Coordination and Adaptation of Human Movements in Human-Robot Interaction

Michael Herzog

Karlsruher Institut für Technologie

Michael Herzog

Coordination and Adaptation of Human Movements in Human-Robot Interaction

Karlsruhe Sports Science Research
Volume 91.2026

Coordination and Adaptation of Human Movements in Human-Robot Interaction

by
Michael Herzog

Karlsruhe Institute of Technology

Karlsruher Institut für Technologie
Institut für Sport und Sportwissenschaft

Coordination and Adaptation of Human Movements in Human-Robot Interaction

Zur Erlangung des akademischen Grades eines Doktors der Philosophie
von der KIT-Fakultät für Geistes- und Sozialwissenschaften des
Karlsruher Instituts für Technologie (KIT) genehmigte Dissertation

von Michael Herzog

Tag der mündlichen Prüfung: 6. Oktober 2025
KIT-Dekan: Prof. Dr. phil. Alexander Woll
1. Gutachter: Prof. Dr. rer. nat. Thorsten Stein
2. Gutachter: Prof. Andrea d'Avella, Ph.D.

Impressum

Karlsruhe Institute of Technology

Karlsruhe Institute of Technology (KIT)
Kaiserstraße 12
76131 Karlsruhe

Institute of Sports and Sports Science (IfSS)
www.ifss.kit.edu

2026

ISSN 2943-0380
DOI 10.5445/IR/1000187586

To my parents Roseliese and Herbert

Acknowledgements

First of all, I would like to express my sincere gratitude to all the people involved, without whom this dissertation would not have been possible.

I want to thank Prof. Dr. Thorsten Stein for offering me the possibility to write this dissertation. Thank you very much for your tireless support, dedication, and the many insightful discussions, for making it possible to delve into, enjoy, and pursue research. I am very grateful to my second supervisor, Prof. Dr. Andrea d'Avella. Thank you very much for the many insightful discussions, the always great feedback, and for spreading your inspiring, infinite energy.

I want to thank all the people I had the chance to learn from and collaborate with. I want to thank all the former and current colleagues at the BioMotion Center and the Institute of Sports and Sports Science at the Karlsruhe Institute of Technology (KIT) for their discussions and for making me enjoy working there.

During my dissertation, I got the fantastic opportunity to stay with Andrea, his team, and colleagues in Rome for some time. Thank you, Thorsten and Andrea, for making this possible, and a warm thank you to everyone there who made this stay so enjoyable. I felt welcome even before I was there. I would also like to extend my thanks to the DAAD for their financial support.

Thank you very much to all the participants who volunteered in the studies during my dissertation!

Felix and Denise, thank you for proofreading this dissertation, and Bernd and Lizeth for your constructive criticism and discussions on particular scientific questions.

Last but not least, I want to thank my family, especially my parents, Roseliese and Herbert, and my wife Marina for their unconditional and permanent support during the dissertation and all the years before.

Zusammenfassung

Die Leichtigkeit, mit derer Athletinnen und Athleten ihre Bewegungen ausführen, ist ein beeindruckendes Ergebnis der menschlichen Koordination. Um Bewegungen ausführen zu können, löst das zentrale Nervensystem (ZNS) mehrere Herausforderungen: die Redundanz des menschlichen Muskelskelettsystems, die daraus resultierende Vielseitigkeit an Bewegungen und die Veränderlichkeit von Körper-, Umgebungs- und Objekteigenschaften.

Das menschliche Muskelskelettsystem umfasst mehr als 600 Muskeln, die sich über mehr als 200 Gelenke mit mehreren Freiheitsgraden spannen. Jede Bewegungsaufgabe kann daher auf mehrere Arten gelöst werden. Diese Redundanz zu kontrollieren wird auch als das „Problem der Freiheitsgrade“ bezeichnet. Des Weiteren ergibt sich durch die enorme Anzahl an Freiheitsgrade ein umfangreiches Repertoire an möglichen Bewegungen. Es ist jedoch unwahrscheinlich, dass das ZNS die Kommandos für jede Bewegung stets neu berechnet. Ebenfalls unwahrscheinlich ist, dass das ZNS die Kommandos für jede Bewegung abspeichert. Wie das ZNS diese Vielseitigkeit an Bewegungen verwaltet, ist demnach ungeklärt. Darüber hinaus ist der Mensch sich ständig verändernden Gegebenheiten ausgesetzt. Sein eigener Körper, seine Umgebung und die Objekte, mit denen er interagiert, sind fortwährend Veränderungen unterworfen und verändern ihre physikalischen Eigenschaften über die Zeit. So weht beispielsweise beim Beachvolleyball der Wind mal stärker oder schwächer oder der neue Tennisschläger ist andersartig bespannt als das Vorgängermodell. Das ZNS meistert die Herausforderung der Veränderlichkeit von Körper-, Umgebungs- und Objekteigenschaften und passt Bewegungen entsprechend an. Der Prozess, der diese Anpassung erzielt, wird als „motorische Adaptation“ bezeichnet. Er beschreibt die Anpassung einer beherrschten Bewegung auf eine Veränderung des eigenen Körpers, der Umgebung, und der Objekte, mit denen er agiert.

Wie das ZNS diese drei Herausforderungen meistert, ist bislang nicht vollständig verstanden. Gemäß einer vorherrschenden Hypothese koordiniert das ZNS mithilfe einer modularen Kontrollarchitektur nicht einzelne Elemente, sondern funktionelle Verbindungen. Anstatt einzelner Muskeln kontrolliert es demnach Gruppen gleichzeitig aktivierter Muskeln. Diese funktionellen Verbindungen gleichzeitig aktivierter Muskeln werden als Muskelsynergien bezeichnet. Bei der Ausführung von Bewegungen realisieren Muskelsynergien biomechanische Funktionen, wie zum Beispiel das Vorwärtsstrecken des Arms.

Muskelsynergien können als Lösung des ZNS für das Problem der Freiheitsgrade, der immensen Redundanz, betrachtet werden. Da das ZNS anstelle einzelner Muskeln Muskelsynergien kontrolliert, reduziert sich die Anzahl der notwendigen Kommandos. Außerdem stellen die Muskelsynergien eine mögliche Lösung dar, wie das ZNS das enorme Bewegungsrepertoire, die Vielseitigkeit, effizient verwaltet. Da Muskelsynergien beliebig und unterschiedlich gewichtet miteinander kombiniert werden, sind schon wenige ausreichend, um eine Vielzahl an Bewegungen zu realisieren. Durch die Nutzung von Muskelsynergien reduziert sich folglich die Anzahl der zu verwaltenden Elemente. Doch welchen Einfluss die Interaktion mit Objekten auf die Muskelsynergien hat und insbesondere, wie die Adaptation, wenn sich Objekteigenschaften ändern, von Muskelsynergien repräsentiert wird, ist nicht vollständig verstanden. Es ist also unklar, wie das ZNS die Herausforderung der Veränderlichkeit von Objekteigenschaften löst.

Roboter bieten die Möglichkeit, diese noch ungeklärten Sachverhalte kontrolliert experimentell zu untersuchen. Somit wird die Herausforderung der Veränderlichkeit von Objekteigenschaften untersucht. Die Roboter werden so programmiert, dass sie ein Objekt mit neuen physikalischen Eigenschaften simulieren, an die sich der Mensch anpassen muss. Zudem wird der Einfluss von Mensch-Roboter-Interaktion untersucht. Roboter können Objekte simulieren, die speziell für die Interaktion mit dem Menschen entworfen sind, wie beispielsweise Rollatoren.

Die vorliegende Arbeit untersuchte die Koordination und Adaptation bei der Mensch-Roboter-Interaktion in Bezug auf die modulare Kontrollarchitektur. Sie gliedert sich in zwei Themen, A und B, mit jeweils zwei Studien.

In Thema A wurde die Koordination und Adaptation von Reichbewegungen mit Hilfe eines Robotermanipulandums und Technologien virtueller Realität untersucht. Wie oben beschrieben, können Menschen ihre Bewegungen adaptieren. Beispielsweise adaptieren Tennisspielerinnen und Tennisspieler sich an die neuen physikalischen Eigenschaften eines neuen Schlägers. Während die ersten Bälle mit dem neuen Schläger noch im Netz oder Aus landen, spielen sie die Bälle nach und nach so gut wie vor dem Wechsel. Bei der motorischen Adaptation wird Wissen erworben, das sowohl nach vergangener Zeit wieder abgerufen wird, als auch bis zu einem gewissen Grad auf bis dahin unbekannte Bedingungen generalisiert werden kann. Verschiedene experimentelle Paradigmen ermöglichen die kontrollierte Untersuchung der motorischen Adaptation, wie zum Beispiel das Kraftfeldparadigma. Hier umfassen Probandinnen und Probanden den Griff eines Robotermanipulandums und steuern damit verschiedene Ziele an. Dabei adaptieren sie an Kräfte, die das Robotermanipulandum ausübt, um die Reichbewegungen zu perturbieren. Diese perturbierenden Kräfte stellen die neuen physikalischen Eigenschaften des Objektes dar, an die das ZNS die Bewegung adaptiert. Im oben genannten Beispiel wird der neue Tennisschläger durch das Robotermanipulandum repräsentiert.

Die erste Studie untersuchte mithilfe des Kraftfeldparadigmas, welchen Effekt die Organisation der Übungsvariabilität auf die Retention und räumliche Generalisierung hat. Alle Probandinnen und Probanden führten Reichbewegungen zu unterschiedlichen Zielen im Arbeitsraum aus. Jedoch wurden die Probandinnen und Probanden in zwei Gruppen eingeteilt und die Übungsvariabilität der beiden Gruppen wurde unterschiedlich organisiert: einmal randomisiert, d.h. mit hoher Interferenz und einmal geblockt, d.h. mit niedriger Interferenz. Es wurde festgestellt, dass ein randomisiertes einem geblocktem Trainingsprotokoll, in Bezug auf die Retention und räumliche Generalisierung, überlegen ist. Diese Ergebnisse wurden zuvor beim Fertigkeitslernen im Zusammenhang mit dem Kontext-Interferenz-Effekt, jedoch noch nicht bei Kraftfeldadaptation und räumlicher Generalisierung, beschrieben. Darüber hinaus konnten die Ergebnisse mithilfe eines erweiterten Zustandsmodells („State-space model“) in Verbindung mit einer der drei vorherrschenden Hypothesen zur Erklärung des Kontext-Interferenz-Effekts, der „Rekonstruktionshypothese“, gebracht werden.

Um tiefere Einblicke in die Kraftfeldadaptation, die Retention und die räumliche Generalisierung zu gewinnen, standen in der der zweiten Studie die Muskelsynergien im Fokus. Die Probanden führten zunächst Reichbewegungen zu fünf Zielen (-90°, -45°, 0°, 45°, 90°) aus und wurden dabei nicht perturbiert. Diese Phase wird als „Baseline“ bezeichnet. Anschließend führten sie Reichbewegungen zum 0° Ziel aus und wurden dabei perturbiert. Nach dieser Adaptationsphase schloss sich eine Auswaschphase an, in der sie die Reichbewegungen ohne Perturbation zum 0° Ziel ausführten. Schließlich wurden die Probanden in drei Gruppen aufgeteilt. Je eine Gruppe führte perturbierte Reichbewegungen zu je einem Ziel aus, d.h. eine Gruppe nur zum -90° Ziel, eine andere zum 0° Ziel und eine zum 45° Ziel. Muskelsynergien wurden aus elektromyographischen Daten extrahiert. Die Ergebnisse zeigten, dass die Muskelsynergien, welche die Aktivierungsmuster der Muskeln der „Baseline“-Bewegungen beschreiben konnten, die Aktivierungsmuster der Muskeln nach der Adaptation nicht beschreiben konnten und dass die Kraftfeldadaptation spezifische Muskelsynergien erfordert. Diese kraftfeldadaptationsspezifischen Muskelsynergien wurden in einem neuartigen, vierphasigen Muster aktiviert. Des Weiteren bildeten die spezifischen Muskelsynergien und deren Aktivierungsmuster auch die Grundlage für die Retention und die räumliche Generalisierung. Zusammenfassend betrachtet, erweitert Thema A zum einen unser Wissen über die Effekte der Organisation der Übungsvariabilität bei der Kraftfeldadaptation, zum anderen liefern sie neue Erkenntnisse bezüglich der Koordination auf muskulärer Ebene, die der Kraftfeldadaptation zugrunde liegt.

Thema B evaluierte, wie sich die Unterstützung durch einen Rollator auf die Koordination der Bewegungen auswirkt. Durch Rollatoren kann die Last von den unteren auf die oberen Extremitäten verlagert werden. Des Weiteren sollen sie die Sturzgefahr reduzieren. Studien zeigten jedoch, dass Rollatoren auch als Risikofaktor für Stürze identifiziert werden können. Um dieses Paradox zu untersuchen, wurden zwei Studien durchgeführt. Die Probandinnen und

Probanden standen auf und saßen hin unter drei Unterstützungsbedingungen. In der Bedingung „ohne Unterstützung“ nutzten Sie die Arme nicht. Bei der Bedingung „leichte Berührung“ legten sie ihre Handflächen leicht auf die Rollatorgriffe. Bei der Bedingung „volle Unterstützung“ umgriffen sie die Rollatorgriffe. Weiter wurden zwei Bodenbedingungen genutzt. Die Probandinnen und Probanden hatten entweder den Standardlaborboden unter ihren Füßen oder Balancierkissen aus Gummi. Ein Roboter-Rollator-Simulator diente als Hilfsmittel, um den Einfluss eines Rollators auf die Übergänge vom Sitzen zum Stehen und vom Stehen zum Sitzen zu untersuchen. Im Gegensatz zu Thema A, in dem die Adaptation mit Reichbewegungen eines Arms und im Sitzen untersucht wurde, untersuchte Thema B eine Ganzkörperbewegung. Die beiden Studien zu Thema B werden als aufeinanderfolgende Analysen betrachtet. In der ersten Studie wurden verschiedene Bewegungsstrategien durch nicht-superversierte maschinelle Lernverfahren auf der Grundlage von Gelenkwinkeln, Körperschwerpunktverläufen und der Interaktionskräfte zwischen den Probandinnen und Probanden und dem Boden und Stuhl identifiziert. In der zweiten Studie wurden die Bewegungen vom Sitzen zum Stehen und vom Stehen zum Sitzen mit Muskelsynergien in Bezug auf die zuvor identifizierten Bewegungsstrategien untersucht. Zusammenfassend zeigten die beiden Studien drei Ergebnisse. Beim Benutzen des Rollators (1) neigten die Probandinnen und Probanden beim Aufstehen und Hinsitzen dazu, den Oberkörper weniger stark nach vorne zu neigen und stattdessen stärker vertikal auszurichten, (2) nahm ihre relative Muskelaktivierung in den Armmuskeln zu und in den unteren Gliedmaßen ab und (3) kontrollierte das ZNS die gleichgewichtskritischen Phasen des Auf- und Absitzens höherfrequentiert im Vergleich zu den Zeitpunkten davor und danach.

Die Ergebnisse der vier Studien verbessern unser Verständnis, wie das ZNS die Herausforderungen der Redundanz, Vielseitigkeit und Veränderlichkeit von Körper-, Umgebungs- und Objekteigenschaften löst. Die Ergebnisse zur Organisation der Übungsvariabilität und zur Koordination auf muskulärer Ebene bei der Kraftfeldadaptation erlauben die motorische Adaptation bei sportlichen Bewegungen perspektivisch besser zu verstehen und zu optimieren. Die Identifikation und Charakterisierung von Bewegungsstrategien und der Einfluss von Rollatoren auf die Koordination verhelfen zu einer sicheren und effizienten Nutzung von Rollatoren.

Abstract

The ease with which athletes perform their movements is an impressive result of the control processes in human motor control and learning. This is because the central nervous system has to solve several challenges: the redundancy of the musculoskeletal system, the versatility of possible movements, and the time-varying properties of the human body, the environment, and objects with which humans interact.

The human musculoskeletal system consists of over 600 muscles spanning over more than 200 joints, with most often several degrees of freedom. Every movement task can thus be solved in multiple ways. Controlling this inherent redundancy is called the “degrees of freedom problem”. Furthermore, the immense number of degrees of freedom allows for a huge number of possible movements. However, it seems implausible that the CNS calculates the commands for the movement each time anew. Likewise, it seems implausible that the CNS stores the commands for every movement. Hence, it is unclear how the CNS solves this versatility challenge. Furthermore, there is the challenge of time-varying properties. Humans’ bodies, their environment, and the objects they interact with change their physical properties on different timescales. For example, the wind becomes stronger or weaker in beach volleyball, or the new tennis racket is tensioned differently than the former one. The CNS solves this challenge of time-varying properties and adapts movements accordingly. The process of adjusting how an already well-practiced action is executed to maintain performance in response to a change of the physical properties of the body, in the environment, or the object the human interacts with, is called “motor adaptation”.

However, how the CNS solves these challenges remains unclear. According to a prevailing hypothesis, the so-called “modular control architecture”, it is proposed that the CNS controls functional linkages instead of single components. In particular, muscle synergies are functional linkages of muscle activations. This means that instead of controlling single muscles, the CNS controls groups of coactivated muscles. These muscle synergies reflect biomechanical functions, such as forward reaching with the arm.

Muscle synergies can be seen as a representation of the solution of the CNS to the redundancy challenge. By controlling groups of coactivated muscles instead of single muscles, the number of necessary commands is reduced. Furthermore, by combining and weighting individual muscle synergies, only a few are necessary to generate an extensive behavioral repertoire. This can be seen as a solution to the CNS for the challenge of versatility. However, the influence of human interactions with objects on muscle synergies remains unclear. In particular, it remains unclear how motor adaptation is represented by muscle synergies. Thus, it is unclear how muscle synergies change as the CNS solves the challenge of time-varying properties.

Robotic devices enable us to study these remaining questions experimentally. The challenge of time-varying properties can thus be investigated. Robotic devices can be programmed to simulate objects with novel physical properties that humans can adapt to. Furthermore, the influence of robotic devices on coordination can be studied using human-robot interaction. For example, robotic devices can also simulate objects, especially designed for human-robot interaction, like rollators.

This dissertation investigated coordination and adaptation in human-robot interaction with respect to the modular control architecture. It is divided into two topics, A and B, each comprising two studies.

In topic A, coordination and adaptation of reaching movements using a robotic manipulandum and virtual reality technologies were examined. As described before, humans can adapt their movements. For example, a tennis player adapts to the new physical properties of their new racket. While the first shots with the new racket land in the net or out, the tennis player subsequently improves until their performance level returns to the level before the racket change. The knowledge acquired through motor adaptation can be recalled after some time and partly generalized to new, inexperienced conditions. Motor adaptation can be investigated with various experimental paradigms. In the force field adaptation paradigm, participants grasp the handle of a robotic manipulandum and reach to multiple targets. Therefore, they adapt to the forces exerted on the handle by the robotic manipulandum, perturbing the reaching movements. These perturbing forces reflect, for example, the new physical properties of the object that the human adapts to. In this case, the new tennis racket's physical properties are simulated by the robotic manipulandum.

In the first study, the force field paradigm was used to investigate the effect of the organization of practice variability on retention and spatial generalization in force field adaptation. All participants performed reaching movements to different targets in the workspace, but the participants were divided into two groups with different organizations of practice variability: one was randomized, i.e., with high interference, and the other was blocked, i.e., with low interference. The random practice protocol was superior to the blocked practice protocol regarding retention and spatial generalization. These results were previously described in skill learning in the context of the contextual-interference effect, but not yet in force field adaptation and spatial generalization. Furthermore, using an extended state-space model, the results could be related to one of the three prevailing hypotheses to explain the contextual-interference effect, the “forgetting-and-reconstruction hypothesis”.

To gain deeper insights into force field adaptation, retention, and spatial generalization, muscle synergies were investigated in the second study. The participants first reached to five targets (-90°, -45°, 0°, 45°, 90°) without any perturbation. This phase was called "Baseline". Then, they reached to the 0° target and got perturbed. After adapting, they washed out by reaching to the 0° target without perturbation. Finally, the participants were split into three groups. Each group reached to one target and got perturbed. One group reached to the -90° target only, another group to the 0° target only, and the last group to the 45° target only. Muscle synergies were extracted from EMG data. The results showed that muscle synergies that facilitated baseline reaching could not explain the muscle activation patterns employed after adaptation and that force field adaptation requires specific muscle synergies. These adaptation-specific muscle synergies were furthermore activated in a novel four-phasic pattern and also underlay retention and spatial generalization. In summary, the two studies expand our knowledge of the effects of the organization of practice variability and underlying coordination in force field adaptation at a muscular level.

In topic B, the effects of rollator support on the coordination of sit-to-stand and stand-to-sit movements were investigated. Rollators can shift the load from the lower to the upper body. Furthermore, rollators are often prescribed to improve postural stability. However, they have paradoxically also been associated with a higher fall risk. To unravel this paradox, two studies were performed. The participants stood up and sat down in three different support conditions. In the unassisted condition, they did not use the handles. In the light touch condition, they placed their palms on the handles, but only with a light touch. In the full support condition, they grabbed the handles with a power grip. Furthermore, two floor conditions were used. They either had the standard lab floor or rubber balance pads beneath their feet. A robot rollator simulator served as an assistive device to study the rollator's influence on transitions between sitting and standing. While topic A investigated adaptation using seated reaching with one arm, topic B investigated a whole-body movement. Therefore, the two studies on topic B can be seen as subsequent analysis steps. In the first study, distinguishable movement strategies were identified by unsupervised machine learning techniques based on joint kinematics, center of mass movement, and ground reaction forces as well as seat interaction forces. In the second study, the sit-to-stand and stand-to-sit movements were investigated using muscle synergies with respect to the previously identified movement strategies. In summary, the two studies showed that participants (1) tended to stand up and sit down with less upper body lean but a more vertical upper body orientation when they used a rollator, (2) relative muscle activation increases in the arm muscles and decreased in the lower limbs when they used a rollator, and (3) the balance-critical phases of seat-off and seat-on were more tightly controlled than before and after these time points.

The results of the four studies enhance our understanding of how the CNS solves the challenges of redundancy, versatility, and time-varying properties. The results regarding the organization of practice variability and coordination at a muscular level in force field adaptation facilitate a better understanding and improvement of motor adaptation in sports. The identification and characterization of movement strategies and the influence of rollator support on coordination help establish a safe and efficient use of rollators.

Contents

Acronyms and symbols

Acronyms

BoS	base of support
CIE	contextual-interference effect
CNS	central nervous system
CoM	center of mass
CoP	center of pressure
CPG	central pattern generator
EC	error clamp
EMG	electromyography
FF	force field
FFCF	force field compensation factor
FS	full support
FWHM	full-width at half-maximum
GRF	ground reaction force
ICA	independent component analysis
LMM	linear mixed model
LT	light touch
NF	null field
NMF	non-negative matrix factorization
PCA	principal component analysis
$\mathbf{PD_{max}}$	maximum perpendicular distance

SSM	state-space model
SVM	support vector machine
UA	unassisted
w.r.t.	with respect to

Symbols and variables

$\mathbf{A}$	matrix
a	scalar
α	angle

List of Figures

List of Tables

1 Introduction and motivation

1.1 Motivation

Human movements are astonishing, e.g., Gymnasts perform Saltos backward with four twists on the floor (FIG, 2024), and tennis players hit balls at each other at speeds of over 180 km/h (Fleisig et al., 2003). Skilled athletes move efficiently, smoothly, and gracefully (Schmidt and Lee, 2011). However, the ease with which they move disguises the complexity of the underlying central nervous system (CNS) processes (Wolpert et al., 2012). Furthermore, the athlete performs in various environments or with specific objects. Gymnastics is performed on special tumbling floors with springs (King and Yeadon, 2004), and tennis players can choose from a wide range of tennis rackets with different physical properties (Allen et al., 2016). Accordingly, the CNS not only needs to coordinate the athlete's movements but must also take into account the interaction with the environment or objects. All these skills require years of practice (Schmidt and Lee, 2011). Furthermore, the physical properties of the athlete's body, their environment and their objects change on different time-scales and require constant adaptation (Karniel, 2011).

Despite years of research, the CNS processes involved in human motor control and learning are not fully comprehended (Wolpert and Bastian, 2021). Thus, they are essential to understanding and optimizing the learning and execution of human movements. Therefore, I aspire to improve our understanding of human motor control and learning with two topics:

Topic A: Coordination and adaptation of reaching movements using a robotic manipulandum and virtual reality technologies

Topic B: Effects of rollator support on the coordination of sit-to-stand and stand-to-sit movements using a robot rollator simulator

These two topics investigate human motor control and learning using reaching, a simple skill (topic A), and complex skills, sit-to-stand and stand-to-sit, (topic B). Hereby and in this dissertation, reaching is called "simple", because it involves primarily only one arm. This means, the number of degrees of freedom in movement is lower compared to the whole-body movements sit-to-stand and stand-to-sit. The latter involve multiple body segments and are therefore called "complex" in this dissertation and according to Cisek and Green (2024) and Wulf and Shea (2002). The two topics further address two crucial time points in human motor control and learning. Topic A concerns the phase when humans adapt their movements to the modified physics of a different object, like a new tennis racket. Topic B, on the other hand, assumes that adaptation has occurred and examines how coordination changes persistently by assistive devices.

Therefore, the different object's physical properties and the assistive device are operationalized with robotic devices. Hence, I use human-robot interaction, on the one hand, as a tool to understand coordination and adaptation (topic A), and on the other hand, with assistive devices specially designed for human-robot interaction (topic B).

1.2 Outline

This dissertation comprises six chapters. This first chapter introduces theoretical and methodological fundamentals. The current state of research concerning the topics of interest for this dissertation is introduced, and the aims and scope of this dissertation finish this first chapter. The subsequent four chapters present individual studies, each addressing the aims and scopes. Each study is either already peer-reviewed and published in a journal or currently in review.

Chapter 2 and 3 focus on topic A, the coordination and adaptation of reaching movements using a robotic manipulandum and virtual reality technologies, and comprise two studies:

Study 1: Random practice enhances retention and spatial transfer in force field adaptation

Study 2: Changes in muscle synergy structure and activation patterns underlie force field adaptation, retention, and generalization

Chapter 4 and 5 focus on topic B, the effects of rollator support on the coordination of sit-to-stand and stand-to-sit movements using a robot rollator simulator, and comprise two studies:

Study 1: Rollator usage lets young individuals switch movement strategies in sit-to-stand and stand-to-sit tasks

Study 2: The central nervous system adjusts muscle synergy structure and tightly controls rollator-supported transitions between sitting and standing

Chapter 6 summarizes and discusses the main findings. Further, it discusses their implications for fundamental and applied sports settings as well as motivates and suggests further research. Figure 1.1 summarizes the structure of this dissertation.

Coordination and Adaptation of Human Movements in Human-Robot Interaction

Chapter 1: Introduction and motivation

Topic A

Coordination and adaptation of reaching movements using a robotic manipulandum and virtual reality technologies

Chapter 2: Study A1

Herzog, M., Focke, A., Maurus, P., Thürer, B. and Stein, T. (2022).

Random practice enhances retention and spatial transfer in force field adaptation.

Frontiers in Human Neuroscience 16: 816197, doi:10.3389/fnhum.2022.816197.

Chapter 3: Study A2

Herzog, M., Berger, D. J., Russo, M., d'Avella A.† and Stein, T.†

Changes in muscle synergy structure and activation patterns underlie force field adaptation, retention, and generalization.

[in review]. Preprint available at https://doi.org/10.1101/2024.12.16.628548

Topic B

Effects of rollator support on the coordination of sit-to-stand and stand-to-sit movements using a robot rollator simulator

Chapter 4: Study B1

Herzog, M., Krafft, F. C., Stetter, B. J., d'Avella, A., Sloot, L. H. and Stein, T. (2023).

Rollator usage lets young individuals switch movement strategies in sit-to-stand and stand-to-sit tasks.

Scientific Reports 13: 16901, doi:10.1038/s41598-023-43401-6.

Chapter 5: Study B2

Herzog, M., Krafft, F. C., Fiedler, J., Berger, D. J., Sloot, L. H., d'Avella A.† and Stein, T.† (2025).

The central nervous system adjusts muscle synergy structure and tightly controls rollator-supported transitions between sitting and standing.

Journal of NeuroEngineering and Rehabilitation 22: 96, doi:10.1186/s12984-025-01622-y.

Chapter 6: General discussion

Figure 1.1: Dissertation outline. Overview of the chapters along with the topics and studies of this dissertation. † Share senior-authorship.

1.3 Challenges in human motor control and learning

Human movements are astonishing, and skilled performers move efficiently, smoothly, and gracefully (Schmidt and Lee, 2011). However, the ease with which they move disguises how complex the underlying CNS processes are (Wolpert et al., 2012). In this context, it has been proposed that the CNS solves multiple challenges for successful movements (Franklin and Wolpert, 2011, Leib et al., 2024, Tresch et al., 1999): delays, uncertainty, noise, nonlinearity, redundancy, versatility, and time-varying properties. This dissertation focuses on redundancy, versatility, and time-varying properties, which will be introduced in the following sections.

1.3.1 Redundancy and versatility

Returning a tennis serve exemplifies the redundancy and versatility challenges of a typical sports movement (Wolpert and Bastian, 2021, Bernstein, 1967). To return the serve, the tennis player must move their racket. However, there is inherent redundancy. The same racket trajectory can be realized with many different joint rotations and muscle activations (Franklin and Wolpert, 2011). The hand holding the racket and the joints involved in the movement can be moved at different speeds and over numerous joint angle trajectories, but still realize the same racket trajectory (Franklin and Wolpert, 2011). Furthermore, various muscles can be combined and activated differently for the same joint movement (Franklin and Wolpert, 2011). Muscles act around the joints and generate the torque to move the limbs. The CNS controls these muscles (Bizzi et al., 1991). However, approximately 600 muscles span over 200 joints with multiple degrees of freedom (Franklin and Wolpert, 2011). These 600 muscles are either active or inactive simultaneously, leading to 2^{600} possibilities at any given time – a number with over 180 digits (Bellman, 1966). Furthermore, muscles act on a single, two, or more joints (mono-, bi-, and multiarticular muscles; Van Ingen Schenau 1989), and often, multiple muscles rotate the same joint in similar directions. Hence, the CNS needs to solve a complex "many-to-one problem" (Rosenbaum, 2009). The same movement can be achieved in multiple, often infinite, ways, leading to many possible solutions (Franklin and Wolpert, 2011). How the CNS copes with this vast number of degrees of freedom is the so-called "degrees of freedom" problem (Bernstein, 1967) and a fundamental question in human motor control and learning (Flash and Bizzi, 2016). This problem becomes even more complex, considering the other above-listed challenges. For example, the muscles that activate to move the limbs are highly nonlinear in their force production (Franklin and Wolpert, 2011). The muscle forces depend on their activation level nonlinearly concerning the muscle force-length, force-velocity relationships, and tendon properties (Zajac, 1989). Lastly, not only is the human body responsible for movement, but it also interacts with the environment and various objects (Flash and Bizzi, 2016). Identical muscle activation patterns can generate different motor outputs, for example, because of a different body posture or environmental forces (Ting and Chiel, 2017).

The redundancy of degrees of freedom not only makes the computations complex but is also the basis of great behavioral versatility, as the vast number of degrees of freedom allows for countless movement possibilities (Bizzi et al., 1991). Indeed, humans learn an immense number of movements over their lifespan and can perform them in various environmental conditions (Bizzi et al., 1991). This raises the question of how the vast versatility and behavioral repertoire are efficiently represented in the CNS. As introduced before, the equations of motion describing rotations around the joints are highly complex as they include multiple terms depending on several interactions between joints. Even if these equations can be solved analytically, the exact determination of each parameter is difficult and leads only to an approximation of human motion (d'Avella, 2016). Despite the possibility that an extensive neural network could implement it, any explicit analytic model would be impossible to learn efficiently due to the degrees of freedom and parameters involved (Wolpert and Ghahramani, 2000). Accordingly, it seems implausible that the CNS uses explicit representations of the limbs' equations of motions and performs analytical calculations; it rather uses implicit and approximate knowledge of the limbs' dynamics resulting from muscle activation (d'Avella, 2016). On the other side of the spectrum concerning the generality of the knowledge of the limbs' dynamic behavior, there is a "one-to-one" mapping. However, a one-to-one mapping also seems implausible as it would mean that the CNS needed to store mappings of an infinite number of movements onto an infinite set of muscle activation patterns (d'Avella, 2016). With respect to the tennis player example, it seems implausible that the CNS stores the mappings of every possible return shot, including all their variants (fast, slow, with little or much spin, etc.), onto sets of muscle activation patterns independently. It therefore seems much more plausible that the CNS uses a compromise of both extremes, the very general mapping and the very large number of "one-to-one" mappings (d'Avella, 2016).

To sum up, there must be a way to reduce the number of components that need control and storage. The modular control architecture has been proposed as a solution to these control problems (Bizzi et al., 2008, Giszter, 2015, d'Avella, 2016) and will be introduced in section 1.4.2.

1.3.2 Time-varying properties

Time-varying properties, also called non-stationarity, describe the fact that physical properties of the human body, the environment, or the objects we interact with change over time (Franklin and Wolpert, 2011, Leib et al., 2024, Karniel, 2011). This poses a challenge for the CNS. Examples of changes in the human body are fatigue and aging. Examples of environmental changes are wind conditions in beach volleyball. An example of a change in an object's physical properties is the change in tennis rackets. Properties change on different time scales, from milliseconds to millions of years, as described by Karniel (2011):

On a very short scale, there is "feedback". Here, sensory information is propagated in the sensorimotor system when a movement is carried out. For example, when an ongoing movement needs to be corrected. No structural change is happening, and the changes in the motor command result from the changes in the sensory signals. That is different from motor adaptation, where a change of parameters occurs based on the received sensory information.

“Motor adaptation refers to a particular type of behavioral change that involves adjusting how an already well-practiced action is executed to maintain performance in response to a change in the environment or the body [...] by modifying how the current action is executed” (Krakauer et al., 2019, p. 616). Hence, motor adaptation aims to improve the future performance of a well-practiced movement based on the observation of previous control and sensory signals. One example is the adjustment of a tennis player’s motor commands when they change rackets. The first shots with the new racket will likely land in the net or out of bounds. After several shots, they become precise again, and the tennis player can perform as well as before the change. No new capabilities emerge in motor adaptation (Karniel, 2011). Performance does not improve beyond baseline; instead, it returns to its level before the change (Krakauer and Mazzoni, 2011, Shadmehr and Wise, 2005). Accordingly, with motor adaptation, the tennis player will improve their performance with the new racket up to the level they had with the old racket, but not beyond. On a wider timescale, but still being motor adaptation, there is also change within a lifetime through growth and development, which requires a recalibration of our motor commands (Krakauer et al., 2019). Motor adaptation is of particular interest in this dissertation and will be elaborated in section 1.4.3.

In contrast to motor adaptation, structural changes happen during (skill) learning (Karniel, 2011). In particular, “skill learning (e.g., learning to ride a bike or to play tennis) involves acquiring new patterns of muscle activation and achieving a higher level of performance by reducing errors without a reduction in movement speed” (Kitago and Krakauer, 2013, p. 93). This means, skill learning facilitates improvements beyond the original level (Diedrichsen and Kornysheva, 2015, Krakauer and Mazzoni, 2011), which stays in contrast to motor adaptation. Furthermore, the induced changes at the level of performance are relatively permanent, another difference to the transient and reversible character of motor adaptation (Krakauer et al., 2019). Furthermore, skill learning takes up to months or even years, distinctly longer than motor adaptation, which can happen within a single experimental session (Krakauer et al., 2019, Kitago and Krakauer, 2013).

Lastly, evolution may take millions of years and includes any possible changes, such as structural, functional, or changes in connectivity, but will not be further discussed in this dissertation.

Given the example of the tennis player and the described challenges, it becomes evident that human motor control and learning are complex. Thus, gaining a better understanding of human motor control and learning will have wide-ranging implications for sports, activity, rehabilitation, and robotics (Rucci et al., 2007, Gollhofer et al., 2012, Schmidt and Lee, 2011). The following sections will introduce the means to investigate the challenges of redundancy, versatility, and time-varying properties.

1.4 Modeling and analysis of human motor control and learning

The previous section outlined the challenges of human motor control faced by the CNS. In addition, the question was raised about how it deals with these challenges. This section introduces the concepts used in this dissertation to study human motor control and learning, focusing on the challenges redundancy, versatility, and time-varying properties. One important aspect concerning the understanding of human motor control and learning is the level of analysis.

1.4.1 Multiple levels in human motor control

The neuroscientist David Marr (1982) suggested a taxonomy for analyzing complex information-processing systems with three levels: (1) "computational theory" (also called "task" and "theory"; Giszter and Hart 2013, Berret et al. 2019), (2) the "representation and algorithm", and (3) the "hardware implementation". Marr's levels provide a useful guide to a better understanding of the CNS behavior (Kriegeskorte and Douglas, 2018). They complement each other but address conceptually different questions (Berret et al., 2019). The three levels are described in the following three paragraphs. Subsequently, it is described how they complement each other.

The "computational theory" addresses questions such as, "What is the goal of the computation, why is it appropriate, and what is the logic of the strategy by which it can be carried out?" (Marr, 1982, p. 25). This level thus seeks to find the actions' driving purpose and logic (Shadmehr and Krakauer, 2008). This level describes the functions that humans are supposed to achieve (Rosenbaum, 2009). These functions can be expressed mathematically with explicit formulas (Rosenbaum, 2009). Even though the CNS does not use the formulas explicitly, they are used implicitly (Rosenbaum, 2009). In Marr's example of bird flight, this level concerns aerodynamics, Bernoulli's equations, which state that birds fly because of lift. In human motor control, this level aims to explain why human movement trajectories have certain characteristics and what makes the chosen movement better than another (Berret et al., 2019). In other words, presuming human behavior is optimal, the aim is to understand the optimality criterion or cost function the CNS uses (Berret et al., 2019). Internal models as a theory underling force field adaptation can for example be positioned at this level (Shadmehr and Wise, 2005, Sensinger and Dosen, 2020). "Optimal feedback control" (Todorov, 2004, Todorov and Jordan, 2002) is another currently prevailing theory at this level (Haith and Krakauer, 2012, McNamee and Wolpert, 2019). However, how the bird or human carries out the movement is not answered at the computational level.

The “representation and algorithm” level addresses the questions, “What is the representation for the input and output, and what is the algorithm for the transformation?” (Marr, 1982, p. 25). In Marr’s example, this would be the bird’s flapping of wings. In human motor control, this level addresses how the sensorimotor system could generate observably optimal trajectories (Berret et al., 2019). Many human motor control theories have been proposed, with the modular control architecture, the one discussed in this dissertation, being one of them (Berret et al., 2019). It will be further introduced in section 1.4.2.

Finally, the “hardware implementation” level addresses the question, “How can the representation and algorithm be realized physically?” (Marr, 1982, p. 25). It refers to the question which physical structure is available. In Marr’s example, these are the bird’s wing feathers. In human motor control, this refers to the physical realization through the nervous and musculoskeletal systems (Shadmehr and Krakauer, 2008). This level thus addresses, for example, which brain regions become active or inactive and how muscles contract and relax to facilitate movement, such as the bird’s flapping of wings and the human’s moving of the arm (Rosenbaum, 2009).

Even though this dissertation primarily focuses on the representational level, one must be aware that the levels are coupled (Kriegeskorte and Douglas, 2018). For example, the choice of an algorithm depends on what it has to do and which physical structure is available (Marr, 1982). Birds, insects, and aircrafts that fly all satisfy the principles of aerodynamics at the computational level. However, they have feathers, thin layers of cutin and veins, or multiple alloys and composite materials available as physical structures at the implementation level, respectively (Duffield, 2018, Bishop, 1997, Mouritz, 2012). Hence, the algorithm differs: Birds and insects flap their wings differently and aircrafts rotate propellers. Likewise, while a robotic and a human arm obey to the same laws of physics and mechanical objectives at the computational level, they differ at the implementation level, for example humans use muscles and robots motors. Consequently, while robotic developers can use concepts in human motor control for robotic algorithms, the robotic algorithms still need more specification and adjustments (Atkeson, 1989).

In summary, Marr’s levels provide a framework to help understand the complex processes in human motor control, from high-level goals and constraints to the physical mechanisms realizing the movement. It pinpoints that the levels are interwoven, which has implications for analyzing human motor control and learning: Findings at the implementation level are especially interpretable only if a certain knowledge of the other two levels is present (Jonas and Kording, 2017, Krakauer et al., 2017). Hence, when analyzing human motor control and learning, all three levels need to be considered. In this dissertation, all levels are addressed, while the primary focus is on the representational level.

1.4.2 Muscle synergies as a potential solution to the challenges of redundancy and versatility

The inherent number of components involved in movements (muscles, joints, etc.) and their nonlinear interactions make the separate control of each component impossible. Thus, the components need to be coordinated. It was Bernstein's intuition that the coordination of movement is the process of mastering redundant degrees of freedom by organizing them into "functional linkages" (Bernstein, 1967). These functional linkages are also known as synergies, modules, or motor primitives. They reduce dimensionality because the number of components to control is reduced. This is because just the functional linkages require control rather than every component. This modular control architecture simplifies human motor control (Savelsbergh et al., 1999, Bizzi et al., 2008, Giszter, 2015, d'Avella, 2016). These functional linkages may exist in different forms in human motor control (Bruton and O'Dwyer, 2018, Flash and Hochner, 2005), for example, as reflexes (Sherrington, 1910), elements of central pattern generators (CPGs; Grillner 1981), convergent force fields (Bizzi et al., 1991), kinematic synergies (Daffertshofer et al., 2004, Santello et al., 1998), or muscle synergies (Saltiel et al., 2001). The following sections first describe the research origins of convergent force fields and muscle synergies with a particular focus on the redundancy challenge. Then, the currently prevailing muscle synergy models are presented. Hereby, the modular control architecture is emphasized by describing the models' hierarchical structures. Afterwards, it is described how muscle synergies can be characterized in terms of their biomechanical properties. Furthermore, it is emphasized how the CNS might utilize muscle synergies as a solution to the versatility challenge. Finally, the calculation of muscle synergies from electromyography (EMG) data is explained.

1.4.2.1 Research origins of the modular control architecture and convergent force fields

Experiments with spinalized frogs (Bizzi et al., 1991, Giszter et al., 1993) and rats (Tresch and Bizzi, 1999) have provided evidence that there may be in fact functional linkages acting as building blocks for movement (Bizzi et al., 2002). For example, a series of pioneering studies used microstimulation of interneuronal regions of frogs' lumbar spinal cords. The frog's ankle was fixed at different positions in the workspace, and the force at the ankle, exerted through microstimulation of the same part of the spinal cord, was measured (Figure 1.2A). Measuring the force at different workspace positions led to observing position-dependent forces, termed "convergent force fields" (Figure 1.2B). These convergent force fields have interesting properties. Firstly, systematic stimulation of different spinal cord regions led to only a few convergent force fields. Secondly, a seminal study by Mussa-Ivaldi et al. (1994) found that when two sides of the spinal cord were stimulated simultaneously, the resulting convergent force field resembled the summation of the convergent force fields obtained by separate microstimulations (Figure 1.2C-F). This means that convergent force fields induced by focal stimulation of the spinal cord follow the principle of vector summations (Bizzi et al., 1991, Mussa-Ivaldi et al., 1994, Lemay et al., 2001). This linear observation is interesting because convergent force field vector summation eliminates the complex nonlinearities among neurons and between neurons and muscles. Thus, the principle of vector summation of a small number of convergent force fields hints that the motor system may employ a computationally simple mechanism to produce a wide range of movements (Bizzi et al., 2000). The organizational mapping of the spinal cord and the distinctiveness of the convergent force field orientations supported the concept of a modular organization in the spinal cord motor circuitry (Bizzi et al., 2002). Similar results with electrical stimulation in the rat spinal cord suggested that these results might generalize across vertebrates (Bizzi et al., 2000, Tresch and Bizzi, 1999). The studies by Mussa-Ivaldi and Giszter (1992) and Mussa-Ivaldi (1997) verified this view with computational analyses. In particular, the simulation study by Mussa-Ivaldi and Bizzi (2000) demonstrated that the combination of convergent force fields could reproduce a wide range of movement trajectories with the basic characteristics of experimentally observed reaching movements.

1.4.2.2 The different models of muscle synergies and the modular control architecture

The vector summation principle described in the previous section was subsequently found in muscle activations (Tresch et al., 1999, Giszter et al., 2010). This supports the idea that the CNS might use so-called muscle synergies to produce behavior (Tresch et al., 1999, Giszter et al., 2010). The microstimulation-activated contractions of sets of muscle were repeatable and well-organized. Cutaneous stimulation of frogs' hindlimbs could describe the evoked muscle activation patterns with linear combinations of a small set of co-activated muscles. Furthermore, while single spinal interneurons are synaptically connected with a set of motor neurons controlling different muscles, Saltiel et al. (2016) and Levine et al. (2014) showed that spinal interneurons are organized in functional linkages. Each of these functional linkages activates a particular set of co-activated muscles. Hereby, the muscles are co-activated in distinctive proportions. Such a set of co-activated muscles is called a spatial muscle synergy (Flash and Bizzi, 2016). Spatial muscle synergies are also called “time-invariant” or “synchronous” muscle synergies.

Another perspective on muscle synergies comes from the observation that an invariant temporal structure of muscle activation is consistently found in human adult locomotion (Ivanenko et al., 2004, 2005, Lacquaniti et al., 2012). Here, only the distinctive proportions of the sets of co-activated muscles vary (Ting and Chvatal, 2010). In other words, the timing at which sets of

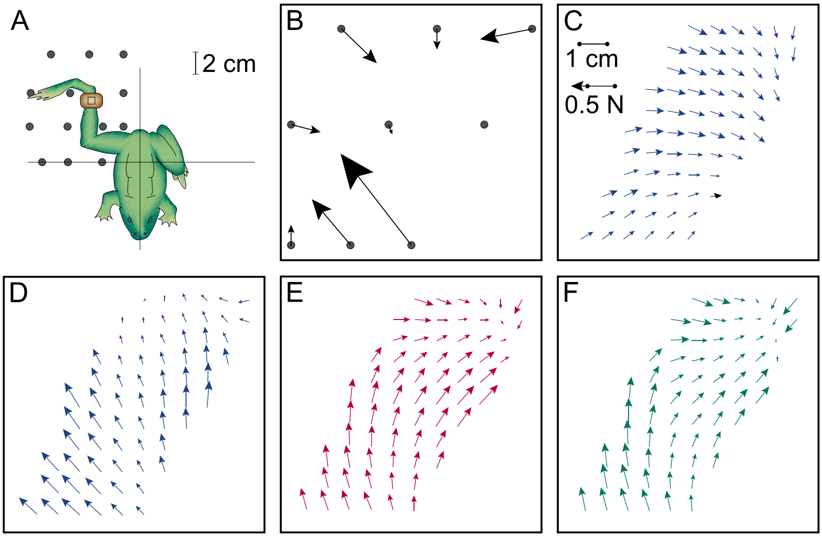

Figure 1.2: Force fields are evoked by microstimulation of the frog's spinal cord. A: The frog's ankle was fixed at different locations as indicated by filled circles. Electrical stimulation of the spinal cord or noxious stimulation of the skin led to muscle activation patterns and their resulting forces were measured at the ankle. B: Force measurements at different ankle locations. The set of forces is called "convergent force field". C and D: Convergent force fields, by stimulation of different sides of the frog's spinal cord. E: Prediction of the convergent force field by summation of the force vectors from C and D. F: Convergent force field produced from co-stimulation of the sides of C and D, with remarkable similarity to E (adapted from Bizzi et al. 1991, Mussa-Ivaldi et al. 1994, and Bizzi et al. 2000; reproduced with permission from Springer Nature).

co-activated muscles are active is invariant. The timing is stereotypical across gait cycles and gait modes. These stereotyped, invariant temporal structures of muscle activation are called temporal muscle synergies. This means that the sets of co-activated muscles are active once and at distinct phases of the gait cycle. The timings are hardly affected by walking speed (Ivanenko et al., 2004), walking mode (walking or running; Cappellini et al. 2006), direction (forward and backward walking; Ivanenko et al. 2008). Temporal muscle synergies are also called "temporal components" or "basic patterns".

To sum up, two different models of muscle synergies were introduced: spatial muscle synergies and temporal muscle synergies. In addition to these two, further models of muscle synergies exist, such as spatiotemporal muscle synergies – also called time-varying muscle synergies – (d'Avella and Tresch, 2002, d'Avella et al., 2006) and space-by-time muscle synergies (Delis et al., 2014), but the latter two are not further discussed in this dissertation.

The different models of muscle synergies differ with respect to which part is trial-dependent and which is trial-independent (Berger et al., 2020, Delis et al., 2014, Russo et al., 2014). This is an important distinction between the models of muscle synergies as this links to the idea that muscle synergies are hierarchically organized in the modular control architecture. According to a hierarchical organization, movement is generated through a combination of a trial-independent and a trial-dependent part (Ting and McKay, 2007). The trial-independent part is presumably stored in subcortical areas of the CNS and reused across movements. In contrast, the trial-dependent part is presumably under cortical control and accounts for variations across trials (d'Avella et al., 2003, Ting and Chvatal, 2010). As the trial-dependent part is presumably under cortical control, it is also called a "descending command". In spatial muscle synergies, the trial-independent part comprises the sets of muscles which are co-activated in distinctive proportions. These sets of the trial-independent part are called "muscle weightings". The muscle weightings are combined with trial-dependent activation functions (also called time-varying coefficients). The activation functions represent how much and when the muscle weightings are activated (Figure 1.3). The activation functions are the descending commands. In contrast, temporal muscle synergies consist of stereotyped, invariant temporal structures of muscle activation and trial-dependent muscle weightings. Here, the activation functions are invariant and the muscle weightings vary across trials. In other words, it is assumed that the CNS uses fixed temporal structures of muscle activation. Here, the muscle weightings vary as their distinctive proportions is given by descending commands (Safavynia and Ting, 2012).

1.4.2.3 Muscle synergies and their biomechanical characterization

Many study results suggest that muscle synergies can be correlated to functional outputs and task performance, or in other words, support the idea that they represent biomechanical functions (Ting et al., 2015). In reaching movements, muscle synergies usually represent arm flexion and extension or elevation of the scapula (d'Avella et al. 2006; Figure 1.3); in sit-to-stand movements, for example, the forward-bending movement of the trunk or the hip and knee extensions to rise (Yang et al., 2017). In addition, Neptune et al.'s (2009) forward dynamics simulation showed that combining five muscle synergies could reconstruct the basic parts of walking, such as body support in early stance or propulsion in late stance phases.

Furthermore, muscle synergies are often tuned. In reaching movements, this means that the descending commands show higher activation of muscle synergies for specific reaching directions, often resembling a cosine function. Hence, one muscle synergy might be most active in medial reaching movements and gradually less for reaching movement away from the medial direction. Another might be most active for lateral reaching movements and less for more medial reaching movements, respectively (d'Avella et al. 2006; Figure 1.3). Similar findings were revealed in reactive postural responses following perturbations in different directions (Ting and Macpherson, 2005, Torres-Oviedo et al., 2006, Torres-Oviedo and Ting, 2007).

1.4.2.4 Muscle synergies underlie behavioral versatility

The previous section described how the CNS might use muscle synergies with regard to the challenge of redundancy. The redundancy is reduced by coordinating muscle synergies instead of single muscles. With respect to the challenge of versatility, the findings that the same muscle synergies contribute to different movements and different behaviors are of particular interest (d'Avella et al., 2003). This means, muscle synergies are shared across movements. Different movements are constructed by combining the same muscle synergies with different timings and amplitudes, i.e., tunings (Bizzi and Ajemian, 2015). In other words, flexibly recruiting and combining muscle synergies generates an extensive behavioral repertoire and versatility (d'Avella et al., 2003, Bizzi et al., 2008, Mussa-Ivaldi et al., 1994, Mussa-Ivaldi and Bizzi, 2000, Ting and Macpherson, 2005). For example, muscle activation patterns for reaching to different directions can be reconstructed by a number of muscle synergies lower than the number of reaching directions and muscles (Figure 1.3). This is even true for via-point or change-in-target reaching movements (d'Avella et al., 2006, 2008, 2011, Muceli et al., 2010, Coscia et al., 2014). Likewise, shared muscle synergies underlie the responses to perturbations in different directions in postural tasks (Torres-Oviedo et al., 2006, Torres-Oviedo and Ting, 2007). However, similar yet distinctive movements typically require specific muscle synergies in addition to the shared muscle synergies. For example, shared muscle synergies underlie a series of locomotion movements, like walking, turning, or sit-to-walk transitions (Carey et al., 2021). In particular, the three locomotion movements share around 80% of the muscle synergies. However, all three locomotion movements still require their few specific muscle synergies, for example, one specific to the turning movement.

1.4.2.5 Muscle synergy analyses in human motor control and learning

Muscle synergy analysis has played a major role for research in human motor control and learning (see reviews from Bizzi et al. 2008, Tresch and Jarc 2009, Lacquaniti et al. 2012, Giszter 2015, Ting et al. 2015, Mileti et al. 2020, Cheung and Seki 2021, Zhao et al. 2023, Borzelli et al. 2024, Singh et al. 2018, Ivanenko et al. 2006). Nevertheless, it needs to be acknowledged that the extent to which muscle synergies extracted from EMG are neurally encoded has remained controversial, despite these numerous findings (Cheung and Seki, 2021, Tresch and Jarc, 2009). However, much evidence supporting the modular control architecture stems from the observation of low dimensionality in the muscle activation patterns recorded during a variety of movements, from different species or patients (Berger et al., 2020, Torres-Oviedo et al., 2006, Cheung et al., 2012, d'Avella et al., 2003, Overduin et al., 2008). Further supporting evidence stems from experimental studies that are designed to distinguish a modular controller from a non-modular one and directly allow testing causality (Berger et al., 2013).

1.4.2.6 Extraction of muscle synergies from EMG data

The following sections provide experimental and mathematical introductions to the extraction of muscle synergies from EMG data.

Recording and processing of EMG data

The first step in calculating muscle synergies is the capturing and processing of EMG data. EMG data must be obtained from as many muscles as possible but at least from those playing an important role in the movement under investigation (Torricelli et al., 2016). In particular, the number of measured muscles and experimental conditions or variations must be high enough to capture different muscle activation patterns (Cheung et al., 2005, Ting and Chvatal, 2010), following the hypothesis that few muscle synergies underlie an extensive behavioral repertoire. Usually, the EMG recordings are contaminated with noise from electronic equipment or the electromagnetic radiation resulting from the electrical power lines (Torricelli et al., 2016). Additionally, motion artifacts such as those resulting from movements of the electrode on the skin or the cables connecting the electrode and amplifier may appear in the signal (Torricelli et al., 2016). Further artifacts may result from the heartbeat or the quasi-random firing of motor units (Boyer et al., 2023, Torricelli et al., 2016). A series of steps is usually employed to remove all the raw EMG data artifacts that do not relate to muscle activation patterns in the best possible way. These steps include but are not limited to low- and high-pass filtering, application of a “notch” filter, rectification, and envelope extraction of the EMG data. Afterward, the EMG data are often segmented to the relevant time of the movement under investigation, time-normalized, and amplitude-normalized (Kieliba et al., 2018, Turpin et al., 2021, Steele et al., 2013). It must be noted that the processing of the EMG data is a critical part for the extraction of muscle synergies. Differently processed EMG data lead to different inputs for the algorithm, which extracts muscle synergies, and thus possibly result in somewhat dissimilar muscle synergies and interpretations (Kieliba et al., 2018, Turpin et al., 2021, Steele et al., 2013). The next step is to choose the algorithm that extracts muscle synergies.

The choice of the algorithm to extract muscle synergies

Matrix factorization algorithms like principal component analysis (PCA; Hotelling 1933, Pearson 1901), independent component analysis (ICA; Jutten and Herault 1991) and non-negative matrix factorization (NMF; Lee and Seung 1999, 2001) make it possible to obtain functional linkages in muscle activation patterns, i.e., to identify muscle synergies from multidimensional EMG data (Tresch et al., 2006). The algorithms are unsupervised source decomposition machine learning methods (Cichocki et al., 2009). Applied to EMG data, they aim to reconstruct the original EMG data with a relatively small number of muscle synergies, i.e., to obtain a low-dimensional representation of muscle activation patterns (Flash and Bizzi 2016, Ting and Chvatal 2010; Figure 1.3). NMF is particularly suitable for the extraction of muscle synergies because it constrains the outcome matrices to be non-negative, unlike PCA and ICA. This non-negativity relates well to muscles which can either pull or be idle (Ting and Chvatal, 2010).

Another interesting property of NMF is that NMF yields parts-based decompositions, as demonstrated by Lee and Seung (1999). Their original paper showed that faces are decomposed into specific parts, such as the nose, eyes, and mouth. Combining each part with a scaling factor specific to it (e.g., large eyes) enables the creation of many faces. With respect to muscle synergies, this means all muscle synergies are added up – they cannot be subtracted from each other – resulting in the fact that the single muscle synergies resemble identifiable parts of the complete muscle activation patterns (Ting and Chvatal 2010; Figure 1.3). In other words, a multiplication of a muscle synergy with its activation function yields a specific muscle activation pattern. This specific muscle activation pattern is also found as a part in the EMG data. This is an advantage of NMF over PCA. PCA starts with the mean face and adds or deletes other faces. The resulting face may therefore bear no resemblance to any of the parts resulting from a decomposition with PCA (Ting and Chvatal, 2010). With respect to muscle activity, this means, the resulting pattern from a single principal component and its scores is not necessarily found in the EMG data, it could vanish through a subtraction as another resulting pattern could be negative. Hence, the non-negativity constraint and the parts-based decomposition property ease the interpretability of the muscle synergies (Devarajan and Cheung, 2014). The following section describes the calculation of muscle synergies with NMF.

Extraction of muscle synergies with non-negative matrix factorization

After the processing of the EMG data, the next step is the arrangement of the processed EMG data into a matrix. Envelopes are either averaged over repetitions of the same movement or concatenated (Brambilla et al., 2023a). The arrangement depends on the underlying research question and corresponding muscle synergy model (spatial, temporal, etc.; Torricelli et al. 2016). In the following, the steps of the muscle synergy extraction are explained for the spatial muscle synergy model. In terms of the calculation, these steps also apply to temporal muscle synergies, with the difference being a different arrangement of the data in the EMG matrix.

To extract spatial muscle synergies, the EMG data are arranged in a matrix $\mathbf{V}$ such that the single muscles are arranged in rows, and one column represents one point in time. Usually, $\mathbf{V}$ contains multiple time points and multiple trials. Therefore, the columns comprise the different trials that hold the time points of the single trials chronologically. NMF decomposes the EMG data in $\mathbf{V}$ into a low-dimensional approximation $\mathbf{WC}$, with $\mathbf{W}$ and $\mathbf{C}$ being matrices that contain only non-negative values. $\mathbf{W}$ contains the sample-independent muscle weightings, and $\mathbf{C}$ the sample-dependent activation functions (Delis et al., 2014, Russo et al., 2014).

To extract temporal muscle synergies, the matrix $\mathbf{V}$ is altered. Specifically, the multiple time-points are arranged in rows, with the first time-point in the first row. The columns comprise the single muscles and multiple trials are concatenated horizontally (Russo et al., 2014). NMF decomposes $\mathbf{V}$ into $\mathbf{CW}$. $\mathbf{C}$ contains the sample-independent activation functions and $\mathbf{W}$ the sample-dependent muscle weightings (Delis et al., 2014, Russo et al., 2014).

In detail, to obtain spatial muscle synergies, NMF factorizes the matrix $\mathbf{V}$ into two matrices, $\mathbf{W}$ and $\mathbf{C}$. Thereby, all matrices $\mathbf{V}$, $\mathbf{W}$, and $\mathbf{C}$ contain only non-negative values. Again, this non-negativity constraint makes physiological sense, as motor neurons are either firing (positive value) or in a resting state (zeros; Ting and Chvatal 2010). Mathematically formulated, NMF tries to solve the problem

$$\begin{aligned} \mathbf{V} &\approx \mathbf{WC} \\ \text{w.r.t. } \mathbf{V} &\in \mathbb{R}_{\geq 0}^{n\times m}, \\ \mathbf{W} &\in \mathbb{R}_{\geq 0}^{n\times r}, \\ \mathbf{C} &\in \mathbb{R}_{\geq 0}^{r\times m} \end{aligned}$$

Here, n denotes the number of recorded muscles, m the number of envelopes multiplied by the number of time samples, and r the number of muscle synergies. The number of muscle synergies r is an input to NMF and therefore needs to be chosen by the researcher. Usually, r is chosen to be smaller than n or m so that $\mathbf{WC}$ is a low-dimensional representation of $\mathbf{V}$ (Lee and Seung, 2001). The matrix $\mathbf{V}$ is therefore approximated by a multiplication of $\mathbf{W}$ and $\mathbf{C}$.

The critical choice of the number of muscle synergies to be extracted

NMF aims to find $\mathbf{W}$ and $\mathbf{C}$ that best approximate $\mathbf{V}$. To quantify the approximation and determine how well the EMG data is approximated, a measure of the reconstruction quality is necessary. The muscle activation patterns in $\mathbf{V}$ and their reconstruction $\mathbf{WC}$ are multivariate time series (d'Avella et al., 2006). Thus, the reconstruction quality should be assessed with a multivariate-based measure of data variability. Accordingly, d'Avella et al. (2006) defined the multivariate R^2 using the total variation method proposed by Mardia et al. (1979): the trace of the muscle activation patterns' covariance. This R^2 relates the ratio of the sum of the squared residuals

(*SSE*) to the sum of the squared residuals from the mean activation (*SST*) according to d'Avella et al. (2006) and Russo et al. (2024). In other words, it shows how much the reconstruction $\mathbf{WC}$ can account for the total variation in $\mathbf{V}$.

$$R^2 = 1 - \frac{SSE}{SST} = 1 - \frac{tr[(\mathbf{V} - \mathbf{WC})(\mathbf{V} - \mathbf{WC})^T]}{tr[(\mathbf{V} - \bar{\mathbf{V}})(\mathbf{V} - \bar{\mathbf{V}})^T]}$$

Here, tr denotes the trace, the T superscript the matrix transpose. $\bar{\mathbf{V}}$ contains the mean muscle activations.

The choice of r, the number of muscle synergies to extract, is critical. To obtain a low-dimensional but still good representation of $\mathbf{V}$, r needs to be chosen carefully (Banks et al. 2017, Zhao et al. 2023, Turpin et al. 2021; Figure 1.3). The problem of selecting r has been addressed extensively in the literature, and multiple criteria have been proposed (Zhao et al., 2023, Turpin et al., 2021). Generally, the aim is to choose r such that the structural variation in the EMG data is captured and that any additional muscle synergy would add only unstructured noise to the reconstruction (Tresch et al., 2006). Usually, a measure of the reconstruction quality (e.g., R^2) is used to determine r and assessed with a plot showing R^2 against the number of extracted synergies (Figure 1.3). The most widely used criterion is to select r when R^2 exceeds an *a priori*-defined threshold value, most often a number between 0.8 and 0.9 (Zhao et al., 2023, Turpin et al., 2021). Furthermore, a second criterion is often used to ensure no structural data variation is neglected. This criterion can for example be that the increase of R^2 with additional bases is lower than an *a priori*-defined threshold, such as 0.05 (Zhao et al., 2023, Turpin et al., 2021). Another method with the same aim of capturing structural data variation and neglecting noise is based on the shape of the R^2 curve and selects r where the R^2 curve shows a knee point. After this knee point, the R^2 curve usually plateaus (d'Avella et al., 2006). Many more methods exist (Zhao et al., 2023) and are still being developed (Ranaldi et al., 2023). In any case, the correct number r is unknown because the ground truth is unknown. Hence, it is always necessary to question the choice of r critically and in terms of the content (Torricelli et al., 2020).

Muscle synergies are extracted using multiple starts and iterations of the non-negative matrix factorization

The NMF problem $\min \|\mathbf{V} - \mathbf{WC}\|$ with respect to $\mathbf{W}$ and $\mathbf{C}$, subject to $\mathbf{V}, \mathbf{W}, \mathbf{C} \geq 0$, is not convex, meaning that finding an algorithm that finds global minima is unrealistic (Lee and Seung, 2001). Therefore, the algorithm is usually ran 10 to 100 times with initial random starting points for $\mathbf{W}$ and $\mathbf{C}$ (Turpin et al., 2021). Then, after every start, the update rules are iteratively applied so that $\min \|\mathbf{V} - \mathbf{WC}\|$ converges to a local minimum or the algorithm is terminated by reaching the user-defined maximum number of iterations (Ting and Chvatal, 2010). There are several update rules (Scano et al., 2022), but often the "multiplicative update rule" according to Lee and Seung (2001) is used:

$$\mathbf{C_{i+1}} = \mathbf{C_i} \frac{\mathbf{W_i^T V}}{\mathbf{W_i^T W_i C_i}}$$
$$\mathbf{W_{i+1}} = \mathbf{W_i} \frac{\mathbf{V C_{i+1}^T}}{\mathbf{W_i C_{i+1} C_{i+1}^T}}$$

In every iteration i, the distance $\|\mathbf{V} - \mathbf{WC}\|$ is reduced and the R^2 is increased. Finally, the result from the last iteration of the best run in terms of the least distance $\|\mathbf{V} - \mathbf{WC}\|$ is chosen (Turpin et al., 2021).

Figure 1.3: Schematic of the modular control architecture and overview of the extraction of muscle synergies (next page). Top: Spatial muscle synergies are extracted from EMG data of medial, forward, and lateral reaching movements. Activation functions or descending commands modulate subcortical muscle synergies. A muscle synergy is a group of co-activated muscles with characteristic relative activation levels (muscle weightings). Each modulated muscle synergy activates multiple muscles to realize a mechanical output (biomechanical characterization). The whole muscle activation is realized through the sum of the modulated muscle synergies. This can be seen, for example, in the biceps muscle (Bic, enlarged plot). Bottom: The reconstruction $\mathbf{WC}$ of the original EMG data improves with the number of muscle synergies. This can be seen (1) by the R^2 plot on the left and (2) the reconstruction of the forward reaching EMG data on the right. The higher the number of muscle synergies, the better EMG data (gray area) and reconstruction (red solid line) align. If not enough muscle synergies are extracted, the reconstruction does not capture the EMG data satisfactorily, as can be seen by the mismatches between the original and reconstructed EMG data. However, the extraction with seven muscle synergies, which equals the number of measured muscles, does not result in a low-dimensional representation, as most "muscle synergies" consist primarily of one active muscle. Abbreviations: DelA Musculus deltoideus anterior part, DelM Musculus deltoideus middle part, DelP Musculus deltoideus posterior part, Trap Musculus trapezius, Pect Musculus pectoralis, Tric Musculus triceps, Bic Musculus biceps. The depicted human model was created using OpenSim and the DAS3 model (Delp et al., 2007, Chadwick et al., 2014).

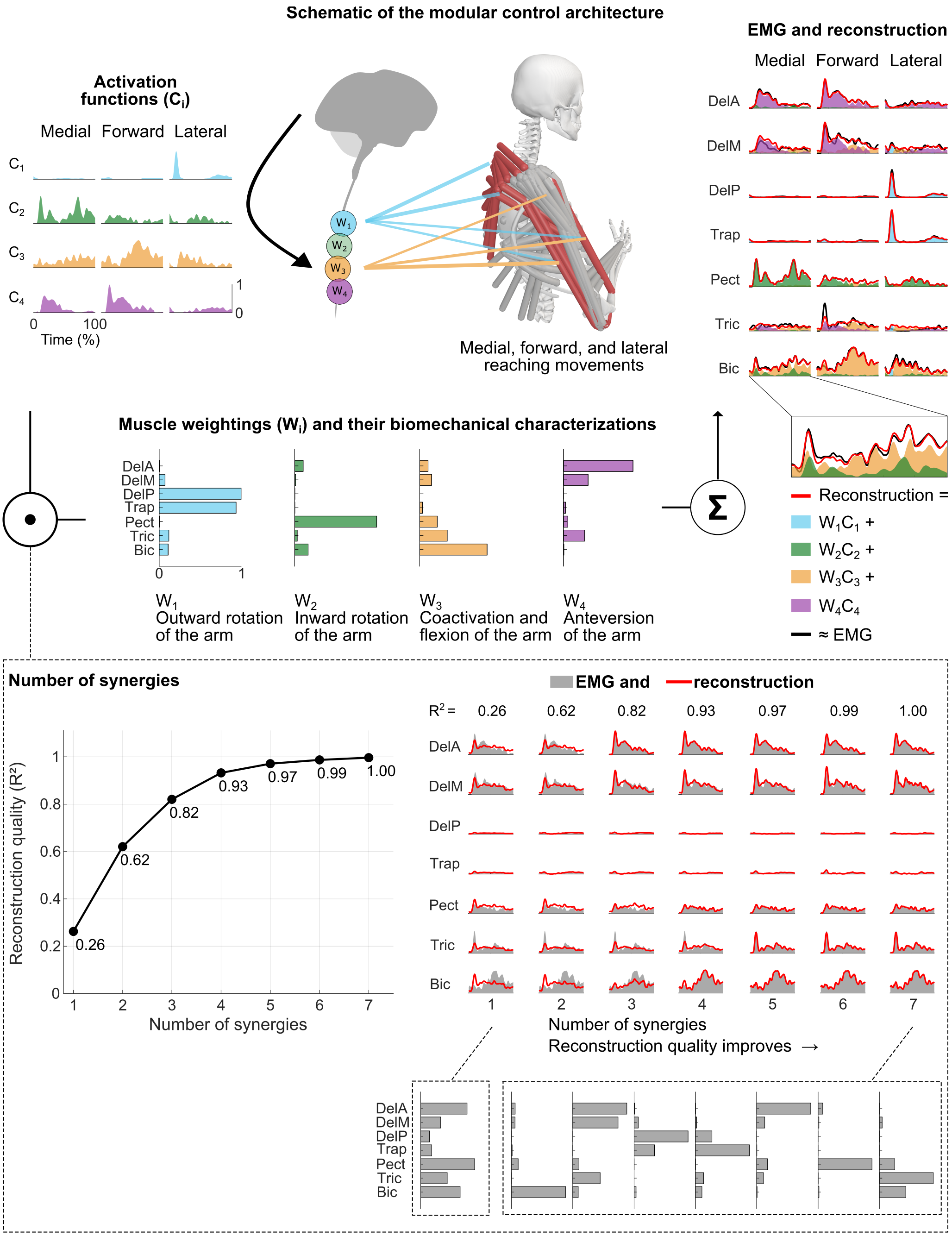
Schematic of the modular control architecture
Activation functions (C_i)
Medial Forward Lateral
C_1
C_2
C_3
C_4
0
100
Time (%)
1
0
W_1
W_2
W_3
W_4
Medial, forward, and lateral reaching movements
EMG and reconstruction
Medial Forward Lateral
DelA
DelM
DelP
Trap
Pect
Tric
Bic
Reconstruction =
W_1C_1 +
W_2C_2 +
W_3C_3 +
W_4C_4
≈ EMG
Muscle weightings (W_i) and their biomechanical characterizations
DelA
DelM
DelP
Trap
Pect
Tric
Bic
0
1
W_1 Outward rotation of the arm
W_2 Inward rotation of the arm
W_3 Coactivation and flexion of the arm
W_4 Anteversion of the arm
Σ
Number of synergies
Reconstruction quality (R^2)
0
0.2
0.4
0.6
0.8
1
1
2
3
4
5
6
7
0.26
0.62
0.82
0.93
0.97
0.99
1.00
Number of synergies
EMG and reconstruction
R^2 =
0.26
0.62
0.82
0.93
0.97
0.99
1.00
DelA
DelM
DelP
Trap
Pect
Tric
Bic
1
2
3
4
5
6
7
Number of synergies
Reconstruction quality improves →
DelA
DelM
DelP
Trap
Pect
Tric
Bic

1.4.3 The force field adaptation paradigm to study the challenge of time-varying properties

A remarkable feature of the human is their ability to adapt movements to new physical and environmental conditions. Tennis players change their rackets time and again for various reasons. The new racket has different physical characteristics; for example, it might weigh more, or the strings are tensioned differently. An experienced tennis player can change the racket and effortlessly adapt to the new racket's different physical properties. After a few shots with the new racket, the player performs as well as with his old racket. This phenomenon is called motor adaptation (Krakauer et al. 2019; see section 1.3.2).

Motor adaptation has been extensively studied under laboratory conditions, such as using prism glasses while throwing balls (Martin et al., 1996) or displacing targets while executing saccadic eye movements (McLaughlin, 1967). A large body of research has also come from studying reaching movements, such as the visuomotor rotation paradigm, by which the cursor on a virtual reality display systematically moves in a rotated direction depending on where the participant's hand moves (Krakauer et al., 1999, 2000). Furthermore, motor adaptation has been studied in gait (Dietz et al., 1994) and with exoskeletons (Poggensee and Collins, 2021).

In force field adaptation, participants grasp the handle of a robotic manipulandum and perform target-directed point-to-point movements in the horizontal plane. The robot produces perturbing forces that act on the participant's hand via the handle (Shadmehr and Mussa-Ivaldi 1994; Figure 1.4). Typically, the forces are viscous, i.e., dependent on the current handle's velocity, and directed orthogonally to the handle's current movement direction (Figure 1.4B). This means the robot creates a specific kind of perturbation. It simulates a physical object with novel dynamic properties. These novel dynamic properties change in real time and are unusual. This means, it is highly unlikely that participants have experienced such a perturbation before. That these properties are unusual is especially suited for studying motor adaptation, because they allow to gain an understanding of how dynamics are represented and changed in a trial-by-trial manner (Wolpert and Flanagan, 2010b), without the potentially mediating effect of prior experiences.

Typically, participants produce roughly straight trajectories before the perturbation forces are applied (Figure 1.4C). With the onset of the perturbation forces, the participants produce curved trajectories (Figure 1.4D). The perturbing forces have led to an unforeseen change of the object's physical properties, which now requires an adjustment of the motor commands (motor adaptation). The deviations predominantly stem from a prediction error, a mismatch between the predicted and the experienced movement (Krakauer and Mazzoni, 2011, Shadmehr, 2017). This prediction error seems to foster trial-by-trial adjustments of an internal model, leading to motor commands that enable the participants to iteratively counter-act the perturbing forces better and re-gain baseline performance (Shadmehr, 2017, Shadmehr et al., 2010). With increasing repetitions, the participants compensate for the perturbing forces and produce baseline-similar movement trajectories again (Figure 1.4E). Motor adaptation occurs on a short timescale compared to skill learning. The participants usually adapt within 300-600 trials when different reaching directions are practiced (Gandolfo et al., 1996, Shadmehr and Brashers-Krug, 1997).

When the force field is suddenly disabled after the participants have adapted, the participants produce errors again. They produce trajectories mirror-inverted to the ones from the force field's onset. These errors are called "after-effects" (Figure 1.4F). Their presence suggests the acquisition of model knowledge (Shadmehr and Mussa-Ivaldi, 1994). In particular, after-effects show that participants do not only co-contract antagonist muscle groups to counteract the forces, as in this case, trajectories would be baseline-like and without visible after-effects. The internal model has interesting properties (Shadmehr, 2017), some of which are examined in this dissertation and elaborated in the following.

1.4.3.1 Savings and generalization in motor adaptation

When the participants continue reaching after the force field was turned off, called "washout", one observes that the after-effects vanish fast, within far less trials than the initial adaptation. When re-exposed to the force field, participants adapt faster than the first time. This phenomenon is called "savings" (Brashers-Krug et al., 1996, Mathew et al., 2021, Shadmehr and Brashers-Krug, 1997). The acquired knowledge during adaptation frees the participant from having to learn the new physical properties the next time they use the object (Shadmehr, 2017). Accordingly, the motor memory, the acquired internal model, does not seem to be erased entirely. Savings hint that despite the transient and reversible nature of motor adaptation, a long-term memory is associated during the initial adaptation (Huberdeau et al., 2015a).

Furthermore, the acquired knowledge not only serves the movement that was explicitly practiced but also similar movements in other contexts. A successful transfer from practice to a new situation is commonly called generalization (Krakauer et al., 2019, 2006). Yet, generalization and transfer will be used interchangeably in chapters 2 and 3 (study A1 and study A2) and denote successful transfer. Generalization suggests that the CNS uses a shared neural representation of the internal model (Shadmehr, 2004). Studying generalization can thus provide insights into the neural representations underlying motor adaptation (Krakauer et al., 2019). Generalization has been found across arms (Criscimagna-Hemminger et al., 2003, Stockinger et al., 2015) or to unpracticed reaching directions (Gandolfo et al., 1996, Ghez et al., 1999, Rezazadeh and Berniker, 2019). However, generalization is not unlimited. For example, spatial generalization seems to be local or narrow, i.e., the amount of spatial generalization decreases with distance from the practiced direction, following a Gaussian-like function with almost no spatial generalization to targets in a direction 90° rotated from the practiced one (Donchin et al. 2003, Howard and Franklin 2015, Rezazadeh and Berniker 2019; Figure 1.5A-B).

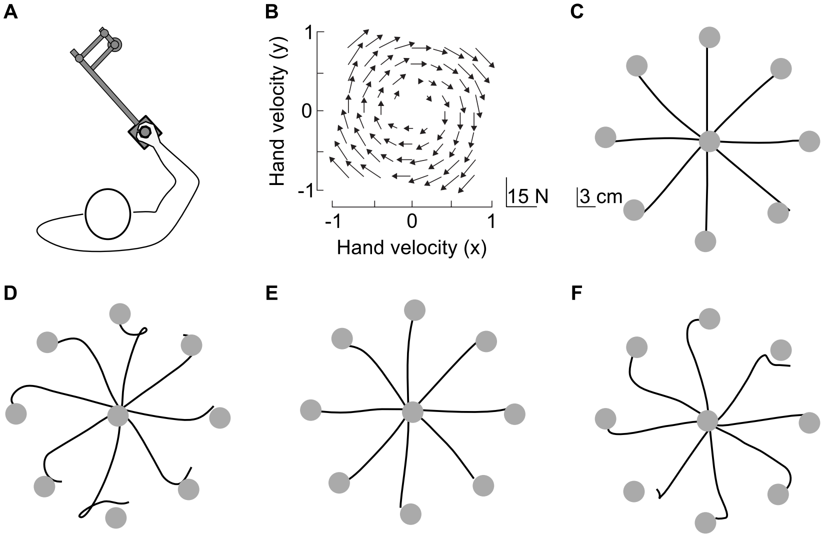

Figure 1.4: Force field adaptation paradigm. A: A participant holds the handle of a robotic manipulandum. B: A velocity-dependent force field based on the hand velocity. The force acts orthogonally to the current direction of motion and increases with velocity. C: When the handle is freely movable (null field (NF) condition), the participant reaches from the middle to the eight targets with an almost straight trajectory. D: Once the force field is turned on (force field (FF) condition), the first trajectories are perturbed and show large deviations. E: After several hundred repetitions, the participant has adapted and performs baseline-like trajectories again. F: When the force field is turned off, the trajectories resemble those of the initial force field perturbation but are mirror-inverted. This observation is called “after-effect” (Wolpert and Bastian 2021 and Shadmehr and Brashers-Krug 1997, adapted from Shadmehr and Brashers-Krug 1997; Copyright (1997) Society for Neuroscience).

1.4.3.2 Multiple processes in motor adaptation and retention

The adaptation progress resembles an exponential function (Figure 1.5C). An initial fast increase is followed by a slower, more gradual increase. Linear, time-invariant multi-rate state-space models can model this progress well, offering a mathematical approach to the trial-by-trial error reduction in motor adaptation (Donchin et al., 2003, Smith et al., 2006, Thoroughman and Shadmehr, 2000). In principle, the state-space model (SSM) takes the error in terms of lack of adaptation as input, the update of the internal model as a hidden variable, and outputs the adjusted, subsequent movement performance (Krakauer and Mazzoni, 2011). Mathematically, in a simple form as described by Smith et al. (2006), the SSM is given by the formula:

$$
\begin{aligned}
x(k+1) &= x_s(k+1) + x_f(k+1) \\
x_s(k+1) &= a_s x_s(k) - b_s e(k) \\
x_f(k+1) &= a_f x_f(k) - b_f e(k) \\
e(k) &= f(k) - x(k) \\
\text{with } a_s, a_f, b_s, b_f &\in [0,1], \text{and } a_s < a_f, b_s < b_f
\end{aligned}
$$

with e denoting the error in trial k, calculated as the difference between the motor output x and the perturbation f. a_s and a_f are the retention factors for the slow and fast process, respectively. The retention factor quantifies the tendency of the motor output to decay to baseline levels with each movement, with 1 indicating no decay or perfect retention and 0 total decay. b_s and b_f quantify the error sensitivity or learning rate, i.e., the proportion of the error being compensated for in the subsequent trial (Kim et al., 2021). The sum of x_s and x_f, the internal slow and fast states, results in the motor output x (Krakauer et al., 2019, Smith et al., 2006). Accordingly, the adaptation progress can be decomposed into fast and slow processes. The fast process learns quickly from error but has weak retention, whereas the slow process learns more slowly but has better retention. Regarding the overall adaptation progression, the fast initial increase is attributed to the fast process and the subsequent phase to the slow process (Smith et al., 2006).

In the context of sports, the two processes allow adequate motor adaptation to changes that persist on different time scales. For example, short-lasting perturbations, such as a change in wind conditions in beach volleyball or fatigue, can be covered by the fast process. In contrast, more lasting changes, such as a change of tennis racket or bodily changes, can be covered by the slow process (Wolpert and Flanagan, 2010a).

Although the model suggests it, it is unlikely that the processes underlying motor adaptation differ only in their speed of forgetting and learning. Instead, the different learning components correspond to different learning processes employed simultaneously on the same problem (Krakauer et al., 2019). For example, literature suggests that the fast process reflects an explicit learning and is sensitive to reward, while the slow process reflects implicit learning and is error-driven (Huberdeau et al., 2015b).

SSMs have characterized and predicted a host of motor adaptation phenomena, such as savings, spontaneous recovery, and anterograde interference (Krakauer et al., 2019, Shadmehr et al., 2010, Smith et al., 2006). SSMs are being further developed to account, for example, for inter-trial breaks (Albert and Shadmehr, 2018), multiple targets (Schweighofer et al., 2011, Tanaka et al., 2012), or variable error sensitivities (McDougle et al., 2015). Accordingly, SSMs offer a window into the study of processes underlying motor adaptation.

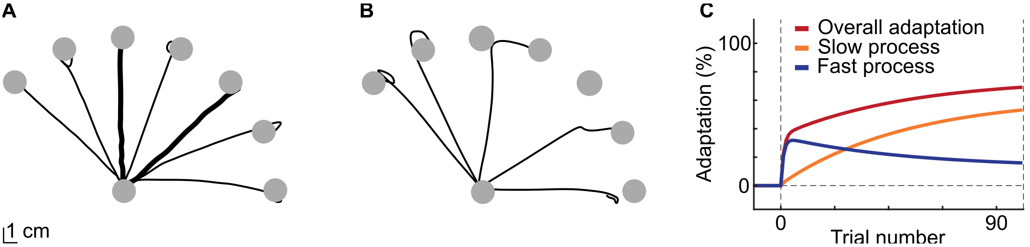

Figure 1.5: Spatial generalization and multiple components in motor adaptation. A and B: Spatial generalization. In A, trajectories are shown for a participant who reaches from the start to seven targets 10 cm away and arranged in a circular shape around the start. The reaches are not perturbed and thus almost straight. Then, an adaptation period follows during which the participant adapts to the two targets illustrated with thick solid lines only (trajectories not shown here). In B, trajectories are shown in the null field after adaptation. The participant only reaches to the targets not used during adaptation. Remarkably, after-effects are stronger the closer their targets are to the two to which the participant adapted (adapted from Gandolfo et al. 1996; Copyright (1996) National Academy of Sciences, U.S.A.). C: Schematic of the multiple components in motor adaptation. The overall adaptation (red) consists of the sum of a slow (orange) and a fast (blue) process. The fast process increases faster than the slow process but decays faster than the slow process. After the perturbation's onset, the overall adaptation's main part consists of the fast process value, but this changes over trials. Ultimately most of the overall adaptation consists of the slow process' value (adapted from Krakauer et al. 2019; used with permission of John Wiley and Sons, Copyright (2019) American Physiological Society, from Krakauer et al. (2019); permission conveyed through Copyright Clearance Center, Inc.).

1.4.4 Human-robot interaction as a tool to understand human motor control and learning

Robotic devices have tremendously helped to understand human motor control and learning (Wolpert and Flanagan, 2010b, Floreano et al., 2014). One example is the robotic manipulandum used in the force field adaptation paradigm, which perturbs reaching movements to allow the study of motor adaptation (see section 1.4.3). This manipulandum consists of several links converging to a handle which can be moved by a participant in the horizontal plane (see Figure 1.4A). Sensors track the robot configuration at a high frequency, allowing, for example, the precise measurement of the handle's velocity. A computer controls the robot configuration, allowing the robotic manipulandum to exert forces on the handle. This sets up a controlled environment to study motor adaptation. In particular, this set-up allows the creation of objects with novel dynamic properties, which can also be changed in real time. A wide range of novel dynamic properties can be generated, especially unusual ones, like the viscous force field in force field adaptation (Wolpert and Flanagan, 2010b). This enables us to study motor adaptation in novel, unusual situations, which is important in motor adaptation experiments. For example, studies on force field adaptation have led to an understanding of representations of dynamics, trial-by-trial learning, and much more. In this case, human-robot interaction is used to study human motor control and learning. This is done in topic A in this dissertation.

However, robotic devices can not only be used to perturb movements. Robotic devices can assist humans in their movements and extend their physical capabilities (Burdet et al., 2013). This is of particular interest when movement can no longer be carried out the same way, for example, as a result of aging, injuries, or pathologies (Seidler et al., 2010). By studying the neural mechanisms underlying human-robot interaction, robots can be designed to work safely alongside humans (Sheridan, 2016). This is particularly important in settings where close collaboration is required, e.g., with surgical robotics or assistive devices. The emerging field of human-robot interaction has provided promising results as the first paraplegic patients can walk with exoskeletons, and advanced prosthetic arms can be controlled through targeted muscle reinnervation (Cheesborough et al., 2015, Coser et al., 2024). However, many robotic devices are limitedly effective because of technical limitations but also due to insufficient knowledge about humans (Beckerle et al., 2017, Dollar and Herr, 2008, Windrich et al., 2016, Yan et al., 2015). Furthermore, human-robot interaction is highly complex, as two nonlinear-dynamic systems are coupled, which can generally lead to unpredictability (Schaal, 2007). Accordingly, to be used effectively, robotic device developers require a good understanding of how humans control their limbs and interact with the robotic devices (Burdet et al., 2013). To facilitate the study of human-robot interactions, one approach is to keep the robot invariant and focus on the human side of the interaction. This is done in both topics A and B in this dissertation.

In sum, this dissertation uses human-robot interaction as a tool to understand human motor control and learning in two ways: in topic A as a tool to study coordination and adaptation of reaching movements and in topic B to study the effects of support by a robot rollator simulator on the coordination of sit-to-stand and stand-to-sit movements.

1.5 Aims and scope of this dissertation

This dissertation aims to increase our current knowledge of human motor control and learning using human-robot interaction. It will primarily address the challenges of redundancy, versatility, and time-varying properties using experimental studies. Thereby, topic A addresses the coordination and adaptation of reaching movements using a robotic manipulandum and virtual reality technologies, and topic B effects of rollator support on the coordination of sit-to-stand and stand-to-sit movements using a robot rollator simulator.

1.5.1 Topic A: Coordination and adaptation of reaching movements using a robotic manipulandum and virtual reality technologies

A major goal in motor learning is to optimize practice to maximize the amount of learning, retention, and generalization (Schmidt and Lee, 2011). Therefore, it is interesting to know (1) what influence different practice protocols have on adaptation, retention, and spatial generalization, as well as (2) how processes underlying practice are represented at the muscular level. However, multiple facets influence the practice of sports movements, not only the design and amount of practice but also motivation or how instructions are delivered (Schmidt and Lee, 2011). Thus, to examine single facets in a targeted and isolated manner, controlled experimental setups are necessary. In other words, to understand underlying mechanisms, specific hypotheses along with targeted experiments are needed (Cisek and Green, 2024). This way, foundational insights into components of learning can be gained and help us approach perspectively an understanding of complex skills (Krakauer et al., 2019). Therefore, I used two force field adaptation studies, which will be briefly introduced below.

Study A1 in chapter 2: The contextual-interference effect (CIE) describes a frequently examined skill learning phenomenon related to the organization of practice variability (Battig, 1972, Shea and Morgan, 1979). Accordingly, when participants practice a movement in different contexts in an interleaved (high contextual interference) rather than a blocked order (low contextual interference), they show better retention and generalization despite potentially worse performance during practice (Wright and Kim, 2019, Magill and Hall, 1990). The CIE is therefore particularly relevant for learning and improving sports skills, as practice protocols should be organized in such a way that the participant builds up the ability to successfully perform the practiced movement sustainably and in similar situations (Schmidt and Lee, 2011). However, the CIE has hardly found attention in force field adaptation. Study A1 addresses how practice variability is best organized to facilitate these aspects in force field adaptation, particularly retention and spatial generalization. Furthermore, despite the vast number of studies, mainly in skill learning, (Czyż et al., 2024a,b, Ammar et al., 2023, Wright and Kim, 2019, Magill and Hall, 1990), not one but three major hypotheses exist that try to explain the CIE (Wright and Kim, 2019). Hence, it is unclear, if the CIE is found in force field adaptation, retention, and spatial generalization, and if it is found, which hypothesis may explain the findings. One of the hypotheses is the forgetting-and-reconstruction hypothesis (Lee and Magill, 1983, Lee et al., 1985). It assumes that “action planning” is necessary to perform a movement and that the action plan is forgotten over time. When the same movement is practiced repetitively until other movements are practiced (blocked practice), the action plan can be retrieved from short-term memory. In contrast, when the movements are practiced in a random order, their action plan gets forgotten every time the other movements are practiced. Hence, the action plans must be reconstructed every time. This repeated reconstruction slows down acquisition, but fosters retention and generalization. Force field adaptation offers a way to study the CIE with respect to the forgetting-and-reconstruction hypothesis (Lee and Magill, 1983, Lee et al., 1985, Schweighofer et al., 2011). In particular, it allows us to relate the forgetting and reconstructing to a well-established computational model in motor adaptation, the state-space model (Schweighofer et al., 2011, Smith et al., 2006). Accordingly, the first study assessed how the organization of practice variability affect retention and spatial generalization in force field adaptation with task-related variables using end-point kinematics and kinetics. The adaptation process was modeled mathematically with a state-space model, which was extended to relate the findings to the forgetting-and-reconstruction hypothesis.

Study A2 in chapter 3: Study A2 investigates how the acquired knowledge in force field adaptation, retention, and spatial generalization may be represented. It is, in particular, unclear how the CNS coordinates force field adaptation at the level of muscle activations. Despite the fact that the concept of muscle synergies is well-accepted, it has not yet been related to force field adaptation, retention, and spatial generalization. While it has been shown that in isometric visuomotor rotation, a related motor adaptation paradigm, unperturbed reaching muscle synergies account for adaptation (De Marchis et al., 2018, Gentner et al., 2013, Severini and Zych, 2020), studies in force field adaptation with single muscles' activation may suggest otherwise. For example, muscles that act in the force field's opposite direction are activated early in the reaching movement, and co-contraction is also observed (Thoroughman and Shadmehr, 2000, Milner and Franklin, 2005, Huang et al., 2012). Thus, we first tested whether combinations of unperturbed reaching muscle synergies can account for force field adaptation. Then we continued to test if specific muscle synergies are required. Finally, assuming muscle synergies can represent force field adaptation, we expect them to also represent retention and the narrow spatial generalization (Rezazadeh and Berniker, 2019, Gandolfo et al., 1996, Ghez et al., 1999).

Even though reaching with a robotic manipulandum restricts the end-effector movement to a 2D space, the reaching movement itself involves at least the seven mechanical degrees of freedom (excluding the hand) of wrist, elbow, and shoulder joints, and all the muscles acting on these joints (Rosenbaum, 2009). For example, 24 muscles cross the elbow joint (Hamill and Knutzen, 2009), leading to theoretically 2^{24} combinations of them being active or inactive. This means that although the movement in topic A is more constrained than the whole-body movement of topic B, the redundancy and versatility challenges can be addressed. In other words, the reaching movement is constrained just to the degree where confounding factors irrelevant to the research question and potentially causing artifacts and hindering an interpretation are excluded (Cisek and Green, 2024). Nevertheless, it needs to be acknowledged that reaching in the horizontal plane is still a constrained movement when compared to whole-body movements.

1.5.2 Topic B: Effects of rollator support on the coordination of sit-to-stand and stand-to-sit movements using a robot rollator simulator

Human motor control, learning, and human-robot interactions are of particular importance in rehabilitation. Assistive devices aim to support humans in need to perform activities of daily living (Mohebbi, 2020). For example, rollators, also called four-wheeled walkers, are often prescribed to improve postural stability (Mundt et al., 2019). However, rollators have also been associated with a higher fall risk (Bateni and Maki, 2005). Therefore, in topic B, two studies investigated how rollator support affects coordination in sit-to-stand and stand-to-sit movements, two typical activities of daily living.

As already elaborated, the CNS has to cope with multiple degrees of freedom, i.e., redundancy. This redundancy provides many options to perform a certain movement. Furthermore, there are individual differences across humans, like different segment lengths and muscle fiber distributions (James and Bates, 1997). It comes as no surprise that humans perform movements with different movement strategies. “A movement strategy is a selected neuromuscular solution for the performance of a motor task” (James and Bates, 1997, p. 58). The existence of multiple movement strategies has also been termed “strategic variability” (Cowin et al., 2022) or “behavioral flexibility” (Ranganathan et al., 2020) and is one of the multiple forms of variability (Cowin et al., 2022). The movement strategy selection can be voluntary or involuntary. Furthermore, the movement strategy selection may differ between or even within the participant. This variability or flexibility is advantageous on the one hand as it allows humans to adapt to varying environmental or body conditions (aging, fatigue) and execute various tasks. However, it makes an analysis difficult on the other hand (Choudry et al., 2013). Different movement strategies lead to a substantial amount of variability (James and Bates, 1997). If analyses do not account for movement strategies, important information and effects may be masked, leading to missing, misleading, or incorrect interpretations (James and Bates, 1997).

Accordingly, two subsequent studies for topic B were set up. First, movement strategies were identified based on the kinematic-kinetic level with regard to joint kinematics, center of mass (CoM) movement, and ground reaction forces (GRFs), as well as seat interaction forces (study B1 in chapter 4). Then it was investigated if and how rollator support affects them. The subsequent study B2 in chapter 5 applied muscle synergy analysis to understand how the strategies are represented by muscle synergies and what effects rollator support has on them. Topic B can be seen as a step toward studying human motor control in more natural conditions, i.e., conditions with relaxed restrictions (Cisek and Green, 2024). In other words, it can be seen as a step toward studying movement with its richness, or “behavioral flexibility” and still complying with the crucial trade-off between seeking naturalistic behavior and guaranteeing experimental control (Maselli et al., 2023) as the same instructions were given to and the general setup was the same for all participants. With this two-step approach, the two complex whole-body movements, sit-to-stand and stand-to-sit, in interaction with a robot rollator simulator, could be assessed on the kinematic, kinetic, and muscular levels.

1.5.3 Overview

Taken together, the aims of this dissertation were to

1. analyze the influence of the organization of practice variability on force field adaptation, retention, and spatial generalization. Based on the CIE, the hypothesis was that a random practice protocol is superior to a blocked protocol in retention and spatial generalization, while practice performance is inferior. Further, it was hypothesized that a state-space model could reflect these findings based on the forgetting-and-reconstruction CIE hypothesis. The challenge of time-varying properties was addressed. A simple reaching movement and a robotic manipulandum were used. The focus was on the computational level using end-point kinematic and kinetic variables.

2. analyze the underlying coordination of force field adaptation, retention, and spatial generalization at the muscular level. Based on the modular control architecture, the hypothesis was that muscle synergies can represent the underlying coordination of force field adaptation, retention, and spatial generalization at the muscular level. The challenges of time-varying properties, redundancy, and versatility were addressed. A simple reaching movement and a robotic manipulandum were used. The focus was on the representational level using muscle synergies extracted from EMG data.

3. analyze the influence of rollator support on movement strategies for transitions between sitting and standing. The hypothesis was that rollator support influences the movement strategies and their choice when standing up and sitting down. The challenges of redundancy and versatility were addressed. Complex movements and a robot rollator simulator were used. The focus was on the representational level using joint kinematics, CoM movement, and ground reaction forces as well as seat interaction forces.

4. analyze the underlying coordination for transitions between sitting and standing at the muscular level with respect to movement strategies. The hypotheses were that muscle synergy activation differs across movement strategies and that rollator support influences the weightings between upper body and lower limb muscles for standing up and sitting down. The challenges of redundancy and versatility were addressed. Complex movements and a robot rollator simulator were used. The focus was on the representational level using muscle synergies extracted from EMG data.

2 Topic A, Study A1: Random practice enhances retention and spatial transfer in force field adaptation

This is a post-peer-review, pre-copyedit, and slightly adapted[1] version of the published article

Herzog, M., Focke, A., Maurus, P., Thürer, B. and Stein, T. (2022). Random Practice Enhances Retention and Spatial Transfer in Force Field Adaptation. *Frontiers in Human Neuroscience* 16: 816197, doi:10.3389/fnhum.2022.816197.

---

[1] The citation and cross-reference style, as well as the figures' fonts, have been adjusted for consistency in this dissertation.

2.1 Abstract

The contextual-interference effect is a frequently examined phenomenon in motor skill learning but has not been extensively investigated in motor adaptation. Here, we first tested experimentally if the contextual-interference effect is detectable in force field adaptation regarding retention and spatial transfer, and then fitted state-space models to the data to relate the findings to the "forgetting-and-reconstruction hypothesis". Thirty-two participants were divided into two groups with either a random or a blocked practice schedule. They practiced reaching to four targets and were tested 10 min and 24 h afterward for motor retention and spatial transfer on an interpolation and an extrapolation target, and on targets which were shifted 10 cm away. The adaptation progress was participant-specifically fitted with 4-slow-1-fast state-space models accounting for generalization and set breaks. The blocked group adapted faster ($p = 0.007$) but did not reach a better adaptation at practice end. We found better retention (10 min), interpolation transfer (10 min), and transfer to shifted targets (10 min and 24 h) for the random group (each $p < 0.05$). However, no differences were found for retention or for the interpolation target after 24 h. Neither group showed transfer to the extrapolation target. The extended state-space model could replicate the behavioral results with some exceptions. The study shows that the contextual-interference effect is partially detectable in practice, short-term retention, and spatial transfer in force field adaptation; and that state-space models provide explanatory descriptions for the contextual-interference effect in force field adaptation.

2.2 Introduction

Motor skills enable people to interact with the environment in many different ways. Motor skills are not innate but learned throughout life, which indicates the importance of understanding motor learning processes. In the literature, two types of motor learning are usually distinguished: (1) skill learning, which "is a set of processes associated with practice or experience leading to relatively permanent changes in the capability for skilled movement" (Schmidt et al., 2019); and (2) motor adaptation, where the motor system responds to changes in the body and/or the environment to return to a previous level of performance under these new environmental conditions (Krakauer and Mazzoni, 2011). For both types of learning, practice is the most important factor and a central question of research in motor learning is to understand how different practice protocols (e.g., amount of practice, distribution of practice or variability of practice) affect motor learning processes on different time scales.

In this regard, the contextual-interference effect (CIE) is a well-studied phenomenon in motor skill learning. The CIE states that interleaved (high contextual interference) as opposed to repetitive (low contextual interference) practice results in lower performance gains during practice but superior retention and transfer (Shea and Morgan, 1979). Originally formulated by Battig (1972) for verbal learning, a large body of research has supported the CIE in motor skill learning, especially for simple laboratory tasks but also in more complex sport tasks (for an overview; see Schmidt et al. 2019). However, compared to skill learning, the CIE has not been widely studied in the context of motor adaptation (Thürer et al., 2019). Accordingly, this study focuses on the analysis of the CIE in a motor adaptation task.

There are different experimental paradigms to analyze motor adaptation (Krakauer et al., 2019). In this study, we use the force field paradigm (Shadmehr, 2017, Shadmehr and Mussa-Ivaldi, 1994) to study the CIE in motor adaptation. Here, participants perform reaching movements and experience forces on their hand, leading them to laterally deviate from straight trajectories. The deviations predominantly result from a sensory prediction error, i.e., a mismatch between the predicted and the experienced movement (Krakauer and Mazzoni, 2011). This error is assumed to drive trial-by-trial adjustments of an internal model (Albert and Shadmehr, 2016, Donchin et al., 2003, Kawato, 1999, Shadmehr et al., 2010). Thereby, the motor commands are updated. This enables the participants to counteract successively better the perturbances and to ultimately perform a straight trajectory. This means that the participants returned to a previous level of performance (Shadmehr et al., 2010). The acquired internal model can be interpreted as a motor memory that is partially transferrable to new situations (Shadmehr, 2017). For example, there is evidence for transfer to different movement speeds and amplitudes (Goodbody and Wolpert, 1998, Joiner et al., 2010, Mattar and Ostry, 2010). Also, contralateral transfers could be shown (Criscimagna-Hemminger et al., 2003, Joiner et al., 2013, Stockinger et al., 2015). A host of literature found spatial transfer capabilities in force field adaptation, such as to different reaching directions or to arm configurations that are shifted by several centimeters (Gandolfo et al., 1996, Ghez et al., 1999, Rezazadeh and Berniker, 2019, Shadmehr and Moussavi, 2000, Shadmehr and Mussa-Ivaldi, 1994).

The adaptation progress itself resembles an exponential function with a fast initial increase followed by a slower, more gradual increase (Krakauer et al., 2019). This progress can be modeled well with linear, time-invariant (multi-) state-space models (SSMs) (Smith et al., 2006). Thereby, the error serves as input, the update of the internal model as a hidden variable, and the adjusted, subsequent movement as output (Krakauer and Mazzoni, 2011). In particular, the fast initial increase is attributed to a fast process with a high learning rate and rapid decay, and the subsequent phase to a process with a slower learning rate but greater retention (Smith et al., 2006). SSMs have successfully characterized and predicted numerous phenomena in force field adaptation (Kim et al., 2021). Thus, they offer the possibility of investigating potential processes underlying practice related to behavioral changes (Smith et al., 2006).

As described above, adaptation progress, retention, and spatial transfer characteristics in force field adaptation have been thoroughly examined. However, no study so far has explicitly investigated CIE, i.e., the different effects of interleaved and repetitive practice schedules on retention and spatial transfer in force field adaptation. Further, despite the large host of studies in motor skill learning, there is no sole hypothesis to fully explain the CIE (Wright and Kim, 2019). The three prevailing hypotheses are “elaboration-and-distinctiveness” (Shea and Morgan, 1979), “retroactive inhibition” (Shea and Titzer, 1993), and “forgetting-and-reconstruction” (Lee and Magill, 1983, Lee et al., 1985). According to the first, interleaved practice requires performing comparative and distinctive analyses on a trial-by-trial basis, which increases the cognitive effort compared to repetitive practice. This increased effort slows down the acquisition, but fosters better retention performance by a more distinct or better representation of the task in the memory. The retroactive inhibition hypothesis explains the CIE such that learning a similar task in a repetitive manner inhibits recalling a memory of a preceding, different task. However, this hypothesis is probably not valid for the CIE in motor adaptation tasks (Thürer et al., 2019, 2018). The forgetting-and-reconstruction hypothesis proposes that the action plan for a task is forgotten over time and vanishes from short-term memory. If it is repeatedly needed during random practice, it must always be reconstructed. This, in turn, slows down acquisition, but fosters retention and transfer. Due to the interplay of learning and decay, SSMs in particular enable the study of the CIE in terms of the forgetting-and-reconstruction hypothesis (Schweighofer et al., 2011).

Accordingly, this study follows a combined approach to investigate the CIE in force field adaptation. The first objective is to experimentally investigate if there is a CIE regarding retention and spatial transfer in a force field adaptation task. The second objective is to fit an extended SSM to the experimental data to infer possible latent mechanisms. We hypothesize that: (1) participants with an interleaved practice schedule achieve a lower adaptation level at practice end than participants with a repetitive schedule and adapt slower; (2) participants of the interleaved group demonstrate better retention and (3) spatial transfer; and (4) the superior effect of the interleaved practice schedule can be explained by the two-rate characteristic of the learning process.

2.3 Materials and methods

2.3.1 Participants

Thirty-two right-handed (Oldfield, 1971), healthy female and male volunteers (age 24 ± 3 years) participated in the study. All participants were naïve to force field adaptation experiments, informed about the experimental protocol and gave their written informed consent. The study protocol was submitted to and approved by the Ethics Committee of the Karlsruhe Institute of Technology.

2.3.2 Apparatus and task

The participants sat at a KINARM End-Point Lab (BKIN Technologies, Kingston, Canada), and performed 10 cm point-to-point movements with their right hand in the transverse plane. The manipulandum was equipped with a virtual reality display showing the handle's position and the start and target points, but occluding vision of the handle itself, their arms, and hands (Figure 2.1A). Participants were instructed to reach from the start to the target within 500 $\pm$ 50 ms. When the target was reached, its color changed, providing the participants with feedback on whether the specified time was met. Shortly after the target was reached and the cursor had resided in it for 800 ms, the manipulandum moved the handle back to the start for the next trial.

To comprehensively investigate the effects of different practice schedules on spatial transfer, we considered three different spatial transfer tasks, for which literature has shown different amounts of transfer. Following the dial of a clock for orientation, the points were located as follows (Figure 2.1B-D): the first start point was at (0,0). The "practice targets" were positioned at 1.30, 12, 9, and 7.30 h (Figure 2.1B). Figure 2.1C shows the "interpolation" (10.30 h) and "extrapolation" (4.30 h) targets. The second starting point was shifted 10 cm to 1.30 h (Figure 2.1D). The remaining four targets had the same directions as the practice targets but were shifted like the second starting point (Figure 2.1D). We expected a good transfer for the interpolation target, as its direction is similar to the one practiced (Castro et al., 2011, Gandolfo et al., 1996, Rezazadeh and Berniker, 2019). In contrast, we expected no transfer for the extrapolation target as its direction deviates at least 90 degrees from the practice targets (Castro et al., 2011, Ghez et al., 1999). Based on studies by Ghez et al. (1999) and Shadmehr and Moussavi (2000), we expected fractional transfer for the shifted origin targets.

2.3.3 Experimental design

2.3.3.1 Trial conditions

Three different trial types were used: null field (NF), force field (FF), and error clamp (EC). During NF trials, the handle was freely movable without perturbing forces. FF trials were carried out in a viscous (velocity-dependent), counter-clockwise force field. Hereby, the force field was specified by the formula

$$\mathbf{F} = k \cdot [cos\theta, -sin\theta; sin\theta, cos\theta] \cdot [\dot{x}; \dot{y}];$$

where k denotes the force field magnitude and was fixed at 20 Ns/m. The angle θ was set to 90°. The velocity components of the handle are given by the vector $[\dot{x}; \dot{y}]$. Accordingly, the force field always deviated the handle's movement orthogonally to its movement direction. For EC trials, the manipulandum restricted the movement to a small channel connecting the start and end points (Joiner and Smith, 2008, Scheidt et al., 2000). Therefore, the manipulandum created virtual walls, with a wall viscosity of 10 kNs/m and a wall stiffness of 1 kN/m.

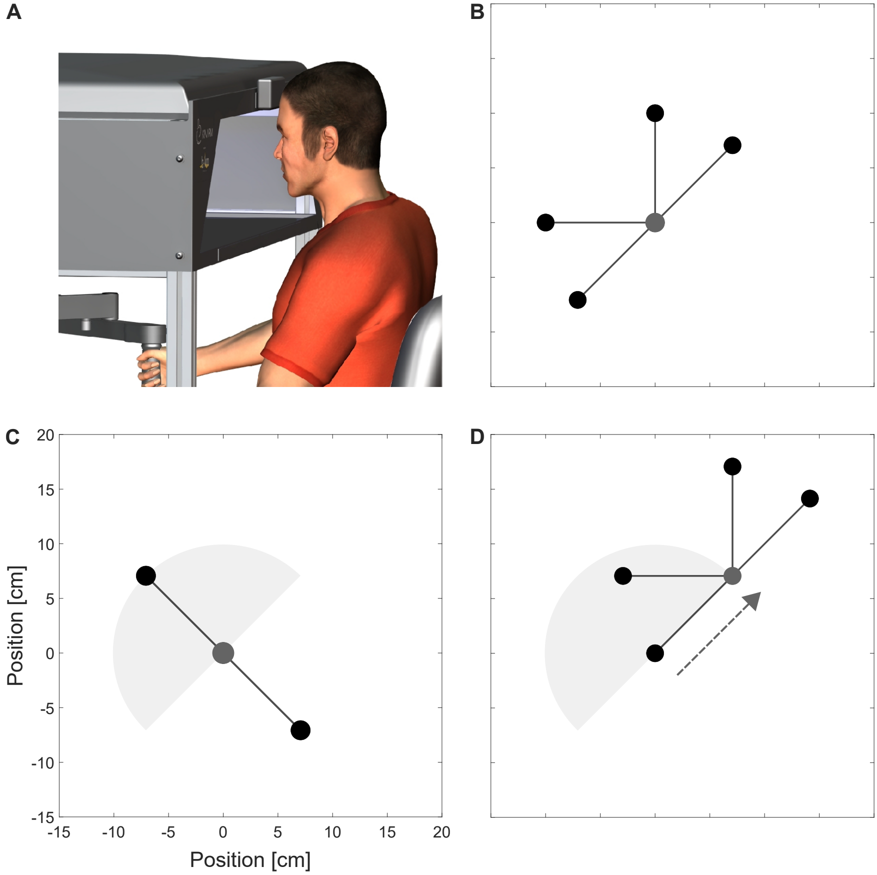

Figure 2.1: (A) Participant sits at a KINARM End-Point Lab (BKIN Technologies Ltd., dba Kinarm, Kingston, Canada). (B) Start point (0,0) in gray and target points (practice targets) in black. (C) Start (0,0) in gray, interpolation target (10.30 h), and extrapolation target (4.30 h) in black. (D) Targets with shifted origin. The dotted gray arrow illustrates the translational shift. In (C,D) the gray semicircle illustrates the area spanned by the practice targets, but this was not visible during the experiments.

2.3.3.2 Group assignment and schedule

Thirty-two participants were randomly assigned to two groups called “blocked” and “random” (each N = 16, with 8 females and 8 males). The experiment consisted of five different phases: familiarization, baseline, practice, short-term test, and long-term test. The first three phases were separated by 5 min breaks, and there was a 10 min break between practice and the short-term test. The long-term test followed 24 h later. During the practice phase, there were 30 s breaks after every 80 trials, during which participants could let go of the handle but remained seated. The various phases differed in the types of trials and targets used (Table 2.1).

To enable the participants to become accustomed to the manipulandum and the desired movement speed, the familiarization consisted of 120 NF trials. Targets appeared in block-randomized order (4 targets × 30 blocks). The baseline phase consisted of three reaches to each of the practice targets, and one reach to each of the interpolation, extrapolation, and shifted origin targets in the NF condition. Then, all targets were approached once in the EC condition.

Practice consisted of 800 trials. The practice targets of the random group appeared in a random order, although each target was reached once within a block of four trials (interleaved practice). In contrast, each participant in the blocked group practiced one of the four practice targets 200 times before proceeding to the next (repetitive practice). Eighty EC trials were randomly interspersed. Both groups were divided into four sub-groups (N = 4 each), each of which began with a different practice target.

The short-term test consisted only of EC trials. Thereby, we assessed short-term retention and short-term spatial transfer. First, two blocks of practice targets appeared (retention test), followed by transfer tests. Two blocks with the inter- and extrapolation target appeared, then two blocks with the shifted-origin targets. The targets' ordering varied within the test blocks for each participant, with one of each group (blocked and random) with the same ordering. To exclude a potentially occurring retroactive inhibition effect, the four subgroups were further divided into two sub-subgroups. The order of the targets in the retention test was equal to the order of the subgroup for the first sub-subgroup and in reverse order for the second sub-subgroup (e.g., blocked subgroup B1: 200 × 1.30 h, 200 × 12 h, 200 × 9 h, and 200 × 7.30 h; sub-subgroup 1: 1.30 h, 12 h, 9 h, 7.30 h; sub-subgroup 2: 7.30 h, 9 h, 12 h, 1.30 h). The exact ordering for all participants is shown in Supplemental Table A.1. The long-term tests followed a similar protocol as the short-term tests, but every second reach to a target was a FF trial, viz., not an EC trial. The exact ordering is shown in Supplemental Table A.1.

Table 2.1: Practice schedule. There was a 10 min break between practice and the short-term test, and 24 h between the short- and long-term tests. Between all other phases, there were 5 min breaks. Targets are abbreviated: practice targets (pr), interpolation (in), extrapolation (ex) and shifted origin (so). [*]Each target was reached 200 times before switching to the next. [†]The order was random, but all targets were reached within four trials. [‡]Each target group was reached in the EC condition first and then in FF. [§]Detailed ordering for every participant is listed in the Supplemental Table A.1.

	Familiarization	**Baseline**	**Practice**	**Short-term test**[§]	**Long-term test**[§]
Targets	pr	pr, in, ex, so	pr	pr, in, ex, so	pr, in, ex, so
Number and type of trials	120 NF	18 NF, 10 EC	720 FF, 80 EC	20 EC	10 EC, 10 FF
Trials per target	30	Practice targets: 3 NF, 1 EC Others: 1 NF, 1 EC	200	2	1 EC, 1 FF
Trial ordering *Blocked group*	Random[†]	3x pr, in, ex, so (NF), pr, in, ex, so (EC)	N = 4: 1.30, 12, 9, 7.30 h[*] N = 4: 12, 9, 7.30, 1.30 h[*] N = 4: 9, 7.30, 1.30, 12 h[*] N = 4: 7.30, 1.30, 12, 9 h[*]	N = 8: pr, in, ex, so N = 8: pr, ex, in, so	N = 8: pr, in, ex, so[‡] N = 8: pr, ex, in, so[‡]
Trial ordering *Random group*	Random[†]	3x pr, in, ex, so (NF), pr, in, ex, so (EC)	Random[†]	N = 8: pr, in, ex, so N = 8: pr, ex, in, so	N = 8: pr, in, ex, so[‡] N = 8: pr, ex, in, so[‡]

2.3.4 Data analysis

Kinematic data, including hand position and velocity, and forces measured at the manipulandum's handle were recorded at 1,000 Hz with KINARM Dexterit-E software (BKIN Technologies Ltd., Kingston, ON, Canada).

2.3.4.1 Pre-processing

Following our previous studies (Stockinger et al., 2015), raw kinematic and force data were filtered with a fourth-order Butterworth low-pass filter and a cut-off frequency of 6 Hz (kinematic) and 10 Hz (force). Movement start and end were defined as the time points where the hand velocity exceeded or fell below 10% of the trial's peak velocity. Segmented data were time-normalized to 101 time points using cubic spline interpolation.

2.3.4.2 Dependent variables

The dependent variables were calculated with ManipAnalysis (Stockinger et al., 2012) and self-written Matlab scripts (R2020a; The MathWorks, Inc., Natick, Massachusetts, United States). Following studies by Sing et al. (2009) and Heald et al. (2018), we assessed adaptation with a kinematic and a dynamic parameter. The maximum perpendicular distance (PD_{max}) between the participant's trajectory and a virtual straight line connecting the start and target points served as kinematic measure on FF trials. It quantifies the net motor output as it includes all control processes involved (Stockinger et al., 2015).
While PD_{max} quantifies the kinematic output, the force field compensation factor ($FFCF$) is a dynamic measure, quantifying the participant's force field prediction (Joiner and Smith, 2008, Scheidt et al., 2000). The $FFCF$ was calculated on EC trials, i.e., when the kinematic error was kept to zero. The force the participant applied orthogonally toward the virtual wall was computed (F_{actual}). The ideal force field profile F_{ideal} was calculated as a product of the velocity profile of the trial and the force field matrix. The $FFCF$ was then obtained using linear regression of F_{ideal} and F_{actual} according to the formula

$$F_{actual}(t) = a_1 \cdot F_{ideal}(t) + a_0 + e(t).$$

Thereby, e denotes the error that is to be minimized in least-squares sense, and a_0 and a_1 are the regression coefficients of the fit. The coefficient a_0 denotes the axis intercept. The slope a_1 serves as the $FFCF$. If F_{ideal} coincides with F_{actual}, the $FFCF$ is 1. If they are unrelated, the $FFCF$ is 0. All $FFCF$ values after the baseline are participant- and target-specific baseline-subtracted values, to ensure only the learning-induced changes in the force profile are considered (Wagner and Smith, 2008).

The PD_{max} progress was investigated by fitting (Matlab `lsqcurvefit`) the following exponential model to the PD_{max} curve (Davidson and Wolpert, 2004, Stockinger et al., 2015):

$$PD_{max}(tr) = a_0 + a_1 \cdot e^{(-tr/\tau)},$$

where tr is the number of the trial, and τ serves as the time constant of adaptation used to compare the adaptation progress. The scalar a_0 represents the participant's performance learning plateau and a_1 the gain. Considering that the blocked group successively reached to the same and the random group to varying targets, we used the following approaches to compare the progress between the two groups. Firstly, we fit the model to the participant-specific PD_{max} curves of the whole practice. The fitting procedure was repeated 1,000 times with random initial values for a_i and τ. The fits with the highest R^2 were taken for further analyses. Secondly, we fit the model to participant- and target-specific PD_{max} curves (Krakauer et al., 2000). For the target-specific fits, we used a bootstrapping procedure as individual data were noisy, sampling 1,000 times per group with 64 (4 targets × 16 participants) randomly sampled PD_{max} curves with replacement and random initial values. Thirdly, we fit the exponential model to the target-specific mean PD_{max} curves.

2.3.4.3 Fitting of the extended SSM to behavioral data

We fitted the following extended SSM to each participant's data:

$$\begin{aligned} e(t) &= f(t) - y(t) \\ y(t) &= \mathbf{x_f}(t)\mathbf{c}(t) + \mathbf{x_s}(t)\mathbf{c}(t) \\ \mathbf{x_f}(t+1) &= \mathbf{A_f}\mathbf{x_f}(t) + \mathbf{c}(t)\mathbf{b_f}e(t) \\ \mathbf{x_s}(t+1) &= \mathbf{A_s}\mathbf{x_s}(t) + \mathbf{c}(t)\mathbf{b_s}e(t) \end{aligned}$$

Our extended SSM entails a fast process x_f and a slow process x_s running in parallel (Lee and Schweighofer, 2009, Smith et al., 2006). Their sum produces the model output y for each trial t. Model output y and perturbation f correspond to the $FFCF$ and their difference constitutes the error e. As it is corresponding to the $FFCF$, the perturbation f is always equal to one (Trewartha et al., 2014). However, because no error is experienced during a block of EC trials, the error e is set to zero during short-term retention (Albert and Shadmehr, 2018). Each process's progress depends on the preceding error, a process-specific error-sensitive learning (b_f, b_s), and decay (A_f, A_s) rate. In the formula above, $\mathbf{A_f}$ ($\mathbf{A_s}$) is a 4 × 4 matrix with A_f (A_s) value on the diagonal and zeros otherwise, $\mathbf{b_f}$ is a vector $[b_f b_f b_f b_f]$, and $\mathbf{b_s}$ analogous.

The two-rate SSM as proposed by Smith et al. (2006) cannot account for multiple targets (Schweighofer et al., 2011, Tanaka et al., 2012), as long as they cannot be averaged out over a few trials (Albert and Shadmehr, 2018, Tanaka et al., 2012). Therefore, we extended the SSMs to have them account for multiple targets (Schweighofer et al., 2011, Tanaka et al., 2012). The vector **c(t)** defines the currently active context (target direction), according to (Lee and Schweighofer, 2009). It contains four elements, each representing one of the practice targets if four contexts are assumed or a single one if a single context is assumed (see below).

Literature (Donchin et al., 2003, Howard and Franklin, 2015, Rezazadeh and Berniker, 2019) suggests a Gaussian-tuned trial-by-trial generalization with the mean at about the target direction, a standard deviation of about 45° and almost no transfer to ± 90°. Accordingly, the value $c(t, a)$ for the currently active context a is 1. The values for the others $c(t, b)$ ($b \in \{$practice targets $\setminus a\}$) correspond to the value of the tuning function (Ingram et al., 2011).

$$c(t, b) = \frac{\Delta(\mathcal{N}(180), \mathcal{N}(b))}{\Delta(\mathcal{N}(0), \mathcal{N}(180))}, \text{ with } \mathcal{N}(b) = \frac{1}{\sqrt{2\pi\sigma^2}} e^{(-\frac{(\theta(b))^2}{2\sigma^2})}$$

Hereby, $\theta(b)$ is the absolute angular difference between the direction of target a and the direction of target b. As only the four practice targets are learned during practice, the transfer targets' performances are constituted at the time they appear as follows. The value c for the interpolation target is set as the sum of the average states of the fast and slow processes. The value c for the extrapolation target is set to zero as we do not expect transfer to it (Castro et al., 2011, Ghez et al., 1999). The value c for a shifted origin trial is set as if it were the practice target with the same direction. This is a simplification as transfer to shifted workspaces is evident, however, setting a specific transfer coefficient was avoided due to controversial results (Berniker et al., 2014, Criscimagna-Hemminger et al., 2003, Malfait et al., 2002, Mattar and Ostry, 2007, Shadmehr and Moussavi, 2000, Shadmehr and Mussa-Ivaldi, 1994). Based on previous findings that prolonged intervals between trials led to considerable decrease of previously achieved adaptation levels (Ethier et al., 2008, Huang and Shadmehr, 2007, Kim et al., 2015b), we extended our SSM so it accounted for the forgetting between extended inter-trial pauses and set-breaks (Albert and Shadmehr, 2018, Kim et al., 2015b). Thus, when a set-break occurred, a factor d was used, which accounted for additional decay during breaks (Albert and Shadmehr, 2018).

$$A = \begin{cases} A \\ A^{d+1} \end{cases} ; b = \begin{cases} b & \text{no set break} \\ A^{d} b & \text{set break} \end{cases}$$

The factor d was set at 2, 20, and 2580 for the 30 s, 10 min and 24 h breaks respectively, being multiples of the average inter-trial interval (Albert and Shadmehr, 2018, Coltman et al., 2019).

Fitting was performed to minimize the root mean squared error ($RMSE$) between the model output and the experimental data (Matlab `fmincon`). The stability of the model fits and sensitivity of the constraints and initial values were evaluated with a grid search and bootstrapping procedure (McDougle et al., 2015, Sadeghi et al., 2018, Tanaka et al., 2012). Bootstrapping was performed 1,000 times per group with 16 randomly sampled participants with replacement and random initial values. We varied the number of processes (4-slow-1-fast, 1-slow-4-fast, and 4-slow-4-fast). We excluded 1-fast-1-slow as such a model would only be able to account for performance decreases after target changes by altering the decay parameter d or an overall worse fit. In case of the 4-slow-1-fast model, A_f and b_f were scalar values. Analogously, for the 1-slow-4-fast model, A_s and b_s were scalar values. We varied the search space for $A_f \in \{]0, 1[,]0.5, 1[,]0.5, 0.9[\}$, $A_s \in \{]0, 1[,]0.9, 1[\}$, $b_f \in \{]0, 1[,]0, 0.5[\}$, and $b_s \in \{]0, 1[,]0, 0.5[\}$ (Albert and Shadmehr, 2018, Forano and Franklin, 2020). Fitting was robust with respect to the constraints (Supplemental Table A.2), so we chose a 4-slow-1-fast model as it can reproduce a larger amount of force field adaptation phenomena (Lee and Schweighofer, 2009). Parameters were constrained to $0.5 < A_f < 0.9 < A_s < 1$ and $0 < b_s < b_f \leq 0.5$, ensuring each process met the appropriate scale (Forano and Franklin, 2020, McDougle et al., 2015). Initial values of x_f and x_s were constrained to be within $[0, 0.5]$, as no participant showed an initial $FFCF$ value > 0.5.

2.3.5 Statistics

2.3.5.1 Adaptation progress

Adaptation to the force field during the practice phase was assessed with ANOVAs (Group: Blocked vs. Random, Time: Start, End) on the two dependent variables PD_{max} and $FFCF$. For PD_{max}, the first eight and last eight trials of the practice phase were used for both groups. This number of trials was selected so that each target direction was included twice in each sample. For $FFCF$, each participant's first and last EC trial was selected to constitute the start and end sample. The PD_{max} progresses were compared between the groups with a Mann-Whitney U-test on the time constant of adaptation τ.

2.3.5.2 Retention

To test for differences between groups, short-term retention was tested with one ANOVA on $FFCF$ values (Group: Blocked vs. Random, Time: Practice end, Short-term) and long-term retention with two separate ANOVAs on PD_{max} and $FFCF$ values (Group: Blocked vs. Random, Time: Practice end, Long-term). The sample for "practice end" constituted the last four trials of the practice (blocked), or the last trials per target (random). The first four EC trials of the short-term retention and the four EC trials (FF for PD_{max}) of the long-term retention were selected, respectively, for the short-term and long-term sample. For each time point, values were averaged per participant, so that each sample contained 16 values per group.

2.3.5.3 Spatial transfer

Spatial transfer was tested in two steps. First, we determined whether transfers had taken place with one-sample t-tests vs. 0 separately for each group and spatial transfer task. Second, if there was transfer, we tested for differences between the groups with t-tests as we expected differences in the amount of transfer between the groups. These tests were repeated for short-term ($FFCF$ values) and long-term (PD_{max} and $FFCF$ values) tests. All short-term samples consisted of participant-specific mean values. All long-term samples consisted of single-trial values.

2.3.5.4 Modeling results and robustness

To assess whether the SSM reflects behavioral findings, all tests for adaptation, retention, and spatial transfer were carried out on the predicted model data. Additionally, we tested whether the slow and fast process at the practice end, as well as the error-sensitive learning rates, differ between the groups.

The ranges of the 95% confidence intervals (CIs) were determined by the 2.5th and 97.5th percentile values over every 1,000 fits. For all statistics conducted, the significance level was set a priori at two-sided p = 0.05. The normal distribution of the data was tested with the Kolmogorov-Smirnov test, and homoscedasticity with Levene's test. If several analyses were performed regarding the same construct, the Holm-Bonferroni method was used to adjust the significance level of the post-hoc t-tests. The effect sizes were determined with partial eta squared (η_p^2), Cohen's |d| or Cohen's |r| (Mann-Whitney U-test). Mean and standard deviation of R^2 were calculated with forth-and-back Fishers z-transformations. All statistical tests were carried out in SPSS (IBM Corp., v26.0. Armonk, NY).

2.4 Results

2.4.1 Practice performance

Participants' hand trajectories in both groups during baseline, start, and end of practice resembled those typically observed in force field adaptation (Figure 2.2; Shadmehr and Mussa-Ivaldi 1994). During baseline, trajectories were almost straight. At practice start, they showed high deviations along the force field direction. At the end of practice, the trajectories resembled those of the baseline phase.

We analyzed adaptation with the two variables PD_{max} and $FFCF$. Their progression during the practice is shown in Figure 2.3 and Figure 2.4. Remarkably, $FFCF$ (PD_{max}) values of the blocked group showed negative (positive) peaks around trial numbers 200, 400, and 600, i.e., every time the target changed for the blocked group.

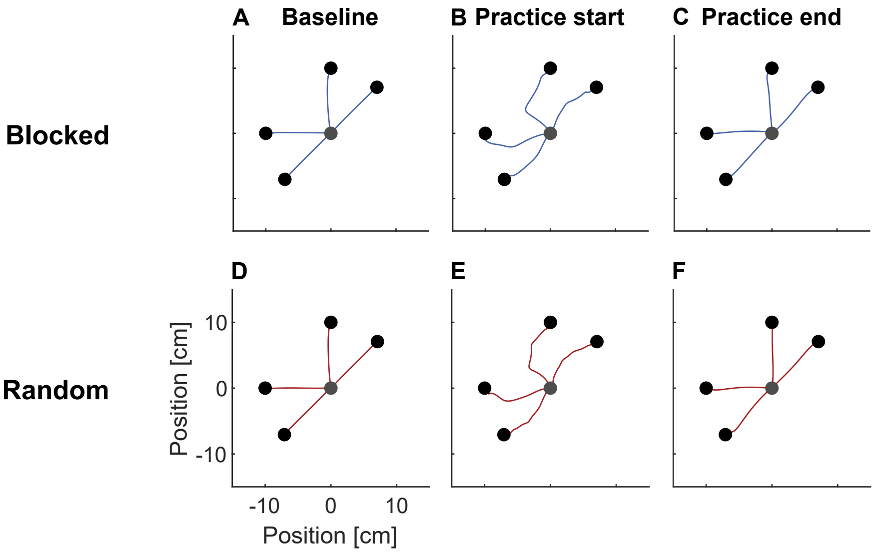

Figure 2.2: Mean trajectories of the NF baseline (A, D), the first (B, E) and last FF practice trials (C, F) separated for the two groups. At practice start, trajectories deviated from the straight trajectories seen during baseline, but became similar to baseline again at practice end.

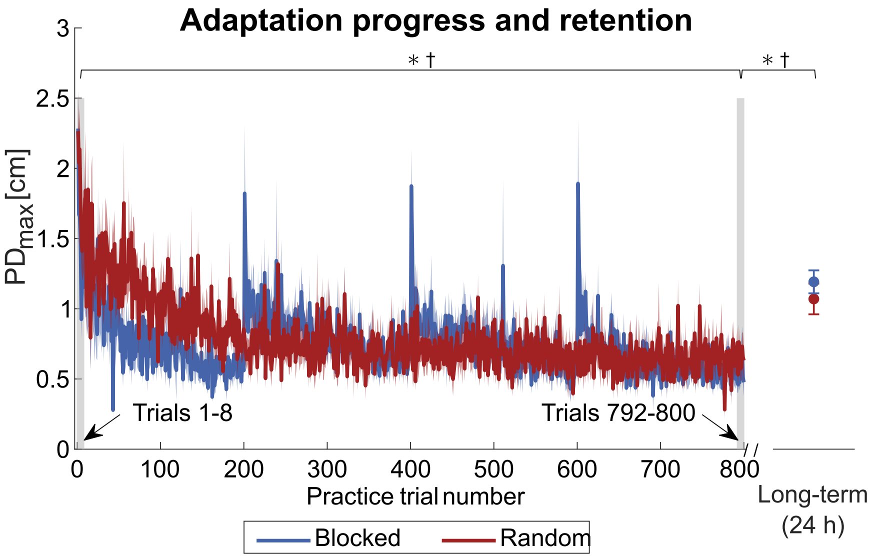

Figure 2.3: Adaptation progress and retention by PD_{max}. The blue and red solid curves show the mean values of the respective groups, and the shaded area the corresponding standard error. The gray shaded rectangles pinpoint the trials used for statistics. Symbols indicate statistically significant differences ($p < 0.05$) in adaptation level for the blocked group (∗) and the random group (†) obtained by post-hoc t-tests.

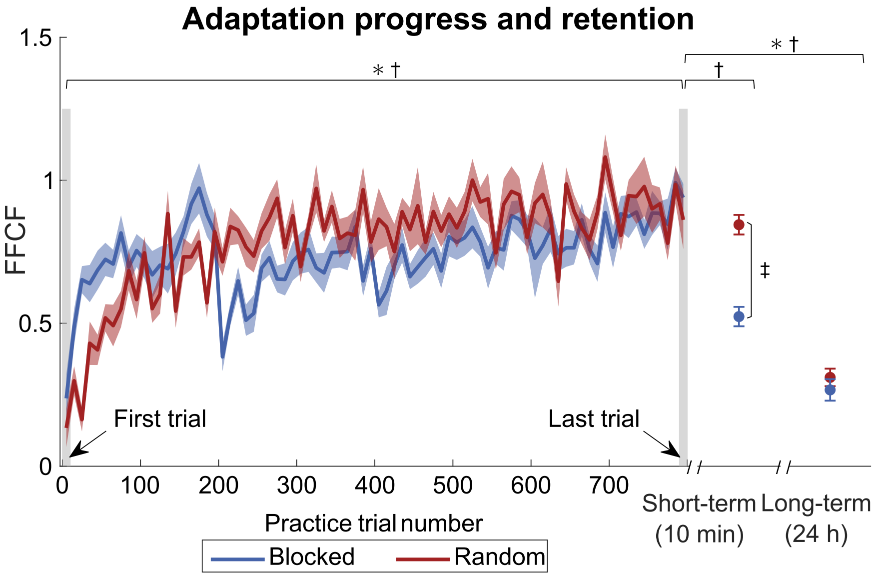

Figure 2.4: Adaptation progress and retention by $FFCF$. The blue solid curve shows the $FFCF$ values of the blocked group, and red of the random group. The gray shaded rectangles pinpoint the trials used for statistics. Symbols indicate statistically significant differences ($p < 0.05$) in adaptation level for the blocked group ($*$), the random group (†), and between the groups (‡) obtained by post-hoc t-tests.

To test the first part of our first hypothesis that participants with an interleaved practice schedule achieve a lower adaptation level at practice end than participants with a repetitive schedule, we used one ANOVA for the PD_{max} and one for the $FFCF$ values. We expected a significant time and interaction effect. The ANOVA with respect to the PD_{max} values showed a time effect [F(1, 30) = 65.431, $p < 0.001$, $\eta_p^2 = 0.686$], confirming that the participants adapted. The ANOVA showed no group [F(1, 30) = 1.118, p = 0.299, $\eta_p^2 = 0.036$] or interaction effect [F(1,30) = 0.168, p = 0.685, $\eta_p^2 = 0.006$]. Using post-hoc tests, we compared the time effect separately for the two groups and found differences in both cases [blocked: t(15) = 4.197, $p < 0.001$, |d| = 1.049; random: t(15) = 10.525, $p < 0.001$, |d| = 2.631; Figure 2.3], which indicates that both groups adapted. However, there was no group difference regarding the adaptation level at practice end.

In addition, we tested the force field prediction with the $FFCF$. Again, we found a time effect [F(1,30) = 104.641, $p < 0.001$, $\eta_p^2 = 0.777$], but neither a group [F(1,30) = 0.775, p = 0.386, $\eta_p^2 = 0.025$] nor an interaction effect [F(1,30) = 1.176, p = 0.287, $\eta_p^2 = 0.038$]. Post-hoc tests also showed a time effect for both groups [blocked: t(15) = -7.846, $p < 0.001$, |d| = 1.962; random: t(15) = -6.961, $p < 0.001$, |d| = 1.740; Figure 2.4]. Consequently, the $FFCF$ yielded the same results as the PD_{max}.

To test the second part of our first hypothesis that the random group adapts slower, we compared the PD_{max} progress. Regarding the whole curve of practice, the time constant of adaptation τ

was higher for the random group, indicating slower adaptation compared to the blocked group [U = 57.000, p = 0.007; random: τ = 77 trials (SEM 10), R^2 = 0.133 (SEM 0.044); blocked: τ = 22 trials (SEM 19), R^2 = 0.175 (SEM 0.023), Figure 2.5A]. Regarding the target-specific curve of the practice, i.e., without intervening trials for the random group, the median time constant of adaptation τ was 23.6 for the random and 19.1 trials for the blocked group. However, fits were poor, as 21.4% of the whole pool of bootstrap samples yielded an R^2 below 0.1, and the confidence intervals were (0.83, 327.12) for the random and (0.35, 941.9) trials for the blocked group. As a third step, we compared the two groups based on the fit to their target-specific mean progressions. Here, the time constant of adaptation τ was 37.9 for the random group and 23.9 trials for the blocked group (Figure 2.5B). The quality of the fit R^2 was 0.75 (random group) and 0.85 (blocked group).

In summary, the statistical results of the practice phase show that both groups adapted to the force field. Compared to the blocked group, the random group did not reach a different adaptation level at practice end but adapted slower. Therefore, we cannot confirm the first part of our first hypothesis that participants with an interleaved practice schedule achieve a lower adaptation level at practice end, but can confirm that adaptation is slower in the random group.

2.4.2 Retention

Our second hypothesis was that random practice improves retention. We tested for retention at two time points: 10 min (short-term retention) and 24 h (long-term retention) after practice. For each comparison, we used ANOVA to compare the adaptation levels at the end of practice to those of the retention test.

The ANOVA for the short-term retention revealed time [F(1,30) = 11.992, p = 0.002, η_p^2 = 0.286], group [F(1, 30) = 6.317, p = 0.018, η_p^2 = 0.174] and interaction effects [F(1, 30) = 5.494, p = 0.026, η_p^2 = 0.155] for the $FFCF$. With post-hoc tests, we only found a time effect for the blocked group [t(15) = 7.513, p < 0.001, |d| = 0.879], which revealed that the adaptation level decreased from practice end to short-term retention test. In addition, we found that the random group showed a superior performance in the short-term retention test compared to the blocked group [t(30) = -5.854, p < 0.001, |d| = 2.138; Figure 2.4].

We used two ANOVAs to test for long-term retention, one for the PD_{max} values and one for $FFCF$ values. For PD_{max}, we found a time effect [F(1, 30) = 89.390, p < 0.001, η_p^2 = 0.749], indicating a decrease of the adaptation level. We found neither a group [F(1, 30) = 0.002, p = 0.962, η_p^2 < 0.001], nor an interaction effect [F(1, 30) = 4.182, p = 0.050, η_p^2 = 0.122]. Hence, the performance did not differ between the groups. Post-hoc tests revealed a time effect for both groups [blocked: t(15) = -8.081, p < 0.001, |d| = 2.020; random: t(15) = -5.273, p < 0.001, |d| = 1.318; Figure 2.3], indicating that both groups' adaptation levels were lower 24 h after practice end. We also conducted an ANOVA on the $FFCF$ values. It also revealed a time effect [F(1, 30) = 123.535, p < 0.001, η_p^2 = 0.805], but likewise no group [F(1, 30) = 0.154, p = 0.697, η_p^2 = 0.005] or interaction effect [F(1, 30) = 0.076, p = 0.784, η_p^2 = 0.003]. As with PD_{max}, post-hoc tests revealed a time effect for both groups [blocked: t(15) = 11.299, p < 0.001, |d| = 2.825; random: t(15) = 6.275, p < 0.001, |d| = 1.569, Figure 2.4].

In summary, the random group's retention was better 10 min after practice but did not differ from the blocked group 24 h after practice. Hence, we can accept our second hypothesis regarding short-term retention, but must reject it regarding long-term retention.

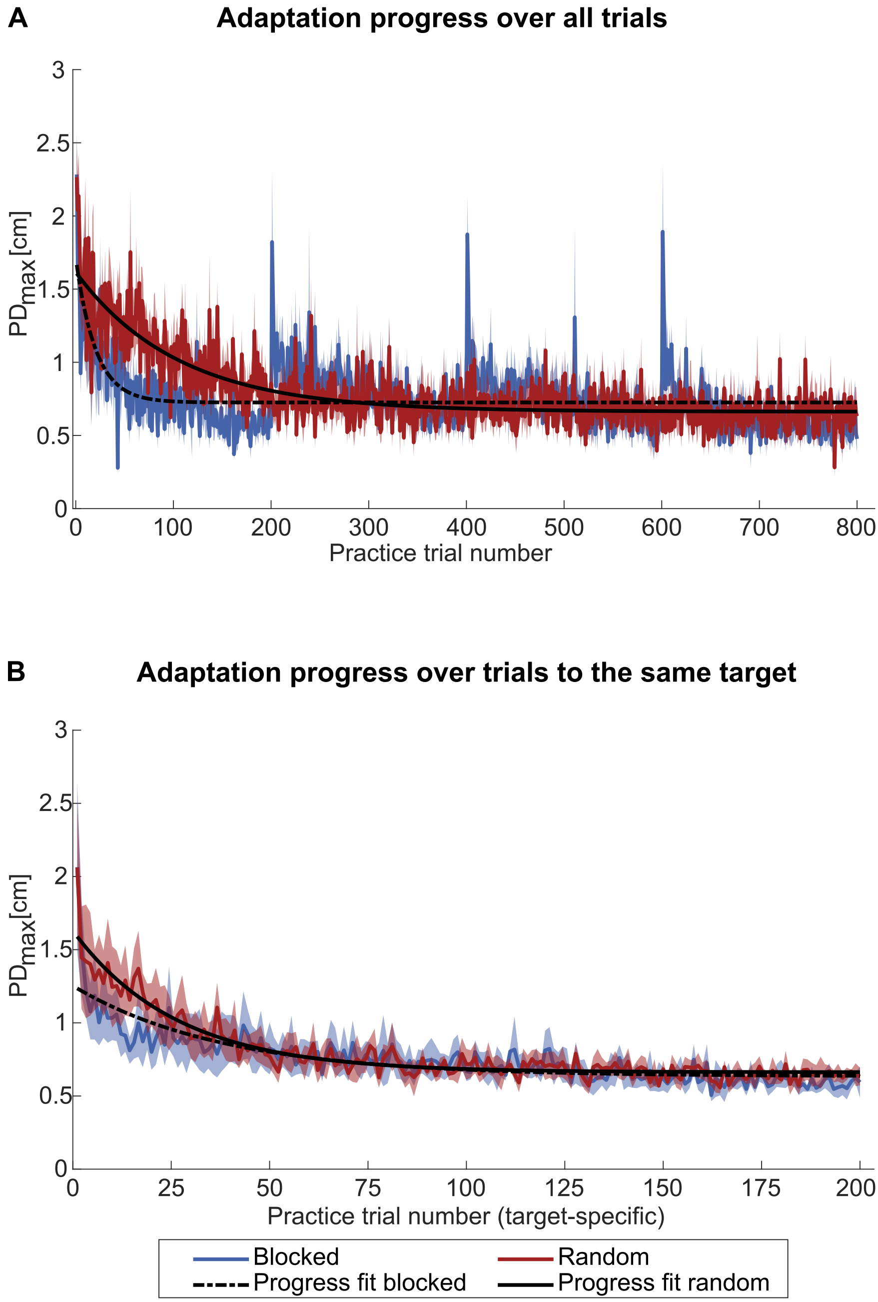

Figure 2.5: PD_{max} progression fits. The blue and red solid curves show the mean values of the respective groups, and the shaded area the corresponding standard error. The black curves illustrate the PD_{max} progression fits, the fit over the groups' means. In (A) the fits were calculated over all trials and in (B) by target.

2.4.3 Spatial transfer

Our third hypothesis was that random practice improves spatial transfer. We tested for transfer at two time points: 10 min (short-term transfer) and 24 h (long-term transfer) after practice, with three different kinds of targets: interpolation, extrapolation, and shifted origin (Figure 2.6).

For the short-term transfer, we first tested for every transfer task whether there was transfer for either group. If there was transfer, we tested which group performed better. Both groups showed transfer for the interpolation [blocked: t(15) = 7.490, p < 0.001, |d| = 1.934; random: t(15) = 11.821, p < 0.001, |d| = 3.052] and shifted origin targets [blocked: t(15) = 12.179, p < 0.001, |d| = 3.145; random: t(15) = 15.122, p < 0.001, |d| = 3.904]. No group showed transfer for the extrapolation target [blocked: t(15) = 0.279, p = 0.784, |d| = 0.072; random: t(15) = 0.036, p = 0.972, |d| = 0.009]. Then, we tested for differences between the blocked and the random group on the interpolation and shifted origin target. The random group showed a better interpolation and shifted origin transfer than the blocked group [interpolation: t(30) = -4.453, p < 0.001, |d| = 1.626; shifted origin: t(30) = -4.627, p < 0.001, |d| = 1.689].

Analogously to the short-term transfer tests, we first tested whether the groups showed long-term transfer to the different targets. Like with the short-term tests, both groups showed transfer for the interpolation [blocked: t(15) = 7.900, p < 0.001, |d| = 2.050; random: t(15) = 11.871, p < 0.001, |d| = 3.065] and shifted origin targets [blocked: t(15) = 15.875, p < 0.001, |d| = 4.099; random: t(15) = 15.685, p < 0.001, |d| = 4.043]. No group showed transfer for the extrapolation target [blocked: t(15) = -0.913, p = 0.376, |d| = 0.236; random: t(15) = -0.634, p = 0.535, |d| = 0.164]. We then examined if there was a group difference for the interpolation and shifted origin targets. The groups did not differ for the interpolation target [$PD_{max}:$ t(30) = 0.727, p = 0.473, |d| = 0.266; $FFCF$: t(30) = -1.642, p = 0.111, |d| = 0.600]. Regarding the long-term tests for the shifted origin targets, we found that PD_{max} values did not differ between the groups [t(29.726) = 0.342, p = 0.734, |d| = 0.125]. However, we found better transfer for the random group regarding the $FFCF$ [t(30) = -2.582, p = 0.015, |d| = 0.943].

In summary, the random group revealed a better interpolation test performance than the blocked group 10 min after practice. We found no group difference 24 h after practice for the interpolation test. No group showed transfer to the extrapolation target, neither 10 min, nor 24 h after practice. In the shifted origin transfer task, the random group outperformed the blocked group 10 min as well as 24 h after practice ($FFCF$).

We hypothesized that interleaved practice fosters transfer, but found mixed results. We can therefore only partially accept the hypothesis.

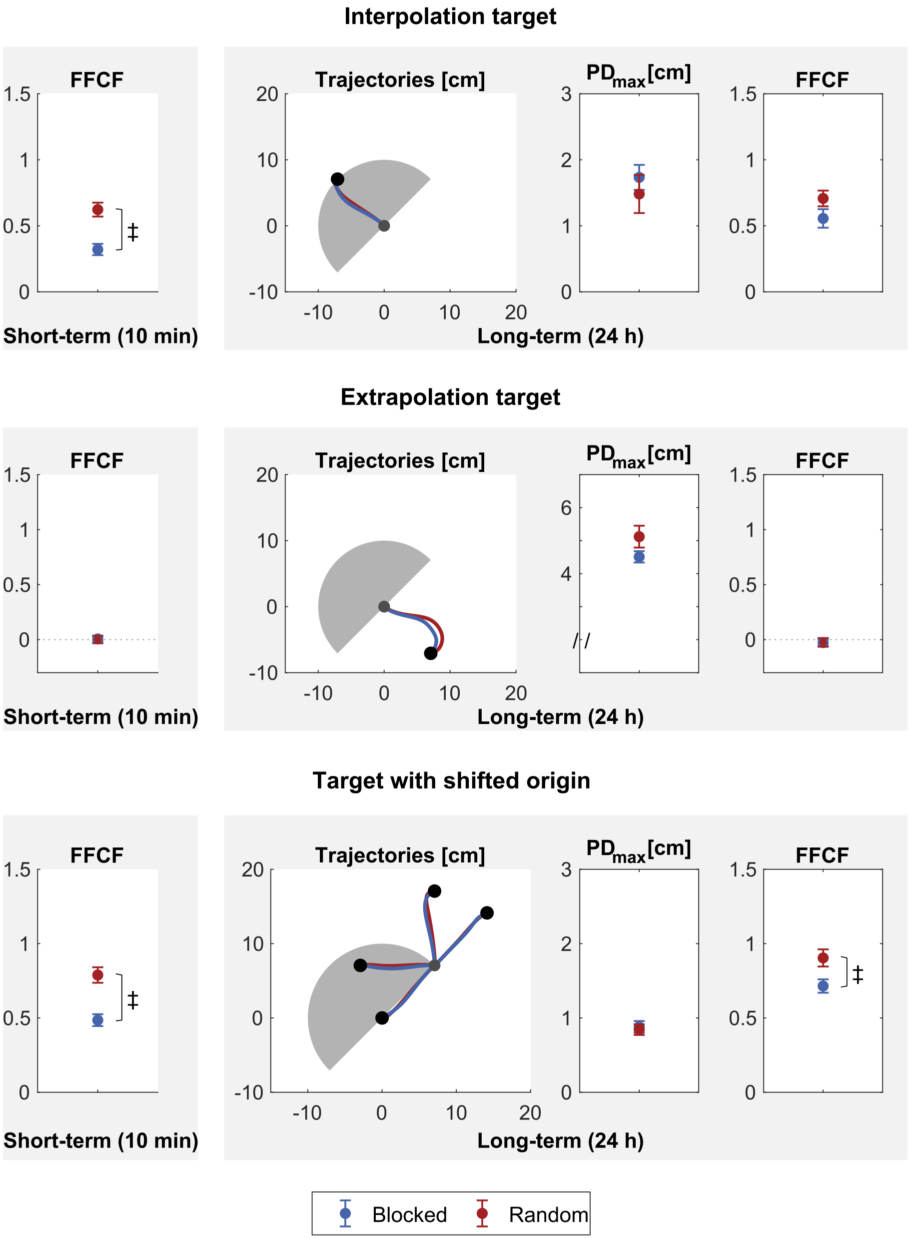

Figure 2.6: Spatial transfer 10 min (left column) and 24 h (right column) after practice. Top: interpolation target, middle: extrapolation target, bottom: targets with shifted origin. All values are mean and standard error over the blocked (blue) and random (red) groups. The gray shaded semicircle illustrates the area spanned by the practice trials for orientation. Trajectories are means over the groups. Group differences ($p < 0.05$) are indicated by the ‡ symbol.

2.4.4 State-space model to model the contextual-interference effect

2.4.4.1 General characteristics of the model data

The SSM captured the overall adaptation progress, retention and transfer for both groups [$RMSE_{blocked}$ = 0.27 (CI 0.03), [$RMSE_{random}$ = 0.31 (CI 0.02), $R^2_{blocked}$ = 0.78 (CI 0.04), R^2_{random} = 0.70 (CI 0.04); Figure 2.7]. The error-sensitive learning rates were $b_{f, blocked}$ = 0.31 (CI 0.07), and $b_{f, random}$ = 0.23 (CI 0.05), as well as $b_{s, blocked}$ = 0.04 (CI 0.03), and $b_{s, random}$ = 0.04 (CI 0.01). The decay rates were $A_{f, blocked}$ = 0.79 (CI 0.10), and $A_{f, random}$ = 0.86 (CI 0.05), as well as $A_{s, blocked}$ = 0.99 (CI 0.01), and $A_{s, random}$ = 0.99 (CI 0.01). The decay factors during breaks were $d_{blocked}$ = 1.05 (CI 0.56), and d_{random} = 0.23 (CI 0.21). Differences in the learning rates of the fast process between the groups were not significant but revealed a large effect size, indicating a slower rate and thus a slower adaptation for the random group ($b_{f, blocked}$ vs. $b_{f, random}$: t(26.33) = -2.052, p = 0.050, |d| = 0.800).

We tested for differences in the processes' values at the end of practice as they can possibly explain differences in the retention performances. For the slow process, the difference was not significant with a medium effect size [blocked: mean 0.51 (SE 0.05); random: mean 0.66 (SE 0.06), t(30) = 1.802, p = 0.082, |d| = 0.658]. The difference of the fast process' activity was not significant either, with a weak correlation [blocked: mean 0.30 (SE 0.04); random: mean 0.24 (SE 0.04); U = 96.000, Z = -1.206, p = 0.239, |r| = 0.22].

2.4.4.2 Additional analysis of the model data

To examine in more detail whether the model can replicate the performance trends over time induced by the random and blocked practice protocols, the same statistics as for the $FFCF$ values (sections 2.4.1-2.4.3) were calculated from the model data and can be found in the supplementary material A.1.2. The statistical results of the model data were consistent with the behavioral results except for the practice start, the extrapolation target, and the long-term retention test. Thus, with regard to our fourth hypothesis, our SSM allows to provide and discuss explanatory mechanisms underlying some, but not all behavioral results.

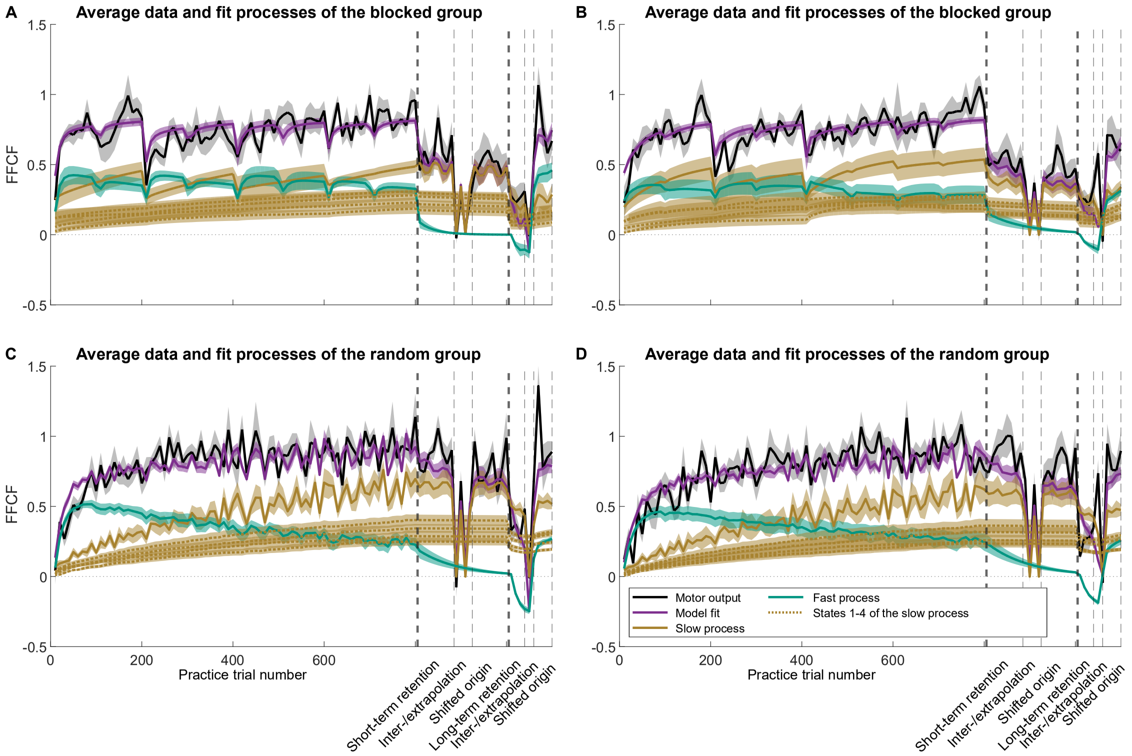

Figure 2.7: Results of the SSM fit showing mean motor output (black) and model fit (purple) with slow (brown) and fast (green) processes. The thin dotted brown lines illustrate the different states of the slow process. The dashed vertical lines separate the different phases. Means are calculated over the eight participants of each group (blocked: A, B; random: C, D) whose schedules start with the extrapolation before the interpolation target (A, C) or vice versa (B, D) during the spatial transfer phase.

2.5 Discussion

The CIE is a well-studied phenomenon in motor skill learning. It states that interleaved (high contextual interference) as opposed to repetitive (low contextual interference) practice results in lower performance gains during practice, but superior retention and transfer (Schmidt et al., 2019, Shea and Morgan, 1979). The aims of the study were to investigate whether a CIE can be observed with respect to retention and spatial transfer in a force field adaptation task, and whether a SSM can reproduce the CIE and thus partly explain the underlying mechanisms of the CIE. The main findings of our study are: (1) a random practice schedule does not lead to different performance levels at practice end but to a slower adaptation than a blocked schedule. A random schedule is superior to a blocked schedule in (2) short-term retention and (3) spatial transfer. (4) SSMs reflect the experimental findings with some exceptions and provide possible explanatory mechanisms.

2.5.1 Random practice does not lead to different performance levels at practice end but to a slower adaptation

Participants of both groups adapted to the force field perturbation. Based on the typical results of the CIE in skill learning (Wright and Kim, 2019), we expected and hypothesized that the adaptation at practice end would be worse for the random group than for the blocked group. However, we found no difference between the groups. Former studies on the CIE in our lab are inconsistent in this regard. The finding in this study concurs well with Thürer et al. (2019, 2017), but differs to Thürer et al. (2018). In the latter, a difference was only found for the enclosed area parameter (kinematic error) but not for the $FFCF$. However, these studies cannot be directly compared to ours, since they varied the force field magnitude rather than the reaching direction. A possible explanation for the same adaptation level at practice end is the long duration of the practice phase of our study. Usually, adaptation progression plateaus after 300-600 trials when different reaching directions are practiced (Gandolfo et al., 1996, Shadmehr and Brashers-Krug, 1997). Other CIE studies have also shown that adverse effects of random practice can be overcome during long acquisition phases (Maslovat et al., 2004, Pauwels et al., 2014).

Participants with a random schedule adapted slower than those with a blocked schedule, as indicated by the blocked group's lower time constant of adaptation and the higher error-sensitive learning rate of the fast process (large effect size). The difference in the higher error-sensitive learning rate of the fast process indicates that the blocked group shows faster adaptation, especially in the movements at the beginning. The finding that participants in the blocked group adapted faster is in good agreement with CIE findings in the skill learning literature (Magill and Hall, 1990, Shea and Morgan, 1979) as well as with motor adaptation tasks (Thürer et al., 2018). However, not all studies explicitly compared adaptation speed (Thürer et al., 2019, 2017). Although not explicitly measured, but apparent, the blocked group seemed to adapt faster in the study of Schweighofer et al. (2011). In motor adaptation studies, there is support that increased environmental variability slows down adaptation or, in other words, a consistent environment speeds up the adaptation rate (Gonzalez Castro et al., 2014, Wei and Körding, 2009). Nonetheless, to the best of our knowledge, no study so far has compared a blocked with a random schedule regarding different movement directions in terms of adaptation speed. With the help of the SSMs, this could be described as follows. The faster adaptation can be explained by the fact that in blocked practice, the learning gain toward the next trial is maximal, since the same movement direction is practiced. In contrast, the learning gain after a trial in random practice only partially serves the next trial, as it has a different movement direction (section 2.5.4.1).

During practice, the blocked group showed a decrease in the $FFCF$ and an increase in PD_{max} every time the target changed. Yet, the values did not fully revert to the baseline level. A possible explanation could be the breaks that took place after 200 trials. A closer look at behavioral results of force field adaptation studies (Heald et al., 2018, Taubert et al., 2016) also showed that performance decreases after short breaks, although the performance decreases are much smaller in these studies than in our study. Also, the random group took the same breaks, but no distinct steps are visible in their performances. Therefore, we suggest, with the help of our SSM, that the performance decrease can be explained by the contextual switches when a new target appeared. Due to the constant target change, the random group learned each target equally, either as it was practiced itself or by the Gaussian trial-by-trial generalization. This resulted in constant fluctuations rather than distinct steps in the adaptation progress. In contrast, the blocked group always learned the recurrent target the most and the others only by the Gaussian trial-by-trial generalization. The target after the target change was therefore less learned by the blocked group which resulted in the visible steps (section 2.5.4.1).

2.5.2 Random practice yields better short-term retention but not necessarily long-term retention

We hypothesized that random practice results in better retention performance. Therefore, we assessed the performance 10 min (short-term) and 24 h (long-term) after practice. While short-term retention benefitted from random practice, long-term retention did not. Furthermore, for both groups, long-term retention showed a lower adaptation level than short-term retention. These results match with those of Schweighofer et al. (2011) for both short- and long-term retention. However, based on our SSM, we cannot fully support in our study that the better retention performance is merely due to a higher level of the slow process (section 2.5.4.2). Our results on long-term retention are partially consistent with our previous studies. Thürer et al. (2017) found a difference only in $FFCF$, but not in PD_{max}. While Thürer et al. (2018) did not find a group difference, Thürer et al. (2019) did find an advantage in the random group (only kinematic metric assessed). However, these comparisons are difficult as in these studies force field magnitudes were varied rather than movement directions. A better retention performance is often seen for randomly practicing groups in motor skill learning (Shea and Morgan, 1979). It must be noted, however, that motor adaptation is just a temporary transient adjustment of an existing internal model and that, generally, adaptation rapidly returns to baseline performance, which is in stark contrast with skill learning (Krakauer et al., 2019).

Factoring out differences in the practice schedule, there is much support in the literature stating that retention worsens with time in motor adaptation (Huberdeau et al., 2015b, Krakauer et al., 2019). Thereby, the passage of time plays a crucial role as the adapted state passively decays over time without any interfering trials in-between (Criscimagna-Hemminger and Shadmehr, 2008, Kitago et al., 2013). Furthermore, the adapted state also reverts toward baseline if EC trials are inserted (Kitago et al., 2013, Scheidt et al., 2000). These two findings concur well with the results of our retention tests: long-term retention is worse than short-term retention. In between the two tests, there was a 24 h pause and the short-term retention trials were only EC trials. However, the decrease in performance after 24 h without practice can be caused by a warm-up decrement being a temporary loss of an internal state that had been acquired (Kantak and Winstein, 2012, Schmidt et al., 2019). Therefore, if we had inserted a few FF trials before the long-term retention tests, maybe a group difference would have been visible.

2.5.3 Random practice yields better short-term transfer but not necessarily long-term transfer

To the best of our knowledge, studies so far have only examined the influence of the CIE on intermanual but not spatial transfer in force field adaptation (Thürer et al., 2019, 2018). According to skill learning studies (Goode and Magill, 1986, Wright and Kim, 2019), we expected a superior transfer performance from the random group. In light of this, and for the purpose of a comprehensive examination of spatial transfer, we investigated three different spatial transfer tasks: interpolation, extrapolation, and shifted origin. Since the time passing between practice and test trials plays a major role in force field adaptation (Criscimagna-Hemminger and Shadmehr, 2008, Krakauer et al., 2019), first short- and then long-term transfer test results are discussed separately.

2.5.3.1 Short-term

Both groups showed transfer for the interpolation and shifted origin targets. Remarkably, performance decreased to no transfer for the extrapolation target. We then found benefits for the random group compared to the blocked group in short-term transfer for the interpolation target as well as for the shifted origin targets. Our SSMs provide a possible explanation, relating the better transfer in the random group to the higher and more balanced activity of the slow process (2.5.4.3).

Factoring out the group differences, the superior transfer performance in the short-term interpolation task compared to the extrapolation task finds support in the literature. Many studies have shown that transfer is local to the practiced movement directions in the work space and decreases with increasing angular difference between the targets (Castro et al., 2011, Gandolfo et al., 1996, Rezazadeh and Berniker, 2019). The performance results of both groups in the inter- and extrapolation tasks correspond to these findings. In addition, we found that practicing in one workspace transfers to a shifted one. These results correspond to previous studies (Berniker et al., 2014, Criscimagna-Hemminger et al., 2003, Malfait et al., 2002, Mattar and Ostry, 2007, Shadmehr and Moussavi, 2000, Shadmehr and Mussa-Ivaldi, 1994). The shifted origin targets had the same direction as the practice targets in view of extrinsic coordinates. Yet, we did not explicitly control for the coordinate system in which the targets are moved. Furthermore, there is controversy over which coordinate systems are responsible for successful transfer (Franklin et al., 2016).

2.5.3.2 Long-term

Analogously to the short-term transfer, we first separately tested both groups for transfer and then tested for differences between the groups. Both groups showed transfer for the interpolation and shifted origin trials but not for the extrapolation target. This is alike our findings for the short-term transfer. However, in the long-term transfer tests, the random group did not outperform the blocked group, except for the transfer test for the shifted origin trials. For the latter, we only saw benefits when we assessed performance with the $FFCF$ but not with PD_{max}. Potentially, this is due to the different control mechanism the two parameters quantify (Stockinger et al., 2015): the $FFCF$ serves as a measure of the force field prediction and thus the internal model, whereas the PD_{max} reflects the net motor output. The theoretical framework of optimal feedback control (OFC) (Scott, 2004, Todorov, 2004, Todorov and Jordan, 2002) and its extension robust optimal feedback control (Crevecoeur et al., 2019) may help understand why differences in $FFCF$ values but not in PD_{max} values are visible. OFC assumes a tradeoff between the reliance on internal models and sensory feedback. Furthermore, the reliance on sensory feedback is upregulated when accurate internal models cannot be formed (e.g., due to uncertainty) (Franklin et al., 2012, 2017). We speculate that the shift in start and end points increased the uncertainty about the environment. This uncertainty especially increased for the blocked group but not for the random group since the latter group already experienced higher uncertainty inherent in their practice schedule. Therefore, the blocked group could have increased their feedback gains following the target shift allowing for more vigorous corrective responses when encountering the force field (Crevecoeur et al., 2019). Collectively, the increased feedback gains and thus the more vigorous corrections during the ongoing movement in the blocked group would essentially cancel out the difference in the force field prediction ($FFCF$) yielding in a similar motor net output (PD_{max}).

We saw a group difference for the shifted-origin trials in both short- and long-term tests but no group difference in the long-term tests for the interpolation target. Possibly, a retrieval effect may have played a role. This refers to the phenomenon that relearning of a force field occurs at a more rapid rate than initial learning and of overcoming a warmup-decrement (Haith and Krakauer, 2014, Huberdeau et al., 2015a,b, Krakauer, 2005, Krakauer and Shadmehr, 2006, Schmidt et al., 2019). Maybe the warm-up decrement was overcome through the FF trials during the long-term tests until the long-term shifted origin tests started. Then, the better transfer performance of the random group, which was found during the short-term tests, could emerge again.

2.5.4 State-space models provide further explanations for the contextual-interference effect

In addition to the experimental testing of the CIE, we developed SSMs to explain potential superior performance effects of the random practice schedule by the two-rate characteristic of the learning process. Except for the practice start, the extrapolation test, and partially long-term retention, the SSM could reproduce the performance trends in the behavioral data. Therefore, its underlying processes provide explanations to some but not all behavioral findings.

2.5.4.1 Practice

In the blocked group (Figure 2.7A, B), both processes were active throughout practice. When the target changed, activity in the fast process always increased, and decreased in the slow process. During the periods when the blocked group approached the same target 200 times, the context did not change and the Gaussian trial-by-trial learning had the strongest effect on the recurrent context. Whenever the target changed, the responsible context for the new target became active. Since the new context has been solely learned by trial-by-trial generalization and became active for the first time then, this resulted in a lower adaptation for the new context than for the preceding at the time the new context became active. When the new context became active, fast process activity increased and contributed more to the overall adaptation than at the end of the preceding context. Every time a new context became active, the preceding one was increasingly forgotten. The observation that first the fast process and then the slow process lead to adaptation when the target changed can be related to the respective process characteristics (Huberdeau et al., 2015b). The fast process is sensitive to reward and its activity level rises fast, whereas the slow process seems to be more error-driven and rises more slowly. Regarding the underlying physiological cause, the literature suggests that adaptation, in the beginning, is achieved by stiffening the arm either as a result of an impedance control strategy (Heald et al., 2018, Milner and Franklin, 2005) or to upregulate feedback gains (Crevecoeur and Scott, 2014, Crevecoeur et al., 2019) as the internal model was inaccurate for the new target (Franklin et al., 2012). When targets changed after every 200 trials, participants probably analogously first used these reactive responses as a result of a reward-based mechanism and then – on a slower timescale – adapted an internal model which was able to predict the force field (Franklin et al., 2012). Another possibility could be that the visible change of the target addressed the explicit component of the learning process, which has been shown to resemble the fast process (McDougle et al., 2015). Though, we did not control for explicit and implicit processes and thus this remains speculative.

In the random group (Figure 2.77C, D), overall performance was determined by activity of the fast process until approximately halfway through practice. Toward the end of practice, the slow process became very active, and the activity of the fast process decreased. Both slow and fast processes revealed fluctuations which resulted from the continuous context switches. Whenever the target changed, the responsible context became active. The time that passed until the target was reached again caused a decrease in activity of the corresponding context. However, since the time was short, the decrease was only small, which resulted in the fluctuations.

2.5.4.2 Retention

Participants with a random practice schedule showed better short-term retention than participants with a blocked practice schedule. There were no differences between the long-term retention performances. Schweighofer et al. (2011) explained, without a statistical test, the increased immediate retention performance of the random group with a more pronounced activation of the slow process during practice. This ultimately led to a higher level of the slow process at practice end when compared to the slow process level of the blocked group. They explained that the slow process, which started from a higher level at practice end and then decayed slowly in the random group, led to better retention. In our study, we also observed a higher level of the random group's slow process, yet the difference was not significant with a medium effect. It must be noted that we did not test retention for each target individually. With respect to the forgetting-and-reconstruction hypothesis, it could be that in the blocked group the earlier a target was practiced the more it got forgotten. So, the earliest practiced targets got considerably forgotten. In contrast to the random group in which all targets were practiced in a block-randomized manner and no target got forgotten more than another. Possibly, this difference between the slow processes of the two groups yields different average retention values and thus is reflected in the worse retention for the blocked group. Joiner and Smith (2008) showed the slow process to be the main contributor for the adaptation level during long-term retention (24 h), whereas the fast process does not contribute. This holds true for our modeling results as the adaptation level during long-term retention is only influenced by the slow process level. Also, our SSM is able to reflect the decrease of adaptation for both groups after 24 h. However, it fails to reproduce the experimental finding that the groups' performances do not differ significantly. Possibly, it is not only the decay of the slow process that is responsible for the long-term retention performance. Other mechanisms may happen, like a fractional transition of the fast process into the slow process as suggested by Criscimagna-Hemminger and Shadmehr (2008) or model-free learning mechanisms occurring along with error-based learning (Huang et al., 2011). With regard to this, our experimental procedure and state-space modeling did not allow us to verify if the described phenomenon happened. Additionally, maybe the decrease in retention results from the interference of daily task reaching movements, like grabbing a cup of coffee in front of you, and thereby promoting a wash-out, which we did not consider with the SSM approach. Thus, this question cannot be addressed here and remains speculative.

2.5.4.3 Transfer

To be applicable to adaptation to multiple targets, SSM must also include multiple contexts (Albert and Shadmehr, 2018, Schweighofer et al., 2011, Tanaka et al., 2012). However, new targets did not appear after adaptation in any of these studies. This contrasts with our study, as the interpolation, extrapolation, and shifted origin targets were not practiced. Hence, we used a simplified approach to let the SSMs account for the new targets (section 2.3). Our SSMs reproduced the statistical results we found in our behavioral analyses results with little exceptions (Supplemental Data A.1.2). Therefore, it seems that the Gaussian trial-by-trial generalization can account for transfer to new targets. The SSMs provide a possible explanation for the better short-term interpolation transfer performance of the random group in light of the forgetting-and-reconstruction hypothesis. Since the activity of the slow process for the four contexts increased much more uniformly in random than in blocked practice and resulted in a higher value for the interpolation target, this possibly explains the higher transfer for the interpolation target of the random group. The SSM fits showed minor transfer for the extrapolation target for both groups stemming from the fast process. The fast process does not consist of context-specific states, and so cannot revert from a high value to zero within a single trial. For the shifted origin targets, the context of the practice target with the same direction served as the context of the respective shifted-origin target. This is a simplification in the sense that we do not consider whether the context of the direction is embedded in an intrinsic, extrinsic, or a mixed coordinate system (Berniker et al., 2014). However, for the purposes of our study, this simplification seems valid as the SSM reproduced the behavioral data.

The SSM can also account for the fact that no significant differences were found for the long-term interpolation test. In the absence of error, i.e., during EC trials or breaks, the adaptation level decays exponentially (Orozco et al., 2021). Due to the exponential decay, the difference of the slow process between the two groups which was possibly responsible for the group difference in the short-term interpolation test also quickly became smaller. As a result, significant differences no longer occurred after 24 h. The model data are in line with the experimental findings of the long-term transfer test for the shifted origin targets, i.e., a superior performance of the random group. The SSM supports the explanation based on a possible retrieval effect and warmup-decrement

(section 2.5.2). Every second block during long-term retention and tests, we used FF trials. With them, the SSMs accounted again for learning and the values of the processes increased.
Despite support in the literature (Smith et al., 2006), there is criticism that SSMs cannot validly account for the underlying mechanisms of all savings or retrieval phenomena in force field adaptation (Herzfeld et al., 2014, Krakauer et al., 2019). Based on SSMs, savings are explained with the higher onset value of the slow process after being re-exposed to the force field (Smith et al., 2006). However, savings are also found after a prolonged washout period during which the slow process diminishes almost to zero (Zarahn et al., 2008). A possible extension to SSMs is the use of variable error sensitivities (Coltman et al., 2019, Herzfeld et al., 2014, Zarahn et al., 2008) or different parallel states as supposed by Lee and Schweighofer (2009).

2.5.5 Operationalization of the contextual interference in force field adaptation

The size of the CIE seems to be dependent on the type of variation practiced (Magill and Hall, 1990). In this regard, a certain amount of challenge seems to be critical (Guadagnoli and Lee, 2004). This means that, up to a certain degree, the more difficult or dissimilar the tasks are, the better participants would benefit from an interleaved practice schedule. In this adaptation study, participants practiced reaching to different targets in a force field. Even though, there is fractional transfer of learning between neighboring targets (Donchin et al., 2003, Howard and Franklin, 2015, Rezazadeh and Berniker, 2019), we propose that reaching to different directions can be considered dissimilar in the context of an CIE as it requires different joint movements (Morasso, 1981) and muscle activations (Flanders, 1991, Karst and Hasan, 1991, Thoroughman and Shadmehr, 1999). Furthermore, transfer of learning to neighboring targets seems to decrease with increasing direction difference (Gandolfo et al., 1996). Taken together, reaching to different directions in the force field may constitute a sufficient interference and thus a challenge in the context of the CIE to provoke better retention and transfer for the interleaved group. Studies in a similar laboratory setting, where practicing one task variation can presumably transfer to the others, also showed a CIE: Schweighofer et al. (2011) found a CIE in grip force pattern, Chalavi et al. (2018) in a visuomotor task, Lelis-Torres et al. (2018) in a manual aiming task, and Thürer et al. (2019), where force field magnitudes varied. We therefore considered the different reaching directions to be dissimilar enough to see a CIE.

2.5.6 Neuronal mechanisms related to the contextual-interference effect and state-space model

Recent studies have started to address the question of the underlying neuronal mechanisms related to the decomposition of adaptation into two distinct processes (Farrens and Sergi, 2019, Kim et al., 2015a, Sarwary et al., 2018). Kim et al. (2015a) demonstrated in a visuomotor adaptation that slow formation of memory relates to activity in the inferior parietal cortex and anterior-medial part of the cerebellum; and fast formation to areas in the prefrontal and parietal lobes and the posterior part of the cerebellum. Studies of the CIE associated the improved retention and transfer performance of a random schedule to increased activity in the parietal lobe (Thürer et al., 2018) or the dorsolateral prefrontal cortex (Kantak et al., 2010), and showed increased activity with blocked practice in the motor cortex (Kantak et al., 2010). SSMs as applied in our study are descriptive models of behavior and so do not allow us to infer the underlying neural mechanisms (Krakauer et al., 2019). Especially, it is yet unresolved whether the processes can be associated with short- and long-term memory to fully support the forgetting-and-reconstruction hypothesis (Schweighofer et al., 2011). As the CIE is detectable in both motor adaptation and skill learning studies, and these two types of motor learning are likely to have overlapping neural circuitry (Krakauer et al., 2019), future studies may further investigate the CIE and the neural differences between blocked and random practice which lead to the different behavioral results.

2.5.7 Limitations

There are a few limitations that need to be considered. Firstly, we used two approaches (fit over all trials vs. by target) to compare adaptation speed by comparing the PD_{max} progression, which both come with limitations. Comparing τ over all trials obscures the difference between practicing targets block-wise versus in a row, yielding a τ for the random group around four times larger than τ for the blocked group. However, if τ is compared by target, the occurring transfer of learning between the different targets and the decay of learning of a target until it is reached again is obscured for the random group. Furthermore, let t be the n^{th} trial for target i. For the blocked group, t would be trial number $(n + 200 + n + 400 + n + 600 + n)/4 = 300 + n$ on average. For the random group, t would be between trial numbers $4n - 3$ and $4n$. Thus, on average, t appears earlier in the random schedule than in the blocked for the first half of the trials, where adaptation progresses most $(4n < 300 + n; n = 1 \leq n \leq 99)$. The blocked group would therefore have more practice trials before t. Secondly, the interspersed FF trials during the long-term tests may blur the results of the CIE. The savings or retrieval effect likely plays a more dominant role than the CIE for our long-term tests. Future research may assess the CIE after a 24 h break without an FF trials effect to gain more insights into the CIE in motor adaptation because, in motor skill learning, an increased retention is also observed after 48-72 h (Wright and Kim, 2019). Thirdly, our SSMs did not account for biomechanical differences of the different reaching directions (Molier et al., 2011, Rand and Rentsch, 2017). Another limitation of our SSM is that it did not account for possible non-linear error sensitivity (Fine and Thoroughman, 2007, Wei and Körding, 2009) or context-dependent decay (Ingram et al., 2013).

2.6 Conclusion

The study shows that the CIE, which has been primarily investigated in motor skill learning studies, can partially lead to better retention and spatial transfer in motor adaptation tasks. Studying the influence of different practice schedules on retention and transfer is of theoretical as well as of practical interest. The study of the CIE in motor adaptation helps to better understand the underlying processes, as skill learning and motor adaptation are likely to make use of some shared neural circuitry and the causes of the CIE are still inconclusive. The study of the effects of different practice schedules also aims at providing practitioners with the most efficient practice schedules which ultimately may help foster the learning and execution of motor skills.

3 Topic A, Study A2: Changes in muscle synergy structure and activation patterns underlie force field adaptation, retention, and generalization

This is a slightly adapted[1] version of the original research submitted as:

Herzog, M., Berger, D. J., Russo, M., d’Avella A.[2] and Stein, T[2]. Changes in Muscle Synergy Structure and Activation Patterns Underlie Force Field Adaptation, Retention, and Generalization. [in review].

A preprint version is available at https://doi.org/10.1101/2024.12.16.628548[1].

---

[1] The citation and cross-reference style, as well as the figures’ fonts, have been adjusted for consistency in this dissertation. Figure 1 was added, according to the version in review.

[2] Share senior-authorship

3.1 Abstract

Humans can adapt their motor commands in response to errors when they perform reaching movements in new dynamic conditions, a process called motor adaptation. They acquire knowledge about the new dynamics, which they can use when they are re-exposed and, limitedly, generalize to untrained reaching directions. While force field adaptation, retention, and generalization have been thoroughly investigated at a kinematic and kinetic task level, the underlying coordination at a muscular level remains unclear. Many studies propose that the central nervous system uses low-dimensional control, i.e., coordinates muscles in functional groups: so-called muscle synergies. Accordingly, we hypothesized that changes in muscle synergy structure and activation patterns represent the acquired knowledge underlying force field adaptation, retention, and generalization. To test this, 36 male humans practiced reaching to a single target in a viscous force field and were tested for retention and generalization to new directions, while we simultaneously measured muscle activity from 13 upper-body muscles. We found that muscle synergies used for unperturbed reaching cannot explain the muscle patterns when adapted. Instead, muscle synergies specific to this adapted state were necessary, alongside a novel four-phasic pattern of muscle synergy activation. Furthermore, these structural changes and patterns were also evident during retention and generalization. Our results suggest that reaching in an environment with altered dynamics requires structural changes to muscle synergies compared to unperturbed reaching, and that these changes facilitate retention and generalization.

3.2 Introduction

Humans can adapt their motor commands in response to errors when their reaching movements are perturbed, a process called motor adaptation (Shadmehr and Mussa-Ivaldi, 1994). Furthermore, they can re-use the acquired knowledge when they are perturbed again and can partly generalize it to unpracticed reaching directions (Brashers-Krug et al., 1996, Gandolfo et al., 1996, Ghez et al., 1999, Rezazadeh and Berniker, 2019, Shadmehr, 2004, 2017). Many studies have thoroughly analyzed force field adaptation, retention, and generalization at the level of task-related variables; describing and modeling the mapping of end-point kinematics and kinetics (Diedrichsen et al., 2010, Krakauer and Mazzoni, 2011, Thoroughman and Shadmehr, 2000, Wolpert and Kawato, 1998). However, how the CNS coordinates motor adaptation at the level of muscle activations has not been fully investigated. The CNS may implicitly represent acquired knowledge and generate motor commands by organizing muscle synergies (d'Avella, 2016, Bernstein, 1967, Bizzi et al., 2008, Giszter, 2015, Mussa-Ivaldi, 1999). Through muscle synergies – coordinated recruitment of groups of muscles acting together as functional units – the CNS may control a small number of units rather than every muscle, thereby reducing the dimensionality of the control problem (Bernstein, 1967, Bizzi et al., 1991, Tresch et al., 1999). Furthermore, by flexibly combining and sharing synergies, a large behavioral repertoire can be generated (d'Avella et al., 2003, Bizzi et al., 2008, Mussa-Ivaldi et al., 1994, Mussa-Ivaldi and Bizzi, 2000, Ting and Macpherson, 2005).

To date, it remains unexplored how muscle synergies are related to force field adaptation, retention, and generalization; and what changes in their structure and activation patterns lead to the observed task-level kinematics and kinetics. While isometric visuomotor rotation studies (De Marchis et al., 2018, Gentner et al., 2013, Severini and Zych, 2020) showed that adaptation and spatial generalization do not require additional muscle synergies, a study by Oscari et al. (2016) hints that force field adaptation does require additional synergies. Furthermore, studies with a few muscles' EMGs in force field adaptation show two principal mechanisms. First, there is co-contraction of muscles acting around the elbow and shoulder joints, which decreases during adaptation but does not vanish completely (Franklin and Franklin, 2021, Milner and Franklin, 2005, Thoroughman and Shadmehr, 1999). Secondly, activity of specific muscles counteracting the force field increases, and their activation timing shifts toward the movement start (Albert and Shadmehr, 2016, Huang et al., 2012, Thoroughman and Shadmehr, 1999). Furthermore, even after a plateau in kinematic- and kinetic-dependent variables, muscle activity continues to decrease, presumably to reduce effort (Franklin et al., 2003, Huang et al., 2012). Accordingly, adaptation may be represented either by a combination of baseline reaching muscle synergies or by specific, effort-optimized muscle synergies. Either way, if muscle synergies viably represent the coordination of force field adaptation at a muscular level, we expect them to also represent retention and spatial generalization. In particular, if muscle synergies change to accommodate specific requirements for adaptation to reaching in some directions, they are a poor choice for capturing muscle patterns in unpracticed reaching directions, in line with previous narrow spatial generalization findings (Gandolfo et al., 1996, Ghez et al., 1999, Rezazadeh and Berniker, 2019).

To investigate how muscle synergies underlie force field adaptation, retention, and generalization at a muscular level, we first examined task-level variables. Accordingly, we hypothesized that (H_{Task} 1) people adapt, de-adapt, and re-adapt to the force field and that (H_{Task} 2) spatial generalization decreases with distance from the practiced movement direction. Building on this, we then analyzed muscle activation patterns and hypothesized that ($H_{\mathrm{Synergies}}$ 1) the muscle patterns of force field adaptation can be reconstructed by a combination of baseline reaching synergies. As this hypothesis did not hold, we hypothesized that ($H_{\mathrm{Synergies}}$ 2) specific muscle synergies are required. Lastly, we hypothesized that ($H_{\mathrm{Synergies}}$ 3) muscle synergies acquired through adaptation are only locally applicable, reflecting the narrow spatial generalization force field adaptation findings.

3.3 Materials and methods

3.3.1 Participants

Thirty-six right-handed (Oldfield, 1971) male volunteers (25.9 ± 2.8 years, 1.80 ± 0.05 m height, 77.2 ± 9.5 kg mass) naïve to force field adaptation experiments gave written informed consent before participating. The Karlsruhe Institute of Technology (KIT) Ethics Committee approved the study.

3.3.2 Apparatus and task

The participants sat at a KINARM End-Point Lab with a virtual reality (VR) display (KINARM, Kingston, Canada, Figure 3.1). The chair's height was individually adjusted so the participant sat upright, leaning his forehead against the VR frame, and had a 90° angle between the upper and forearm. In the starting position, the handle was located on the mid-sagittal plane in front of the torso. The participants performed 15 cm center-out point-to-point movements in the horizontal plane with their right hand. The VR display showed the handle's position as well as the starting and target points but obscured the view of the handle, hands, and arms. Participants were instructed to move the handle from the start to the target within 550 ± 50 ms after the handle had resided at the start point for at least 800 ms. The target color changed when reached, giving participants feedback on whether the specified movement time was met (green: within the time frame, blue:


[redacted]

Figure 3.1: Experimental setup. A participant with EMG electrodes attached sits at the KINARM End-Point Lab (KINARM, Kingston, Canada).

too fast, red: too slow). After the handle remained within the target for 800 ms, the manipulandum moved it back to the start for the subsequent trial. The five targets were located at -90°, -45°, 0°, 45°, and 90° (Figure 3.2).

3.3.3 Experimental design

3.3.3.1 Trial conditions

Three trial types were used: null field (NF), force field (FF), and error clamp (EC). In NF trials, the handle was freely movable without perturbing forces. In FF trials, a counterclockwise, velocity-dependent force field acted according to the formula:

$$\vec{\mathbf{F}} = k \cdot \begin{pmatrix} cos\ \theta & -sin\ \theta \\ sin\ \theta & cos\ \theta \end{pmatrix} \cdot \begin{pmatrix} \dot{x} \\ \dot{y} \end{pmatrix},$$

with k being the force field magnitude fixed at 20 Ns/m. The angle θ was fixed at 90°. Therefore, the force field always steered the handle's movement orthogonally to its direction of motion. The handle's velocity components are given by $\begin{pmatrix} \dot{x} \\ \dot{y} \end{pmatrix}$. In EC trials, the End-Point Lab restricted the motion to a small channel connecting the start and end points (Joiner and Smith, 2008, Scheidt et al., 2000). Therefore, the manipulandum created virtual walls with a viscosity of 10 kNs/m and a stiffness of 1 kN/m.

3.3.3.2 Groups assignment and schedule

The schedule consisted of six successive phases: familiarization, baseline, practice, short-term retention and generalization, washout, and long-term retention and generalization (Figure 3.2). Participants accustomed themselves to the task during the familiarization phase, which consisted only of NF trials with the directions in a random order (same order for all participants). During baseline, they reached for each target 20 times without perturbing forces (NF trials) and three times in the EC condition in a random order. The last three were FF trials in the -90°, 0°, and 45° directions. During practice, they performed 250 reaches in the FF condition to the 0° target. Therein, 26 EC trials were randomly interspersed. After a 30-second break, participants were tested for short-term retention (0° target) and generalization (-90° and 45° targets). Therefore, the three targets were reached first once in the EC and then twice in the FF condition. The short-term retention and generalization started with the 0° target. Half of the participants continued with the -90° target, the other with the 45° target. This was followed by the washout, consisting of 125 trials (114 NF and 11 EC). After a 10-minute break, the long-term retention and generalization phase followed. Every participant was randomly assigned to one of three groups (-90°, 0°, or

45°; each N = 12). The participants reached 250 times to one of the three targets only (target depending on groups assignment) with perturbing forces. Twenty-six EC trials were interspersed at the same trial number as during the practice phase. Participants could let go of the handle during the breaks.

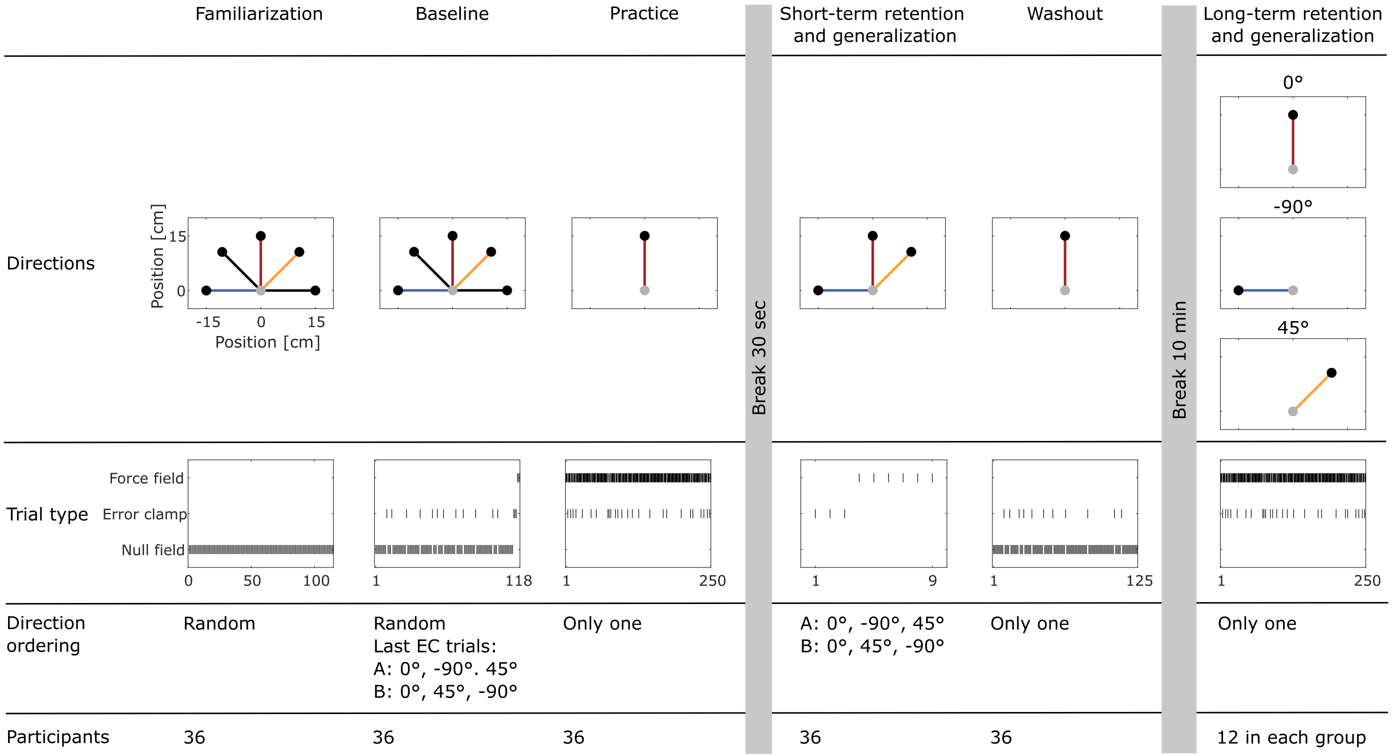

Figure 3.2: Experimental protocol. Participants performed center-out reaching movements of 15 cm in length. Start points are indicated by gray circular markers and target points by black circular markers. The top row shows the movement directions, and the second row shows the sequences of trial types. After washout, the 36 participants were randomly and evenly assigned to either the long-term retention, -90° generalization, or 45° generalization group.

3.3.4 Data analysis

Kinematic (hand position and velocity) and kinetic (interaction forces) data measured at the manipulandum's handle were recorded at 1,000 Hz with KINARM Dexterit-E software (KINARM, Kingston, ON, Canada).

Thirteen surface EMG electrodes (4,000 Hz; Noraxon USA, Scottsdale, AZ, USA) captured upper-body muscle activity of the following muscles (Figure 3.1): trapezius (descending “TrapD”, transverse “TrapT”, ascending “TrapA”), deltoid (anterior “DeltA”, middle “DeltM”, posterior “DeltP”), latissimus dorsi (“LatDorsi”), pectoralis major (“PectMaj”), serratus anterior (“SerrA”), triceps brachii (lateralis “TriLat” and medialis “TriMed”), biceps brachii (long head, “Bic”), and brachioradialis (“Bra”). Participants' skin was prepared by shaving, abrasion, and cleansing with alcohol to ensure good electrode-skin contact. Then, Ag/AgCl electrodes were attached according to SENIAM guidelines (Hermens et al., 2000) and Perotto (2011).

3.3.4.1 Pre-processing

Raw kinematic and kinetic data were filtered with a 4th-order Butterworth low-pass filter and a cut-off frequency of 6 Hz (kinematic) and 10 Hz (kinetic) following previous studies (Herzog et al., 2022, Stockinger et al., 2015). Movement start was defined as the instant the participant left the start point, and movement end when he reached the target point for the first time. Raw EMG data were bandpass filtered with a 20-450 Hz, 4th-order zero-lag Butterworth filter (Albert and Shadmehr, 2016). ECG artifacts apparent in the recordings of the trunk muscles were removed with a template-matching procedure (Peri et al., 2021). Subsequently, 50 Hz noise was removed with a 2nd-order zero-lag Butterworth notch filter (50 Hz and harmonics up to 500 Hz; Ahmad et al. 2013, Anwar et al. 2011). The filtered EMG data were full-wave rectified and envelopes were calculated using a 4th-order Butterworth low-pass filter with a cut-off frequency of 10 Hz. EMG data were segmented from 200 ms before the participant left the start point until 200 ms after they reached the target for the first time, e.g., including potential overshooting corrections. The segmented data were time-normalized to 101 time points. Then, the data were amplitude-normalized per muscle and participant to the maximum activity across all trials. Finally, the tonic EMG component was removed from all trials (d'Avella et al., 2006). To do so, a linear ramp was modeled using the average EMG envelope of each muscle in the 200 ms before the movement start and the 200 ms after target reach. Each calculation of averages included all baseline trials to the same direction. This direction-, muscle-, and participant-specific estimation of the tonic component was then subtracted from all respective trials. The remaining phasic parts of the EMG could contain negative values, which were clipped to zero. After careful observation, TrapD was excluded as it contributed only noise. All processing and analysis steps were performed in Matlab (R2023b, Natick, MA, USA).

3.3.4.2 Kinematic and kinetic dependent variables

Following previous studies, adaptation was assessed with a kinematic and a kinetic measure (Heald et al., 2018, Sing et al., 2009). The kinematic variable PD_{max} quantifies the maximum perpendicular distance between a trial's trajectory and a virtual straight line connecting the start and target. While it quantifies the net motor output with all control processes involved (Stockinger et al., 2015), the kinetic force field compensation factor ($FFCF$) quantifies the participant's force field prediction (Joiner and Smith, 2008, Scheidt et al., 2000). $FFCF$ was calculated by linear regression according to the formula:

$$F_{actual}(t) = a_1 \cdot F_{ideal}(t) + a_0 + e(t),$$

where the error $e(t)$ was minimized (least-squares). The regression coefficient a_0 was the axis intercept, and a_1 was the slope. The slope serves as $FFCF$. F_{actual} was the force with which the participant pressed the handle against the virtual wall. F_{ideal} was the product of the force field matrix and the trial's velocity profile, resulting in the force profile with which the participant would have produced a straight trajectory in the force field. If F_{ideal} and F_{actual} are identical, the $FFCF$ is 1; if unrelated, the $FFCF$ is 0. To consider only changes based on adaptation and generalization, all PD_{max} and $FFCF$ values were participant- and target-specific baseline-subtracted (Wagner and Smith, 2008).

3.3.4.3 Extraction and fitting of muscle synergies

We set up three hypotheses to investigate how force field adaptation, retention, and spatial generalization are represented in a modular structure, using the following "extract-and-fit" approach (Figure 3.3). To test $\text{H}_{\text{Synergies}}$ 1, that the muscle patterns of force field adaptation can be reconstructed by a combination of baseline reaching synergies, we extracted muscle synergies from the baseline trials (section 3.3.4.3) and tested their ability to explain the muscle patterns of the adapted state by fitting them on adapted state trials (see 3.3.4.3). To test $\text{H}_{\text{Synergies}}$ 2, that specific muscle synergies are required, we extracted shared-and-specific muscle synergies of the baseline and adapted state (see 3.3.4.3). A shared-and-specific muscle synergy extraction approach stems from the observation that synergy combinations span specific subspaces in muscle activation space, and that different sets of synergies may span the same subspace, as they can result from a rotation within the subspace. Thus, the approach aims to best identify the intersecting (i.e. shared) and the disjunct (i.e. specific) parts of the two subspaces spanned by two sets of muscle synergies (d'Avella and Bizzi, 2005, Cheung et al., 2005).

Alternatives to the shared-and-specific extraction have the following limitations. First, extracting from the pooled EMG would yield a muscle synergy representation underlying the two datasets, assuming that dimensions are shared, though this assumption is what is to be tested. Second, separate extractions with a subsequent similarity analysis may be misleading as the similarity value is not unambiguous but depends on the single sets muscle synergy extraction (Cheung et al., 2009). Finally, to test $\text{H}_{\text{Synergies}}$ 3, that muscle synergies acquired through adaptation are only locally applicable, reflecting the narrow spatial generalization force field adaptation findings, we fitted the shared-and-specific muscle synergies to the first 20 retention/generalization trials (see 3.3.4.3). Subsequently, we extracted shared-and-specific synergies from the baseline and adapted state together and the first retention/generalization trials (see 3.3.4.3), with the aim of identifying a muscle synergy representation of what facilitates retention and generalization.

Extraction of baseline muscle synergies

For every participant, a matrix $\mathbf{EMG} \in \mathbb{R}_{\geq 0}^{12\times 101\cdot 5}$ was composed, with the EMG data of the 12 muscles in rows and the five averaged trials with 101 time points each in columns. Each averaged trial consists of the averaged EMG data of the 23 baseline trials to the same target. We extracted spatial muscle synergies with non-negative matrix factorization (NMF; Lee and Seung 1999, 2001, Russo et al. 2024). NMF reduces the dimensionality of the EMG dataset by approximating it with N trial-invariant spatial muscle synergies $\mathbf{W_n} \in \mathbb{R}_{\geq 0}^{12\times 1}$, vectors specifying relative muscle activation levels, as well as N synergy activation profiles $\mathbf{C_n} \in \mathbb{R}_{\geq 0}^{1\times 101}$:

$$\mathbf{EMG}(t) \approx \sum_{n \in N} \mathbf{W_n} \cdot \mathbf{C_n}(\mathbf{t})$$

The decomposition was repeated 50 times with random initial conditions to avoid convergence to local minima and was limited to 3,000 iterations (Bach et al., 2021, Carey et al., 2021). The reconstruction quality was assessed using the multivariate $R^2 = 1 - SSE/SST$. SSE was calculated as the sum of the squared residuals and SST as the sum of the squared residuals from the mean vector (d'Avella et al., 2006). The number of extracted synergies N was chosen at the R^2-knee point, after which the R^2 curve remained approximately straight. The R^2 knee point was calculated using a series of linear regressions fitted to the R^2 versus N curve (Matlab `polyfit`), beginning with a regression across the interval $[1,\ 12]$. We then iteratively excluded the smallest value from the regression interval. We identified the optimal number of synergies N as the first N with a regression line from N to 12 with a mean square error smaller than 10^{-4} (d'Avella et al., 2006).

Quality of reconstruction of adapted state data with baseline muscle synergies

To investigate if baseline reaching muscle synergies can reconstruct the muscle patterns of force field adaptation, they were tested for their ability to explain the muscle patterns (R^2) in the adapted state. In particular, NMF was applied to the averaged EMG data from the last four force field trials of the adaptation phase, keeping the baseline synergies ($\mathbf{W_N} \in \mathbb{R}_{\geq 0}^{12\times 1}$) fixed and updating only the activation profiles ($\mathbf{C_N} \in \mathbb{R}_{\geq 0}^{1\times 101}$). Then, we compared the R^2 values of the reconstruction with a cross-validated R^2_{CV} of the baseline extraction. Therefore, we repeated the following process 100 times. Four randomly selected baseline trials to the same direction were averaged and constituted the test part of the cross-validation. The remaining 19 trials were averaged and horizontally concatenated with the remaining four average baseline trials, constituting the training part of the cross-validation (see 3.3.4.3). Muscle synergies were extracted from the training part and fitted to the test part. Cross-validation was used to prevent a misleading overestimation of the synergies' reconstruction ability on the baseline phase (Stone, 1974).

Extraction of shared-and-specific muscle synergies of baseline and the adapted state

To investigate if specific muscle synergies are required for force field adaptation, we extracted three sets of synergies from the combined baseline and adapted state data: one set shared between baseline and adapted state data, a second set specific to the baseline data, and a third set specific to the adapted state data (d'Avella and Bizzi, 2005, Cheung et al., 2005). We determined the number of shared synergies as the dimension of the shared subspace spanned by the synergies extracted separately from baseline and adapted state. To estimate such a dimension, we used a bootstrapping procedure that differentiated noise and structural differences (Brambilla et al., 2023b, Sylos-Labini et al., 2020). This procedure assumes that differences in the synergies extracted from different subsets of trials in the same conditions are due to noise rather than structural differences.

The procedure consisted of four steps. First, muscle synergies were extracted from the baseline and adapted state separately following the description in section 3.3.4.3. Thereby, the EMG data matrix of the baseline state consisted of the 12 muscles in rows and the five averaged trials in columns. Each trial was the average of the 20 NF baseline trials to the same direction. The adapted state matrix consisted of 12 muscles in rows and one averaged trial over the last 20 FF. The principal angles between the subspaces spanned by the two sets of muscle synergies were calculated ($\theta_{\mathit{Baseline\ vs.\ adapted\ state}}$; Golub and Van Loan 1989). Secondly, both baseline and adapted state datasets were split into two disjunct, equal-sized sub-datasets. The two baseline sub-datasets comprised five averaged trials, each from 10 randomly selected trials to the same direction. The two adapted state sub-datasets constituted one averaged trial, calculated on 10 randomly selected trials of the last 20 FF trials during adaptation. Muscle synergies were extracted from each subset, and the principal angles between the subspaces spanned by the muscle synergies of the same phase were calculated. The second step was repeated 500 times, each time with a random drawing with replacement of trials included in the sub-sets. This resulted in two principal angle distributions, one for the baseline and one for the adapted state. These distributions quantify the noise inherent in the baseline and the adapted state data. Thirdly, the principal angles from each

subset were used to obtain a new distribution of principal angles between baseline and adapted state synergies due only to noise. To do so, two new subspaces representing the "noise subspaces" for the baseline and adapted state were calculated starting from a common base and rotating each subspace according to the respective principal angle distribution. Then, the principal angles between the two newly constructed "noise subspaces" of the baseline and adapted state were calculated. The third step was repeated 500 times, providing a distribution of the principal angles from the "noise subspaces". Fourthly, the latter distribution's 95th percentile (θ_{95}) was calculated and compared to the principal angles between the original baseline and original adapted state synergies (step one, $\theta_{Baseline\ vs.\ adapted\ state}$). The number of shared synergies was defined as the number of principal angles between the baseline and the adapted state, which were smaller than the corresponding θ_{95}. This is based on the assumption that structural differences between muscle synergies are represented by much larger principal angles than those due to noise.
After these steps, which resulted in the number of muscle synergies shared between the baseline and adapted state, shared-and-specific muscle synergies were simultaneously extracted with an iterative process. The horizontal concatenation of the baseline and adapted state datasets, as described in the first step, constituted the input matrix for the NMF algorithm. Starting with the number of shared synergies, muscle synergies were extracted. The reconstruction qualities $R^2_{baseline}$ and $R^2_{adapted\,state}$ were calculated and compared to the original R^2 values obtained during the first step of the shared extraction. If the original R^2 values were not reached, a new NMF decomposition was performed with the number of shared synergies plus one or two, depending on the R^2 comparisons. Additionally, the matrix $\mathbf{C}$ with the synergy activation profiles was provided. $\mathbf{C}$ was initialized with random values in the cells for the shared synergies, baseline- and adapted state-specific synergies to extract. The remaining cells were filled with zeros. Therefore, using the properties of the NMF multiplicative update rule, activation profiles specific to one phase were not considered for the other phase.

Fitting shared-and-specific muscle synergies of baseline and the adapted state to the first trials of the long-term retention and generalization phase

To test $\mathrm{H}_{\mathrm{Synergies}}$ 3, that muscle synergies acquired through adaptation are only locally applicable, reflecting the narrow spatial generalization force field adaptation findings, we fitted (1) the baseline synergies and (2) the shared-and-specific muscle synergies extracted from baseline and the adapted state (see 3.3.4.3) to the average of the first 20 FF trials of the long-term retention and generalization phase and tested their ability to reconstruct the respective muscle pattern (R^2). If the hypothesis holds, then the reconstruction using the shared-and-specific synergies compared to using baseline synergies would be best for the 0° group (retention), higher than zero for the 45° group (limited generalization) and zero for the -90° group (no generalization).

Extraction of shared-and-specific muscle synergies of the baseline and the adapted state together and the start of the long-term retention and generalization phase

With a similar approach to the four steps described in the section 3.3.4.3 we extracted shared-and-specific synergies from the baseline and adapted state together and the first 20 FF retention/-generalization trials. The aim was to identify a muscle synergy representation of what facilitates retention and generalization. For the EMG data matrix of the baseline and adapted state, the same baseline matrix as described in the section 3.3.4.3 was concatenated horizontally with one averaged trial over the last 20 FF trials during adaptation. For the EMG data matrix of the retention/generalization trials, the first 20 FF trials during this phase were averaged. We then calculated the noise distributions in a similar way as described in section 3.3.4.3, with subsets of 10 averaged trials. We ensured that the muscle synergies extracted from the baseline and adapted state kept their structure as extracted in the section 3.3.4.3, i.e., their number of shared and specific synergies. Therefore, we initialized the $\mathbf{C}$ matrix with random numbers in cells according to the shared and specific synergies and zeros otherwise. Hence, in these calculations, the synergy vectors' values and the activation functions' values could vary, but the general structure of the synergy extraction remained. The combined shared-and-specific extraction in the last step also used a specific initialization of the $\mathbf{C}$ matrix. $\mathbf{C}$ was initialized with random values in the cells for the shared and specific synergies between the baseline and adapted state together and the first retention/generalization trials and zeros otherwise.

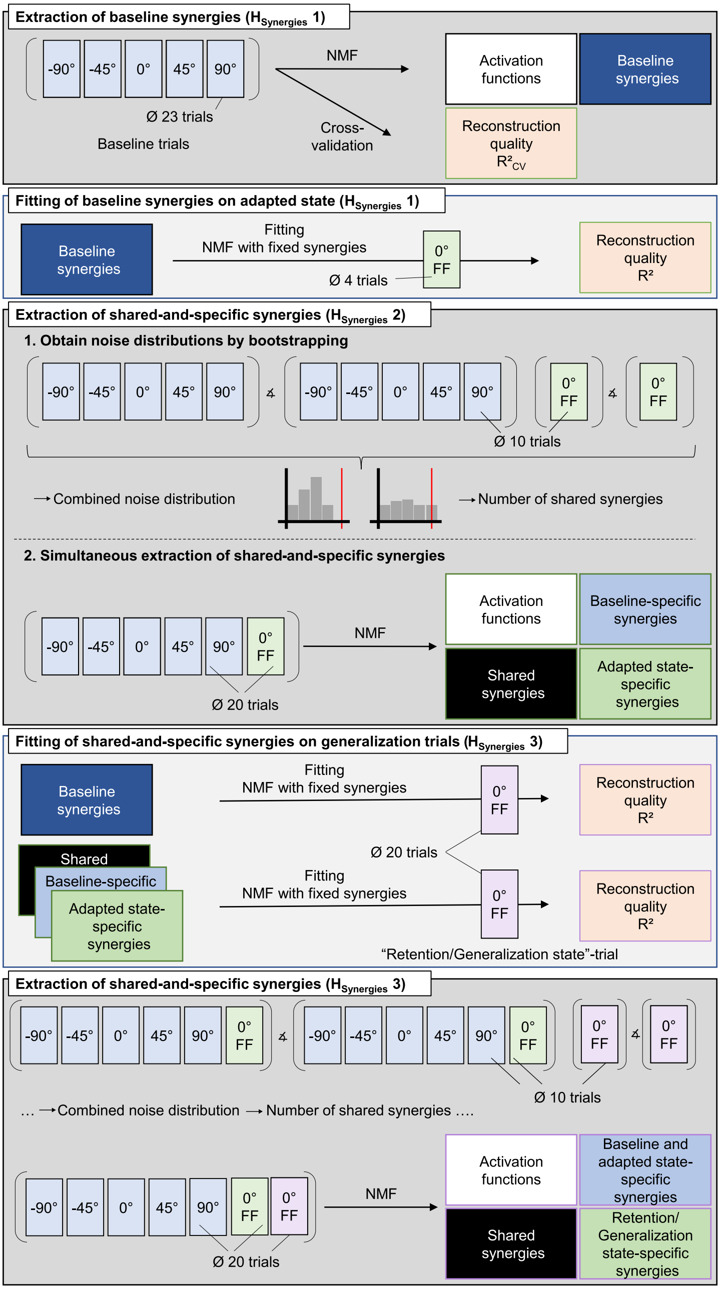

Figure 3.3: Summary of muscle synergy analyses. We followed an iterative "extract-and-fit" approach. First, baseline synergies were extracted and fitted to the adapted state. Next, shared-and-specific synergies of the baseline and adapted state were extracted and fitted to the first generalization trials. Finally, shared-and-specific synergies were extracted from the baseline and adapted state together and the first generalization trials. The ∡ sign illustrates the calculated principal angle.

Clustering of similar muscle synergies

To compare synergies extracted from different participants, we grouped them using cluster analysis. Each synergy was normalized to the maximum of its elements. First, hierarchical clustering (Matlab `pdist` (Minkowski distance; p = 3), linkage (Ward option), and cluster; Allen et al. 2019) was used to determine the optimal number of clusters. The number was chosen by assessing (1) the scree plot, which plots the within-cluster sum of squares of the linkage distance against the number of clusters, and (2) the silhouette method (Matlab `silhouette`), which quantifies the similarity of a given synergy to the other synergies in its cluster with respect to synergies from other clusters. The silhouette value s_{syn} for the synergy *syn* is calculated as follows:

$$s_{syn} = \frac{b_{syn} - a_{syn}}{\max(a_{syn}, b_{syn})}$$

Here, a_{syn} is the average distance (cosine similarity) from *syn* to the other synergies of the same cluster, and b_{syn} is the minimum average distance (cosine similarity) from *syn* to the synergies in a different cluster, minimized over the clusters. Silhouette values range from -1 to 1, with higher values indicating a better similarity. The number of clusters was chosen at the knee point of the scree plot and increased when a cluster contained low negative values (< -0.3).

Secondly, the synergies were clustered with k-means++ based on their cosine similarity. The centroids are the synergies with the least distance (1 - cosine) to all synergies within one cluster (Sylos-Labini et al., 2020).

3.3.4.4 Cosine tuning of the baseline synergy clusters

Synergy tuning curves were calculated for each baseline synergy cluster by a cosine fit using the integral under the mean activation of each synergy cluster and the target position (-90°, -45°, 0°, 45°, 90°; d’Avella et al. 2006). Therefore, the integrals were fitted with a linear regression according to the following formula (Matlab `regress`):

$$act(\theta) = \beta_0 + \beta_x cos(\theta) + \beta_y sin(\theta),$$

where $act(\theta)$ is the integral under the mean activation of each synergy cluster toward the target in the direction of θ. Synergies can be used to decelerate a movement going in the direction opposite to its “acting direction”. Therefore, synergy tuning curves were calculated for the first 25% of the movement duration, ensuring tuning only to the “acting direction”. The quality of the fits was assessed using R^2, and significance of the cosine tuning was assumed when the p-value of the regression between the data and the optimal cosine tuning was smaller than 0.05.

3.3.5 Statistical analysis

3.3.5.1 Kinematic and kinetic dependent variables

Differences in the kinematic and kinetic dependent variables, PD_{max} and $FFCF$, were tested as follows. Normality was assessed with Shapiro-Wilk tests and the homogeneity of variances with Levene's tests.

Whether the participants adapted and washed out (H_{Task} 1) was tested separately with dependent t-tests comparing the means of the first and last two FF trials and the first and last EC trials, respectively.

The short-term retention and generalization (H_{Task} 2) were assessed as follows: first, a one-way repeated-measurements ANOVA with subsequent post-hoc t-tests identified differences between the three groups (-90°, 0°, 45°) on the PD_{max} -mean of the two FF trials. Second, the $FFCF$ values were tested for differences against zero (zero = no retention/generalization) with one-sample t-tests separately for each direction. Third, $FFCF$ differences between the groups were tested with a one-way repeated-measurements ANOVA with subsequent post-hoc t-tests.

To determine if people (re-)adapt in the long-term retention and generalization phase, the three groups were tested separately with dependent t-tests on (1) the first and last two FF trials (PD_{max}) and (2) the first and last EC trials ($FFCF$). Furthermore, the first $FFCF$ values were tested for differences against zero (zero = no retention/generalization) with one-sample t-tests to assess retention and generalization.

To investigate H_{Task} 2, that generalization decreases with distance from the practiced movement direction, a linear mixed model (LMM) was used (Matlab `fitlme`). LMM allows the consideration of repeated measures (level 1) of a single participant (level 2), instead of the required aggregation of data as in t-tests or ANOVAs, which suits an adaptation experiment featuring inter-trial changes. The group assignment was included as a dummy variable using reference coding (either *DIR90* or *DIR45* set to 1, or both to 0 for the *DIR0* group). The first LMM was calculated with *DIR0* as the reference group and the second LMM with *DIR90* as the reference group, allowing investigation of all pairwise comparisons. LMM further allows the inclusion of both FF and EC trials into the model and also the interaction of trial type with trial duration; this improved the model fit based on the change in the -2 log-likelihood and the Akaike's information criterion (Matlab's `linearmixedmodel.compare` function; Ippersiel et al. 2021, Russell and Haworth 2014). The residual plots were inspected to assess linearity and homoscedasticity as prerequisites for LMM, and no gross violations were found (Hox et al., 2017).

The LMM regression formula was:

$$\begin{aligned} \mathit{Adaptation}_{tp} &= (\gamma_0 + u_{0p}) + \gamma_1 \mathit{DIR90}_{tp} + \gamma_2 \mathit{DIR45}_{tp} \\ &+ \gamma_3 \mathit{TrialType}_{tp} + \gamma_4 \mathit{TrialDuration}_{tp} \\ &+ \gamma_5 \mathit{TrialType}_{tp} \times \mathit{TrialDuration}_{tp} + \epsilon_{tp} \end{aligned}$$

Adaptation$_{tp}$ represents the PD_{max} or $FFCF$ value of the t^{th} trial for the p^{th} participant. The variable u_{0p} is a participant-specific random component and the γs are fixed effect parameters for the group assignment (dummy coding), trial type, trial duration, and the interaction of trial type and duration. Accordingly, the following formula was used for the function specification of the `fitlme` function: Adaptation $\sim$ DIR90 + DIR45 + TrialType $*$ TrialDuration + (1 | Participant). The LMM was implemented using the maximum likelihood method. Twenty trials were included.

3.3.5.2 Muscle synergy analyses

A dependent t-test was used to determine differences in the reconstruction quality of the baseline muscle synergies (R^2_{CV}) and their fit to the adapted state ($\mathrm{H}_{\mathrm{Synergies}}$ 1; section 3.3.4.3). The Kruskal-Wallis and Wilcoxon tests were used to test for improvements in the reconstruction quality between fitting the baseline synergies and fitting the shared-specific synergies on the retention/generalization trials, as the distribution was not normal ($\mathrm{H}_{\mathrm{Synergies}}$ 3).

3.3.5.3 General procedure

For all statistics, the significance level (two-tailed) was set a priori at 0.05. It was adjusted for multiple comparisons post-hoc with the Holm-Bonferroni correction (Holm, 1979), and to 0.025 for the LMM statistics as the test was carried out with two reference groups. The effect sizes were determined with η^2_p and Cohen's |d|; and classified as small (η^2_p $\geq$ 0.01, |d| $\geq$ 0.2), medium (η^2_p $\geq$ 0.06, |d| $\geq$ 0.5), and large (η^2_p $\geq$ 0.14, |d| $\geq$ 0.8; Cohen 1988).

3.4 Results

We were interested in how muscle synergies reflect force field adaptation, retention, and generalization at a muscular level. Therefore, we first examined whether all participants adapted, washed out, and showed retention/generalization ($\mathrm{H}_{\mathrm{Task}}$ 1 and $\mathrm{H}_{\mathrm{Task}}$ 2, Figure 3.4) based on the kinematic and kinetic dependent variables (PD_{max} and $FFCF$). Then, we examined the underlying muscle synergies of adaptation, retention, and generalization ($\mathrm{H}_{\mathrm{Synergies}}$ 1-3).

3.4.1 Participants adapted to the force field and washed out successfully

When first exposed to the force field, participants' trajectories became typically curved and then, with practice, became almost straight again ([PD_{max}: t(35) = 14.03, $p < 0.001$, d = 2.86; $FFCF$: t(35) = -9.15, $p < 0.001$, d = -2.28], Figure 3.4). Therefore, we can state that participants adapted to the force field. At the beginning of the washout, participants' trajectories became curved again, mirroring the initial trajectories of the adaptation phase, and then became almost straight again

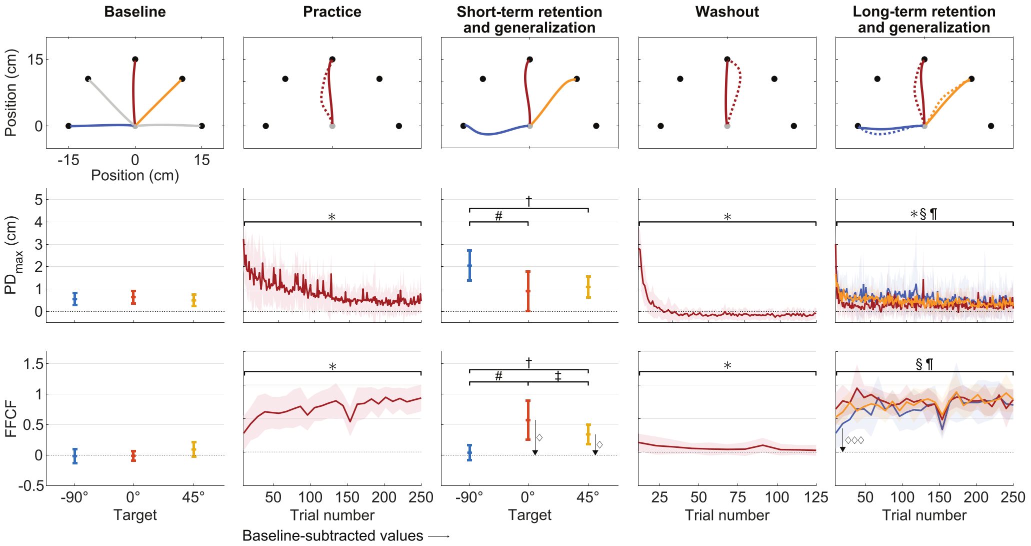

Figure 3.4: Kinematic and kinetic results. In columns: the different phases are arranged chronologically from left to right. Top row: Mean trajectories. Solid lines in baseline and short-term retention and generalization are mean values across all NF and FF trials and all participants. Dashed lines in practice, washout, and retention/generalization show mean values across all participants' first two trials in the respective phases. Solid lines, likewise, for the last two trials. Middle and bottom rows: PD_{max} and $FFCF$ mean and standard deviation values. The signs ∗, §, and ¶ indicate statistically significant differences over time for the 0°, -90°, and 45° targets, respectively. The # indicates a statistically significant difference between performance for the -90° and 0° target, the †between the -90° and the 45° and the ‡ between the 0° and 45° target. The ◇ indicates a statistically significant different value from zero.

[PD_{max}: t(35) = 22.60, p < 0.001, d = 5.15; $FFCF$: t(35) = -9.15, p < 0.001, d = -2.30]. Hence, participants washed out. We therefore accept H_{Task} 1, that the participants adapt to the force field and de-adapt after its removal.

3.4.2 Participants generalized better to the 45° than to the -90° target at the short-term retention and generalization test

After the adaptation period, all participants were tested for retention and generalization to the -90° and 45° targets. The ANOVA [F(2, 58.01) = 216.45, p < 0.001, η_p^2 = 0.86] and post-hoc t-tests on the PD_{max} values revealed no difference between the 0° and the 45° target [t(35) = -1.59, p = 0.120, d = -0.28] but indicated that there were differences between 0° and -90° [t(35) = 8.79, p < 0.001, d = 1.58] as well as between the -90° and 45° targets [t(35) = 8.22, p < 0.001, d = 1.56]. Hence, the generalization to the 45° was not worse than the 0° retention, and better than the generalization to the -90° target.

The $FFCF$ values were significantly different from zero for the 0° [t(35) = 10.77, p < 0.001, d = 1.76] and 45° target [t(35) = 12.91, p < 0.001, d = 2.11] but not the -90° target [t(35) = 1.84, p = 0.075, d = 0.30], indicating retention (0° target) and generalization to the 45° target only. The ANOVA [F(2, 50.32) = 53.37, p < 0.001, η_p^2 = 0.60] and post-hoc t-tests on the $FFCF$ values showed the best performance for retention, and better performance (i.e., better generalization) for the 45° than for the -90° target [-90° vs. 0°: t(35) = -8.86, p < 0.001, d = -2.15; -90° vs. 45°: t(35) = -9.43, p < 0.001, d = -2.06; 0° vs. 45°: t(35) = 4.01, p < 0.001, d = 0.91].

In summary, in the short term, participants showed retention, and also generalized better to the 45° than the -90° target.

3.4.3 Participants re-adapted to the practiced direction and showed better generalization to the 45° than to the -90° target at the long-term retention and generalization test

After the successful washout and a 10-minute break, the participants were randomly assigned to one of the three groups (-90°, 0°, 45°) and tested if they adapted (again) and presented differences across the directions.

All groups showed retention or generalization on the first trial as assessed with t-tests vs. 0 on the $FFCF$ values [-90°: t(11) = 5.47, p < 0.001, d = 1.47; 0°: t(11) = 13.61, p < 0.001, d = 3.66; 45°: t(11) = 13.83, p < 0.001, d = 3.71].

All groups showed a lower PD_{max} value at the end of the long-term retention and generalization phase than at the beginning [0° group: t(22) = 6.95, p < 0.001, d = 2.64; -90° group: t(22) = 4.73, p < 0.001, d = 1.80; 45° group: t(22) = 7.91, p < 0.001, d = 3.00]. The 0° group did not show a higher $FFCF$ value at the end than at the beginning but the -90° and 45° groups did [0° group: t(11) = -0.25, p = 0.807, d = -0.07; -90° group: t(11) = -4.66, p = 0.001, d = -1.63; 45° group: t(11) = -4.56, p = 0.001, d = -1.41]. To sum up, all participants showed retention or generalization at the beginning. Then, the -90° and 45° groups improved their performances further during the generalization phase, while improvement of the 0° group was only apparent in PD_{max}.

We used LMM analysis to assess differences between the groups during the initial phase of retention and generalization (20 trials · 36 participants = 720 observations, ICC = 0.09; Table 3.1), which revealed statistically significant differences between the groups. The retention performance was better than generalization (p < 0.001 and p = 0.021). Generalization was better for the 45° than the -90° target (p = 0.017).

Table 3.1: Statistical results of the LMM on the first 20 FF trials of the long-term retention and generalization phases. The asterisks indicate statistical significance after Bonferroni correction for multiple testing.

Reference group: 0°			
Fixed effects	**ß estimate (lower, upper 95% CI)**	**t**	**p**
(Intercept)	0.03 (-0.01, 0.07)	1.54	0.249
DIR90	-0.06 (-0.08, -0.04)	-5.19	<0.001*
DIR45	-0.03 (-0.05, -0.01)	-2.56	0.021*
TrialType is EC	0.64 (0.53, 0.75)	11.33	<0.001*
TrialDuration	0.01 (-0.05, 0.07)	0.40	1.000
TrialType is EC × *TrialDuration*	-0.07 (-0.30, 0.15)	-0.62	1.000
Random effects			
(Intercept)	0.01 (0.00, 1.78		
Error	0.12 (0.12, 0.13)		
Reference group: -90°			
Fixed effects			
(Intercept)	-0.03 (-0.07, 0.01)	-1.43	0.305
DIR0	0.06 (0.04, 0.08)	5.19	<0.001*
DIR45	0.03 (0.01, 0.05)	2.63	0.017*
TrialType is EC	0.64 (0.53, 0.75)	11.32	<0.001*
TrialDuration	0.01 (-0.05, 0.07)	0.40	1.000
TrialType is EC × *TrialDuration*	-0.07 (-0.30, 0.15)	-0.62	1.000
Random effects			
(Intercept)	0.01 (0.00, 1.78)		
Error	0.12 (0.12, 0.13)		

3.4.4 Two to five muscle synergies are employed during baseline

We used muscle synergy analysis to assess the changes in muscle patterns underlying force field adaptation. First, we extracted muscle synergies from the baseline phase. Over all participants, 3.6 ± 0.6 synergies led to a reconstruction quality (R^2) of 0.82 ± 0.04 (Table 3.2). Figure 3.5 displays the R^2 and EMG for every participant, as well as synergies and their reconstruction for one exemplary participant. Across all participants, baseline muscle synergies comprised simultaneous activations of multiple muscles, including mono-articular and bi-articular muscles. Five of the eight baseline muscle synergy clusters were directionally tuned according to a cosine tuning function (Figure 3.6).

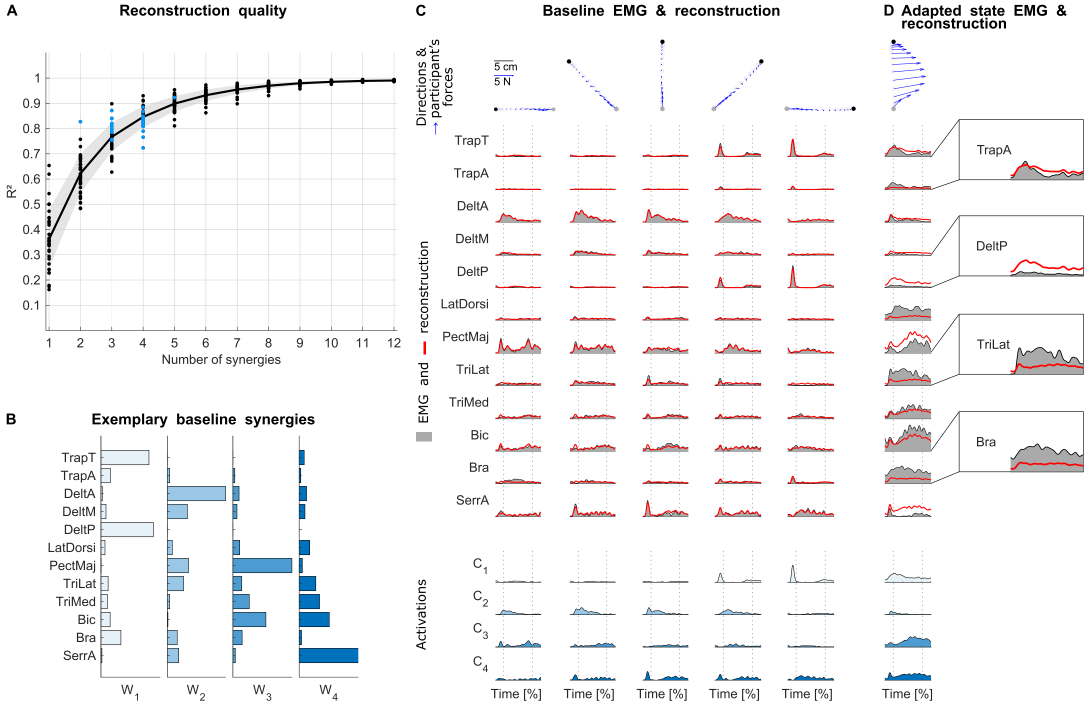

Figure 3.5: Muscle synergy extraction from baseline. A: Reconstruction quality R^2 as a function of the number of extracted synergies. The dots represent individual values and the solid, shaded line represents mean and standard deviation. Blue colored dots show the participant-specific selected numbers based on the R^2-knee criterion. B: Baseline muscle synergies extracted from one exemplary participant. C Top: Mean trajectory and forces averaged over all trials for every direction during baseline from the same exemplary participant. The distances of the dots illustrating the trajectories display the reaching speed (inter-dot distance corresponds to 8% of the trial duration). C Middle: EMG averaged over all trials for each direction during baseline from the same exemplary participant (gray) and the respective reconstructions (red). C Bottom: Activation functions for every direction in columns. Each activation function belongs to one muscle synergy (e.g., C_1 belongs to W_1). D: Trajectories, forces, and EMG averaged over the last 20 FF trials during adaptation for the same participant and the respective reconstruction by the baseline synergies (“baseline fit”). The enlargements show the mismatches in detail for four muscles. The dotted lines in C and D show the time points when the participant left the start point and reached the target point.

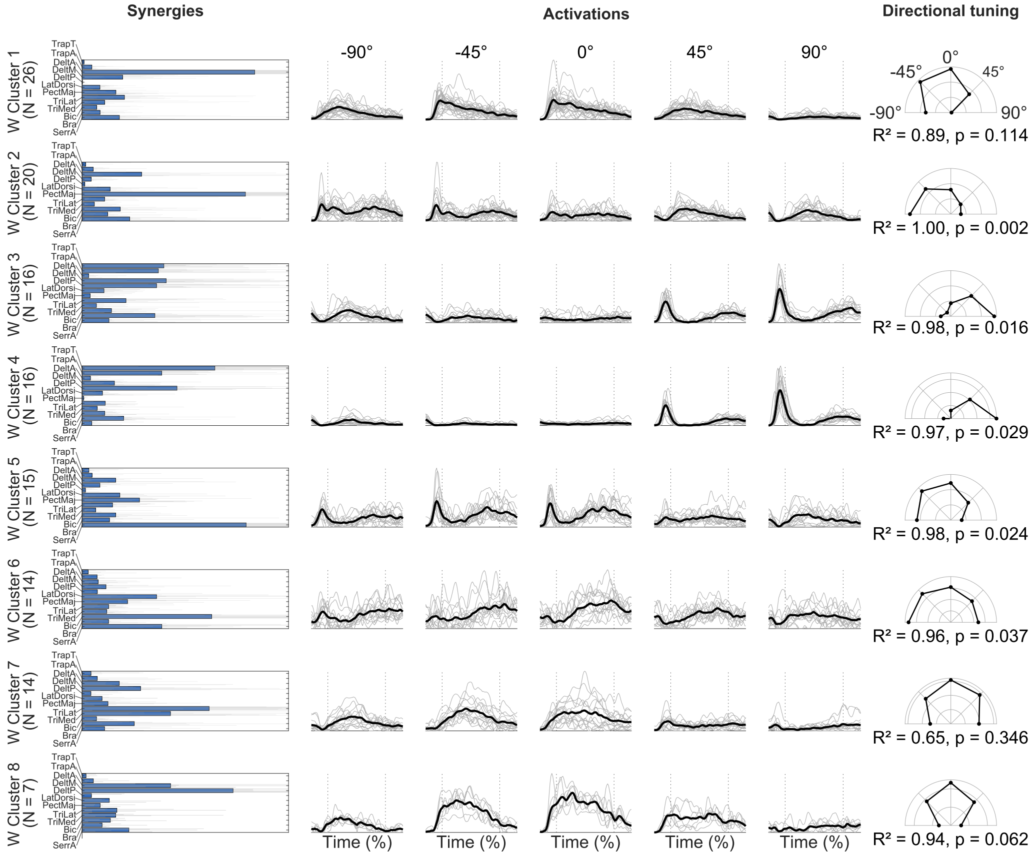

Figure 3.6: Clustering and cosine fit of the baseline synergies. The left column shows the centroids (filled bars) and the individual synergies in gray solid lines. The middle column shows the mean (black, solid lines) and the individual (gray, solid lines) activation functions separated for the five directions. The dotted lines show the average time points when the participants left the start point and reached the target point. The right column shows the cosine tuning.

Table 3.2: Individual results from the muscle synergy analysis. The last three rows present the results aggregated for the three groups (-90°, 0°, 45°).

Participant	Group	Baseline synergies	R^2 baseline	R^2_{CV} baseline (mean and SD)	R^2 fit of baseline synergies on the first 4 FF trials of the practice phase	Shared synergies baseline & adapted state	Specific baseline synergies	Specific adapted state synergies	R^2 fit of baseline synergies on first retention/generalization trials	R^2 fit of shared-and-specific synergies on first retention/generalization trials	Shared synergies with first retention/generalization trials	Specific synergies of first retention/generalization trials
1	0°	4	0.88	0.75 ± 0.14	-0.90	2	3	2	-5.07	0.71	2	1
2	0°	3	0.75	0.72 ± 0.17	0.31	0	3	2	-0.10	0.84	2	1
3	45°	4	0.72	0.71 ± 0.16	-0.40	3	2	1	-0.20	-0.11	3	2
4	-90°	4	0.85	0.73 ± 0.15	0.33	2	3	3	-1.45	-1.31	3	2
5	45°	4	0.81	0.73 ± 0.16	-1.54	1	4	2	0.39	0.46	3	2
6	45°	3	0.81	0.74 ± 0.15	0.51	2	2	2	-0.47	-0.07	3	1
7	45°	3	0.84	0.74 ± 0.13	-1.24	1	3	2	-3.79	0.26	3	2
8	0°	3	0.79	0.70 ± 0.24	-0.60	1	2	2	0.01	0.78	3	1
9	0°	3	0.81	0.72 ± 0.15	-0.03	2	2	1	-0.73	-0.10	3	1
10	-90°	4	0.82	0.73 ± 0.16	-0.52	2	3	1	0.20	0.41	2	2
11	45°	2	0.83	0.75 ± 0.13	-0.92	1	2	2	-2.55	-1.76	2	3
12	0°	4	0.81	0.73 ± 0.17	0.43	2	3	1	-0.21	-0.49	2	2
13	45°	4	0.87	0.70 ± 0.20	-0.14	1	4	2	-1.95	-0.14	2	2
14	-90°	3	0.81	0.75 ± 0.14	0.20	2	2	2	-0.45	-0.06	3	2
15	-90°	3	0.79	0.74 ± 0.13	-2.45	0	3	2	-3.89	-1.08	3	2
16	0°	4	0.81	0.71 ± 0.21	-1.39	1	4	3	-1.85	0.39	2	1
17	-90°	3	0.84	0.72 ± 0.19	-0.37	1	3	2	-0.77	-0.27	2	1
18	45°	4	0.79	0.72 ± 0.26	0.09	2	3	1	-1.35	-0.73	3	1
19	-90°	4	0.84	0.69 ± 0.23	0.16	2	3	2	-0.24	0.02	3	1
20	-90°	4	0.84	0.73 ± 0.15	-0.09	1	4	3	-5.68	-2.02	3	2
21	0°	4	0.81	0.70 ± 0.23	0.52	3	2	2	-0.19	0.06	2	1
22	0°	3	0.82	0.69 ± 0.23	-1.03	0	3	2	-1.68	0.52	3	2

23	-90°	5	0.92	0.73 ± 0.15	0.46	1	5	1	-0.29	-0.23	2	2
24	0°	4	0.82	0.72 ± 0.14	-0.15	2	3	2	-1.00	0.03	2	2
25	45°	3	0.76	0.75 ± 0.11	-0.40	1	3	2	-1.24	-0.40	2	3
26	-90°	3	0.82	0.74 ± 0.15	-1.93	1	3	2	-1.65	0.65	2	2
27	45°	4	0.77	0.73 ± 0.13	-0.30	1	4	3	-3.65	0.07	3	1
28	0°	3	0.79	0.73 ± 0.16	-1.25	1	3	2	-0.49	0.82	2	1
29	0°	3	0.87	0.73 ± 0.17	0.24	1	3	2	-0.47	0.55	2	2
30	45°	3	0.79	0.75 ± 0.11	0.35	2	2	1	-2.81	-0.34	3	2
31	45°	3	0.80	0.73 ± 0.16	0.14	2	2	1	-1.28	-0.75	0	4
32	0°	4	0.85	0.73 ± 0.22	-0.35	2	3	2	-5.10	-0.22	3	2
33	-90°	4	0.83	0.75 ± 0.13	-0.97	2	3	2	-0.59	0.52	2	2
34	-90°	4	0.84	0.72 ± 0.18	-0.33	2	3	2	0.19	0.66	3	2
35	-90°	4	0.85	0.72 ± 0.16	-0.38	2	3	2	-0.78	-0.45	3	2
36	45°	4	0.83	0.73 ± 0.18	-0.33	1	4	3	-1.49	-1.14	2	1
Mean ± SD	0°	3.5 ± 0.5	0.82 ± 0.04	0.72 ± 0.04	-0.35 ± 0.67	1.42 ± 0.09	2.83 ± 0.58	1.92 ± 0.51	-1.41 ± 1.82	0.32 ± 0.45	2.33 ± 0.49	1.42 ± 0.51
Mean ± SD	-90°	3.8 ± 0.6	0.84 ± 0.03	0.73 ± 0.03	-0.49 ± 0.89	1.50 ± 0.67	3.17 ± 0.72	2.00 ± 0.60	-1.28 ± 1.74	-0.26 ± 0.84	2.58 ± 0.51	1.83 ± 0.39
Mean ± SD	45°	3.4 ± 0.7	0.80 ± 0.04	0.72 ± 0.04	-0.35 ± 0.62	1.50 ± 0.67	2.92 ± 0.90	1.83 ± 0.72	-1.70 ± 1.31	-0.39 ± 0.62	2.42 ± 0.90	2.00 ± 0.95

3.4.5 The muscle patterns after adaptation cannot be reconstructed by baseline reaching synergies only, and require additional adaptation-specific muscle synergies

We tested if the muscle patterns of force field adaptation can be reconstructed by a combination of baseline reaching synergies ($\text{H}_{\text{Synergies}}$ 1). The reconstruction quality R^2 was significantly worse for the adapted state than the cross-validated R^2_{CV} of the baseline [t(35) = 7.61, p < 0.001, d = 1.76], with R^2 values on average 0.98 ± 0.69 lower for every participant (Table 3.2). This low reconstruction quality, i.e., the mismatch between the reconstructed EMG and the original EMG, is illustrated in the example of Figure 3.5D. Hence, muscle synergies of unperturbed reaching cannot explain muscle patterns for reaching in a force field, and we reject $\mathrm{H}_{\mathrm{Synergies}}$ 1.

Subsequently, we tested if specific muscle synergies are required using the bootstrap approach ($\mathrm{H}_{\mathrm{Synergies}}$ 2). The higher the number of shared synergies, the more subspace dimensions are shared. Across all participants, we found 1.47 ± 0.74 shared synergies but 2.97 ± 0.74 baseline-specific and 1.92 ± 0.60 adapted state-specific synergies. All synergies were clustered across all participants into four shared, seven baseline-specific, and three adapted state-specific synergies clusters (Figure 3.7, Figure 3.8).

Three of the four shared synergies are directionally tuned, two toward the left and one to the right. Two synergies (clusters 1 and 4) show high activation in the middle and end of the adapted state trial and may, therefore, represent a deceleration of the reach. One synergy tuned to the right side is active at the beginning of the adapted state trial, probably to counteract the perturbation. However, the shared synergies do not contribute much to representing adapted state reaching, as an additional 1.92 ± 0.60 adapted state-specific synergies were necessary to describe the muscle pattern in the adapted state.

The baseline-specific synergies and their activation function overall resemble those of the synergies extracted solely from the baseline. The baseline clusters 1, 2, 3, 4, 5, 6, and 7 from the shared-and-specific extraction resemble baseline clusters 3 and 4, 2, 1, 5, 8, 7, and 6 from the baseline extraction only (Figure 3.6 and Figure 3.7). Accordingly, the synergies employed during the baseline are specific to this phase and are not used in the adapted state.

The adapted state-specific synergy cluster 1 (Figure 3.8) shows high activations of muscles that extend the elbow and the shoulder horizontally, i.e., rotate the arm outward while extending it. This synergy is activated early in the movement, with its peak activity shortly after the start. Cluster 2 shows high activations of TriLat and TriMed, the two main contributors for elbow extension; it is active over the whole trial, with the peak in the middle of the movement. Cluster 3 shows the co-activation of many muscles that act in opposing directions (e.g., DeltA and DeltM, PectMaj and LatDorsi), probably reflecting co-contraction, and especially high activations of Bic, DeltA and DeltM, and PectMaj. These muscles can be seen as antagonists of the aforementioned muscles during the reaching movement toward the 0° target. This synergy shows two peak activations, the first before the beginning of the movement and the second before reaching the target. The three synergies are activated in four phases. After an initial co-contraction (cluster 3), clusters 1 and 2 are activated, leading to forces toward the target ($\mathrm{Force}_{\mathrm{y}}$) and against the counter-clockwise force field ($\mathrm{Force}_{\mathrm{x}}$). Interestingly, the two synergies' activations overlap but have their peaks one after the other; yet $\mathrm{Force}_{\mathrm{x}}$ has a Gaussian shape without any jitter. Afterward, the arm is decelerated by cluster 3, which is reflected in the negative values of $\mathrm{Force}_{\mathrm{y}}$.

Figure 3.9 shows the detailed reconstruction of the adapted state for the exemplary participant with the shared-and-specific synergy extraction. One synergy is shared between the baseline and the adapted state (Figure 3.9B, W_1), as obtained by evaluating the principal angle distributions (Figure 3.9C). There are four baseline-specific synergies (W_2-W_5), resembling those of the baseline-only extraction (Figure 3.5), except that the high PectMaj activity is now present in the shared synergy W_1. Most interestingly, the adapted state-specific synergies W_6 and W_7 show the subsequent but overlapping activation of two synergies which reflect arm extension and outward rotation, probably leading to forces necessary for adapted reaching. This stays in contrast with unperturbed reaching. While one synergy (W_5) showed agonistic muscle activations for unperturbed 0° reaching, two muscle synergies showed it in adapted state reaching (W_6 and W_7). One specialty of this participant is the high activation of the Bic throughout the movement.

In summary, the adapted state EMG patterns are represented predominantly by adapted state-specific muscle synergies with a four-phasic activation pattern.

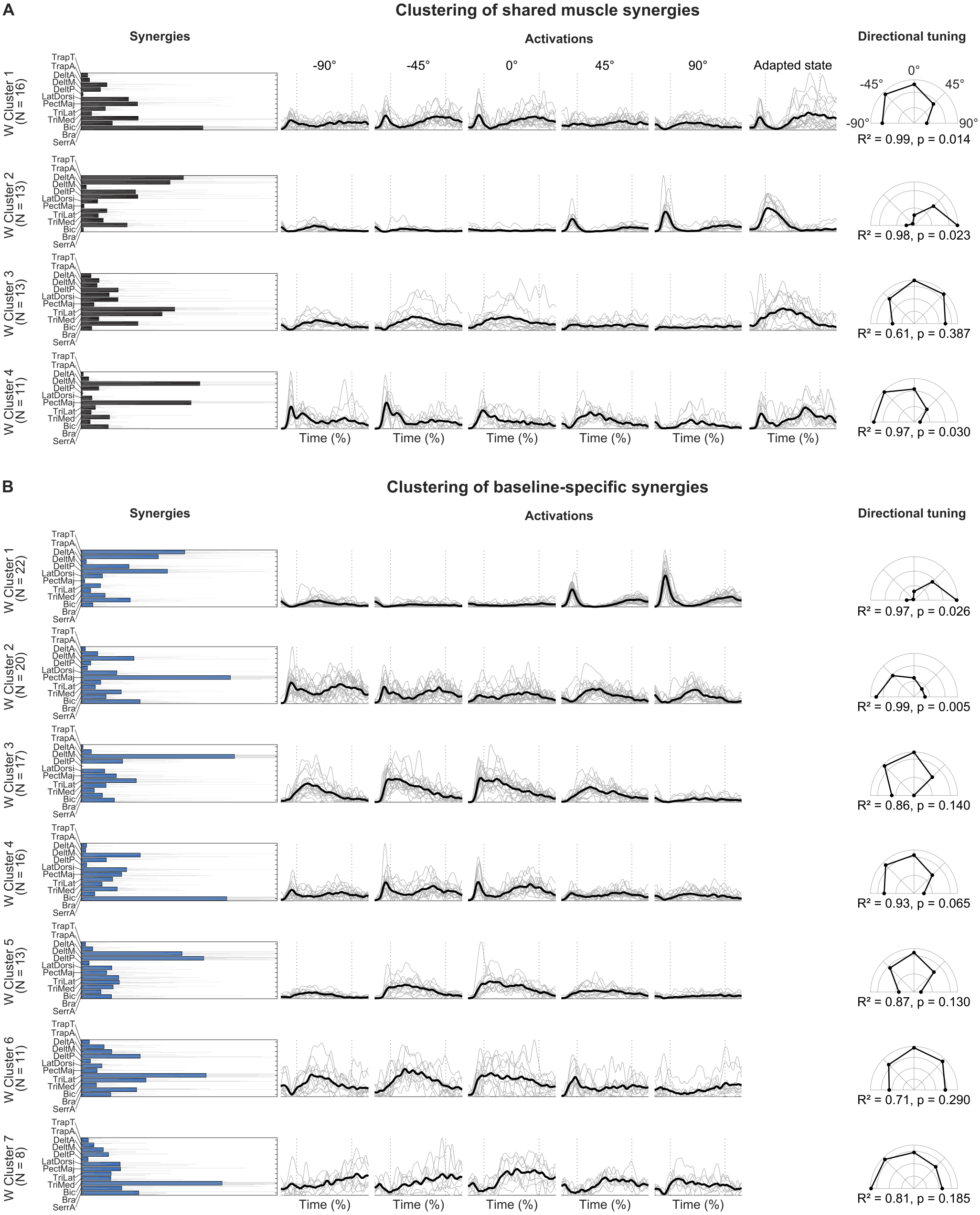

Figure 3.7: Results of the clustering of the shared-specific muscle synergy extraction of baseline and adapted state. A: Clusters of the shared muscle synergies. B: Clusters of the adapted state-specific muscle synergies. The left column shows the centroids (filled bars) and the individual synergies in gray solid lines. The middle column shows the mean (black, solid lines) and the individual (gray, solid lines) activation functions. The dotted lines show the average time points when the participants left the start point and reached the end point. The right column shows the cosine tuning based on the baseline activation functions.

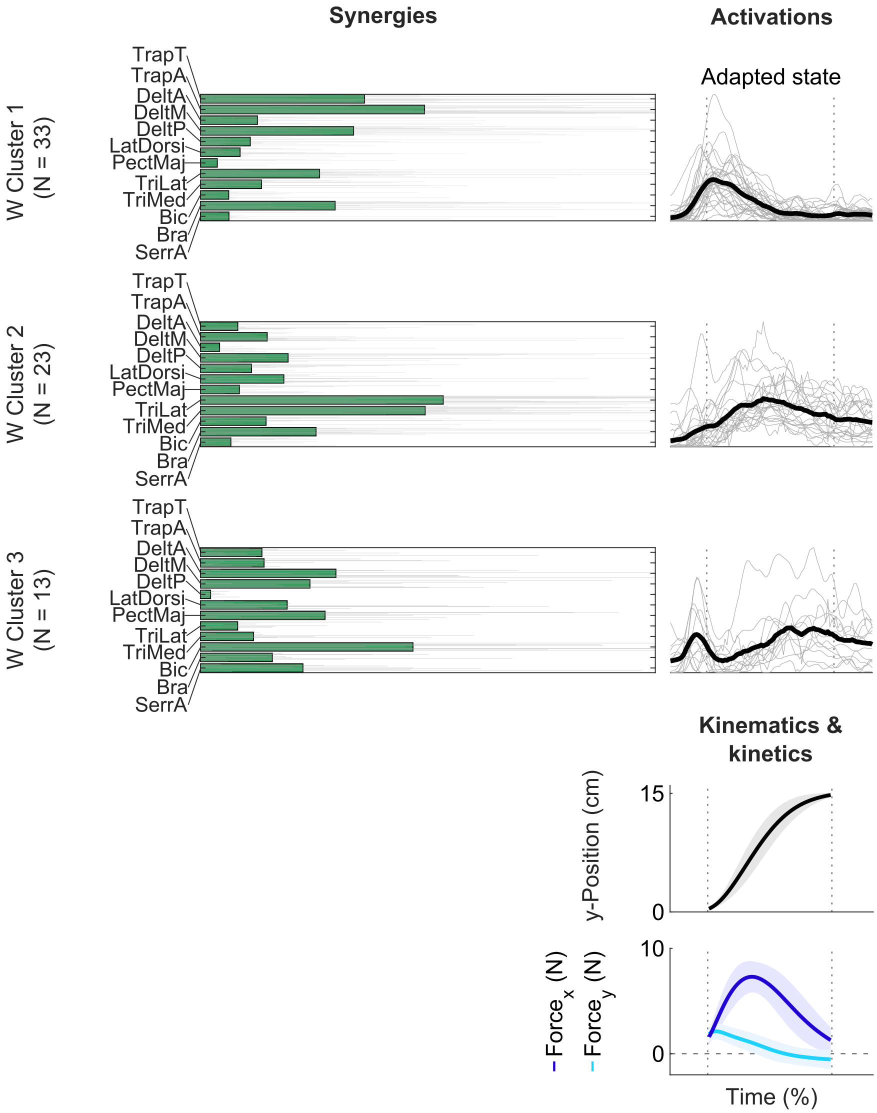

Figure 3.8: Shared-and-specific synergy extraction and clustering of the adapted state-specific synergies. The left column shows the centroid (filled bars) and the individual synergies in gray solid lines. The right column shows the mean (black, solid lines) and the individual (gray, solid lines) activation functions. Below, the position of the handle in the y-direction is shown as mean (solid black line) and standard deviation (gray shaded) across all participants and the last 20 FF trials. Similarly, the participant's mean forces in the x- and y-direction are shown as mean (blue solid lines) and standard deviations (blue shaded line). The dotted lines show the average time points when the participants left the start point and reached the end point. The dashed line shows 0 N.

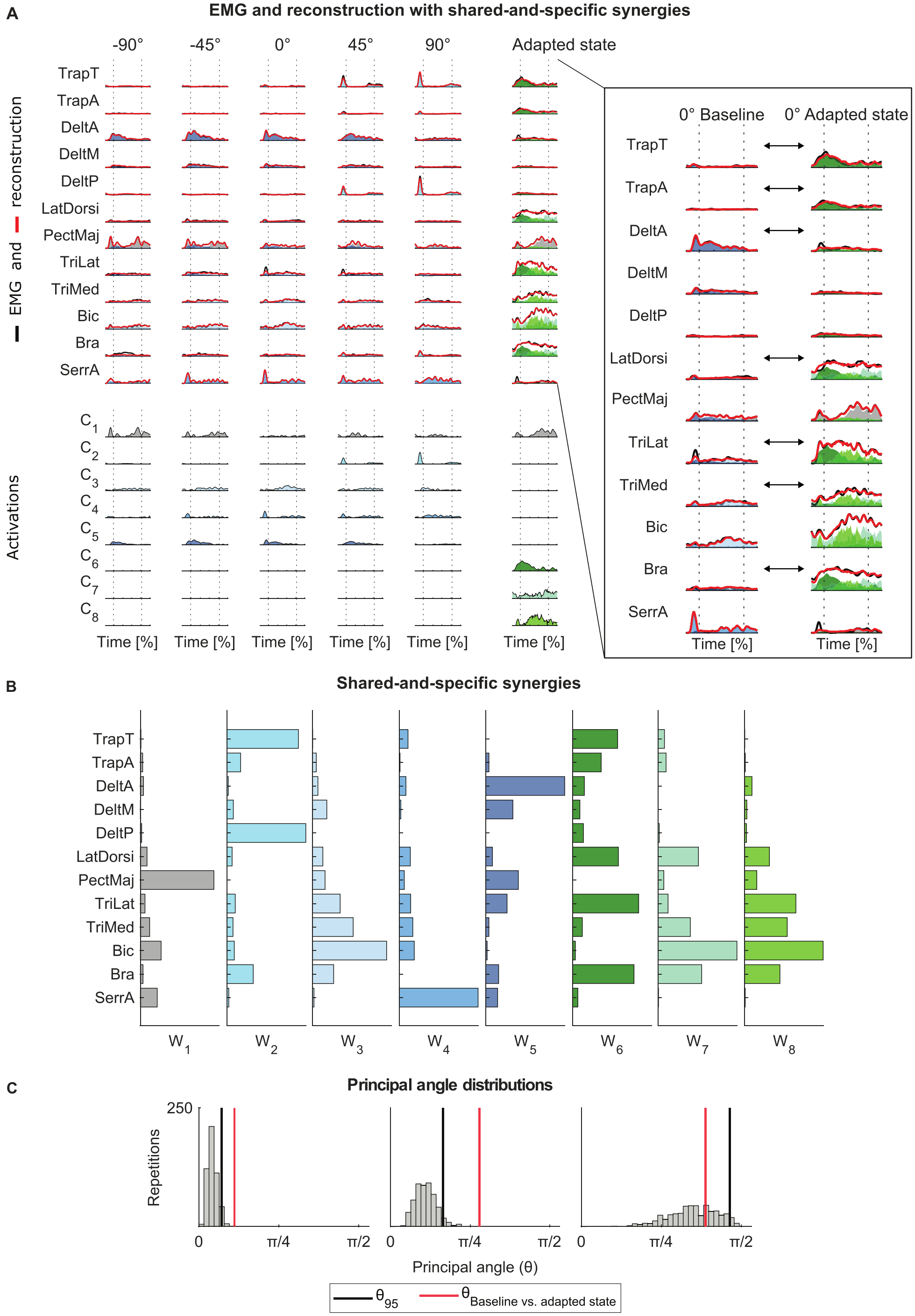
A
EMG and reconstruction with shared-and-specific synergies
-90°
-45°
0°
45°
90°
Adapted state
TrapT
TrapA
DeltA
DeltM
DeltP
LatDorsi
PectMaj
TriLat
TriMed
Bic
Bra
SerrA
EMG and reconstruction
Activations
C_1
C_2
C_3
C_4
C_5
C_6
C_7
C_8
Time [%]
0° Baseline
0° Adapted state
B
Shared-and-specific synergies
W_1
W_2
W_3
W_4
W_5
W_6
W_7
W_8
C
Principal angle distributions
250
Repetitions
0
π/4
π/2
Principal angle (θ)
θ_{95}
$\theta_{\text{Baseline vs. adapted state}}$

Figure 3.9: Reconstruction of the baseline and adapted state EMG with the shared-and-specific muscle synergies. A: EMG (solid black lines) and reconstruction (solid red lines) of shared-and-specific synergy extraction of one exemplary participant. The reconstruction is calculated as the sum of the products of the synergies with their respective activation functions. Here, the reconstruction of each product is plotted transparently to illustrate their contributions to the overall reconstruction. The activation functions of the synergies are plotted below. The enlargement shows the reconstruction of the 0° baseline and adapted state in greater detail; arrows guide the reader to substantial differences in synergy activations. B: Muscle synergies. The shared synergy is gray, the baseline-specific synergies in blue shades, and the adapted state-specific synergies in green shades. C: Combined principal angle distributions obtained with the bootstrapping procedure for the exemplary participant. The vertical black line signifies each distribution's 95th percentile (θ_{95}), and the red line is the principal angle between the baseline and adapted state synergies.

3.4.6 Muscle synergies acquired during adaptation facilitate long-term retention and generalization

Kinematics and kinetics indicated that the 0° group showed retention and that the 45° and 90° groups showed generalization, with slightly better values for the 45° group (see 3.4.3). Therefore, we tested whether muscle synergies can reflect these findings using the shared-and-specific synergies extracted from the baseline and adapted state to reconstruct the muscle patterns of the long-term generalization phase ($\mathrm{H}_{\mathrm{Synergies}}$ 3).

We found that the shared-and-specific synergies explained the muscle patterns at the beginning of the long-term retention and generalization phase better than the baseline synergies, as all groups showed a significant improvement in the reconstruction quality R^2 (-90°: W = 78, $p < 0.001$, d = 1.02; 0°: W = 78, $p < 0.001$, d = 0.93; 45°: W = 78, $p < 0.001$, d = 1.16; Table 3.2, Figure 3.10A). This means that the muscle patterns during the first trials of the long-term retention and generalization phase can be better explained by the synergies that capture the changes occurring during adaptation (shared-and-specific synergies) than those that do not (baseline synergies). However, there was no difference between the groups regarding the improvement in reconstruction achieved with shared-and-specific synergies with respect to baseline synergies [H(2, 35) = 1.76, p = 0.415, $\eta_p^2 = 0.05$].

Next, we investigated the dimensionality and the structure of the muscle synergies that facilitate retention and generalization. This was done by comparing the shared-and-specific synergies extracted from the baseline and adapted state together and the synergies extracted from retention/-generalization trials. We found 2.50 ± 0.50 shared dimensions between the subspaces spanned by the baseline and adapted state synergies and retention/generalization synergies. Hence, more synergies are shared in this case than between baseline and adapted state synergies (Figure 3.10B). Accordingly, the higher number of shared dimensions indicates that the muscle synergies reflect the findings of retention and generalization in the kinematic and kinetic variables. The acquired structural changes in the synergies that occurred during adaptation may facilitate retention and generalization. Figure 3.10C shows the clusters of the shared synergies between the baseline and adapted state synergies and the retention/generalization synergies. The first three resemble the adapted state-specific synergies reported in the section 3.4.5 (clusters 1, 2, and 3 in Figure 3.10C resemble clusters 2, 3, and 1 in Figure 3.8). Furthermore, for the retention, we observe the described four-phasic pattern again. Also, the 45° group shows a similar four-phasic pattern, with the same synergies activated one after another, as the 0° retention group. The -90° group differs from the 0° and 45° groups. Cluster 1 is activated later in the movement and cluster 2 is activated earlier, probably accelerating the arm toward the target instead of decelerating, and only two participants show synergies for cluster 3. Still, we observe that two muscle synergies are activated in an overlapping matter with subsequent activity peaks when the handle moves between the start and stop targets, just like the 0° and 45° groups.

However, the differences between the groups observed with PD_{max} and $FFCF$ are not well reflected in the modular structure, as we found no differences regarding the reconstruction quality of the baseline and adapted state shared-and-specific synergies on the first retention/generalization trials or the number of specific synergies between the -90° and the 45° groups. Hence, we reject $\mathrm{H}_{\mathrm{Synergies}}$ 3.

Figure 3.10: Difference in reconstruction quality (R^2) between fitting of shared-and-specific and baseline synergies on first retention/generalization trials (next page). Bars represent the mean and dots individual values. The values are presented according to their group. A value larger than zero indicates that shared-specific synergies better reconstructed the EMG of the first retention/generalization trials than baseline synergies. The $\diamond$ sign indicates a significant difference from zero B: Comparison of how many synergies are shared between (1) the baseline and the adapted state and (2) the shared-and-specific synergies of the baseline and adapted state together and the first retention/generalization trial. The box chart shows the median and the lower and upper quartiles, and lines show individual values. C: Clustering results of the shared synergies from the shared-and-specific synergy extraction of baseline and adapted state together and the retention/generalization trials. The left column shows the centroid (filled bars) and the individual synergies in gray solid lines. The right columns show the mean (solid lines) and the individual (gray, solid lines) activation functions, separated for the three groups. The dotted lines show the average time points when the participants left the start point and reached the target point.

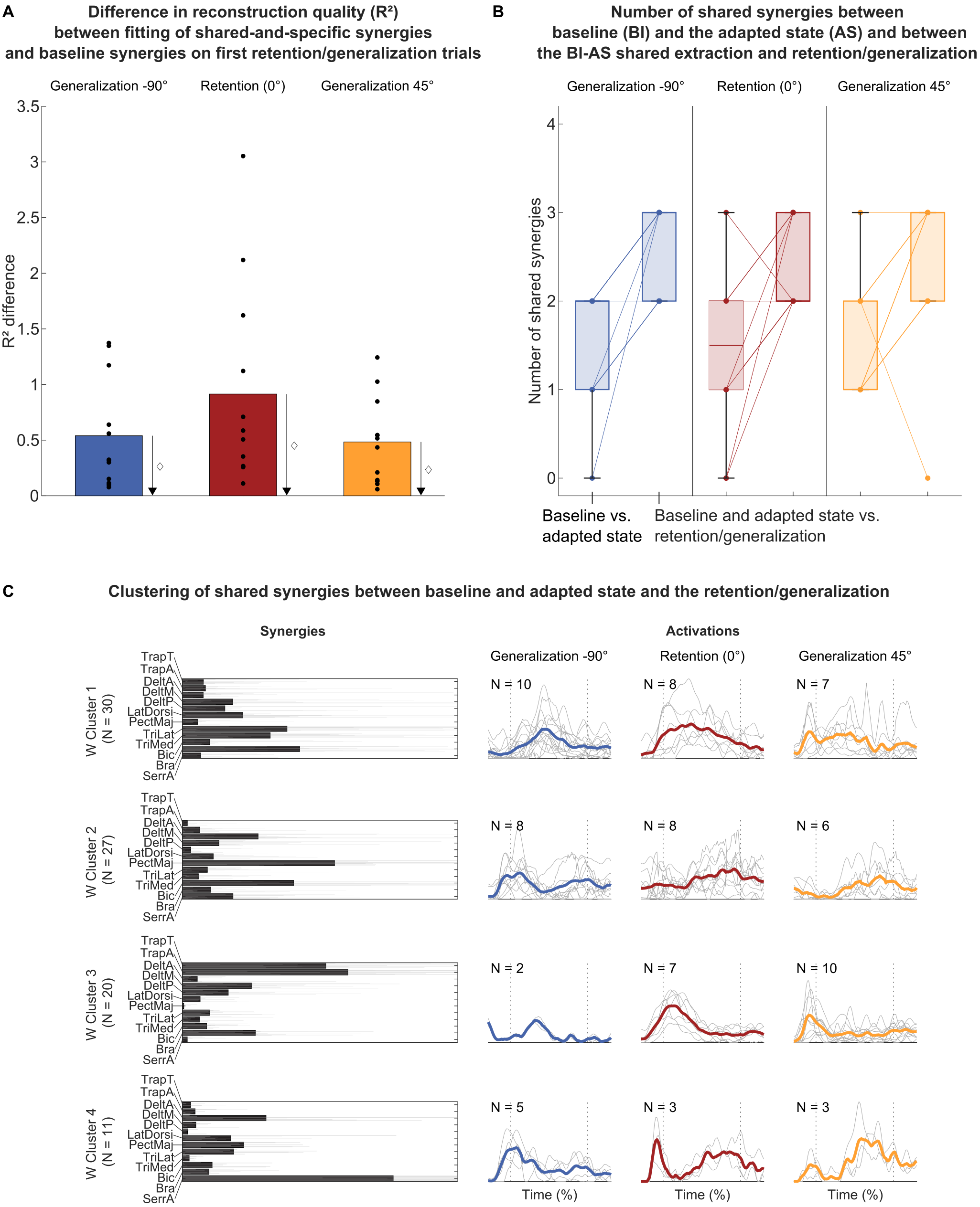
A
Difference in reconstruction quality (R²) between fitting of shared-and-specific synergies and baseline synergies on first retention/generalization trials
Generalization -90°
Retention (0°)
Generalization 45°
R² difference
3.5
3
2.5
2
1.5
1
0.5
0
B
Number of shared synergies between baseline (Bl) and the adapted state (AS) and between the Bl-AS shared extraction and retention/generalization
Generalization -90°
Retention (0°)
Generalization 45°
Number of shared synergies
4
3
2
1
0
Baseline vs. adapted state
Baseline and adapted state vs. retention/generalization
C
Clustering of shared synergies between baseline and adapted state and the retention/generalization
Synergies
Activations
Generalization -90°
Retention (0°)
Generalization 45°
W Cluster 1 (N = 30)
W Cluster 2 (N = 27)
W Cluster 3 (N = 20)
W Cluster 4 (N = 11)
TrapT
TrapA
DeltA
DeltM
DeltP
LatDorsi
PectMaj
TriLat
TriMed
Bic
Bra
SerrA
N = 10
N = 8
N = 7
N = 8
N = 8
N = 6
N = 2
N = 7
N = 10
N = 5
N = 3
N = 3
Time (%)
Time (%)
Time (%)

3.5 Discussion

This study investigated the relationship between muscle synergies and force field adaptation, retention, and generalization. Our findings show that adaptation involves structural changes in muscle synergies compared to reaching in unperturbed conditions, alongside a novel four-phasic synergy activation pattern. Moreover, these structural changes and activation patterns likely facilitate retention and generalization, as the same synergies and their activation patterns are also reflected there.

3.5.1 Participants adapted to the force field, showed retention to the 0° target, and generalization to the 45° and -90° targets

Participants adapted to the force field during their first exposure, washed out after its removal, and re-adapted and generalized when re-exposed ($\mathrm{H}_{\mathrm{Task}}$ 1). Also, we found that generalization decreased with distance from the practiced movement direction ($\mathrm{H}_{\mathrm{Task}}$ 2). These results align with related force field studies (Brashers-Krug et al., 1996, Gandolfo et al., 1996, Mathew et al., 2021, Rezazadeh and Berniker, 2019, Shadmehr and Mussa-Ivaldi, 1994). The fast re-adaptation for the 0°, i.e., the same direction as during the first exposure, has been previously described as the "savings" effect (Brashers-Krug et al., 1996, Mathew et al., 2021, Shadmehr and Brashers-Krug, 1997). However, based on the aforementioned studies, we expected no generalization to the -90° target at the beginning of the long-term retention and generalization phase. This disagreement may stem from participants already being exposed to the -90° FF condition during the short-term retention and generalization test, as adaptation starts from the very first trial (Joiner et al., 2017). The adaptation, washout, savings, and generalization we identified allowed us to examine the underlying modular structure of the muscle patterns.

3.5.2 Reaching in an environment with altered dynamics requires structural changes to the muscle synergies for unperturbed reaching

We first extracted muscle synergies from the planar, center-out reaching movements in the null field during the baseline. The number, composition, and tuning of the extracted baseline synergies are in accordance with the literature (d'Avella et al., 2006, Muceli et al., 2010).

Since a possible mechanism for reaching in a force field could be to combine the synergies employed in the baseline, we hypothesized that the muscle patterns of force field adaptation can be reconstructed by a combination of baseline reaching synergies ($\mathrm{H}_{\mathrm{Synergies}}$ 1). However, our results indicate this is not the case, and force field adaptation requires structural changes in muscle synergies ($H_{\text{Synergies}}$ 2). We found adapted state-specific synergies activated in a four-phasic pattern. First, a synergy reflecting co-contraction is active. Then, there is an early onset of a synergy reflecting arm extension and outward rotation, which is active until halfway through the trial until a second synergy overtakes, mainly reflecting triceps activity and, thus, elbow extension. At the trial end, the movement is decelerated and stabilized through a synergy of antagonistic muscles.

Reaching movements have been found to follow a triphasic pattern of muscle activation, leading to acceleration, deceleration, and damping of the movement (Flanders et al., 1994, Happee, 1992, Wadman et al., 1979). This pattern is generally also reflected in the activation of muscle synergies, showing an interplay between agonistic and antagonistic muscle synergies (d'Avella et al., 2006, Chiovetto et al., 2013). These observations regarding EMG and muscle synergies hold for baseline reaching in our study. Also, when adapted, participants employed a triphasic pattern of muscle activity as previously described (Darainy and Ostry, 2008, Thoroughman and Shadmehr, 1999). However, the novelty of our findings is that the muscle activity used to move the hand to the target is realized through two synergies with overlapping activations, peaking sequentially. Interestingly, the transition between the two synergies is seamless, as the force curves are bell-shaped and smooth. We provide a novel characterization of changes in the synergistic organization of many muscles after adaptation to a perturbing force field. Nevertheless, our findings align with literature examining activities in a few muscles, when looking at the muscle activity in our study without looking at the muscle synergies. We also observed early activity in these muscles, probably reflecting co-contraction (Darainy and Ostry, 2008, Milner and Franklin, 2005), and the muscles for reaching forward and counteracting the force field are already active early in the movement (Albert and Shadmehr, 2016, Thoroughman and Shadmehr, 1999).

Huang et al. (2012) showed that muscle activity is reduced to minimal levels even after a plateau in kinematic- and kinetic-dependent variables. Accordingly, the CNS might optimize effort while adapting, which leads to specific muscle synergies. The synergy that reflects arm extension with high triceps activation is sparse, and may reflect this tendency to realize movements with less effort. However, there is a lack of clarity over the process of how the structural changes happen, i.e., if adaptation expands the subspaces spanned by baseline synergies by learning new synergies or if adapted state-specific subspaces are the results of other control processes not requiring new synergies. This unmet need motivates future studies.

Force field adaptation with a muscle synergy perspective has received little research attention. Oscari et al. (2016) found that moving a joystick in a force field involves two additional muscle synergies during adaptation. This supports the notion of structural changes during force field adaptation, even though their results may be limited. Sampling a single direction may limit the validity of extracted synergies (Steele et al., 2015), characterizing only acceleration and deacceleration patterns (Chiovetto et al., 2013) and neglecting the versatile use of baseline reaching synergies to different directions. In contrast to our findings, a structural change in muscle synergies has not previously been reported during visuomotor rotations (De Marchis et al., 2018, Gentner et al., 2013, Severini and Zych, 2020). Here, muscle synergies extracted from the baseline could reconstruct the muscle patterns during adaptation and generalization, indicating structural robustness. Although force field and visuomotor adaptation are related motor adaptation paradigms, there are some differences, especially when the latter is done under isometric conditions. In contrast to isometric reaching, in dynamic reaching the joint angles and muscle length change throughout the movement; and the force exerted by the participant on the handle depends on the joint angle, muscle length, and their derivatives (Bizzi et al., 1991, Giszter et al., 1993, Mussa-Ivaldi et al., 1994, Shadmehr and Wise, 2005). It is, therefore, plausible that force field adaptation requires muscle synergies to be appropriate and effort-optimized at all joint angle configurations used during the reach, and that a re-aiming strategy by tuning baseline synergies does not suffice.

3.5.3 Retention and generalization are represented in the modular structure after adaptation

We found that retention and generalization muscle patterns can be better explained with synergies extracted from both baseline and adaptation than from baseline synergies alone. Therefore, the structural changes acquired during adaptation are re-used during retention and generalization. The retention (0° target) muscle pattern is well described by the shared synergies. Hence, our results show that muscle synergies and their activation timing are re-used when re-exposed to the same force field, presumably allowing a fast re-adaptation. This suggests that the shared muscle synergies represent a mechanism capturing the savings effect at a modular level (Brashers-Krug et al., 1996, Mathew et al., 2021, Shadmehr and Brashers-Krug, 1997).

However, contrary to our hypothesis $\mathrm{H}_{\mathrm{Synergies}}$ 3, the different amount of generalization between the -90° and 45° directions is not evident in the reconstruction quality, the number of shared synergies, or the number of direction-specific synergies. Accordingly, the structural changes in muscle synergies through adaptation reflect retention and generalization but not the differences between the 0°, -90°, and 45° groups. The observed structural changes through adaptation probably represent a general, i.e., direction-invariant, coordinative solution to the force field perturbation. This supports the notion that muscle synergies represent low-dimensional, modular control and are re-used in reaching to multiple directions (d'Avella et al., 2006), yet motivates future studies to further investigate the relationship between muscle coordination and task-level generalization performances. For example, future studies may investigate the trial-by-trial changes separately for the -90° and 45° directions to investigate possible mechanisms related to different generalization speeds.

3.5.4 Limitations

Baseline reaching directions comprised a semi-circle, and only center-out movements were analyzed. This restricts the possible subspaces and, thus, potentially shared subspace dimensions with the adapted state. Also, all participants adapted to the 0° target first, so future studies may generalize our findings with different directions. Due to the limited number of movements, we cannot conclusively state whether the CNS acquired new synergies during adaptation, or if these synergies are stored in the CNS but were not recruited in the baseline. Furthermore, future studies may investigate how the structural changes in muscle synergies evolve with practice.

3.5.5 Conclusions

This study found that reaching in an environment with altered dynamics requires structural changes and novel activation patterns in muscle synergies. These structural changes facilitate retention when re-adapting to the same direction, and generalization when adapting to new directions. Thus, our results provide new insights into how force field adaptation, retention, and spatial generalization are represented at the level of muscular coordination.

4 Topic B, Study B1: Rollator usage lets young individuals switch movement strategies in sit-to-stand and stand-to-sit tasks

This is a post-peer-review, pre-copyedit, and slightly adapted[1] version of the published article

Herzog, M., Krafft, F. C., Stetter, B. J., d'Avella, A., Sloot, L. H. and Stein, T. (2023). Rollator usage lets young individuals switch movement strategies in sit-to-stand and stand-to-sit tasks. *Scientific Reports* 13: 16901, doi:10.1038/s41598-023-43401-6.

---

[1] The citation and cross-reference style, as well as the figures' fonts, have been adjusted for consistency in this dissertation.

4.1 Abstract

The transitions between sitting and standing have a high physical and coordination demand, frequently causing falls in older individuals. Rollators, or four-wheeled walkers, are often prescribed to reduce lower-limb load and to improve balance but have been found a fall risk. This study investigated how rollator support affects sit-to-stand and stand-to-sit movements. Twenty young participants stood up and sat down under three handle support conditions (unassisted, light touch, and full support). As increasing task demands may affect coordination, a challenging floor condition (balance pads) was included. Full-body kinematics and ground reaction forces were recorded, reduced in dimensionality by principal component analyses, and clustered by k-means into movement strategies. Rollator support caused the participants to switch strategies, especially when their balance was challenged, but did not lead to support-specific strategies, i.e., clusters that only comprise light touch or full support trials. Three strategies for sit-to-stand were found: forward leaning, hybrid, and vertical rise; two in the challenging condition (exaggerated forward and forward leaning). For stand-to-sit, three strategies were found: backward lowering, hybrid, and vertical lowering; two in the challenging condition (exaggerated forward and forward leaning). Hence, young individuals adjust their strategy selection to different conditions. Future studies may apply this methodology to older individuals to recommend safe strategies and ultimately reduce falls.

4.2 Introduction

Falls are the leading cause of unintentional injuries in older individuals, often causing hospitalization and death (Gelbard et al., 2014, Kenny et al., 2017, Stevens, 2005). Approximately 30% of individuals over 65 years old fall at least once a year (O'Loughlin et al., 1993, Tinetti et al., 1988). Risk factors include lower-body weakness and impaired balance (Ambrose et al., 2013, Rubenstein, 2006, Stevens, 2005). Rollators, or four-wheeled walkers, are often prescribed for patients needing gait assistance (Bateni and Maki, 2005) to reduce lower-limb loading, compensate for weakness and injury, and improve balance (Bateni and Maki, 2005, Bradley and Hernandez, 2011, Ko et al., 2014). They aim to empower the residual motor capacities and facilitate natural locomotion (Cifuentes and Frizera, 2016). Rollator users can shift the load from the lower body to the upper body (Youdas et al., 2005) and increase their base of support (BoS) by using the handles as additional contact points (Bateni and Maki, 2005). However, rollators paradoxically have also been found to be a risk factor for falls (Ambrose et al., 2013, Bateni and Maki, 2005). It is not yet clear what underlies the increased fall risk and how rollator usage affects movement coordination during different tasks (Mundt et al., 2019), as evaluations of rollator usage have been mostly limited to spatiotemporal parameters during walking (Mundt et al., 2019). Furthermore, a recent review points to a lack of data on gait aid prescription relative to fall risk or balance performance in older individuals (Lee et al., 2022).

To start walking, we often need to stand up from a sitting position and sit down afterward. Hence, standing up and sitting down are fundamental tasks in daily life essential for mobility. Indeed, non-disabled adults stand up 60 to 100 times a day (Dall and Kerr, 2010, McLeod et al., 1975). Devices like sit-to-stand lifts, rails, and exoskeletons are available to provide specific assistance with standing up (Afsar et al., 2023). But these devices have disadvantages, such as being expensive and needing installation, space, batteries, and power outlets (Afsar et al., 2023). Thus, in many situations, individuals may want or need to use a rollator to stand up and sit down. However, the transitions between standing and sitting are complex. Difficulties standing up correlate with the risk of falling (Yamada and Demura, 2009) and increase the need for assistance (Perry et al., 2006), leading to reduced independence and earlier institutionalization (Branch and Meyers, 1987). Studies in residential aged care facilities report that 21%-41% of falls happen during transfers (Rapp et al., 2012, Robinovitch et al., 2013, van Schooten et al., 2018). Lehtola et al. (2006) reported the second-highest fall risk for sit-to-stand and stand-to-sit transfers in home-dwelling adults over 85 years.

Transitioning between sitting and standing becomes more demanding with increasing age, mostly due to changes in muscle composition and a decline in motor control (Jeon et al., 2021, Seidler et al., 2010). Knee and hip extension muscles provide less force to stand up (Hughes et al., 1996), and knee extensor activity correlates with stability in sitting down (Jeon et al., 2021). Transitions between sitting and standing require the simultaneous, coordinated motion of the lower extremities and the upper body (Jeon et al., 2019, Schenkman et al., 1990). Standing up means shifting the CoM from above the buttocks to above the feet by hip flexion and anterior movement of the head-arms-trunk segment, followed by rising through the extension of the hips, knees, and ankles (Bohannon, 2012, Roebroeck et al., 1994, Schenkman et al., 1990, Vander Linden et al., 1994). This poses a challenge to balancing as the body transfers from a stable seated position with three contact points (feet and buttocks) through an unstable, dynamic movement with the CoM outside the base of support (BoS) to standing, where the base of support is smaller, the CoM is higher, and only two contact points are used (Dall and Kerr, 2010, Hughes et al., 1994, Pai et al., 1994). Sitting down requires a balanced and smooth transition of the CoM from above the feet onto the chair seat. However, sitting down cannot be assumed to be simply the opposite of standing up (Dubost et al., 2005). Sitting down is performed with – rather than against – gravity, and the transition phase begins with a trunk flexion while standing, which is a less stable position than sitting (Dubost et al., 2005). Thus, three questions arise on how these complex movements are executed and if rollator use can improve the transition between sitting and standing.

First, for standing up, individuals have been observed to use different strategies: (1) leaning or sliding forward, (2) upper body flexion, (3) moving the feet backward, and (4) pushing through the arms on armrests (Dolecka et al., 2015, Frykberg and Häger, 2015, Hughes et al., 1994, Komaris et al., 2018). When the feet remain parallel and unchanged throughout standing up, two main strategies were observed: (1) the forward leaning, or momentum transfer strategy, and (2) the (dominant) vertical rise strategy, which has also been called the force control strategy (Anan et al., 2012, Frykberg and Häger, 2015, Hughes et al., 1994, van der Kruk et al., 2021b). With the forward leaning strategy, individuals use the upper body to generate forward momentum, which is smoothly transferred to mostly vertical momentum after seat-off by extending the knees and hips (Anan et al., 2012, Riley et al., 1991). Thereby, as the thorax, abdomen, and pelvis rotate in the same direction during the forward lean, energy is transferred from the thorax to the thigh (mechanical energy flow; Aleshinsky 1986, Anan et al. 2012). As a result, knee torque is reduced Scarborough et al. (2007) compared to a rise solely by lower-body muscles (vertical rise strategy). In the latter, the trunk stays relatively vertical throughout the movement (Coghlin and McFadyen, 1994, Hughes et al., 1994), and the CoM shows only anterior and upward movement (Anan et al., 2012) but no downward movement before it rises. The forward leaning strategy has generally been said to be the most efficient strategy for healthy individuals, as demonstrated in various studies (Scarborough et al., 2007). It is especially efficient, such that it reduces the knee torque compared to rising without the help of upper body momentum (Anan et al., 2012, Scarborough et al., 2007). Enough muscle strength in the knee extensors is one of the most dominant factors for a successful transfer (Alexander et al., 1997). A rollator may help individuals use the advantageous forward leaning strategy, with less force required, and still perform the movement safely.

Secondly, as described earlier, sitting down is also a complex movement and cannot be assumed to be simply the opposite of standing up (Dubost et al., 2005). It is, therefore, even more surprising that sitting down has been little described in the biomechanical literature (Dubost et al., 2005, Frykberg and Häger, 2015), let alone when using a rollator. Possibly, there are different strategies for sitting down, which may also be influenced by rollator use.

Thirdly, observational studies have often described arm use in transitioning between sitting and standing (Bohannon and Corrigan, 2003). However, arm movement is rarely described in biomechanical analyses since these are mostly restricted for standardization purposes (Frykberg and Häger, 2015, van der Kruk et al., 2021b). Yet, arm swing or push might play a vital role in easing the generation of horizontal and vertical momentum (Carr and Gentile, 1994). Indeed, Wretenberg et al. (1993) found a 44% and 34% reduction in hip and knee load, respectively, when their participants could push on armrests. Aging muscles often weaken (Candow and Chilibeck, 2005, Lynch et al., 1999), meaning that 50% of healthy older individuals cannot stand up without using their arms if the seat is at knee height (Mazzà et al., 2004). This makes armrests a necessity. Hence, arms play a major role in generating propulsive forces during standing up, which can compensate for deficits in lower body strength (Bahrami et al., 2000, Munro and Steele, 1998, Wretenberg et al., 1993). Also, the additional contact point of the hands helps maintain balance (Bahrami et al., 2000, Schultz et al., 1992) through somatosensory input by a tactile or proprioceptive haptic cue (Bateni and Maki, 2005, Jeka, 1997, Jeka and Lackner, 1994). In walking and standing, it has been shown that touching a plate or railing with the fingertip improves balance rather than offering mechanical support when allowing strong interaction forces (Kouzaki and Masani, 2008, Oates et al., 2017). In support, van der Kruk et al. (2022) recently observed that the preference of arm use is likely related to the perception of stability and the fear of falling. Thus, rollator handles could greatly simplify standing up and sitting down via mechanical and/or proprioceptive support. However, the few studies that include arms in a biomechanical analysis used armrests rather than rollator handles. Armrests are low and directly lateral to the trunk when sitting, in contrast to anterior-lateral and high as with a rollator (Arborelius et al., 1992, Schultz et al., 1992, Wretenberg et al., 1993). Our previous study (Krafft et al., 2022) found that movement stability (i.e., $\mathrm{CoP}_{\mathrm{feet}}$-length, duration) was enhanced by full rollator support in standing up and sitting down. However, the strategies individuals use when arm support is given are not yet known. Potentially, there exist strategies which make transitions manageable and safe.

This study's purpose was to investigate how rollator support affects strategies for sit-to-stand and stand-to-sit movements. We aimed to identify the strategies used when the rollator usage level changes from no assistance to light touching (supposed proprioceptive cue) and full support (supposed load reduction). Due to the lack of biomechanical studies on movement strategies during standing up and sitting down and the heterogeneity in the physical status of older individuals, this first study investigated non-disabled young adults. As older individuals often struggle with balance, we added a balancing aspect to make the transitions challenging. To mimic age-related balance problems, icy water or convex lenses have been used (Yoshida et al., 2019), and for aging suits, a foam material is glued to the bottom of shoes to create imbalance (Lavallière et al., 2017). There is agreement that proprioception signals from leg muscles provide an essential source of information for postural control (Henry and Baudry, 2019, Wiesmeier et al., 2015). Hence, we aimed to trigger the proprioceptive component, focusing more generally on postural instability, which can result in falls and injuries (Henry and Baudry, 2019). Therefore, we used balance pads in addition to the normal floor condition.

We hypothesized that (1) individuals switch their strategy depending on the level of rollator assistance, (2) we would find specific strategies for (2a) the different degrees of rollator assistance, and (2b) floor condition.

4.3 Materials and methods

We used the same raw and pre-processed data described in our previously-published article (Krafft et al., 2022). All steps after pre-processing (section 4.3.4) are novel in this article.

4.3.1 Participants

Ten females and ten males (25.5 ± 3.8 years, 1.71 ± 0.08 m height, 67.6 ± 10.9 kg mass) participated in the study and gave written informed consent before participation. The number of participants was selected based on comparable, recent biomechanical studies (Jeon et al., 2021, Norman-Gerum and McPhee, 2020, Wang et al., 2021). Informed consent was obtained by the participant shown in Figure 4.1 to publish the image. The study was approved by the Ethics Committee of the Medical Department of Heidelberg University (S-105/2021) and has been performed in accordance with relevant guidelines/regulations and the Declaration of Helsinki.

4.3.2 Experimental protocol

The participants stood up and sat down at their preferred speed, separated by at least two seconds of rest as instructed with the commands "stand up, stand still, sit down." They used a custom-made robot rollator simulator under three different support conditions (Figure 4.1). The participants were instructed not to use the rollator in the (1) unassisted condition and to let their arms hang loosely at their sides as long as they sat. In the (2) light touch condition, they were instructed to place their hands with a palm grip onto the handles to induce a proprioceptive cue, and in the (3) full support condition, they were instructed to use a power grip on the handles. Handle height was individually set at the participant's wrist height in a standing position as recommended by health care literature (Boelen, 2009, Lockette, 2011, Wilkins, 2008). Seat height was individually adjusted to the height of the lateral epicondyle of the femur. To induce a higher demand on balance capabilities, an additional "challenging condition" was set up by placing a circular rubber-made

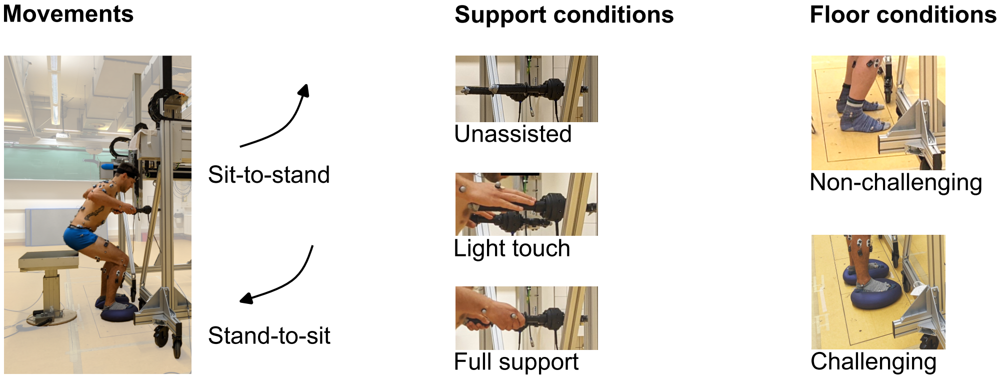

Figure 4.1: Experimental setup. Left: Participant stands up from an instrumented chair with the custom-made robot rollator simulator. Full-body passive markers for motion tracking and EMG electrodes (data not included in this article) were placed on the body. Two movements were studied: sit-to-stand and stand-to-sit. Middle column: Three different support conditions were used: unassisted (top, handles not used), light touch (middle, palm on the handles), and full support (bottom, power grip). Right column: Two floor conditions were used: non-challenging (lab floor, top) and challenging (balance pads, bottom).

balance pad with a compliant surface (Dynair® Ballkissen®, diameter 33 cm, height 8 cm, TOGU GmbH, 83209 Prien-Bachham, Germany) underneath each foot. Participants performed two trials in each condition to familiarize themselves with the setup. Everyone performed three valid, non-consecutive trials in a random order for every support (unassisted, light touch, full support) and floor condition (non-challenging and challenging).

4.3.3 Data collection

Full-body 3D kinematics were recorded (150 Hz, 10 type 5+ cameras, Qualisys, Gothenburg, Sweden) using retroreflective markers placed according to the IOR full-body gait model (Cappozzo et al., 1995, Leardini et al., 2011). Ground reaction forces (GRF) (1000 Hz; Bertec Corp., Columbus, OH, USA) and forces on the seating surface (142 Hz; Phidgets Inc., Calgary, AB, Canada) were measured.

4.3.4 Data processing

Raw kinematic data were processed offline with Qualisys Track Manager (v2018.1, Qualisys Medical Ltd., Sweden) to reconstruct the 3D coordinates of the markers. Subsequently, force and kinematic data were filtered with a 4th-order, 10 Hz, Butterworth low-pass filter. Full-body kinematics and the CoM were then calculated with Visual3D (v6, C-Motion Inc., Germantown, MD, USA). Further data analyses were done in Matlab (R2020a, Natick, MA, USA). Movement start, seat-off, and movement end were segmented using a k-means++ algorithm (Sloot et al., 2020). The trials were time-normalized to 1001 time points (100%).

4.3.5 Data analysis

The following variables were selected for further analyses as they have been described as determinants for the strategies: 3D ground reaction force, normalized to body weight (Borzelli et al., 1999, Gilleard et al., 2008), the 3D CoM, normalized to body height (Hesse et al., 1994, Hughes et al., 1994, Pai et al., 1994, Roebroeck et al., 1994), sagittal angles of the ankle, knee, and hip (Coghlin and McFadyen, 1994, van der Kruk et al., 2021b, Yamasaki and Shimoda, 2016), the sagittal angle between a virtual line connecting the heel and the CoM and the floor perpendicular ("CoM-heel angle") (Anan et al., 2012, Hanawa et al., 2017), and the sagittal angles of thigh, shank, and pelvis relative to the floor perpendicular (Komaris et al., 2018). We focused on the right body side as their values were similar to those of the left side. Kinematic time series of arm movements were not included in the analysis to identify movement strategies. They would have provoked a strict separation between unassisted and light touch/full support trials and thus obscured the similarities of the trials across all support conditions regarding whole-body strategies.

4.3.5.1 Identification of movement strategies

Principal component analysis (PCA) was used to reduce the dimensionality of the data by extracting relevant features. These features were then used to identify movement strategies through k-means++ clustering (Figure 4.2, Deluzio and Astephen 2007, van Drongelen et al. 2021, Robertson et al. 2013). This was done separately for the two movements (sit-to-stand and stand-to-sit) and floor conditions (non-challenging and challenging).

First, the data of each variable was arranged into a matrix $\mathbb{R}^{180\times 1001}$, in which every column represented one timepoint (of 1001 timepoints) and every row one trial (20 participants × three support conditions × three repetitions = 180; Deluzio and Astephen 2007, van Drongelen et al. 2021). After subtracting the mean of the matrix (Leporace et al., 2012, Nüesch et al., 2012), PCA transformed the data into a low-dimensional coordinate system spanned by principal components (Halilaj et al., 2018, Jolliffe, 1986, 2002). We selected the number of principal components so that 90% of the variance was explained (see Table 4.1 for an overview of the number of principal components; Jolliffe 1986, 2002). Following previous studies (van Drongelen et al., 2021, Halilaj et al., 2018, Rein et al., 2010), a single coordinate system was spanned from the PCs of each variable. The scores, i.e., the original data represented in the new coordinate system, were scaled to the interval [0, 1] so that each extracted PC had equal importance in the subsequent clustering (Mohamad and Usman, 2013). First, hierarchical clustering (ward distance) was used to determine the appropriate number of clusters based on the scree and silhouette coefficient plots. Then, k-means++ (Matlab `kmeans` with the 'plus' option) clustering grouped all 180 trials into the determined number of clusters. Each cluster represented one movement strategy. If the strategy of a single trial differed from all identified strategies, it was still assigned to one of the strategies because k-means does not terminate until every trial is assigned to a cluster. These outlier strategies were identified after clustering with the generalized extreme Studentized deviate test for outliers based on their distance to the centroid (Iglewicz and Hoaglin, 1993, Rosner, 1983, Vera et al., 2013). Clustering was repeated ten times to confirm the robustness of the cluster assignments (van Drongelen et al., 2021).

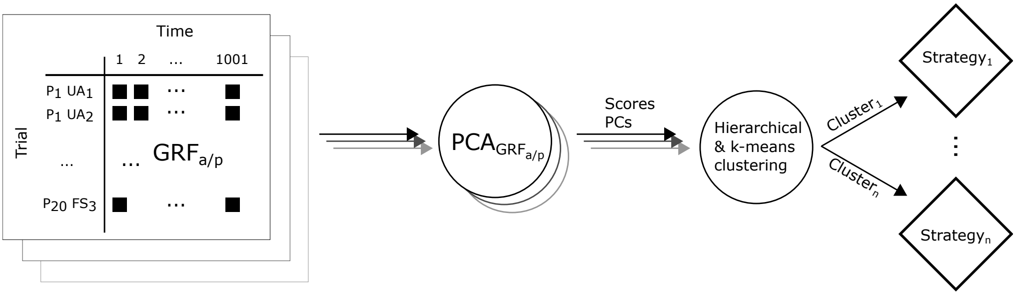

Figure 4.2: Process for identifying strategies, performed separately for each of the four combinations of sit-to-stand, stand-to-sit, and non-challenging, challenging floor conditions. For each variable, a matrix (e.g., $GRF_{a/p}$) served as input for the variable-specific PCA ($PCA_{GRF_{a/p}}$). The input for the clustering consists of a coordinate system with axes formed by the extracted principal components of all variables, as well as the scores obtained from the PCAs. The extracted clusters constitute the strategies. P_i ith participant, UA_i ith unassisted trial, FS_i ith full support trial.

Table 4.1: Number of principal components necessary to explain 90% of the variance within the time series of every selected variable.

	Sit-to-stand		**Stand-to-sit**	
	Non-challenging	**Challenging**	**Non-challenging**	**Challenging**
GRF medio-lateral	3	5	5	8
GRF anterior-posterior	4	6	6	8
GRF vertical	3	4	4	5
CoM medio-lateral	2	2	2	2
CoM anterior-posterior	2	2	2	2
CoM vertical	2	2	2	3
Ankle angle	3	3	3	3
Hip angle sagittal	2	2	2	3
Knee angle sagittal	2	2	2	3
Pelvis-lab angle sagittal	2	2	3	3
Shank-lab angle sagittal	2	2	2	3
Thigh-lab angle sagittal	2	3	2	3
CoM-heel angle sagittal	2	2	2	2

4.3.5.2 Dependent variables

This study aimed to identify if participants switched strategy with support condition. A participant was identified as switching strategies if at least two of the three repetitions of one support condition had a different strategy than in another support condition.

Further, total trial duration and the duration between start and seat-on or -off in seconds were assessed because prolonged times have been associated with increased fall risk and less movement stability (Cheng et al., 2014, Goulart and Valls-Solé, 1999, Krafft et al., 2022, Prudente et al., 2013). As arm movement in the unassisted condition was not restricted to allow for a "natural" movement, it was operationalized as a dichotomous variable: Arms were identified as "involved" when the most anterior elbow position was anterior to the shoulder.

4.3.6 Statistics

Independent tests were used to assess differences between the identified strategies in the time series and dependent variables because trials, not participants, were clustered into strategies (see 4.4.1). First, analyses of the results found that the distributions of the individuals' trials are different across the participants (see section 4.4.1). Hence, dependent tests cannot be used. Therefore, independent tests were used that do not eliminate individuals as a source of variability, which results in less statistical power and thus are more conservative regarding significance than dependent tests. Normality was assessed with Shapiro-Wilk tests, and the homogeneity of variances was confirmed with Levene's tests. Differences between the time series of the respective strategies were assessed with the spm1d toolbox (statistical parametric mapping, SPM; Friston et al. 1994, Pataky et al. 2019). As normality was violated, the non-parametric SPM versions of the ANOVA (three strategies) and t-tests (two strategies) were used (Daly, 2021, Stief et al., 2021). Post-hoc pairwise comparisons by SPM were only performed on regions of interest indicated by the SPM-ANOVA (Pataky et al., 2016, Pickle et al., 2019). In line with recent recommendations (Honert and Pataky, 2021), the aim of applying SPM was to exploratively analyze where the time series tended to differ, to help with the qualitative description of the strategies. Differences in the dependent variables, i.e., trial durations and time until seat contact, were tested with the Kruskal-Wallis and Mann-Whitney U-tests as homogeneity was violated. The significance level (two-tailed) was set a priori at 0.05 and adjusted for multiple comparisons post-hoc to 0.05/3 = 0.017 (Bonferroni correction). All statistics were performed in Matlab (R2020a, Natick, MA, USA).

4.4 Results

Overall, in sit-to-stand, three strategies in the non-challenging and two in the challenging condition were identified (non-challenging: silhouette coefficient = 0.23, scree test SSE = 0.01; challenging: silhouette coefficient = 0.19, scree test SSE = 0.33). In stand-to-sit, three strategies in the non-challenging and two strategies in the challenging condition were also identified (non-challenging: silhouette coefficient = 0.18, scree test SSE = 0.31; challenging: silhouette coefficient = 0.19, scree test SSE = 1.30). The assignment of trials to clusters was robust throughout each instance of the 10 clustering runs.

4.4.1 Most of the participants switched their movement strategies

Figure 4.3 illustrates which strategy was used for every trial. Of the 20 participants, between 14 and 17 (depending on the task) did not use just a single strategy for all their trials. Therefore, we accept our first hypothesis that individuals switch their strategy depending on the level of rollator assistance.

4.4.2 Description and comparison of the identified movement strategies

4.4.2.1 Sit-to-stand movement strategies

Three different strategies were identified for sit-to-stand in the non-challenging condition (Figure 4.4a, Supplementary Video A.1): a “forward leaning” strategy (blue), a “vertical rise” (green) strategy, and a “hybrid” (brown) strategy, inferred by visual inspection of the stick figures and supported by the different courses in the hip and CoM-heel angles before seat-off and the CoM trajectory in the sagittal plane (Figure 4.4b). The kinematics and stick figures of the “hybrid” strategy are either in-between the other two strategies or change from being closer to the one to being closer to the other over the course of the trial, thus named the “hybrid” strategy. These strategies appeared in each support condition, i.e., no strategy was identified to comprise only trials with handle support.

The trial duration with the forward leaning strategy was shorter than the other strategies. However, seat-off timing was not different between strategies (trial duration: forward leaning: 1.16 s ± 0.25, hybrid: 1.24 s ± 0.20, vertical rise: 1.24 s ± 0.22; $\chi^2(2)$ = 10.37, p = 0.006; forward leaning vs. hybrid: z = -2.40, p = 0.016; forward leaning vs. vertical rise: z = -3.04, p = 0.002; hybrid vs. vertical rise: z = 0.04, p = 0.969; seat-off: forward leaning: 0.49 s ± 0.13, hybrid: 0.50 s ± 0.11, vertical rise: 0.50 s ± 0.12; $\chi^2(3)$ = 0.23, p = 0.892).

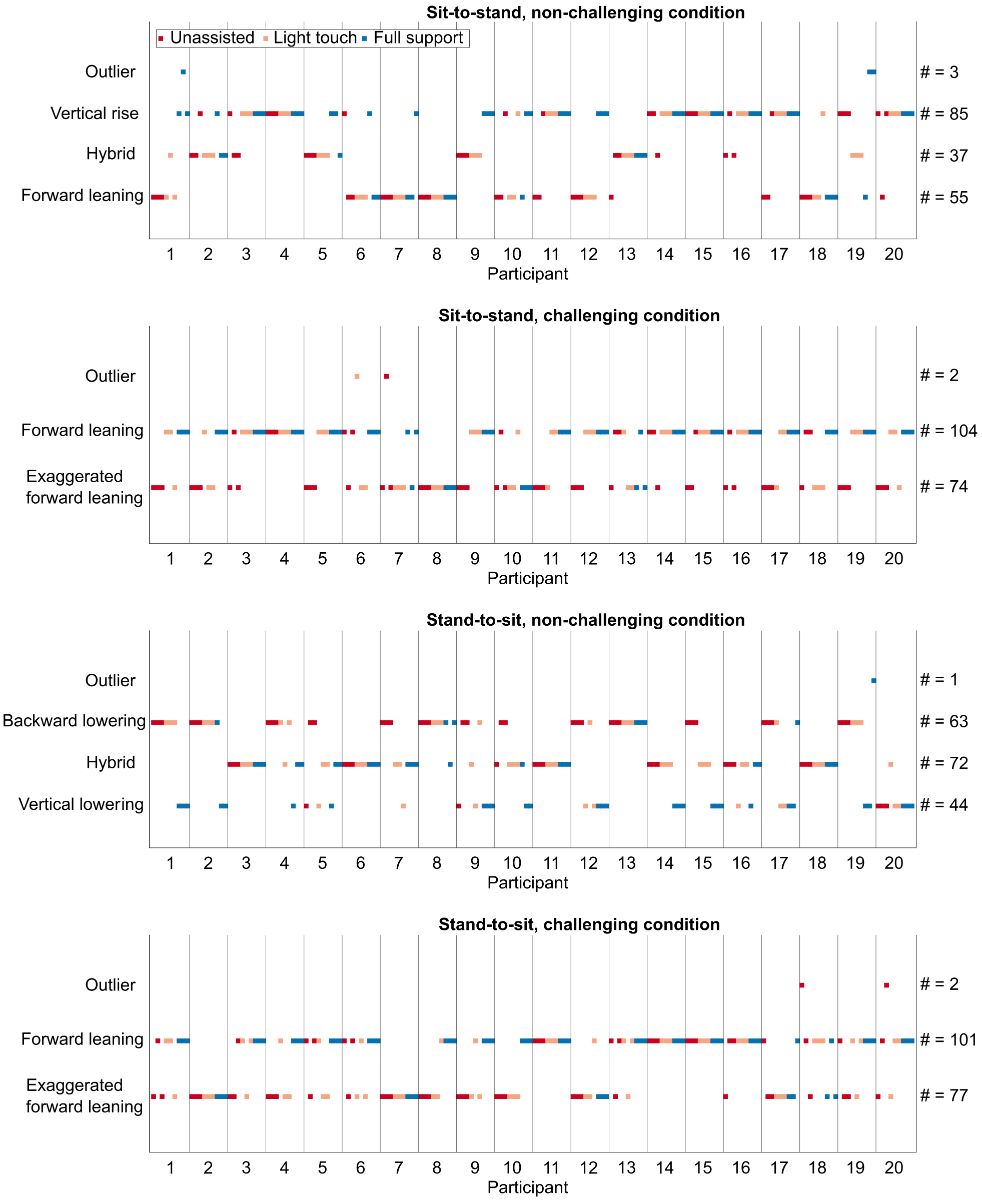

Figure 4.3: Distribution of trials among strategies. One dot represents one trial. The row indicates the strategy to which it belongs. The column shows to which participant it belongs. The support conditions are color coded as indicated by the legend. The labels on the right y-axis show how many trials were associated with the strategy written on the left y-axis.

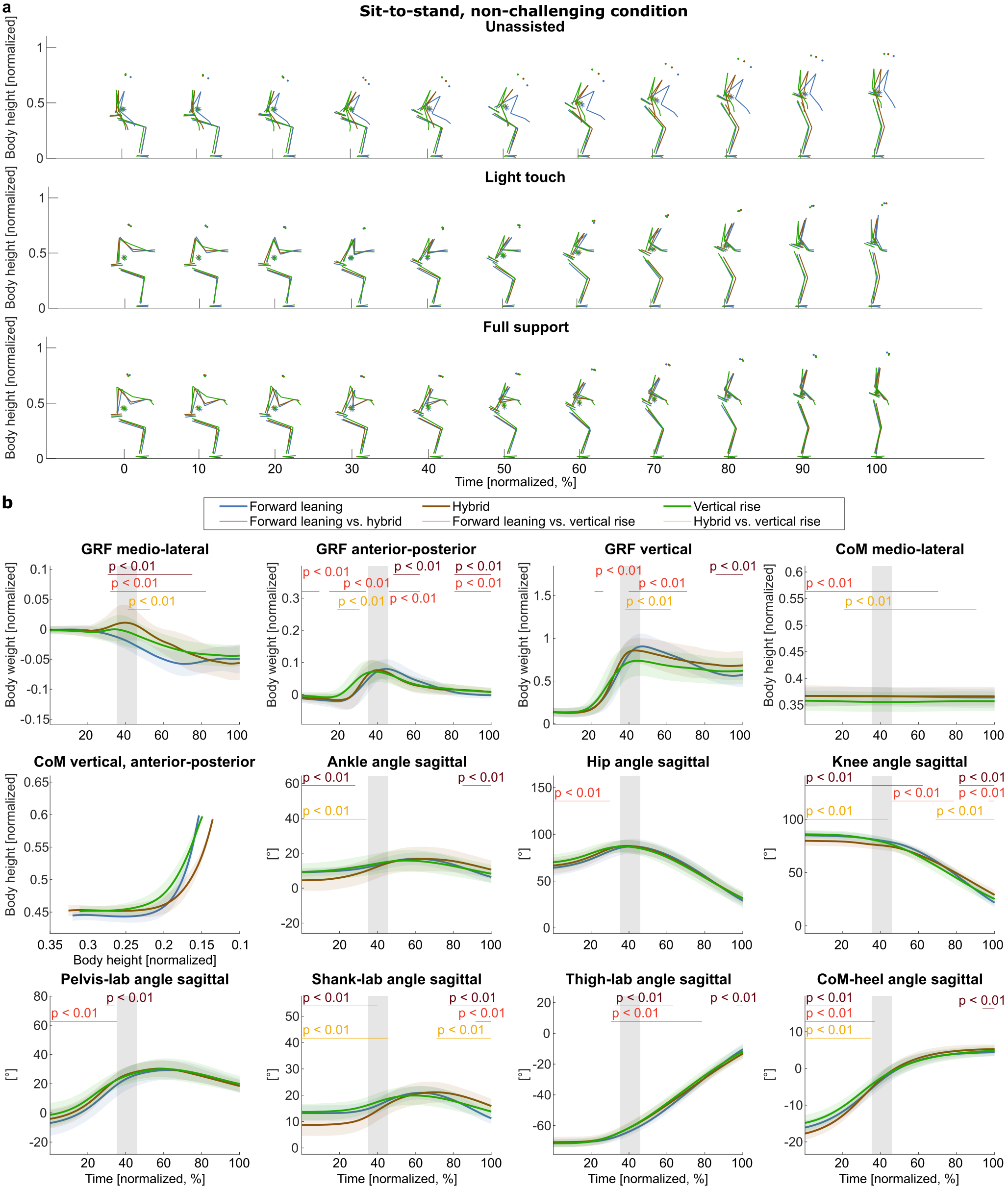

Figure 4.4: Strategies of the non-challenging sit-to-stand task. (a) The strategies are given in different colors (see legend) and separated into rows according to the support condition. The CoM is depicted as an asterisk (∗). (b) Means and standard deviations of the variables, aggregated by cluster. The gray shaded area illustrates the range of seat-off (mean ± s.d.). The red lines and corresponding p-values indicate significant differences revealed by the post-hoc tests ($p < 0.017$).

In the challenging condition, only two strategies were identified (Figure 4.5a, Supplementary Video A.2): an "exaggerated forward leaning" (purple) and a "forward leaning" strategy (blue). In comparison, the exaggerated forward leaning strategy shows a smaller hip angle in the transition phase after seat-off. The wide forward lean is underpinned by the CoM progression in the sagittal plane and the larger CoM-heel angle after seat-off Figure 4.5b). Similar to the normal floor condition, no support-specific strategy was identified. The trial duration was shorter, and seat-on was earlier in the forward leaning strategy (trial duration: exaggerated forward leaning: 1.36 s ± 0.32, forward leaning: 1.27 s ± 0.27; z = 1.99, p = 0.046; seat-contact: exaggerated forward leaning: 0.65 s ± 0.17, forward leaning: 0.54 s ± 0.10; z = 5.07, p < 0.001). The trials identified as outliers are shown in Supplementary Figure A.5. Concerning our hypothesis, we can state that we did not find specific strategies for 2a, the different degrees of rollator assistance, but we did for 2b, the challenging floor condition.

4.4.2.2 Stand-to-sit movement strategies

Three strategies were found in the non-challenging condition (Figure 4.6a, Supplementary Video A.3): a "backward lowering" (blue), a "vertical lowering" (green), and a "hybrid" strategy (brown), inferred from visual inspection of the stick figures and supported by (1) the different CoM progressions and (2) the smaller hip, knee, and ankle angles of especially the backward-lowering strategy (Figure 4.6b). Like with the sit-to-stand tasks, the three identified strategies appeared in each support condition.

Vertical lowering took less time, and seat-on was earlier than in the backward lowering and the hybrid strategy (trial duration: backward lowering: 1.47 s ± 0.29, hybrid: 1.49 s ± 0.26, vertical lowering: 1.33 s ± 0.24; $\chi^2(3) = 17.41$, p < 0.001; backward lowering vs. hybrid: z = -0.09, p = 0.925; backward lowering vs. vertical lowering: z = 2.60, p = 0.009; hybrid vs. vertical lowering: z = 4.24, p < 0.001; seat-on: backward lowering: 0.88 s ± 0.20, hybrid: 0.87 s ± 0.19, vertical lowering: 0.71 s ± 0.15; $\chi^2(3) = 33.44$, p < 0.001; backward lowering vs. hybrid: z = 0.14, p = 0.889; backward lowering vs. vertical lowering: z = 4.64, p < 0.001; hybrid vs. vertical lowering: z = 5.21, p < 0.001).

As with the sit-to-stand task, only two strategies were identified in the challenging condition (Figure 4.7a, Supplementary Video A.4): an "exaggerated forward leaning" (purple) and a "forward leaning" (blue) strategy. These strategies were inferred from visual inspection and underpinned by the smaller sagittal hip and ankle angles after seat-on in the exaggerated forward leaning strategy and the smaller CoM-heel angles after seat-on (indicating that the CoM is more anterior to the heel position than in the forward leaning strategy). As in the other task, no strategy was identified to comprise only trials with handle support. Exaggerated forward leaning took less time, and seat-contact was earlier than with forward leaning (duration: exaggerated forward

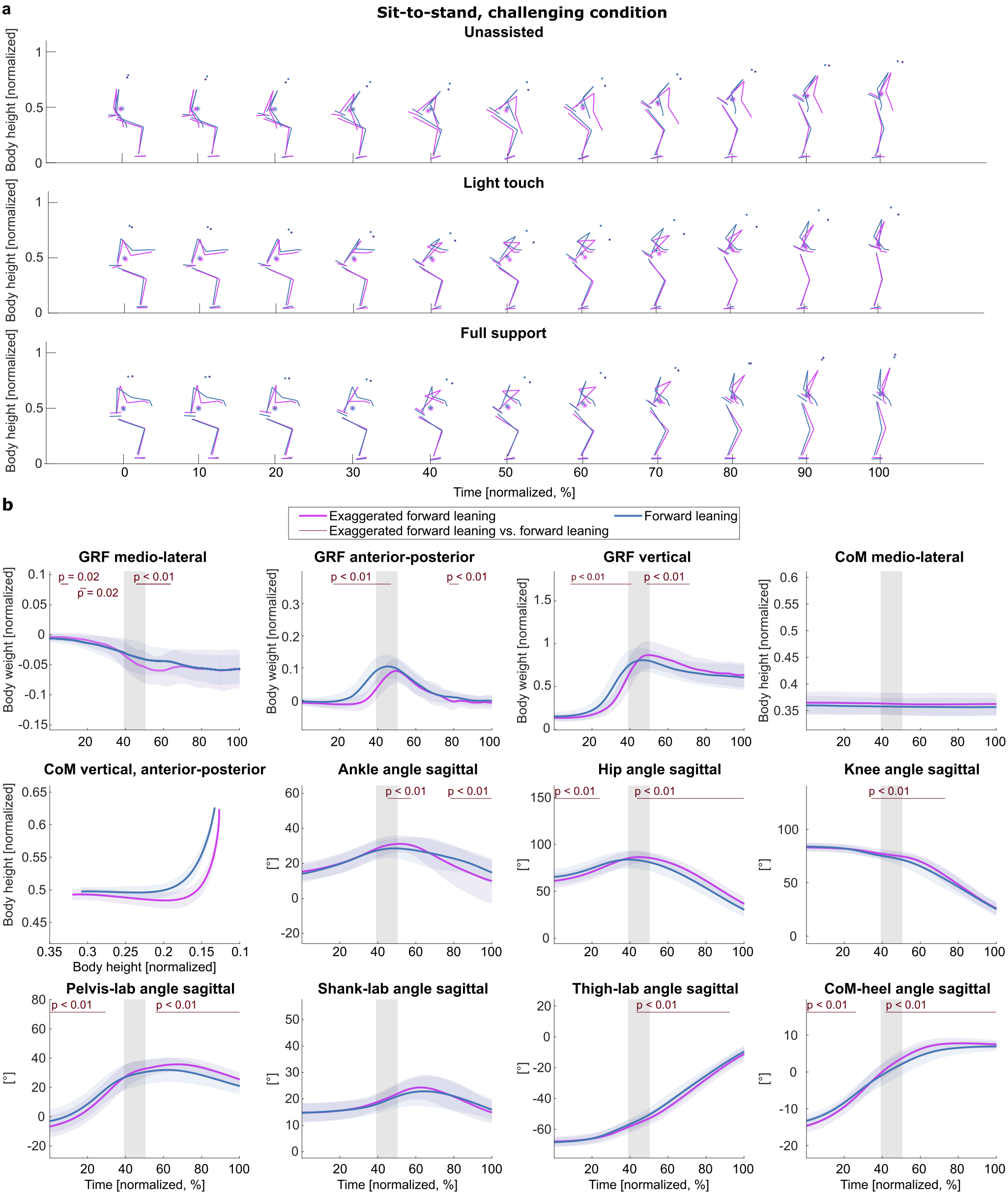

Figure 4.5: Strategies of the challenging sit-to-stand task. (a) The strategies are given in different colors (see legend) and separated into rows according to the support condition. The CoM is depicted as an asterisk ($*$). (b) Means and standard deviations of the variables, aggregated by cluster. The gray shaded area illustrates the range of range of seat-off (mean ± s.d.). The red lines and corresponding p-values indicate significant differences ($p < 0.05$).

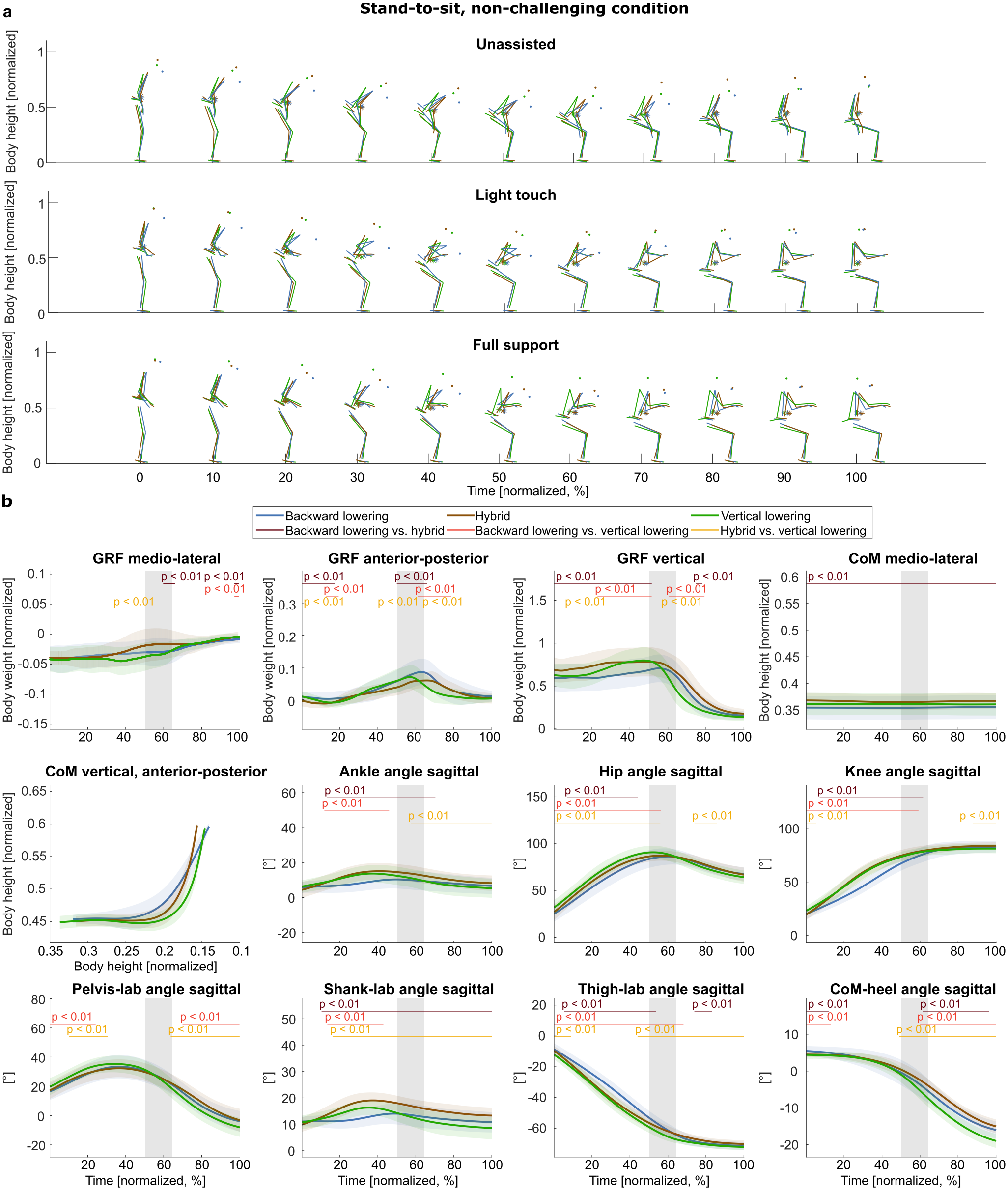

Figure 4.6: Strategies of the non-challenging stand-to-sit task. (a) The strategies are given in different colors (see legend) and separated into rows according to the support condition. The CoM is depicted as an asterisk ($*$). (b) Means and standard deviations of the variables, aggregated by cluster. The gray shaded area illustrates the range of seat-off (mean ± s.d.). The red lines and corresponding p-values indicate significant differences revealed by the post-hoc tests ($p < 0.017$).

leaning: 1.39 s ± 0.30, forward leaning: 1.47 s ± 0.29; z = -2.01, p = 0.044; seat-on: exaggerated forward leaning: 0.70 s ± 0.15, forward leaning: 0.81 s ± 0.19; z = -4.29, p < 0.001).

With respect to our hypotheses and in line with sit-to-stand, we can state that we did not find specific strategies for 2a, the different degrees of rollator assistance, but we did for 2b, the challenging floor condition.

4.4.2.3 The use of the arms in unassisted sit-to-stand and stand-to-sit movements

Arms were only used for two trials of the forward leaning and the hybrid strategy. In the challenging condition, 20 trials included arm movement, 15 of which belonged to the exaggerated forward leaning strategy (Figure 4.8). In stand-to-sit, arms were not involved in the backward lowering, but five were involved in the vertical lowering and two in the hybrid strategy. When challenged, arms were involved in four trials in the exaggerated forward and two trials in the forward leaning strategy (Figure 4.8). As inferred from the parallel lines in Figure 4.8, arms were moved at a similar speed to the CoM, i.e., not swung.

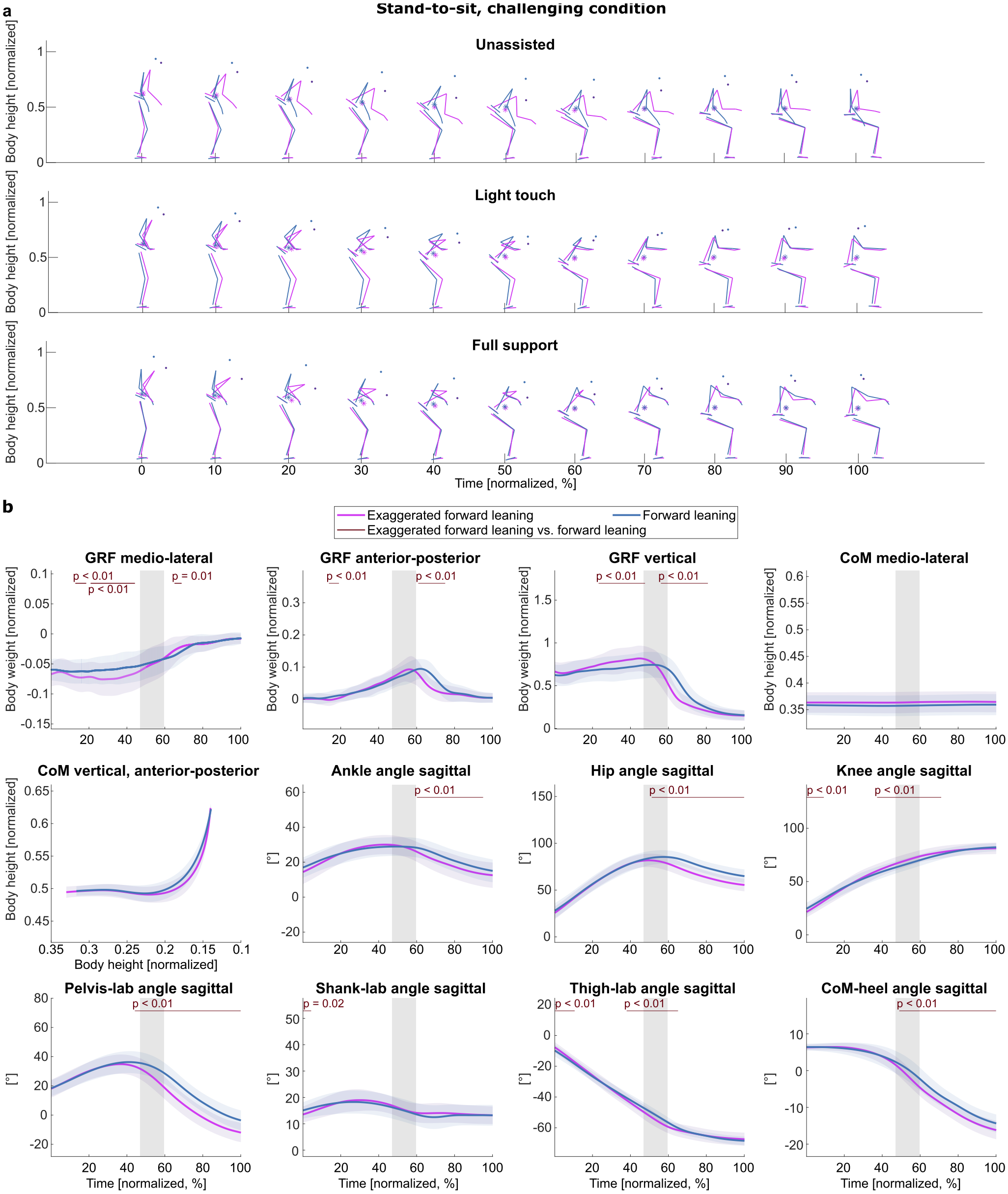

Figure 4.7: Strategies of the challenging stand-to-sit task. (a) The strategies are colored in different colors (see legend) and separated into rows according to the support condition. The CoM is depicted as an asterisk ($*$). (b) Means and standard deviations of the variables, aggregated by cluster. The gray shaded area illustrates the range of seat-off (mean ± s.d.). The red lines and corresponding p-values indicate significant differences revealed by the post-hoc tests ($p < 0.017$).

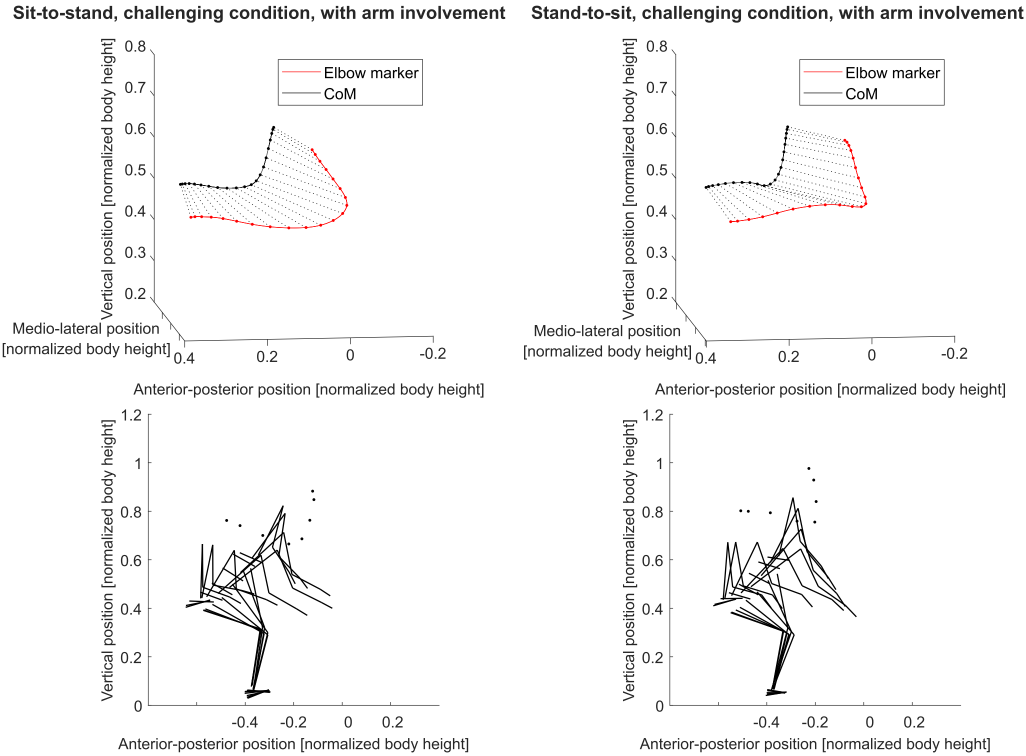

Figure 4.8: Example arm activity for two movements (left: sit-to-stand, right: stand-to-sit). Top: Spatial progression of the CoM and the lateral elbow marker. The black and red lines connecting the points illustrate the spatial progression. The distances between the points illustrate 5% of the total duration in each case. The cross-connections help assess whether the elbow and CoM moved at comparable speeds (as with nearly parallel cross-connections). Bottom: The whole-body movement is shown along with the plots above.

4.5 Discussion

Rollators are often prescribed to assist older individuals in their daily life, but paradoxically have been found to increase fall risk. Standing up and sitting down are often executed, yet are complex and demanding movements for older individuals. To improve this movement for older individuals, this study with young, non-disabled individuals identified if and how rollators affect movement strategies. We found that (1) most (14-17 of 20, task-dependent) participants switched their strategies with rollator assistance, (2a) no support-specific strategies were revealed, but (2b) new strategies emerged when participants' balance was challenged.

4.5.1 Participants switch their strategies with full support, especially when challenged

Participants who stood up with the forward leaning strategy in the unassisted condition did not show a common pattern of which strategy they switched to when having the handle support: some kept leaning forward, and others switched to a vertical rise or hybrid strategy. However, those who used the vertical rise or hybrid strategy unassisted never used the forward leaning strategy with handle support. When their balance was challenged, most participants (16 of 20) switched from the exaggerated forward to the forward leaning strategy with full support. During the light touch trials, one-third used the exaggerated and two-thirds the forward leaning strategy, i.e., presumably the somatosensory input is not the entire reason for changing the strategy. In stand-to-sit, almost all participants who used the backward lowering strategy in the unassisted condition switched their strategy in the full support condition, but not all switched in the light touch condition. When challenged, almost every trial with full support belonged to the forward leaning strategy, i.e., participants who used the exaggerated forward leaning strategy in the unassisted and/or light touch condition switched with full support.

Taken together, full handle support appears to influence strategy selection, especially when the participants were challenged, i.e., the demands on balance control were higher. Further, somatosensory input does not seem to determine the change in strategy under the studied task conditions. A change in the CoM position may be a potential triggering factor for strategy selection. Having the arms on the handles may lead to an anterior shift of the CoM, though rather small, due to the relatively small mass of the arms. This is supported by Jeyasurya et al. (2013), who did not find significant differences in the CoM position when they compared an arm-assist and bar-assist position to the unassisted condition (arm crossed in front of the chest). Furthermore, the causal relationship between CoM-position and strategy selection is debatable. In fact, a recent study (Richmond et al., 2021) argues that the CoM represents the whole body well but questions if the CoM position/movement is optimized regarding a task goal. Hence, it remains an open question if the CoM position may trigger the strategy selection or if anything else triggers the strategy selection resulting in a shifted CoM position. According to a prevailing theory in motor control, the optimal control theory (Todorov and Jordan, 2002), movement strategy selection is based on a cost function that is minimized about the movement goal (e.g., to stand up or sit down). Therefore, a unique control policy is implemented to transform the state estimate (i.e., the internal body representation and task-relevant variables) into motor commands (Kim et al., 2021). The multi-dimensional state estimate could be considered a multi-dimensional input weighted to yield the selected movement strategy. A shift in the weighting, e.g., toward a higher importance of stability in the challenging condition, may explain a change toward a different, then optimal, movement strategy. A previous study (van der Kruk et al., 2021a) proposed that this could explain age-related differences in movement strategies.

4.5.2 Sit-to-stand was achieved with three different strategies

Our data-driven approach revealed three movement strategies (forward leaning, hybrid, and vertical rise). While these three have often been described in unassisted standing up (Anan et al., 2012, Coghlin and McFadyen, 1994, Doorenbosch et al., 1994, Frykberg and Häger, 2015, Hughes et al., 1994, van der Kruk et al., 2021b), we can now add that rollator assistance does not lead to the emergence of new strategies. In line with the literature, we found that participants using the forward leaning strategy showed higher upper body flexion (Coghlin and McFadyen, 1994, van der Kruk et al., 2021b) and stood up faster (Hughes et al., 1994). In Hughes et al.'s study (1994), participants were older than in our study. Thus, we can now conclude that the forward leaning strategy is faster regardless of the individual's age. Scarborough et al. (2007) found that knee moment is smaller with the vertical rise strategy. However, more muscle activity around the knee is needed due to lack of generated upper body momentum. Possibly, rollator use reduces the demand on muscle activity around the knee, as has been shown for walking (Alkjær et al., 2006). To recommend the best strategies, which are safe and with the least demand on knee moment, for older individuals to stand up with a rollator, future studies may investigate muscle activity and joint load in the vertical rise and hybrid strategies with rollator support.

Interestingly, no different strategies were identified for the light touch and full support compared to the unassisted condition. Thus, receiving sensory input and/or weight support to stabilize oneself did not change the movement, even when the balance was challenged. Possibly, the identified strategies are optimal solutions to achieve the task goal, i.e., to stand up, so no new strategies need to emerge. de Rugy et al. (2012) proposed that habitual movement strategies might be retained when the task goal can be achieved, even if conditions change. This could have been the case with our young participants.

4.5.3 When the balance was challenged, participants only used two different strategies to stand up

Participants used an exaggerated forward or forward leaning strategy when their balance was challenged. They did not use a third, vertical rise strategy as they did under non-challenging conditions. An exaggerated forward leaning strategy, based on increased trunk flexion, has been found in older individuals (Papa and Cappozzo, 2000) and in those with pathologies, when stability and safety seem to be of priority, thus often called "stabilization strategy" or "exaggerated trunk flexion strategy" (Cunha et al., 2021, Frykberg and Häger, 2015, van der Kruk et al., 2021b, Nikfekr et al., 2002, Scarborough et al., 2007). Here, participants moved their CoM over the base of support ("stable position") at the earliest time point by an exaggerated trunk flexion and then raised the CoM vertically. This behavior hints at why we found this strategy. The balance pads under the participants' feet contained air, which was re-distributed when the pressure point from above changed. It seems plausible that the transitioning is easier when the CoM is centered above the balance pad at seat-off (CoM-heel angle $\approx 0°$, see Figure 4.5b).

Furthermore, the constantly changing demands due to the pressure distribution in the pads possibly required constant adjustment of the motor commands, as has been shown in studies on postural control (Anderson and Behm, 2005). The higher number of principal components extracted for all GRF directions (Table 4.1) reflects this by indicating a more complex time series structure (Deluzio and Astephen, 2007). Thus, the emergence of the exaggerated forward leaning strategy could result in participants wanting to increase their stability and safety to better cope with the increased balance challenge.

When using handles, the choice in favor of the forward leaning strategy could hint that participants cope with the challenging floor condition by relying more on the rollator handles (Chang et al., 2014): e.g., to lessen the pressure on the pads and so the difficulty standing on them, or to interact with the handles correcting unforeseen instabilities during the transition. This issue can be addressed in more detail in future studies, e.g., with instrumented handles. Possibly, as the hip angle is larger in the forward leaning strategy, this strategy is more suitable for individuals with limited range of motion e.g., due to issues like lower-back-pain (Shum et al., 2005).

That the participants showed two instead of three strategies to successfully perform the sit-to-stand task suggests that young individuals are flexible concerning task demands (Frykberg and Häger, 2015). The vertical rise strategy is possibly not a good solution for this new task demand: here, the CoM-heel angle does not reach 0° until after seat-off (see Figure 4.4b). This could explain why the participants did not use it. Furthermore, we suggest balance pads can be a way to provoke young individuals to use sit-to-stand strategies observed with older individuals or those with pathologies.

4.5.4 Stand-to-sit was achieved with three different strategies

Our data-based approach identified three strategies for sitting down: backward lowering, hybrid, and vertical lowering. To the best of our knowledge, no previous study explicitly identified strategies in the stand-to-sit movement or performed detailed biomechanical measurements on this motion. Only Dubost et al. (2005) observed two general patterns comparable to our study's backward and vertical lowering strategies, although they did not explicitly name them. The main difference between the two patterns they found was the more vertical orientation of the trunk (like in our vertical lowering strategy) in the one predominantly used by their older participants. Their young participants flexed their trunks more (like in our backward lowering strategy).

In contrast to (Dubost et al., 2005), in our study the young participants only used the backward lowering strategy to sit down without rollator support in two of 60 trials. However, unlike in our study, participants had to cross their arms in front of their chests, which makes movement less natural, as supported by studies that evaluated the five-times-sit-to-stand test (Carr, 1992, Khuna et al., 2020). Therefore, not imposing this restriction in our study may have fostered the use of the vertical lowering or hybrid strategy. In both strategies, seat-on occurred earlier than with the backward lowering strategy. Based on this measure, it is suggested that this is a safer strategy as the unstable transition phase is shorter (Prudente et al., 2013). However, this safety assumption needs to be investigated more thoroughly in future studies.

Unlike with the unassisted condition, we found the preferred strategies to sit down with full support to be the backward lowering and hybrid strategies. Here, knee flexion happens more slowly but more steadily. Possibly, this reduces the knee load and muscle activity demand, and handle support helps carrying out this strategy. However, future studies may investigate the three strategies in every condition by imposing these on participants. An examination of muscle activity, interaction forces, and joint moments may then improve understanding of which strategies are optimal for older rollator users.

4.5.5 When the balance was challenged, participants only used two different strategies to sit down

With challenged balance, participants used either a forward leaning or an exaggerated forward leaning strategy to sit down. Like with the sit-to-stand task, participants demonstrated only two instead of three strategies. The backward lowering strategy was not used. With the exaggerated and forward leaning strategies, the CoM is first lowered vertically, presumably to keep the pressure ratio in the balance pads as constant as possible. The rearward movement occurs later (CoM-heel angle $\approx 0^\circ$, not until seat-off, see Figure 4.7b). Probably, shifting the CoM posteriorly earlier, like in backward lowering (CoM-heel angle $\approx 0^\circ$ slightly earlier than seat-off, see Figure 4.6b), would lead to the balance pads filling increasingly in the front, resulting in more air in the anterior area of the balance pads and so the body moving posteriorly. Like with standing up, the higher number of principal components in the GRF variables compared to the non-challenging condition indicates a more complex time series and, thus, constant adjustments of motor commands (Deluzio and Astephen, 2007). This more complex pattern possibly triggered the strategy selection toward a “safer” strategy. Future studies could examine sitting down with older participants and/or those with pathologies. It seems plausible that the exaggerated forward leaning strategy could arise there as a counterpart to the “stabilization strategy” of the sit-to-stand movement.

4.5.6 Arm usage in unassisted sit-to-stand and stand-to-sit does not lead to new strategies

For standardization reasons, arm movement is often restricted, e.g., the arms are to be crossed in front of the chest (Frykberg and Häger, 2015, van der Kruk et al., 2021b). This, however, hinders the participants from performing the transitions naturally, as indicated by validation studies for the five-times-sit-to-stand test (Carr, 1992, Khuna et al., 2020). Furthermore, individuals could possibly keep to their strategy when using the arms to compensate for difficulties (van der Kruk et al., 2021a,b). We only instructed our participants to let their arms hang laterally in the sitting position in the unassisted condition. Trials with arm usage were not identified as outliers, nor did they lead to a new strategy cluster. This is in line with Millington et al.'s 1992 study, in which angles and moments of the trunk, pelvis, and knee remained similar regardless of participants moving to flex their shoulders or elbows in unassisted standing up. Further, Carr and Gentile (1994) found that trunk flexion or peak horizontal and vertical momentum of the CoM did not differ between restricted and flexible arm movement conditions. Hence, arm use does not lead to a new movement strategy. Standing up from a chair at knee height and with "natural" speed may not create difficult task demands for young individuals. Therefore, arm use may not be necessary for them and therefore not done. This is in contrast to the challenging condition, where arms were involved in 23 of 60 unassisted trials. As participants moved their arms at a comparable speed to the CoM (Figure 4.8), rather than using the swing to create extensive, additional momentum as is often done to increase height in jumps (Harman et al., 1990, Lees et al., 2004), they probably used their arms to shift the CoM anteriorly (Swearingen, 1962). This possibly helps to hold the CoM as long as possible over the pads (CoM-heel angle $\approx 0^\circ$) in the exaggerated forward leaning strategy. In stand-to-sit, arms were only used in seven (non-challenging) and six (challenging) of 60 unassisted trials. Here, similar to the sit-to-stand movement in the challenging condition, participants did not extensively swing their arms but seemed to hold them anteriorly, possibly also to hold the CoM in the same horizontal position.

4.5.7 Limitations

Several potential shortcomings need to be considered. First, our simulator device is heavier than a commercially available rollator and can neither dip nor move horizontally, even if the handles are pulled or pushed on heavily. Thus, the outlier "pulling strategy" (Supplementary Material A.2.2), where one participant extensively pulled on the handles to stand up, would not be possible with a real-world rollator. Nevertheless, pulling extensively on rails that are fixed to propel the body upward has been observed as a strategy in older individuals to stand up and sit down (Dekker et al., 2007, Kato et al., 2020) and should therefore be considered in future studies examining older individuals. Secondly, although not uncommon in other biomechanical studies (van der Kruk et al., 2021b), for standardization purposes, we restricted the foot placement to be parallel and underneath the knees, which hindered the participants from pulling their feet backward to stand up, as it is sometimes observed (Dolecka et al., 2015). Thirdly, we applied PCA and k-means clustering. It cannot be excluded that other methods would have led to a different constellation. However, these methods are well-established and frequently used in biomechanics (van Drongelen et al., 2021, Halilaj et al., 2018, Rein et al., 2010), and the allocation of the trials into the identified strategy clusters is plausible and robust. Fourthly, to the best of our knowledge, there are no criteria based on which trials can be assigned a movement strategy in rollator-assisted sit-to-stand and stand-to-sit movements. Thus, there was no prior knowledge regarding the number and composition of the movement strategy clusters, precluding an a priori power analysis. Hence, we used a common unsupervised, data-driven approach to identify movement strategies. With unsupervised algorithms, it is unforeseeable how the data are clustered. Consequently, the number of participants and trials were selected not based on an a priori power analysis but on comparable studies (Jeon et al., 2021, Komaris et al., 2018, Norman-Gerum and McPhee, 2020, Wang et al., 2021). Fifthly, statistics between the strategies were calculated as if the trials between the clusters were independent and single observations. Therefore, these need to be treated with caution. However, statistics were only applied here to give an impression of where the time series tend to differ and to help qualitatively describe the strategies. Lastly, we investigated strategies in young people. Even though we used balance pads to challenge them, this probably limits the validity of the results concerning individuals who are older or physically limited and dependent on a rollator.

4.6 Conclusion

This study found that young individuals switch their strategies to standing up and sitting down with rollator handle support and when their balance is challenged. Our data-driven approach revealed three strategies for sit-to-stand. The strategies found are in line with the literature on unassisted standing up. They have now been shown to hold with rollator support. Our challenging floor condition approach in using balance pads under the participants' feet provoked two strategies, one of which was previously found for older individuals and those with pathologies. We suggest balance pads can be used in future studies as a way to provoke young individuals to use sit-to-stand strategies observed with older individuals or those with pathologies. For the first time, strategies for stand-to-sit have been described based on biomechanical data. Participants used three sit-down strategies, reduced to two in the challenging balance condition. Like with sit-to-stand, rollator support and challenging balance conditions greatly influence strategy selection. In our study, the strategies have been described and discussed predominantly based on kinematics. Future studies may investigate joint loading and muscle activity to assess which strategies can eventually be recommended to fall-prone individuals for safe and efficient rollator usage.

5 Topic B, Study B2: The central nervous system adjusts muscle synergy structure and tightly controls rollator-supported transitions between sitting and standing

This is a post-peer-review, pre-copyedit, and slightly adapted version of the published article [1]

Herzog, M., Krafft, F. C., Fiedler, J., Berger, D. J., Sloot, L. H., d'Avella A.[2] and Stein, T[2]. (2025). The central nervous system adjusts muscle synergy structure and tightly controls rollator-supported transitions between sitting and standing. *Journal of NeuroEngineering and Rehabilitation* 22: 96, doi:10.1186/s12984-025-01622-y.

---

[1] The citation and cross-reference style, as well as the figures' fonts, have been adjusted for consistency in this dissertation.

[2] Share senior-authorship

5.1 Abstract

Background: Older individuals are at risk of falling. Assistive devices like rollators help to reduce that risk, especially by compensating for decreased leg muscle strength and balance problems. Paradoxically, rollators have been found to be a fall risk as well as being difficult to use. To investigate the causes, this study examines how different levels of rollator support (no assistance, light touch, and full support) and balance demands (standard lab floor, balance pads) affect movement coordination during standing up and sitting down movements.
Methods: Twenty young participants stood up and sat down while full-body kinematics and muscle activity (30 channels) were recorded. Participants stood up and sat down using different movement strategies (e.g., forward leaning, hybrid, and vertical rise standing up movement strategies). For each movement strategy, spatial and temporal muscle synergies were extracted from the muscle activity patterns. Temporal muscle synergies provided a more compact, low-dimensional representation than spatial muscle synergies, so they were subsequently clustered with k-means++. The activation duration of the temporal muscle synergies was assessed with full-width at half-maximum at the main peak. Multivariate linear mixed models were used to investigate if the muscle weightings associated with the temporal muscle synergies differed across the support conditions.
Results: The timings of the temporal muscle synergy activations, but not the shape, differed across the movement strategies for both types of movement. Across all tasks, temporal muscle synergies showed a narrower width of activation around the time of seat-off and seat-on than at the movement start and end. No support-specific temporal muscle synergies were found, but lower limb muscle weightings decreased while upper-limb muscle weightings increased with increased support.
Conclusion: The narrow shape of the temporal synergy activation profiles suggests that the central nervous system controls the movements tightly, especially around seat-off and seat-on and in challenging conditions with increased balance demands. Furthermore, rollator support increases the weightings of upper body and decreases the weightings of lower limb muscles, especially around seat-off and seat-on. Future studies may further investigate how the loss of tight movement control may cause falls in older individuals.

5.2 Background

Worldwide, at least one in four individuals over 65 falls every year (Rubenstein, 2006, Salari et al., 2022). Falls and associated injuries often lead to insecurities and restricted mobility, thereby making daily activities challenging and reducing older people's independence (Gaxatte et al., 2011, Rubenstein, 2006). Assistive devices, including canes, crutches, walkers, or rollators, are intended to reduce falls by providing stability and facilitating daily activity independence (Bateni and

Maki, 2005). Rollators, i.e., four-wheeled walkers, are often prescribed to patients who require an assistive device to compensate for muscular weaknesses. By lessening lower limb loading and enhancing balance, they can help alleviate pain and injuries (Bateni and Maki, 2005, Bradley and Hernandez, 2011, Ko et al., 2014, Mann et al., 1995). Paradoxically, studies have shown that rollators are associated with falls (Bateni and Maki, 2005, Kallin et al., 2004). Also, Mann et al. (1995) reported that 57% of the problems with using walkers relate to a "difficult and/or dangerous" use. Although rollators are used widely, the reasons for the difficulties and the increased fall risk have remained unclear due to the lack of thorough biomechanical studies (Mundt et al., 2019).

Rollators are prescribed primarily to help with walking but are also used to stand up and sit down, especially when other assistance, like a handrail or armrest, is missing (Komisar et al., 2023, Leung and Yeh, 2011). Standing up and sitting down are crucial movements to live an independent life but are demanding due to the dynamic balance requirement during the transitions between sitting and standing (Dall and Kerr, 2010, Hughes et al., 1994, Komisar et al., 2023, Pai et al., 1994). Lower limb muscular strength and balance are two main predictors of successful sit-to-stand movements (Frykberg and Häger, 2015). However, these decline with age. In particular, knee extensor strength has been found to decline annually by approximately 2-4% after age 50 (Goodpaster et al., 2006), and a meta-analysis (Moreland et al., 2004) found lower limb weakness to be a statistically significant risk factor for falls. A rollator may help by providing load transfer from the lower limbs to the upper body, reducing the strength demand for the hip and knee extension musculature (Bateni and Maki, 2005, Joyce and Kirby, 1991). Furthermore, the additional contact points through the rollator handles might provide extra positional information next to the feet and enlarge the base of support (BoS), potentially improving balance (Jeka, 1997). However, the evidence is not clear. While a related study found that rollator support increases movement stability during standing up and sitting down movements in young adults (Krafft et al., 2022), a recent observational study in a long-term care setting found that 44.4% of the falls while using a rollator occurred while transitioning between sitting and standing (Nickerson et al., 2024). A possible explanation for the increased fall risk in rollator use could be that they interfere with the movement strategies of different tasks. Literature shows that individuals use different movement strategies, e.g., with or without upper body momentum, to stand up and sit down without a rollator (Dolecka et al., 2015, Frykberg and Häger, 2015, Hughes et al., 1994, Komaris et al., 2018), but with no clear answer as to which movement strategy is the safest (Sadeh et al., 2023). Furthermore, based on kinematic analyses, we have previously found that young individuals change their kinematic movement strategy when provided with rollator support, especially when the balance is challenged (Herzog et al., 2023). These changes in movement strategies indicate that rollators affect the underlying movement coordination patterns, which could be key to understanding human-rollator interactions and safe use.

With approximately 700 muscles and 300 mechanical degrees of freedom, the musculoskeletal system allows countless movement possibilities (Bernstein, 1967, Bruton and O'Dwyer, 2018).

To reduce the inherent complexity, the central nervous system (CNS) may employ a modular control architecture (Bernstein, 1967, Bizzi et al., 2008, Giszter, 2015), of which synergies have been proposed as a possible representation (Berniker et al., 2009, Bizzi et al., 1991, Bruton and O'Dwyer, 2018). Regardless of whether synergies are identified in spinal reflexes (Grillner, 1981), as muscle synergies (d'Avella et al., 2003, Lee, 1984, Tresch et al., 1999), or as kinematic synergies (Daffertshofer et al., 2004, Santello et al., 1998), they may generate movement by activating a few functional groups rather than specifying each single element independently (d'Avella, 2016). Muscle synergies are often used as a compact low-dimensional representation of a set of recorded muscle activity (Bruton and O'Dwyer, 2018). Through flexible recruitment and combinations of synergies, the CNS can generate an extensive movement repertoire (d'Avella et al., 2003). According to a hierarchical organization, movement is generated through a combination of a preexisting, trial-independent part and a flexible, trial-dependent part (Ting and McKay, 2007). The trial-independent part is reused across movements and presumably stored in subcortical areas of the CNS; whereas the trial-dependent part, which accounts for variations across trials, is presumably under cortical control (d'Avella et al., 2003, Ting and Chvatal, 2010). Different models of muscle synergies have been proposed and differ in terms of which part of the decomposition is trial-dependent and which is trial-independent (Berger et al., 2020, Delis et al., 2014, Russo et al., 2014). In spatial muscle synergies, also called time-invariant or synchronous synergies, the trial-independent part is made up of vectors. These vectors, the weightings, represent the activations of multiple muscles, relative in magnitude to each other. These fixed vectors are combined with trial-dependent activation profiles (or time-varying coefficients), representing the amount and timing of the muscle weightings. In contrast, temporal muscle synergies (or temporal components, basic patterns), consist of muscle activation profiles, invariant over muscles and conditions, and trial-dependent muscle weightings. Hence, the relative weightings of muscle activations vary across trials. Another difference between these two models is the compactness of the muscle activity representation. In some studies, temporal muscle synergies provided a more compact representation than spatial synergies (Delis et al., 2014, Brambilla et al., 2023a, Safavynia and Ting, 2012) but this is not always the case (Chiovetto et al., 2013, Safavynia and Ting, 2012). Regardless of the model, muscle synergies are robust against the highly variable and stochastic nature of EMG patterns. Since they therefore reveal the neural organization underlying behavior and functional outcomes of muscular activation (Bizzi and Cheung, 2013, Dominici et al., 2011, Safavynia et al., 2011), they have been used in various settings to investigate questions regarding movement coordination (Singh et al., 2018), as well as in sit-to-stand movements.

Three to four spatial muscle synergies typically explain 87-94% of the variance in unassisted sit-to-stand movements across various age groups (An et al., 2013, Carey et al., 2021, Hanawa et al., 2017, Kogami et al., 2021, Ranaldi et al., 2023, Yang et al., 2017). Usually, each synergy represents one biomechanical function, such as momentum transfer and postural stabilization. While muscle synergy structure seems robust in unassisted standing up, even with visual or vestibular disturbances, the activation timing changes with these disturbances (Yoshida et al., 2019). Furthermore, synergy activation timings have been found to differ across movement strategies (Yang et al., 2017). Consequently, analyzing the temporal structure is crucial. In contrast to unassisted standing up, assistive devices seem to impact not only the activation timing in standing up, but also the number of synergies increased when participants stood up while being pushed up by the chair (Wang et al., 2021), and studies with Nordic walking sticks (Candow and Chilibeck, 2005) or exoskeletons (Lynch et al., 1999, Ashford and De Souza, 2000) show that assistive tools alter movement coordination; such that, for example, synergies specific to the device emerge. Consequently, when studying rollator-assisted standing up, it is essential to consider upper body involvement to account for the involvement of the arms. This is particularly relevant as the aging process leads to muscle weakening (Candow and Chilibeck, 2005, Lynch et al., 1999), and individuals thus often need to push on armrests to master transitioning between sitting and standing. Consequently, it remains an open question how rollator usage influences full-body movement coordination in standing up movements, especially considering the different movement strategies and upper body involvement.

Like in standing up, assistive devices may alter sitting down coordination. Only a few biomechanical and movement coordination studies have analyzed sitting down (Ashford and De Souza, 2000, Carey et al., 2021, Jeon et al., 2021), let alone with a rollator. This is surprising as sitting down is also a complex movement and not simply the opposite of standing up (Dubost et al., 2005, Frykberg and Häger, 2015). For example, the gluteus maximus works concentrically when standing up but eccentrically when sitting down (Ashford and De Souza, 2000). Also, upper body muscles may act differently when sitting down using a rollator, such that the arm extensor muscles presumably work eccentrically rather than concentrically. Accordingly, this implies that rollator usage may influence stand-to-sit movement coordination in a different manner from sit-to-stand.

To improve our understanding of the understudied human-rollator interactions and safe use in transitions between sitting and standing, it is necessary: (1) to develop a protocol and a methodology for assessing coordination during these understudied movements and (2) to establish baseline values in healthy cohorts. Therefore, we apply muscle synergy analysis and examine the movement coordination underlying different movement strategies for standing up and sitting down. We first examine which muscle synergy model is most appropriate, as it is not a priori clear which model best represents the sit-to-stand and stand-to-sit movements (Berger et al., 2020, Brambilla et al., 2023a, Safavynia and Ting, 2012). Then, we explore how different rollator support conditions (no assistance, light touch with haptic cues through the rollator handles, and full support with supposed lower limb load reduction) affect muscle synergies. As thorough studies on movement coordination underlying rollator-assisted movement are scarce (Mundt et al., 2019), and the rollator-prone population is heterogeneous regarding their underlying deficits, this study investigates young participants as a baseline measure, with potentially limited loss of generalizability, even though Hanawa et al. (2017) found that the synergies in standing up remain similar regardless of the participant's age.

Still, to make standing up and sitting down more challenging, and as proprioceptive signals from the leg muscles are the primary source for postural control (Henry and Baudry, 2019), we placed balance pads underneath their feet to evaluate the effect of rollator support while experiencing increased postural instability. Postural instability is common in many neurodegenerative diseases and movement disorders (Djaldetti et al., 2006) and often leads to the prescription of rollators to improve postural stability (Bateni and Maki, 2005, Mundt et al., 2019).

We hypothesized that (1) temporal muscle synergies represent sit-to-stand and stand-to-sit EMG patterns with a different compactness than spatial muscle synergies. Furthermore, we hypothesize that (2) the muscle synergy activation differs across movement strategies and that (3) rollator support influences the weightings between upper body and lower limb muscles for both standing up and sitting down.

5.3 Materials and methods

Our previously published articles on this dataset describe our analysis of the kinematic and kinetic data (Herzog et al., 2023, Krafft et al., 2022). Here, we introduce all the steps regarding the EMG analysis.

5.3.1 Participants

Twenty young and healthy volunteers (10 women, 10 men; 25.5 ± 3.8 years, 1.71 ± 0.08 m height, 67.6 ± 10.9 kg mass) gave written informed consent and participated in the study. The participant shown in Figure 5.1 gave informed consent to publish the image. The Ethics Committee of the Medical Department of Heidelberg University (S-105/2021) approved the study, which was then performed according to the Declaration of Helsinki.

5.3.2 Experimental protocol

The participants sat still and, after hearing "stand up" by the experimenter, they stood up at their own pace. Then, the experimenter said, "stand still". After standing still for at least two seconds, the experimenter said, "sit down," and the participants sat down at their own pace. The seat height was set to the height of the participant's lateral epicondyle of the femur, and a custom-built robot rollator simulator was used to provide rollator support (Figure 5.1). Following recommendations in the health care literature (Boelen, 2009, Lockette, 2011, Wilkins, 2008), the handle height was set at the participant's standing wrist height. According to the support condition, they did not use the rollator handles at all (unassisted, UA), only with a light touch of the hand, i.e., by placing the hand with a palm grip onto the handle to receive a haptic cue (light touch, LT), or with a power grip (full support, FS).

These support conditions were combined with two floor conditions: the standard lab floor and a more “challenging ground”, which was created by positioning a circular rubber balance pad with a compliant surface (Dynair® Ballkissen®, diameter 33 cm, height 8 cm, TOGU GmbH, Prien-Bachham, Germany) under each foot.

Participants familiarized themselves with the task by performing two repetitions in each condition combination (support: unassisted, light touch, full support; floor: non-challenging, challenging). No further instructions on the movement execution were given, allowing the participants to stand up and sit down as naturally as possible. All participants performed three valid, non-consecutive repetitions in each condition combination, resulting in a total of 18 trials per participant. The order of the support and floor conditions was randomized across participants.

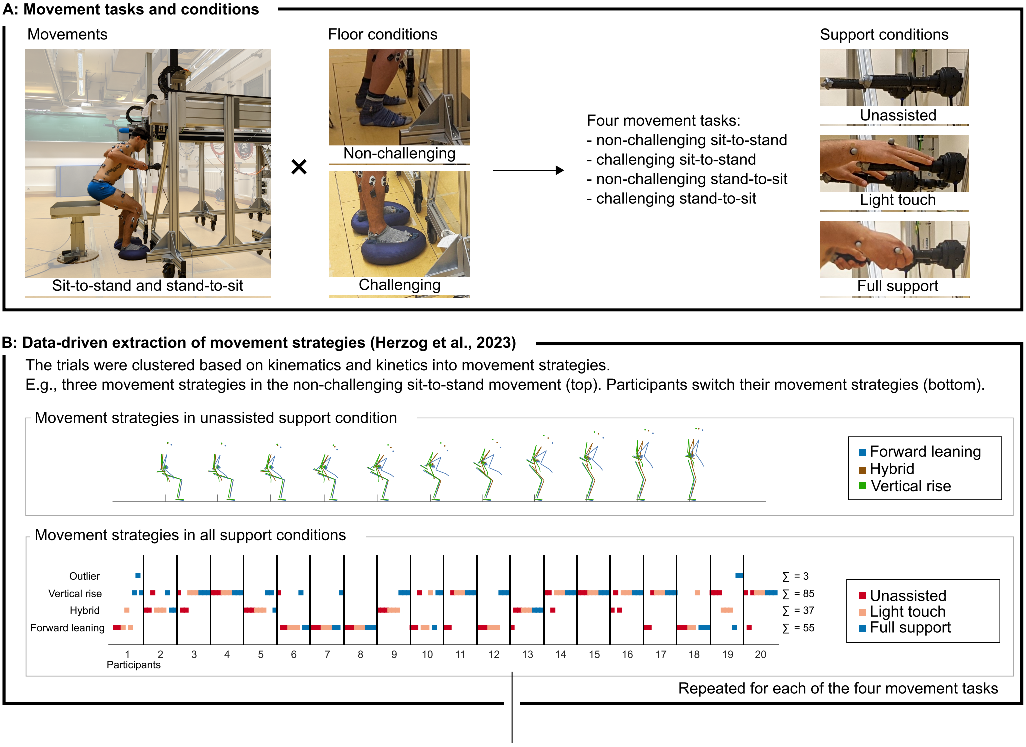

Figure continues on next page.

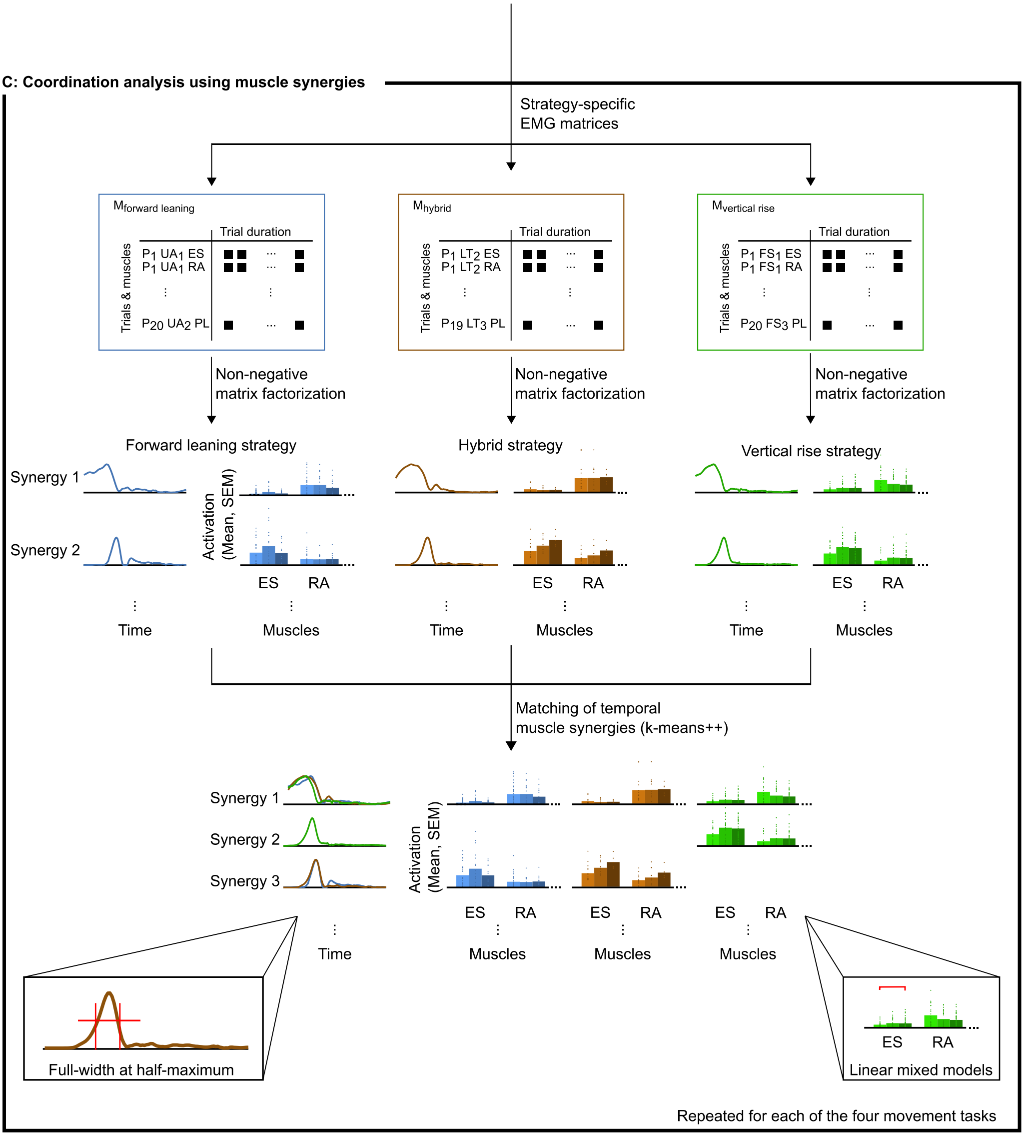
C: Coordination analysis using muscle synergies
Strategy-specific
EMG matrices
M forward leaning
M hybrid
M vertical rise
Trial duration
Trials & muscles
P1 UA1 ES
P1 UA1 RA
P20 UA2 PL
P1 LT2 ES
P1 LT2 RA
P19 LT3 PL
P1 FS1 ES
P1 FS1 RA
P20 FS3 PL
Non-negative
matrix factorization
Forward leaning strategy
Hybrid strategy
Vertical rise strategy
Synergy 1
Synergy 2
Activation
(Mean, SEM)
ES
RA
Time
Muscles
Matching of temporal
muscle synergies (k-means++)
Synergy 1
Synergy 2
Synergy 3
Full-width at half-maximum
Linear mixed models
Repeated for each of the four movement tasks

Figure 5.1: Experimental setup and data analysis. A: The participant stands up from an instrumented chair with the custom-made robot rollator simulator. Full-body passive markers for motion tracking and EMG electrodes were placed on the body. Two movements were studied: sit-to-stand and stand-to-sit. Two floor conditions were used (middle): non-challenging (lab floor) and challenging (balance pads). Three different support conditions were used (right): unassisted (handles not used), light touch (palm on the handles), and full support (power grip). The figure is adapted from (Herzog et al., 2023). B: Participants used different movement strategies and switched between them, as exemplarily shown for the non-challenging sit-to-stand task. The bottom plot shows the distribution of the trials among strategies. One dot represents one trial. The row indicates to which movement strategy it belongs. The column shows to which participant it belongs. The support conditions are color-coded as indicated by the legend. The labels on the right y-axis show how many trials were associated with the strategy written on the left y-axis. The figure is adapted from (Herzog et al., 2023). C: EMG data from the trials of the same movement strategy were arranged into a matrix (for example, $M_{\text{vertical rise}}$). Temporal muscle synergies were extracted from each matrix with NMF (Lee and Seung, 1999, 2001, Russo et al., 2024), resulting in trial-independent activation profiles and trial-dependent muscle weightings. The activation profiles were matched across the movement strategies and ordered chronologically using k-means++ clustering, ensuring a correlation coefficient above 0.9. Bottom: The duration of each activation profile was assessed as full-width at half-maximum. Linear mixed models were used to investigate how rollator support affects the muscle weightings. P_1 participant 1, UA_1 first unassisted trial, LT_1 first light touch trial, FS_1 first full support trial, ES M. erector spinae, RA M. rectus abdominis, NMF non-negative matrix factorization (Lee and Seung, 1999, 2001).

5.3.3 Data collection

Full-body 3D kinematics were obtained using the IOR full-body marker model (Cappozzo et al., 1995, Leardini et al., 2011) and ten cameras (150 Hz; Type 5+, Qualisys, Gothenburg, Sweden). Ground reaction forces (GRF; 1,000 Hz; Bertec Corp., Columbus, OH, USA) and forces on the seating surface (142 Hz; Phidgets Inc., Calgary, AB, Canada) were measured.

Thirty surface EMG electrodes (two systems, 1,500 and 4,000 Hz; Noraxon USA, Scottsdale, AZ, USA) captured full-body muscle activity of the following muscles bilaterally: pectoralis major (Pec), latissimus dorsi (Lat), trapezius (Tra), deltoideus (Del), biceps brachii (Bic), triceps brachii (Tri), gluteus medius (GM), tensor fasciae latae (TF), rectus femoris (RF), vastus medialis (VM), biceps femoris (BF), tibialis anterior (TA), peroneus longus (PL), and gastrocnemius (GA). Additionally, erector spinae (ES) and rectus abdominis (RA) activities were recorded. The participants' skin was prepared by shaving, abrasion, and cleansing with alcohol to ensure good electrode-skin contact before the Ag/AgCl electrodes were attached according to SENIAM guidelines (Hermens et al., 2000) and Perotto (2011).

5.3.4 Data processing

To reconstruct the 3D coordinates of the markers, raw kinematic data were processed offline with Qualisys Track Manager (v 2018.1). Subsequently, force and kinematic data were filtered with a 4^{th}-order zero-lag low-pass Butterworth filter at 10 Hz. Using Visual3D (v6, C-Motion Inc., Germantown, MD, USA), full-body kinematics and the center of mass (CoM) were then calculated. Further data analyses were done in Matlab (R2023b, Natick, MA, USA). Raw EMG data were bandpass (20-500 Hz) and notch (50 Hz) filtered with a 4^{th}-order zero-lag Butterworth filter (Hanawa et al., 2017). ECG artifacts apparent in the trunk muscle recordings were removed with a template-matching procedure (Peri et al., 2021). For robustness, we created a muscle- and participant-specific template of ECG artifacts using the data from the sit-to-stand and stand-to-sit recordings and an additional 9 min of still-standing recordings. Subsequently, filtered EMG data were full-wave rectified and smoothed with a 4^{th}-order zero-lag low-pass Butterworth filter at 10 Hz (Hanawa et al., 2017). Movement start, seat-off/on, and movement end were identified using a k-means++ algorithm on the GRF and CoM data (Sloot et al., 2020). As muscles need to be active before a visible movement starts, data from 200 ms before the detected start of the movement were included (Dehail et al., 2007, Kim et al., 2011). Afterward, data were segmented and time-normalized to 101 time points (100%) using a spline interpolation. Finally, EMG data were amplitude-normalized per muscle and participant to their maximum activity across the 18 trials (Lee and Seung, 2001). Of the 720 trials, 24 were not included in the analyses as some recordings of a few muscles were corrupt (Supplementary table A.3).

5.3.5 Movement strategies

Our previous investigation found that participants switched movement strategies when introduced to a rollator (Herzog et al., 2023). In particular, three movement strategies were identified for the sit-to-stand non-challenging task ("forward leaning", "hybrid", and "vertical rise") and two for the challenging task ("exaggerated forward leaning" and "forward leaning"). Likewise, three and two movement strategies were identified respectively in the stand-to-sit tasks ("vertical lowering", "hybrid", and "backward lowering"; and "exaggerated forward leaning" and "forward leaning"). The naming of these strategies was inferred by visual inspection of their movement progression, the different hip, knee, and ankle sagittal angle courses, and the relative movements between the CoM and the heel. The grouping of trials into the movement strategies was used in the current analysis to extract muscle synergies specific to the movement strategies. Supplementary figure A.6 shows the distribution of trials among strategies.

In short, the forward leaning strategy in the sit-to-stand movement showed more hip flexion and less overlapping anterior and vertical CoM movement than the vertical rise strategy. The hybrid strategy showed kinematic and kinetic time courses sometimes more aligned with one than the other strategy. In the challenging condition, the exaggerated forward leaning strategy was characterized by a wide upper body forward lean and an earlier movement of the CoM over the BoS than the forward leaning strategy. In the stand-to-sit movement, the backward lowering strategy revealed smaller hip, knee, and ankle angles than the other two, and the vertical lowering strategy showed a vertical orientation of the trunk. In the challenging condition, like with the sit-to-stand movement, the exaggerated forward leaning strategy was characterized by a wide upper body forward lean and showed less overlapping vertical and posterior CoM movement than the forward leaning strategy.

5.3.6 Data analysis

5.3.6.1 Muscle synergy analysis

We extracted muscle synergies with respect to our previous findings that participants switched their movement strategies when introduced to a rollator (Herzog et al. (2023); Figure 5.1). As stated in the introduction, the two models (spatial and temporal muscle synergies) describe different aspects of movement coordination (Brambilla et al., 2023a, Chiovetto et al., 2013, Delis et al., 2018, Russo et al., 2014, Safavynia and Ting, 2012). Temporal muscle synergies allow us to follow the underlying assumption that the CNS uses a fixed temporal sequence (trial-independent activation profiles) for the different movement strategies and that muscle weightings vary (trial-dependent muscle activation vectors) across the support conditions. Spatial and temporal muscle synergies are commonly extracted using non-negative matrix factorization (NMF) but with differently arranged EMG input matrices (Brambilla et al., 2023a, Chiovetto et al., 2013, Delis et al., 2018, Russo et al., 2014, Safavynia and Ting, 2012).

For the extraction of temporal muscle synergies, the EMG signals (30 channels) of all trials (tr is the number of trials) belonging to the same strategy (strat) were horizontally concatenated into a data matrix $\mathbf{M}_{strat} \in \mathbb{R}_{\geq 0}^{101 \times 30 \cdot tr}$. NMF decomposed $\mathbf{M}_{strat}$ into a set of N_{strat} trial-independent activation profiles $C_{strat,\,n} \in \mathbb{R}_{\geq 0}^{101 \times 1}$, and trial-dependent muscle weightings $\mathbf{W}^{\mathbf{s}}_{strat,\,n} \in \mathbb{R}_{\geq 0}^{1 \times 30}$ (Lee and Seung, 1999, 2001, Russo et al., 2024). Thus, EMG data from a single trial (s is the trial index) $\mathbf{M}^{\mathbf{s}}_{strat}(t)$ were decomposed with:

$$\mathbf{M}^{\mathbf{s}}_{strat}(t) \approx \sum_{n \in N_{strat}} C_{strat,\,n}(t) \cdot \mathbf{W}^{\mathbf{s}}_{strat,\,n}$$

To investigate hypothesis 1 that temporal muscle synergies represent sit-to-stand and stand-to-sit EMG patterns with a different compactness than spatial muscle synergies, we also extracted spatial muscle synergies. Therefore, the EMG signals (30 channels) of all trials belonging to the same strategy (strat) were horizontally concatenated into a data matrix $\mathbf{M}_{strat,\,spatial} \in \mathbb{R}_{\geq 0}^{30 \times 101 \cdot tr}$. NMF decomposed $\mathbf{M}_{strat,\,spatial}$ into a set of $N_{strat,\,spatial}$ trial-independent muscle weightings $\mathbf{W}_{strat,\,n,\,spatial} \in \mathbb{R}_{\geq 0}^{30 \times 1}$, and trial-dependent activation profiles $\mathbf{C}^{\mathbf{s}}_{strat,\,n,\,spatial} \in \mathbb{R}_{\geq 0}^{1 \times 101}$ (Lee and Seung, 1999, 2001, Russo et al., 2024). Thus, EMG data from a single trial (s is the trial index) $\mathbf{M}^{\mathbf{s}}_{strat\,spatial}(t)$ were decomposed with:

$$\mathbf{M}^{\mathbf{s}}_{strat,\,spatial}(t) \approx \sum_{n \in N_{strat,\,spatial}} \mathbf{W}_{strat,\,n,\,spatial} \cdot C^{s}_{strat,\,n,\,spatial}(t)$$

NMF's iterative decomposition was limited to 3,000 iterations and started 50 times to avoid convergence to a local minimum (Bach et al., 2021, Carey et al., 2021).

A fivefold cross-validation procedure was used to increase the confidence that the extracted muscle synergies were robust and generalizable rather than due to characteristics of single trials. In line with the literature, a training/test split of 80:20 was employed (d'Avella et al., 2003, Muceli et al., 2010). Muscle synergies were extracted from a random 80% portion of the trials. Then, the trial-independent parts were fixed and fitted to the remaining 20% of the trials. Finally, the reconstruction quality R^2_{CV} of the fits to the test sets was used to identify the number of synergies. R^2 is a multivariate measure allowing assessment of the reconstruction quality: R^2 = 1 - SSE/SST, with SSE being the sum of the squared residuals and SST the sum of the squared residuals from the mean vector (d'Avella et al., 2006). The numbers of synergies N_{strat} and $N_{strat,\,spatial}$ were chosen at the R^2-knee point, after which the R^2 curve remained approximately straight (d'Avella et al., 2006). Therefore, a series of linear regressions were fitted to the R^2 curve, starting with the interval $[N_1,\ N_{30}]$ and iteratively removing the smallest N from the interval. Then, the regressions' mean squared residual errors (MSE) were calculated, and N_{strat} and $N_{strat,\,spatial}$ were selected for the first number N with an MSE smaller than 10^{-4}. The number of synergies to extract must be chosen carefully to obtain a good low-dimensional representation of the data with minimum noise (Banks et al., 2017, Tresch et al., 2006), and numerous criteria have been proposed (Zhao et al., 2023). To avoid the results being specific to the choice of N_{strat}, rather than reflecting physiological patterns, an additional criterion was used to compare the results. Therefore, N^*_{strat} was chosen to be the minimum number fulfilling both a global ($R^2_{N_{strat}} \geq 0.9$) and a local criterion ($R^2_n - R^2_{n-1} < 0.05; n = 1 \ldots N_{strat}$).

To investigate hypothesis 1 that temporal muscle synergies represent sit-to-stand and stand-to-sit EMG patterns with a different compactness than spatial muscle synergies, we compared the compactness of the spatial and temporal muscle synergy extractions using two metrics. Firstly, we compared the dimensionality reduction (R^2-knee criterion) between temporal and spatial extractions (N_{strat} and $N_{strat,\,spatial}$). Secondly, the number of trial-dependent parameters (temporal: synergies · muscles, spatial: time samples · synergies) and the number of trial-independent parameters (temporal: time samples · synergies, spatial: synergies · muscles) were also compared between the temporal and spatial extraction, with the number of synergies selected at the respective R^2-knee point (Delis et al., 2014).

This justified the choice of temporal muscle synergies beyond the assumption that the CNS uses a fixed temporal sequence (trial-independent activation profiles) for the different movement strategies and that muscle weightings vary (trial-dependent muscle activation vectors) across the support conditions (degree of handle support). All steps regarding muscle synergy analyses were done separately for the two movements and floor conditions.

5.3.6.2 Matching of similar synergies across the movement strategies

To investigate hypothesis 2 that muscle synergy activation differs across movement strategies, the activation profiles of the different movement strategies were matched with k-means++ clustering (Matlab `kmeans`, with the 'plus' option, 50 restarts with random initial cluster centroid positions, maximum 1,000 iterations; Figure 5.1; Ivanenko et al. 2005). Suppose two movement strategies show n temporal synergies each. If the two movement strategies do not differ in terms of their activation profiles, k-means++ groups them into n clusters, each with two activation profiles, one from the first and one from the second movement strategy. A difference between the movement strategies is identified if there are more than n clusters. In this case, there are clusters with only one synergy. These clusters are specific to one of the two movement strategies. Accordingly, the activation profiles within the same cluster are characterized by a similar shape of activation and timing.

The number of clusters was increased from one until the minimum number for which (1) a correlation coefficient (Ivanenko et al., 2005) of at least 0.9 per match of all activations profiles within each cluster with their centroid was ensured and (2) only one activation profile per strategy was included within each cluster. The clustering was repeated ten times to confirm the robustness of the cluster assignments (van Drongelen et al., 2021).

5.3.6.3 Statistics

Timing and duration of temporal synergies

To investigate hypothesis 2 that muscle synergy activation differs across movement strategies beyond their similarity (see 5.3.6.2), we assessed the duration of activation by measuring the full-width at half-maximum of the main peak ($FWHM$; Matlab `findpeaks`; Ivanenko et al. 2005). Therefore, the time difference between the two points at half-height on either side of the main peak was calculated. As sit-to-stand and stand-to-sit are sequential movements, we cannot assume that the boundary synergies (synergies with the peaks close to the movement start and end) are symmetrical. In the case of boundary synergies, we measured the difference between the movement start and the point of half-height of the descending synergy or the difference between the point of half-height and the movement end.

Linear mixed model to assess differences in the muscle weightings

To investigate hypothesis 3, i.e., to identify the changes in the muscle weightings between the support conditions (unassisted, light touch, full support), a linear mixed model (LMM) was used (Matlab `fitlme`). The LMM considers that repeated measures of a single participant are likely correlated (Aarts et al., 2014, Tirrell et al., 2018) allowing us to manage the distribution of participants' trials over several movement strategies. To account for the simultaneous changes in multiple muscle weightings (trial-dependent muscle activation vectors) with the support condition, a multivariate LMM approach was used (Twisk, 2019).

Single trials (level 1) were nested into participants (level 2). The support conditions were included as dummy variables using reference coding (LT or FS set to 1, or both to 0 for the unassisted condition). The first multivariate LMM was calculated with UA as the reference group, and the second multivariate LMM with LT as the reference group, allowing investigation of all pairwise comparisons within the support conditions. Each vector of muscle weightings belongs to one temporal synergy, i.e., the reference frames in which the muscle weightings lie are different across the temporal synergies, so one multivariate LMM was used for each vector. For example, for the non-challenging sit-to-stand task using the forward leaning strategy, seven synergies led to 14 multivariate LMM tests within this task (seven synergies tested once with UA and once with LT as reference group). Sex was added as a within-participant control variable at level 1 but was not included in the final model as it did not improve the model based on the change in the -2 log-likelihood or the Akaike's information criterion (Matlab's `linearmixedmodel.compare` function; Ippersiel et al. 2021, Russell and Haworth 2014). The residual plots were inspected to assess normality, linearity, and homoscedasticity as prerequisites for LMM, and no gross violations were found (Hox et al., 2017, Snijders and Bosker, 2012).
The multivariate LMM regression formula was:
Level 1:

$$\mathit{Weightings}_{tp} = \beta_{0p} + \beta_{1p} LT_{tp} + \beta_{2p} FS_{tp} + \epsilon_{tp}$$

Level 2:

$$\beta_{0p} = \gamma_{00} + \mu_{0p}$$
$$\beta_{1p} = \gamma_{10}$$
$$\beta_{2p} = \gamma_{20}$$

$\mathit{Weightings}_{tp}$ represents the mean muscle weighting across the left and right limb of each bilaterally assessed muscle and the single weightings of M. erector spinae and M. rectus abdominis of a given synergy on the t^{th} trial for the p^{th} participant. The β_{0p} represents the intercept, β_{1p} and β_{2p} the fixed effects for the support conditions, and ϵ_{tp} represents the trial- and participant-specific residual. The variable μ_{0p} is a support-specific random component of β_{0p} and the γ fixed effect parameters. Accordingly, the following formula was used for the function specification of the `fitlme` function: 'Weightings $\sim$ LT + FS + (1 | Participant)'. To account for the multivariate nature, muscle weightings were vertically concatenated into $\mathit{Weightings}_{tp}$. For the second multivariate LMM test, 'LT' was exchanged with 'UA' to have LT as the reference group. The t-statistic on the β coefficients was used for hypothesis testing with the significance set a priori at a two-sided α = 0.05 (Russell and Haworth, 2014). To reduce the probability of type I errors, the level of significance was adjusted according to the number of tests within one movement strategy (e.g., for the seven synergies in the non-challenging, sit-to-stand forward leaning strategy, the level of significance was adjusted for 14 tests with Bonferroni correction).

If the multivariate LMM showed significance regarding the support groups (Twisk, 2019), **MscName** (a categorical variable representing the muscle names, using effect coding, **MscName** indicates the vector of dummy variables) was used in the second step as a dummy variable of the LMM analyses using effect coding. Therefore, the interaction between the muscles and the support condition was added to the LMM. This revealed the muscles in which the support condition affects their weighting with respect to the mean of the group mean of the reference muscle (M. Rectus abdominis) and support group (effect coding). Consequently, the following model was used:
Level 1:

$$\begin{aligned} \mathit{Weightings}_{tp} &= \beta_{0p} + \beta_{1p} LT_{tp} + \beta_{2p} FS_{tp} \\ &+ \boldsymbol{\beta}_{\mathbf{3p}}^{\mathbf{T}} \mathit{MscName}_{\mathbf{p}} + \boldsymbol{\beta}_{\mathbf{4p}}^{\mathbf{T}} LT_{tp} \mathit{MscName}_{\mathbf{p}} + \boldsymbol{\beta}_{\mathbf{5p}}^{\mathbf{T}} FS_{tp} \mathit{MscName}_{\mathbf{p}} \\ &+ \epsilon_{tp} \end{aligned}$$

Level 2:

$$\begin{aligned} \beta_{0p} &= \gamma_{00} + \mu_{0p} \\ \beta_{1p} &= \gamma_{10} \\ \beta_{2p} &= \gamma_{20} \\ \boldsymbol{\beta}_{\mathbf{3p}} &= \boldsymbol{\gamma}_{\mathbf{30}} \\ \boldsymbol{\beta}_{\mathbf{4p}} &= \boldsymbol{\gamma}_{\mathbf{40}} \\ \boldsymbol{\beta}_{\mathbf{5p}} &= \boldsymbol{\gamma}_{\mathbf{50}} \end{aligned}$$

Matlab model function: Weightings $\sim$ (LT + FS) $*$ MscName + (1 | Participant)
To reduce the probability of type I errors, the significance level (α = 0.05) was adjusted to the number of tests with the second model, at maximum three if a significant effect was found for each pairwise comparison of UA, LT, and FS. The LMM was implemented using the maximum likelihood method.

5.4 Results

5.4.1 Temporal muscle synergies result in a more compact representation than spatial muscle synergies in sit-to-stand and stand-to-sit EMG patterns

To investigate if temporal muscle synergies represent sit-to-stand and stand-to-sit EMG patterns with different compactness than spatial muscle synergies, both types of synergy were extracted from the EMG data. In each movement task, six to ten temporal synergies reconstructed the EMG patterns (Figure 5.2) with an R^2 between 0.84 and 0.89 (Figure 5.2, Table 5.1). In particular, 5.8 ± 2.4 fewer synergies were necessary for the temporal than for the spatial extraction with the R^2-knee criterion. Figure 5.4 shows the EMG and the good reconstruction for an exemplary participant. Furthermore, Figure 5.3 also shows that muscle activity and their reconstruction are very symmetrical between the left and right sides, along with an increase in upper body muscle activity with increasing support. The number of trial-independent parts is smaller for the temporal muscle synergies than for the spatial muscle synergies, and fewer trial-dependent parts are necessary for every trial (Table 5.2). Accordingly, the total number of the trial-independent and trial-dependent parts is smaller for the temporal muscle synergies, which indicates that the higher R^2 of the temporal muscle synergies is not simply due to the number of parts. Thus, temporal muscle synergies represent the EMG patterns more compactly than spatial muscle synergies (hypothesis 1). Accordingly, the subsequent analyses were done with temporal muscle synergies.

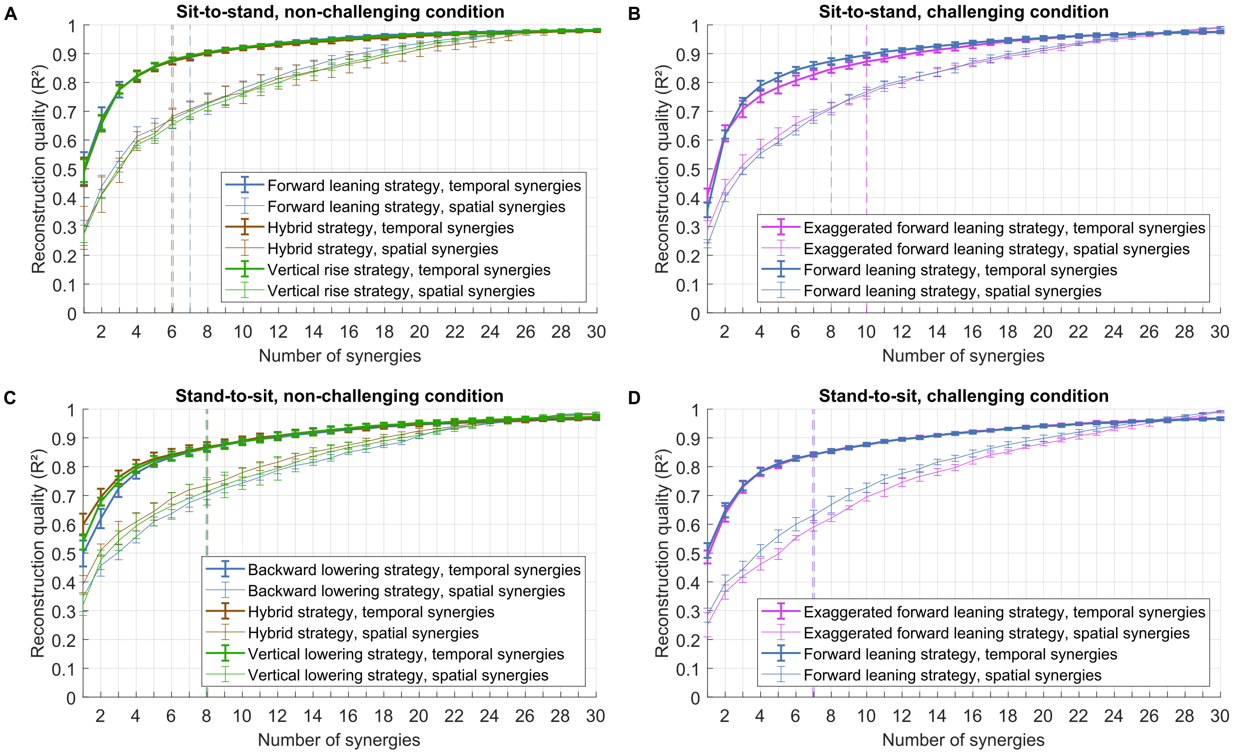

Figure 5.2: Reconstruction quality (R^2) for every movement (A, B, C, D) and movement strategy (color-coded). Thick lines: Temporal muscle synergy reconstruction quality, thin lines: spatial muscle synergy reconstruction quality. The figure shows means and standard deviations over the fivefold cross-validation runs. The vertical dotted lines, color-coded with respect to the movement strategies, indicate the choice for the number of synergies according to Table 5.1.

Table 5.1: The numbers and R^2 of synergies according to the applied criterion and choice of model. R^2 values are mean and standard deviation over the fivefold cross-validation runs.

Movement	**Sit-to-stand, non-challenging**			**Sit-to-stand, challenging**	
Strategy	Forward leaning	Hybrid	Vertical rise	Exaggerated forward leaning	Forward leaning
Temporal	7	6	6	10	8
R^2-knee (N_{strat})	0.888 ± 0.008	0.874 ± 0.012	0.879 ± 0.005	0.873 ± 0.012	0.874 ± 0.011
Temporal	8	8	8	13	11
$R^2 > 0.9$ (N^*_{strat})	0.902 ± 0.005	0.902 ± 0.009	0.905 ± 0.003	0.905 ± 0.009	0.906 ± 0.009
Spatial	15	12	16	11	13
R^2-knee ($N_{strat, spatial}$)	0.952 ± 0.005	0.931 ± 0.007	0.953 ± 0.002	0.882 ± 0.010	0.920 ± 0.006

Movement	**Stand-to-sit, non-challenging**			**Stand-to-sit, challenging**	
Strategy	Backward lowering	Hybrid	Vertical lowering	Exaggerated forward leaning	Forward leaning
Temporal	8	8	8	7	7
R^2-knee (N^*_{strat})	0.865 ± 0.009	0.868 ± 0.017	0.864 ± 0.013	0.842 ± 0.004	0.842 ± 0.007
Temporal	12	11	12	13	13
$R^2 > 0.9$ ($\mathrm{N_{strat}}^*$)	0.902 ± 0.004	0.901 ± 0.014	0.905 ± 0.013	0.902 ± 0.005	0.901 ± 0.005
Spatial	16	13	13	12	12
R^2-knee ($N_{strat, spatial}$)	0.929 ± 0.005	0.915 ± 0.013	0.914 ± 0.011	0.895 ± 0.005	0.896 ± 0.004

Table 5.2: Amount of dimensionality reduction in terms of trial-independent and trial-dependent signals according to Delis et al. (2014).

Movement		**Sit-to-stand, non-challenging**			**Sit-to-stand, challenging**	
Strategy		Forward leaning	Hybrid	Vertical rise	Exaggerated forward leaning	Forward leaning
Number of trial-independent parameters	Temporal: time samples · synergies	707	606	606	1010	808
	Spatial: synergies · muscles	450	360	480	330	390
Number of trial-dependent parameters	Temporal: synergies · muscles	210	180	180	300	240
	Spatial: time samples · synergies	1515	1212	1616	1111	1313
Sum temporal		917	786	786	1310	1048
Sum spatial		1965	1572	2096	1441	1703

Movement		**Stand-to-sit, non-challenging**			**Stand-to-sit, challenging**	
Strategy		Vertical lowering	Hybrid	Backward lowering	Exaggerated forward leaning	Forward leaning
Number of trial-independent parameters	Temporal: time samples · synergies	808	808	808	707	707
	Spatial: synergies · muscles	480	390	390	360	360
Number of trial-dependent parameters	Temporal: synergies · muscles	240	240	240	210	210
	Spatial: time samples · synergies	1616	1313	1313	1212	1212
Sum temporal		1048	1048	1048	917	917
Sum spatial		2096	1703	1703	1572	1572

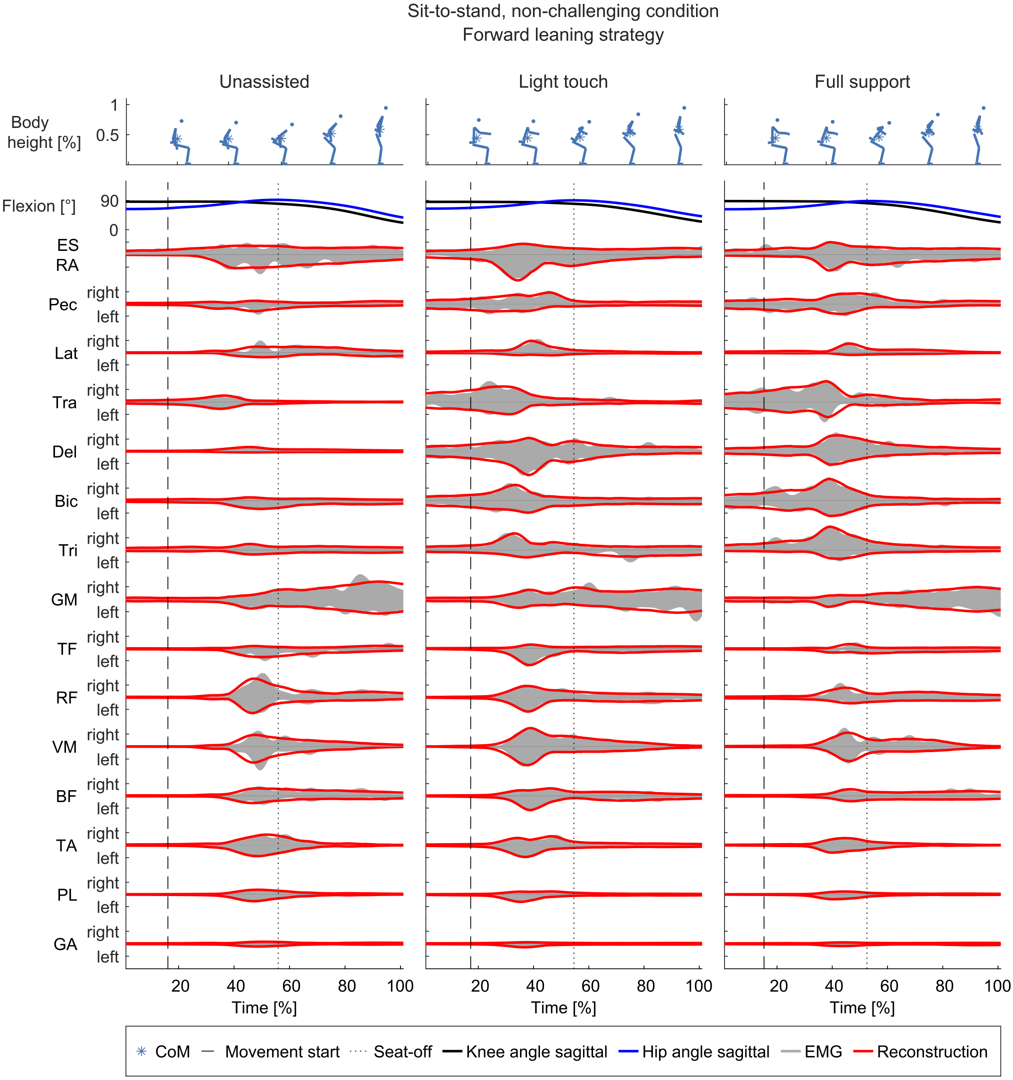

Figure 5.3: Kinematics (top), original EMG (gray areas), and reconstruction (red solid lines). Data from one exemplary participant using the forward leaning strategy to stand up. The dashed line indicates the movement start, i.e., the first visible CoM movement. The dotted line indicates seat-off. Left: unassisted, middle: light touch, right: full support condition. Muscle activity of the right limb is in the positive direction, and the left limb is in the negative direction.

5.4.2 The timing of temporal muscle synergies differs across movement strategies

To investigate hypothesis 2 that muscle synergy activation differs across movement strategies, temporal synergy activation profiles were clustered using k-means++ across the movement strategies and differences were identified if specific clusters were found (see 5.3.6.2).

5.4.2.1 Sit-to-stand movement strategies

In the non-challenging task (Figure 5.4), the activation profiles of the seven forward leaning synergies and the six hybrid and six vertical rise strategies were grouped into eight clusters. Timing differed across the movement strategies between movement start and shortly before seat-off. Also, there is one distinct forward leaning synergy active right after seat-off. At movement start, seat-off, and at movement end, the clusters contained synergies from all three movement strategies. Hence, at these times, the activation profiles do not differ.

In the challenging condition (Figure 5.5), the ten synergies of the exaggerated forward leaning and eight from the forward leaning strategy were grouped into eleven clusters. Right after seat-off, the timing of the synergies differs between the two movement strategies, with three distinct exaggerated forward leaning temporal synergies. This differs from the non-challenging task, where we additionally found differences between movement start and seat-off. Across all movement strategies, the main synergy peaks widths ($FWHM$) were larger at movement start and end than in the middle, especially around seat-off (Table 5.3).

The findings that the timing of the temporal muscle synergies differs across the movement strategies are robust regarding the criterion for selecting the numbers of synergies (Supplementary figure A.7. Therefore, we accept our second hypothesis that muscle synergy activation differs across movement strategies regarding sit-to-stand movements.

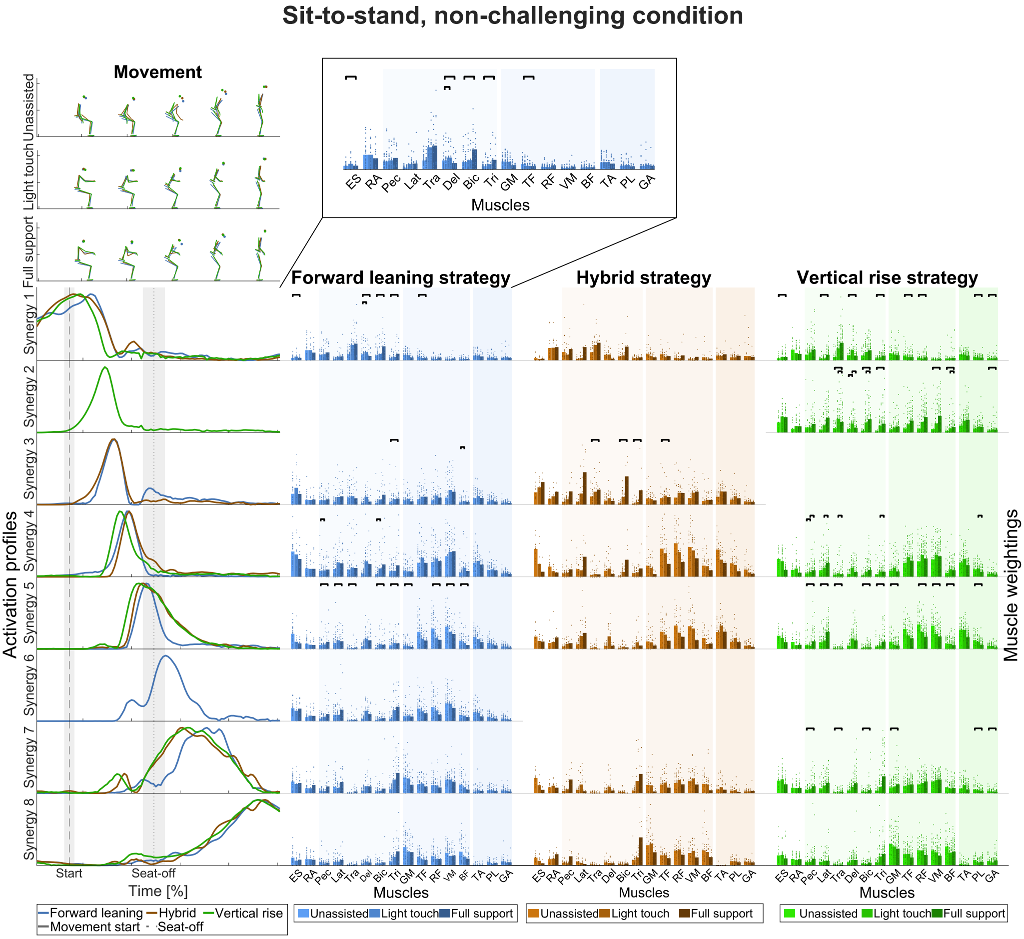

Figure 5.4: Temporal muscle synergies in the sit-to-stand movement and non-challenging condition. Top: Exemplary movements in the unassisted, light touch, and full support conditions (in rows) and movement strategies (color-coded). Bottom, left: Temporal muscle synergies sorted chronologically and color-coded according to the movement strategy. The dashed line indicates the movement start, i.e., the first identified CoM movement. The dotted line indicates seat-off. The timing of the three movement strategies was different, as indicated by the strategy-specific temporal synergies 2, 3, and 6. Bottom, right: Bar graphs show mean muscle weightings across the left and right side (except ES and RA), all trials within a strategy and support condition, and single dots represent trial-specific weightings in two columns for the left and right limbs. The different color shades indicate the support conditions. The bars indicate statistically significant differences according to the LMM statistics (details in section A.3.4).

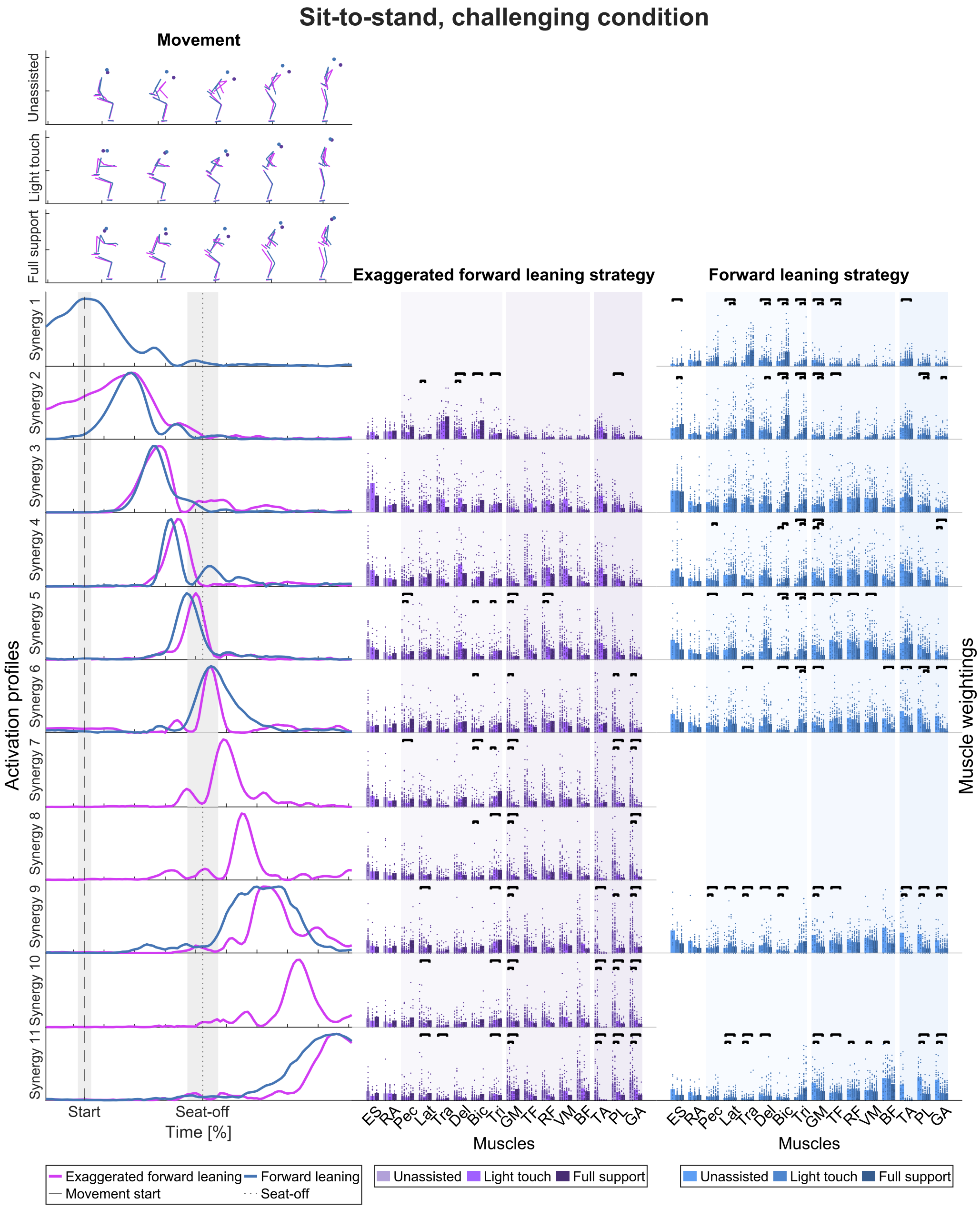
Sit-to-stand, challenging condition
Movement
Unassisted
Light touch
Full support
Exaggerated forward leaning strategy
Forward leaning strategy
Activation profiles
Synergy 1
Synergy 2
Synergy 3
Synergy 4
Synergy 5
Synergy 6
Synergy 7
Synergy 8
Synergy 9
Synergy 10
Synergy 11
Start
Seat-off
Time [%]
ES RA Pec Lat Tra Del Bic Tri GM TF RF VM BF TA PL GA
Muscles
ES RA Pec Lat Tra Del Bic Tri GM TF RF VM BF TA PL GA
Muscles
Muscle weightings
Exaggerated forward leaning
Forward leaning
Movement start
Seat-off
Unassisted
Light touch
Full support
Unassisted
Light touch
Full support

Figure 5.5: Temporal muscle synergies in the sit-to-stand movement and challenging condition. Top: Exemplary movements in the unassisted, light touch, and full support conditions (in rows) and movement strategies (color-coded). Bottom, left: Temporal muscle synergies sorted chronologically and color-coded according to the movement strategy. The dashed line indicates the movement start, i.e., the first identified CoM movement. The dotted line indicates seat-off. The timing of the two movement strategies was different, as indicated by the strategy-specific temporal synergies 1, 7, 8, and 10. Bottom, right: Bar graphs show mean muscle weightings across the left and right side (except ES and RA), all trials within a strategy and support condition, and single dots represent trial-specific weightings in two columns for the left and right limbs. The different color shades indicate the support conditions. The bars indicate statistically significant differences according to the LMM statistics (details in section A.3.4).

5.4.2.2 Stand-to-sit movement strategies

In the non-challenging task (Figure 5.6), the activation profiles of the eight backward lowering, hybrid, and vertical lowering strategies were grouped into ten clusters. Most of the time, the timing across the three movement strategies did not differ. However, there was one distinct synergy for each of the movement strategies: the distinct backward lowering synergy is active after seat-on, the distinct hybrid synergy at seat-on, and the distinct vertical lowering synergy between movement start and seat-on.

In the challenging condition (Figure 5.7), seven synergies of the exaggerated forward leaning and the forward leaning strategy were grouped into eight clusters. As in the non-challenging task, the timing did not differ between the two strategies most of the time. However, each strategy shows a distinct synergy. For the exaggerated forward leaning strategy, the synergy is active at seat-on, and for the forward leaning synergy after seat-on.

Similar to the sit-to-stand movements, the widths of the main synergy peaks ($FWHM$) were larger at movement start and end than in the middle, especially around seat-off (Table 5.3). Also, the finding that the timing of the temporal muscle synergies differs across the movement strategies is robust regarding the criterion for selecting the numbers of synergies (Supplementary figure A.7). Therefore, we accept our second hypothesis that muscle synergy activation differs across movement strategies for stand-to-sit movements.

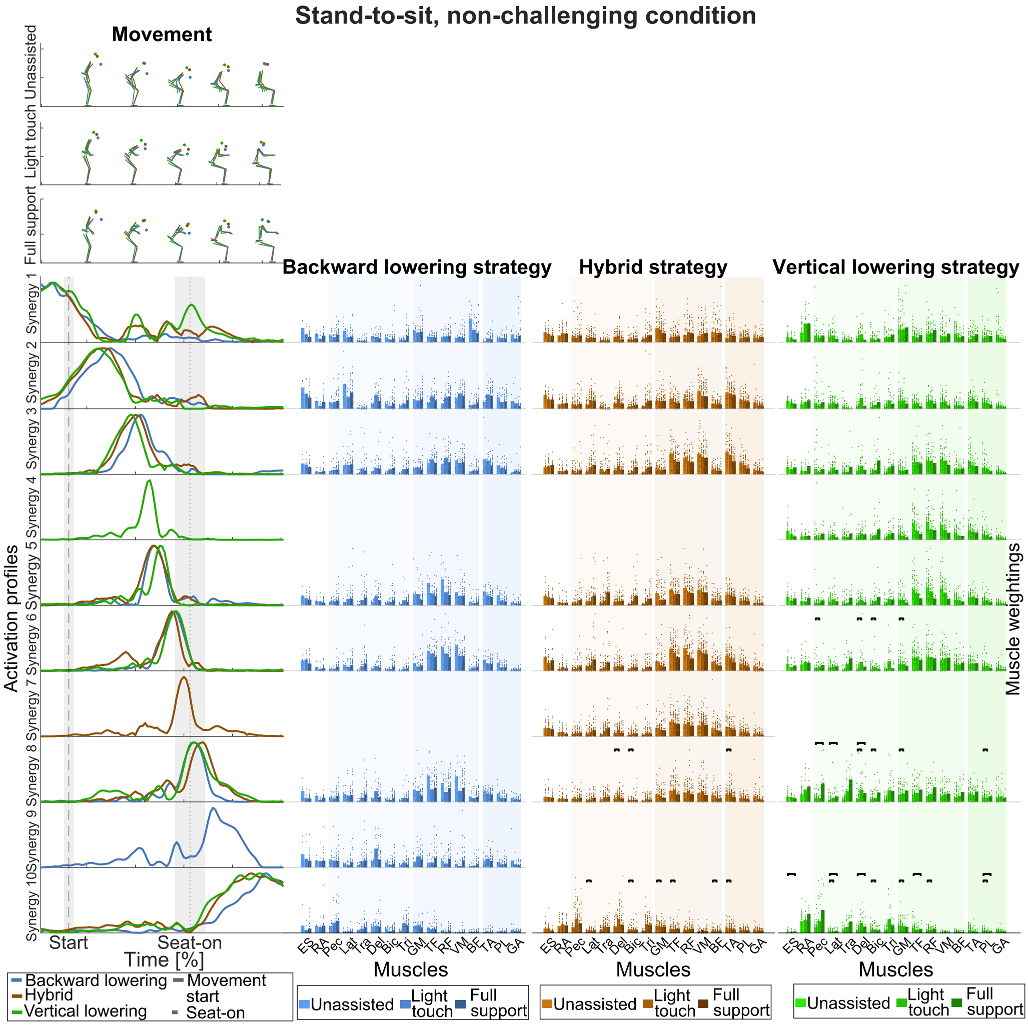

Figure 5.6: Temporal muscle synergies in the stand-to-sit movement and non-challenging condition. Top: Exemplary movements in the unassisted, light touch, and full support conditions (in rows) and movement strategies (color-coded). Bottom, left: Temporal muscle synergies sorted chronologically and color-coded according to movement strategy. The dashed line indicates movement start, i.e., the first identified CoM movement. The dotted line indicates seat-off. The timing of the three movement strategies was different, as indicated by the strategy-specific temporal synergies 4, 7, and 9. Bottom, right: Bar graphs show mean muscle weightings across the left and right side (except ES and RA), all trials within a strategy, and support condition, and single dots represent trial-specific weightings in two columns for the left and right limbs. The different color shades indicate the support conditions. The bars indicate statistically significant differences according to the LMM statistics (details in section A.3.4).

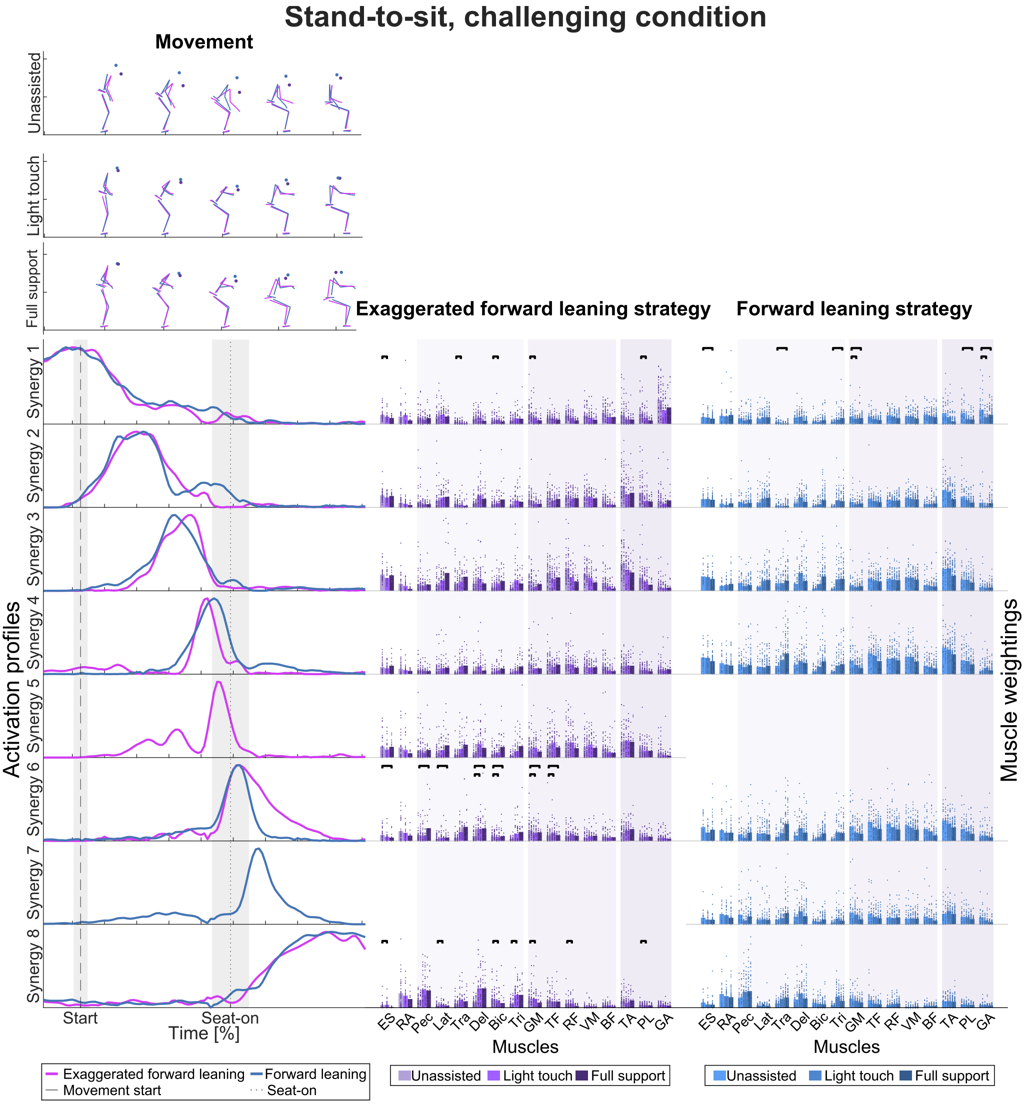

Figure 5.7: Temporal muscle synergies in the stand-to-sit movement and challenging condition. Top: Exemplary movements in the unassisted, light touch, and full support conditions (in rows) and movement strategies (color-coded). Bottom, left: Temporal muscle synergies sorted chronologically and color-coded according to the movement strategy. The dashed line indicates movement start, i.e., the first identified CoM movement. The dotted line indicates seat-off. The timing of the two movement strategies was different, as indicated by the strategy-specific temporal synergies 5 and 7. Bottom, right: Bar graphs show mean muscle weightings across the left and right side (except ES and RA), all trials within a strategy and support condition, and single dots represent trial-specific weightings in two columns for the left and right limbs. The different color shades indicate the support conditions. The bars indicate statistically significant differences according to the LMM statistics (details in section A.3.4).

Table 5.3: Full-width at half-maximum ($FWHM$) of the temporal synergies. Trials are time-normalized to 101 points. Therefore, the numbers in the table represent fractions of the whole trial durations.

Movement	**Sit-to-stand, non-challenging**			**Sit-to-stand, challenging**		**Stand-to-sit, non-challenging**			**Stand-to-sit, challenging**	
Strategy/ synergy	Forward leaning	Hybrid	Vertical rise	Exaggerated forward leaning	Forward leaning	Vertical lowering	Hybrid	Backward lowering	Exaggerated forward leaning	Forward leaning
1	29.1	29.0	25.3		24.4	16.4	15.7	19.4	24.2	24.1
2			9.4	33.2	12.6	23.4	21.3	22.0	18.7	19.9
3	8.7	9.8		11.1	9.0	11.0	13.7	12.7	14.1	14.6
4	9.0	8.4	8.8	8.0	6.3			5.8	11.3	7.4
5	9.5	15.8	18.9	6.7	8.4	8.8	10.8	6.7		6.6
6	13.5			5.8	12.4	10.9	8.4	9.3	8.9	14.2
7	23.1	33.3	32.1	8.2			6.9		8.8	
8	22.8	27.3	25.0	7.1		10.2	10.8	11.4	30.0	30.9
9				12.0	25.5	15.1				
10				9.6		20.0	28.3	31.2		
11				13.1	20.5					

5.4.3 The degree of support influences muscle weighting

To test for differences in muscle weightings (right-hand columns of Figure 5.4, Figure 5.5, Figure 5.6, and Figure 5.7) across the support conditions (UA, LT, FS) with regard to hypothesis 3, that rollator support influences the weightings between upper body and lower limb muscles, LMMs were calculated. Detailed statistical results with p-values corrected for multiple testing are presented in section A.3.4.

5.4.3.1 Sit-to-stand movement strategies

In the non-challenging task, muscle weightings changed from the start of the movement onwards. The main change was an increased weighting of upper body muscles in the full support condition compared to unassisted across all movement strategies. Shortly before and at seat-off, muscle weightings showed a change with increased upper body and decreased lower limb muscle weightings in full support compared to the unassisted condition in the forward leaning and vertical rise strategy. After seat-off, minor changes were only observed in the vertical rise strategy.

More changes were observed in the challenging task than in the non-challenging task. At movement start, upper body muscles were more weighted in the full support condition than in the unassisted condition for all movement strategies. Shortly before and at seat-off, muscle weightings showed increased upper body and decreased lower limb muscle weightings in full support compared to the unassisted condition, as in the non-challenging task. After seat-off, we observed decreased weightings of the muscles acting around the ankle with light touch and full support, which is a specific finding of the challenging condition.

With regard to the sit-to-stand task, we accept the hypothesis that rollator support influences the weightings between upper body and lower limb muscles.

5.4.3.2 Stand-to-sit movement strategies

In the non-challenging task, no significant differences between the support conditions were observed for the backward lowering strategy. However, some changes were observed in the hybrid and vertical lowering strategy: at and after seat-on, the weightings of M. pectoralis major, latissimus dorsi, and arm muscles increased in the light touch and full support conditions.

In the challenging task, no significant changes in muscle weightings were observed in the forward leaning strategy after the movement began. However, muscle weightings changed at seat-on and movement end in the exaggerated forward leaning strategy. Comparable to the non-challenging task, the weightings of M. pectoralis major, latissimus dorsi, and arm muscles increased in the light touch and full support conditions. In addition, the weightings of M. gluteus medius and tensor fasciae latae decreased with support.

With regard to the sit-to-stand task, we accept the hypothesis that rollator support influences the weightings between upper body and lower limb muscles.

5.5 Discussion

The study investigated the influence of rollator handle support on movement coordination in sit-to-stand and stand-to-sit movements while considering that people employ different movement strategies. Three support conditions were investigated: no assistance, light touch (haptic cue), and full support (supposed load reduction in the lower limbs). Furthermore, balance pads were placed underneath the young participants' feet to make the movements challenging by increasing postural instability (non-challenging vs. challenging condition). We hypothesized that (1) temporal muscle synergies represent sit-to-stand and stand-to-sit EMG patterns with a different compactness than spatial muscle synergies. Furthermore, we hypothesized that (2) muscle synergy activation differs across movement strategies and that (3) rollator support influences the weightings between upper body and lower limb muscles.

5.5.1 Temporal muscle synergies represent sit-to-stand and stand-to-sit EMG patterns more compactly than spatial muscle synergies

With six to ten temporal muscle synergies, low-dimensional representations of the sit-to-stand and stand-to-sit movement strategies with 30 EMGs were obtained with R^2 values between 0.84 and 0.89. The number of synergies found was higher than in studies investigating sit-to-stand movements, in which three to four spatial muscle synergies explained 87-94% of the variance (An et al., 2013, Carey et al., 2021, Hanawa et al., 2017, Kogami et al., 2021, Ranaldi et al., 2023, Yang et al., 2017). However, in these studies, no upper body muscle activity was measured, and no assistive device was used. In particular, previous studies also found that the number of synergies increased when participants used assistive devices, for example, Nordic walking sticks (Candow and Chilibeck, 2005) or exoskeletons (Lynch et al., 1999, Ashford and De Souza, 2000) or while they were pushed up by the chair during sit-to-stand (Wang et al., 2021). This supports the higher number of synergies found here compared to earlier sit-to-stand studies (An et al., 2013, Carey et al., 2021, Hanawa et al., 2017, Kogami et al., 2021, Ranaldi et al., 2023, Yang et al., 2017). Also, spatial or spatiotemporal rather than temporal synergies were extracted in the referenced studies. Thus, comparisons regarding the reconstruction quality are limited. Nevertheless, the main functional groups, i.e., groups of coactivated muscles, identified with spatial synergies in the studies mentioned above largely align with the muscle weightings in our study.

We found that temporal muscle synergies provide a more compact representation than spatial synergies, which is supported by studies of upper-limb and postural tasks (Brambilla et al., 2023a, Russo et al., 2014, Safavynia and Ting, 2012) and our finding that the change in slope ("knee") in the R^2 curve was more pronounced with temporal synergies was also found recently during postural tasks (Brambilla et al., 2023a). Spatial and temporal muscle synergies are two of several possible representations of modular control (Delis et al., 2014). In general, the CNS might generate motor commands by a few sample-independent modules, which are thought to be shared across tasks and conditions (d'Avella et al., 2003) and are activated sample-dependently. The sample-independent part is thought to be stored in subcortical areas (Delis et al., 2014). Consequently, with temporal synergies, it is assumed that activation profiles are stored and muscle weightings are sample-dependently composed (Alessandro et al., 2013, Hart, 2004, Hart and Giszter, 2010). The good reconstruction quality with temporal synergies hints that the CNS may store activation sequences for sit-to-stand and stand-to-sit movements, while it has to be acknowledged that the neural underpinning of muscle synergies is still debated (Cheung and Seki, 2021, Tresch and Jarc, 2009).

5.5.2 The activation profiles of the temporal muscle synergies show similar shapes but differ in timing across movement strategies

Across all conditions, the activation profiles of the temporal muscle synergies mostly have a symmetric bell shape with a single point of maximum activation, similar to those found in the literature (Chiovetto et al., 2013, Torricelli et al., 2020). The shapes are similar across the movement strategies, with a narrower width at seat-on and seat-off than at movement start and end. Furthermore, no support-specific synergies emerged with only high lower limb or upper-limb muscle weightings. However, the timing of the temporal muscle synergies differs across the movement strategies, which supports hypothesis 2. Similarly, Yang et al. (2017) found that their momentum transfer and stabilization movement strategy only differed in the activation timing of the spatial muscle synergy, which was predominantly active around seat-off. This aligns with the activation times of the forward leaning, hybrid, and vertical rise strategies (synergies 2, 3, and 6). Accordingly, the differences may stem from strategy-specific biomechanical requirements during this phase, e.g., in the forward leaning strategy to transfer the momentum generated by the upper body from the trunk to the thigh to stand up (Anan et al., 2012, Jeon et al., 2019, Riley et al., 1991). Also, comparing the exaggerated forward leaning to the forward leaning strategy in the sit-to-stand challenging movement, there are distinct activation profiles after seat-off while the body is erected, probably reflecting different biomechanical demands when participants keep their CoM over the BoS for longer in the exaggerated forward leaning strategy (Herzog et al., 2023). Hence, different movement strategies may emerge through different activation sequences, and rollator support does not provoke a different pattern of impulses.

5.5.3 Temporal synergies reveal that tightness of control is increased in balance-critical phases

A recent study related temporal muscle synergies to the model of intermittent control of movement (Brambilla et al., 2023a). According to this model, the CNS sends pulsed commands that are transformed into muscle activation profiles (Leib et al., 2020). The muscle activation profiles are adjusted in amplitude (here: sample-dependent muscle weightings) and finally result in motor output (Gross et al., 2002). Sit-to-stand and stand-to-sit movements consist of multiple phases. Indeed, the literature has identified four to six phases, and even up to eleven (Etnyre and Thomas, 2007, Kotake et al., 1993, Schenkman et al., 1990), each of which has different requirements for motor control.

Numerous temporal synergies have been observed in this study, and their peaks are narrow, especially around the balance-critical seat-off and seat-on (Hughes et al. 1994, Komisar et al. 2023, Pai et al. 1994; see Table 5.3). Regarding the intermittent control model, these narrow, i.e., tight in time, peaks could reflect that each “control action” has a short duration. Accordingly, the CNS might tightly control the movements using multiple, successive pulsed commands to fulfill the demands of the phases’ different requirements. This tight CNS control is further supported by the increased number of temporal synergies in the challenging sit-to-stand condition, where the balance difficulty was increased. The exaggerated forward leaning strategy revealed three more synergies than the forward leaning strategy in the challenging sit-to-stand task. We previously aligned the former with the so-called “stabilization strategy”, based on visual inspection of the stick figures, the hip and CoM-heel angles before seat-off, and the sagittal CoM trajectory (Herzog et al., 2023). We suggested it increases stability and safety when coping with the increased balance challenge due to the longer time the CoM resides inside the BoS (Herzog et al., 2023, Sadeh et al., 2023). The higher number of temporal synergies found here may reflect this coping mechanism. However, the prolonged time keeping the CoM inside the BoS might increase the need for CNS control. In particular, Scarborough et al. (2007) propose that participants might need to sit back if adequate momentum could not be generated (Scarborough et al., 2007). Therefore, the CNS probably increases the tightness of control to enable successful movements and prevent a sit-back. However, the high number of required narrow synergies, and thus a high demand for CNS control, may be critical for older people or people with disabilities. This aligns with Scarborough et al.’s (2007) argument that this strategy might not be the safest because both vertical and anterior momentum need to be generated adequately. Although this cannot be addressed with our healthy cohort, future studies may investigate whether people with reduced balance capacity in standing up and sitting down movements lack tight CNS control.

5.5.4 Rollator support increases upper body and decreases lower limb muscle weightings

In support of hypothesis 3, we found that the weightings of upper body muscles increased with support across movement strategies in general, especially at seat-off and seat-on. Likewise, lower limb muscle weightings decreased with support. In particular, the weightings of muscles acting around the ankle decreased with support in the challenging sit-to-stand task.

Generally, these shifts find support in the literature. Suica et al. (2016) found that walking with a rollator significantly reduced lower limb muscle activity in healthy subjects, and IJmker et al.'s (2015) EMG analysis with stroke survivors showed a drop in lower limb muscle activity when participants touched or held a handrail while walking on a treadmill. However, in these studies, participants walked rather than performing sit-to-stand or stand-to-sit movements, and only lower limb EMG was measured. Chihara and Seo (2014) compared the activity of the anterior deltoid, triceps brachii, rectus femoris, and tibialis anterior in sit-to-stand movements with different handle heights positioned at either side of the participant and found that triceps activity increased while tibialis anterior activity decreased with higher handle height, while the anterior deltoid and rectus femoris were unaffected. This partly supports our findings, yet comparisons are limited as they did not compare muscle activity to unassisted standing up.

Interestingly, the lower limb muscles that often showed reduced weightings with increased support in our study, namely rectus femoris, gluteus medius, tibialis anterior, and peroneus longus, are highly relevant for both knee extension and balance (Donath et al., 2015, Gottschalk et al., 1989, Louwerens et al., 1995, Salzman et al., 1993), exemplifying the easing support of the rollator. These results could be very relevant to balance in older adults. Amiridis et al. (2003) found that older adults rely more on hip muscles to maintain balance than younger adults in a number of static balance tasks, and a systematic review (Lanza et al., 2022) found that hip abductor strength is critical for balance and to avoid falls. In particular, gluteus medius was among those with decreased activity with support in our study. Upper body muscle weightings, most often in the triceps, biceps brachii, and latissimus dorsi, increased with support across all movements. Their contributions likely enabled our participants to stand up and sit down with less lower limb muscle activity. The biceps flexes the elbow, and the latissimus dorsi adducts and medially rotates the humerus at the glenohumeral joints, bringing the body to the arms. The triceps is an elbow extensor (Kholinne et al., 2018), assisting in bringing the body upward against gravity and helping to balance the trunk during sit-to-stand (Munro and Steele, 1998). Thus, the rollator-induced decrease in lower limb muscle weightings can be associated with a reduced leg strength required to fulfill both standing up and sitting down, following the roughly linear EMG/force relationship (Alkner et al., 2000). Therefore, if less force can or needs to be generated by the lower limb muscles, a rollator can help people with problems standing up. An in-depth analysis relating the changes in muscle weightings to the different movement strategies may further help to recommend specific movement strategies, e.g., strategies that most dramatically shift the muscle weightings from lower to the upper body.

5.5.5 Limitations

Several potential limitations of this study need to be considered. First, our rollator-simulator device is heavier than a commercially available rollator and cannot dip or roll, which might influence how much people can lean and pull on the rollator handles. Secondly, we restricted the foot placement to be parallel and underneath the knees for standardization purposes, in line with other biomechanical studies (van der Kruk et al., 2021b). While this is standard practice, it hindered the participants from pulling their feet backward to stand up, which is another everyday common movement strategy while standing up (Dolecka et al., 2015). Thirdly, we included only young people. Even though we used balance pads to challenge them, the generalizability of the results to persons who are older or physically limited and dependent on a rollator may be limited. Nevertheless, Hanawa et al. (2017) found that the synergies in standing up remain similar regardless of the participant's age. Fourthly, despite explanation, familiarization trials, and careful observation, we cannot rule out the possibility that the participants applied more force to the handles in the light touch condition than is typical for studies with haptic cues (Kouzaki and Masani, 2008). Fifthly, the participants are low in number regarding using LMM statistics but at the highest level in the analysis; therefore, their number is not a major problem. Sixthly, even after careful consideration, we cannot exclude that other thresholds or matching procedures might have led to a different grouping of the temporal synergies' activation profiles. Lastly, we observed symmetric activation of the muscles between the right and left limbs. Thus, future studies could focus on unilateral assessment of muscle activity and increase the resolution, e.g., by additionally measuring the hip adductors, M. gluteus maximus, all deltoid parts, and muscles acting on the wrist.

5.6 Conclusion

This study investigated the rollator's influence on the movement coordination for standing up and sitting down, while accounting for different movement strategies. Our temporal muscle synergy analysis found that the timing, but not the shape, of the temporal muscle synergies differs across the movement strategies. Further, we found that the CNS tightly controls standing up and sitting down movements, especially during the balance-critical phases around seat-off and seat-on. Additionally, no support-specific synergies were found, suggesting that the CNS does not need to alter the control if a rollator is used. However, muscle weightings shifted from the lower limbs to the upper body with increased support. In sum, we suggest that people struggling with rollator use practice movement strategies requiring less tight CNS control, like the forward leaning instead of the exaggerated forward leaning strategy to stand up. Further studies should investigate if these findings hold for older and fall-prone individuals, to enable safe and efficient recommendations on rollator usage.

6 General discussion

This dissertation aimed to improve our understanding of human motor control and learning in two topics:

Topic A: Coordination and adaptation of reaching movements using a robotic manipulandum and virtual reality technologies

Topic B: Effects of rollator support on the coordination of sit-to-stand and stand-to-sit movements using a robot rollator simulator

The topics approached human motor control and learning using human-robot interaction. Topic A addressed the challenges of redundancy, versatility, and time-varying properties. Topic B addressed the challenges of redundancy and versatility. In topic A, a simple skill – reaching – and a robotic manipulandum were used. In topic B, complex skills – sit-to-stand and stand-to-sit – and a robot rollator simulator were used. While topic A addressed the adaptation phase, topic B addressed the coordination of human-robot interaction after adaptation. While the primary focus was on the representational level, with movement strategy and muscle synergy analyses, the computational and implementation levels were also addressed and discussed.
The main findings of topic A with respect to the aims and scope were:

- The first aim was to analyze the influence of the organization of practice variability on force field adaptation, retention, and spatial generalization. It was found that the CIE was apparent in force field adaptation. Specifically, a random practice schedule regarding the target locations led to slower adaptation, but not to different performance levels at the practice end, compared to a blocked practice schedule. Furthermore, it led to better short-term retention and spatial generalization. These results were, to a great extent, reflected by a computational state-space model. This model further provided possible explanatory mechanisms with respect to the forgetting-and-reconstruction hypothesis for the CIE. These findings, along with their practical implications, will be further discussed in the sections 6.1.1-6.1.2.
- The second aim was to analyze the underlying coordination of force field adaptation, retention, and spatial generalization at the muscular level. It was found that force field adaptation involved structural changes in muscle synergies compared to reaching in unperturbed conditions, alongside a novel four-phasic muscle synergy activation pattern. Moreover, these

structural changes and activation patterns likely facilitated retention and spatial generalization, as the same muscle synergies and their activation patterns were also reflected in these phases. Accordingly, muscle synergy analysis provided new insights into changes in the representation of internal models in human motor adaptation. These findings, along with their practical implications, will be further discussed in the sections 6.1.3-6.1.4.

The main findings of topic B with respect to the aims and scope were:

- The third aim was to analyze the influence of rollator support on movement strategies for transitions between sitting and standing. It was found that most participants switched their movement strategies with rollator support in sit-to-stand and stand-to-sit movements. They tended to stand up and sit down with less upper body forward lean and a more vertical trunk orientation when they used the rollator handles. This tendency was also found when the participants' balance was challenged by balance pads beneath their feet. Participants stood up and sat down with less upper body forward lean and a more vertical trunk orientation when they used the rollator handles. These findings, along with their practical implications, will be further discussed in the sections 6.2.1-6.2.2.
- The fourth aim was to analyze the underlying coordination for transitions between sitting and standing at the muscular level with respect to movement strategies. It was found that the activation functions of the temporal muscle synergies showed similar shapes but differed in timing across movement strategies. Furthermore, rollator support altered the muscle weightings, such that the weightings of the arm muscles increased and the weightings of the lower limb muscles decreased. This was especially evident during seat-off and seat-on. In addition, regardless of the movement strategy, during both standing up and sitting down, the CNS may employ intermittent control and send impulses at a high frequency during the balance-critical seat-off and seat-on phases. Accordingly, the tightness of control was increased in balance-critical phases. These findings, along with their practical implications, will be further discussed in the sections 6.2.1-6.2.2.

The following section discusses the main findings and their implications. Limitations, outlooks, and the conclusion complete this chapter.

6.1 Main findings in topic A – Coordination and adaptation of reaching movements

Humans have the remarkable capability to adapt their motor commands in response to a systematic perturbation, reapply, and generalize the thereby acquired knowledge to new situations. The two studies in this topic have investigated if motor adaptation, retention, and spatial generalization (1) are affected by the organization of practice variability and (2) how they are represented at the level of muscle activations. Their results are discussed in the following section, along with a perspective on sports-related considerations.

6.1.1 State-space models help unravel why the random group outperforms the blocked group with regard to the forgetting-and-reconstruction hypothesis

The first study investigated the CIE by comparing two practice protocols, a blocked and an interleaved protocol. While the CIE has been studied extensively since it was first mentioned (Battig, 1972, Magill and Hall, 1990, Schmidt et al., 2019), its underlying mechanisms are still unclear. This becomes evident as recent meta-analyses found that CI has only a medium effect on retention and learning in favor of random practice (Czyż et al., 2024a,b). Furthermore, while in laboratory settings, the effect of random practice was medium for retention and generalization, it was at most small in applied settings (Czyż et al., 2024a,b). To shed light on the CIE, the force field adaptation paradigm allows control of different contexts (reaching directions, force field magnitudes). Furthermore, SSMs fit the data with regard to the forgetting-and-reconstruction hypothesis (Schweighofer et al., 2011, Lee and Magill, 1983, Lee et al., 1985).

Study A1's overall findings regarding adaptation, retention, and spatial generalization align with the force field adaptation literature and allowed us to investigate further the group differences stemming from the different practice protocols. The CIE generally states that the random group shows detrimental performance during the acquisition but superior performance in retention and generalization (Shea and Morgan, 1979). Contrarily, our study showed that a random practice schedule does not lead to different performance levels at the practice end. However, as expected, the random practice schedule led to a slower adaptation than the blocked schedule and better short-term retention and spatial generalization (sections 2.5.1-2.5.3). The general agreement with prior CIE studies allowed to examine the results with respect to a potential underlying mechanism. For adaptation, retention, and spatial generalization, the extended SSM provided possible explanations in light of the forgetting-and-reconstruction hypothesis: The SSM output, which is fitted to the experimental data, is calculated as the sum of a fast and a slow process. Each process is the sum of a retention summand, which reflects "forgetting", and an error sensitivity summand, which reflects "reconstruction" (Schweighofer et al., 2011, Joiner and Smith, 2008). However, to account for multiple targets, the slow process was further divided into target-specific sub-processes, along the study by Lee and Schweighofer (2009). Furthermore, these sub-processes reflected the trial-by-trial spatial generalization of adaptation, such that the sub-process values were increased most for the just reached target and less for the neighboring targets, according to a Gaussian function (section 2.3.4.3; Donchin et al. 2003, Howard and Franklin 2015, Rezazadeh and Berniker 2019). These extensions allowed to relate the experimental results to the forgetting-and-reconstruction hypothesis. While section 2.5.4 provides a detailed discussion, in brief, (1) the blocked group's faster adaptation could be attributed to a higher error-sensitivity – "reconstruction" – of the fast process (large effect). This means that with blocked practice, the learning gain toward the next trials is higher than with random practice, at the beginning of the practice when the fast process dominates the overall adaptation. This may reflect that no new action plan, in the notion of Lee and Magill (1983) and Lee et al. (1985), needs to be reconstructed, when the same trials are reached subsequently. (2) The random group's better retention in the short-term tests relates to a higher value of the slow process at the practice end (only medium effect). The slow process contains the values of the sub-processes and these values are the result of forgetting and reconstructing. The higher value of the random group probably comes from the fact that each sub-process' value increases roughly equally, as the targets were constantly being reached. This contrasts the blocked group. Here, the values of the sub-processes decreased when they were no longer reached. For example, the target which was first reached in the blocked schedule gets forgotten while the other targets are practiced (despite a small gain through the trial-by-trial adaptation). Finally, these differences in the sub-processes lead to different levels of the slow process at practice end. Overall, this highlights a difference in the forgetting and reconstruction interplay across the two groups which was made visible by the SSM. This finds support in the literature, a higher value of the slow process was also seen as cause for better retention in the study by Schweighofer et al. (2011), when they compared patients to controls. (3) Finally, the better spatial generalization of the random group are reflected by sub-processes values of the slow process. That the activity of the slow process increased more uniformly for the four contexts in random than in blocked practice resulted in a higher value for the interpolation target, as it was calculated as the average over the four contexts. For the shifted-origin targets, the context of the practice target with the same direction served as the context of the respective shifted-origin target. The higher value of the random group's spatial generalization could be because the targets were constantly reached. Thus, the values of the sub-processes increased evenly and were not forgotten, similar to what was just discussed for retention.

The good fit and gained insights by the SSM support the forgetting-and-reconstruction hypothesis and the detailed decomposition increases our knowledge of the CIE. Future studies can build on this and try to assign the processes and sub-processes to the underlying learning processes, such as the short- and long-term memory, to further understand the CIE (Schweighofer et al., 2011). This study's behavioral and computational results can contribute further to the understanding of the CIE in other motor learning settings. The following section discusses how they can help improve our understanding of the organization of practice variability in sports.

6.1.2 Practical implications for the organization of practice variability in sports

The CIE has extensively been studied in a variety of sports. Yet, in applied settings, the effect of CI is low at most (Ammar et al., 2023, Czyż et al., 2024a,b). However, the successful use of different directions as different contexts for CIE in study A1 motivates the practice of different directions in sports movements, which will be elaborated in the following. Predominantly error-based learning seems to underly the studied force field adaptation (Wolpert and Bastian, 2021). This learning type also underlies or at least contributes to the performance in various sports movements (Spampinato and Celnik, 2021). Hence, the study results may help foster the CIE in sports movements, especially when error-based learning is underlying.

A potential motor adaptation scenario could be the following. Recalling the exemplary tennis player who changes their racket to one with other physical properties and fails with their initial shots. Considering that the goal is to place the shot at a specific position on the court, the discrepancy between the intended landing point and the actual landing point of the ball can be seen as a sensory prediction error. The distance and direction of the discrepancy can be seen as a directional (signed) error, the type of error necessary for error-based learning (Wolpert et al., 2011). In order to be able to play successfully with the new racket in the competition, i.e., to be able to shoot balls where they are intended to land, one could, based on the results of our study, recommend the player to play at different targets at random instead of blocked while getting used to the new physical racket characteristics (motor adaptation). In the sense of the CIE, one would associate the different targets with corresponding contexts and assume a forgetting-and-reconstructing process. With random practice, the player would forget and reconstruct the action plans for the different directions, i.e., contexts, respectively, yet surpass another player who practices the different targets with a blocked schedule. This might be in particular possible when targeting motor adaptation to a longer lasting change, like a change of rackets (see section 1.4.3.2). This is because, we found that the benefits in short-term retention and generalization in study A1 related to the slow process rather than the fast process. However, this is just a gedankenexperiment and has not been tested to the best of my knowledge.

Furthermore, skill learning studies have shown that the CIE is hard to detect in sports movements, even if error-based learning underlies: Error-based learning also seems to underly free throw practice in basketball (Truong et al., 2023), with the difference that motor adaptation does not take place here. Still, the discrepancy between the intended landing point and the actual landing point of the ball can be seen as a directional (signed) sensory prediction error (Truong et al., 2023). Accordingly, players could benefit from a random practice schedule here, too. Indeed, a positive effect of a random practice schedule on the retention test was found for basketball throws from different distances (Landin et al., 1993), yet not when directions and locations were varied (Porter et al., 2020).

Hence, when translating results from study A1 to sports movements, one must be aware of many factors potentially mediating the CIE, which need to be acknowledged. First of all, study A1 investigated motor adaptation. Hence, it needs to be tested how much of the findings can be translated to skill learning, being likely that the underlying processes of motor adaptation overlap with those of skill learning (Krakauer et al., 2019). Yet, error-based learning is presumably not the only principle underlying such a real-world skill (Wolpert and Bastian, 2021). This means that error-based learning presumably does not influence solely the successful acquisition of the described tennis and basketball skills. Furthermore, while reaching to different directions has been an appropriate context in the force field study, it is unclear if this is the case for different shooting directions in tennis or basketball. The CIE seems to take effect only when the practice contexts are dissimilar to the right amount, as the literature suggests that the effect increases with the amount of dissimilarity of the contexts up to a certain degree (Guadagnoli and Lee, 2004).

6.1.3 Muscle synergy analysis reveals structural changes underlying force field adaptation, retention, and spatial generalization

While study A1 investigated the influence of the organization of practice variability on the acquisition, retention, and spatial generalization of internal model knowledge using task-related end-point kinematic and kinetic variables and focused on the computational level, study A2 investigated how internal model knowledge might be represented at a muscular level by muscle synergies. While the SSM is an elegant tool to investigate motor adaptation and many phenomena within, it is a function that maps many complex sensorimotor mechanisms onto a few parameters on the task level. Hence, additional information on the mechanisms can be gained by investigating at a different level of analysis, such as the representational level using muscle synergies. However, force field adaptation, retention, and spatial generalization have not been researched much in relation to muscle synergies. To our knowledge, study A2 was the first to comprehensively investigate muscle synergies underlying force field adaptation, retention, and spatial generalization.

The key finding was that muscle activation patterns after adaptation cannot be explained by baseline, i.e., unperturbed reaching muscle synergies. Instead, structural changes to muscle synergies alongside a novel muscle synergies activation pattern are required. While in line with previously published results on kinematic, kinetic, and single muscles (Brashers-Krug et al., 1996, Darainy and Ostry, 2008, Gandolfo et al., 1996, Milner and Franklin, 2005, Rezazadeh and Berniker, 2019, Shadmehr and Mussa-Ivaldi, 1994, Thoroughman and Shadmehr, 1999), we presented a novel characterization of muscular coordination that underlies force field adaptation. These structural changes were also shown to facilitate retention and spatial generalization, increasing the confidence that the structural changes reflect an actual mechanism underlying force field adaptation. That force field adaptation requires structural changes in muscle synergies compared to unperturbed reaching is an intriguing novel finding concerning the adaptation of reaching movements and motor learning in general. In particular, it concerns the question of how motor learning is represented by muscle synergies.

It is still unclear how changes in muscle synergies relate to improved task performance (Cheung and Seki, 2021). From a more general perspective, a change in task performance could be represented by (1) changes in the number of muscle synergies or by changes in (2) the activation functions or (3) the muscle synergy structure (Park and Caldwell, 2022). All of these changes in relation to motor learning have been found in the literature. (1) The change in the number of muscle synergies has often been found with respect to development (Hinnekens et al., 2024, Sylos-Labini et al., 2020), skill levels (Cheung et al., 2020, Sawers et al., 2015) or impairments (Cheung et al., 2012, Hayes et al., 2014). A comparison regarding the number of muscle synergies would make sense in study A2 when comparing different stages of adaptation. However, a comparison between the baseline and the adapted state is a less fair comparison as the number of conditions (five directions versus one direction) is unequal, and comparing only the 0° direction would probably lead to the aforementioned methodological problems when sampling to few variations, as discussed in section 3.5.2. (2) A change in muscle synergy activation patterns has been found to reflect isometric visuomotor rotation adaptation (De Marchis et al., 2018, Gentner et al., 2013, Severini and Zych, 2020) and was initially hypothesized also for force field adaptation in study A2 ($H_{\text{Synergies}}$ 1). As section 3.5.2 elaborates in detail, literature shows that the muscle activation patterns for unperturbed reaching to different directions can be reconstructed by a number of muscle synergies which is lower than the number of directions and muscles, regardless of the speed or weight support, and that they are even robust for via-point or change-in-target reaching movements (d'Avella et al., 2006, 2008, 2011, Muceli et al., 2010, Coscia et al., 2014). Furthermore, it has been shown that changes in the tuning of the muscle synergies facilitate adaptation and spatial generalization in an isometric visuomotor rotation adaptation task, a paradigm related to the force field adaptation (De Marchis et al., 2018, Gentner et al., 2013, Severini and Zych, 2020). Specifically, in these visuomotor rotation adaptation studies, muscle activation patterns during adaptation and spatial generalization phases could be reconstructed by baseline reaching muscle synergies, and only the tuning changed. However, these findings are in contrast with the study A2's findings and accordingly, (3) muscle synergy structure changed. This is surprising as structural changes have been more closely related to skill learning than motor adaptation (Cheung et al., 2020, Park and Caldwell, 2022). The difference between the force field and isometric visuomotor rotation adaptation may stem from the fact that visuomotor rotation adaptation requires a new mapping between which direction the reach is supposed to go and where it goes (Krakauer, 2009) and that there is no additional perturbation during the reach. In contrast, in force field adaptation, the perturbation endures and changes in magnitude throughout the reach while joint angles and muscle lengths change. The findings of structural changes can probably be better related to the virtual surgery paradigm (Berger et al., 2013), especially to incompatible surgeries. Here, a virtual surgery swaps the tendons of different muscles so that the muscle-to-force mapping is changed. After the virtual surgery, structural changes in muscle synergies are necessary to reach targets, as otherwise, participants cannot adapt to this perturbation successfully. In contrast to the virtual surgery in which participants cannot fully adapt to the perturbation (surgery), need an extensive exploration phase (Berger et al., 2022) or multiple sessions (Borzelli et al., 2022), in study A2, participants successfully adapted to the imposed perturbation within 250 trials. Furthermore, even if the comparability to reaching movements is minor, a recent study of walking adaptation to exoskeletons in stroke survivors also showed structural changes in muscle synergies (Rinaldi et al., 2020). Accordingly, it is to be further explored in which experimental paradigms and how structural changes occur with adaptation, as a strict association of structural changes and skill learning on the one hand and changes in activation functions and motor adaptation, on the other hand, is questioned.

6.1.4 Practical implications for motor learning in sports

Study A2 found that structural changes in muscle synergies are necessary for adaptation during dynamic reaching, contrasting prior isometric visuomotor rotation adaptation results. Against the background of improving the understanding of adaptation in sports movements, the presented findings may be of increased value compared to the isometric visuomotor rotation adaptation results, as most of the sports movements are dynamic – the tennis player's arm moves to strike the ball. Even if the comparability to reaching movements is minor, studies of walking adaptation to exoskeletons in stroke survivors also showed structural changes in muscle synergies (Rinaldi et al., 2020), supporting our findings for non-isometric tasks.

In general, muscle synergy analysis has been applied to sports movements (Taborri et al., 2018), especially in light of different skill and performance levels (Hug et al., 2010, Kim et al., 2018, Kristiansen et al., 2015, Turpin et al., 2011, Vaz et al., 2016). The benefit from these investigations could be to extract information on what aspects of the movement the athlete could practice to improve. Theoretically, weaker performers could optimize their practice to develop their muscle synergy structure toward the good performers' muscle synergies. Or, if the differences between weak and good performers are present in the activation profiles, the athlete could work on the timing of the individual muscle synergies, like the interplay of upper and lower body movements (Carson, 2006, Taborri et al., 2018). The result of study A2, that acquired muscle synergies also enable spatial generalization, can be suggested as an approach to learning movements, while acknowledging that study A2 investigated motor adaptation and carrying-over the findings to skill learning needs to be tested. In light of the modular control architecture that individual muscle synergies are shared across several movements, practicing one movement could simplify the learning of further movements (generalization). Presumably, if both movements share muscle synergies, these muscle synergies could be targeted with practice of the first movement and facilitate the improvement of the second movement. In sports practice, setting up a series of drills for skill progression is an effective and frequently used approach (Irwin et al., 2005, Sands, 2018, Magill and Anderson, 2010). The series of drills is structured in such a way that a generalization takes place between the successive elements of the series: Surf students first learn how to paddle and stand up on the board properly on land before applying what they have learned in the water (Magill and Anderson, 2010). Gymnasts first learn the back extension roll, then a hip circle (Sands, 2018). Likewise, they start with handstands on the floor before proceeding to the balance beam or the parallel bars (Sands, 2018). Künzell and Lukas (2011) compared the snowboarding performance between two groups and found that the group that had previously completed skateboarding exercises showed a better snowboarding performance than those without skateboarding exercises. However, the method of series of drills for skill progression lacks objective foundations, as they are primarily built upon coaches' experimental practice and reflection (Irwin et al., 2005). Furthermore, the generalization is not always clear. For example, humans learning forehand in tennis before learning forehand in badminton often experience an adverse, detrimental effect due to a different technique of holding the racket (Magill and Anderson, 2010). Hence, insights from examining the shared muscle synergies across tasks and with respect to generalization could provide a window and an objective means to better understand and set up a beneficial series of drills for skill progression. Still, this remains speculative, as elaborated in section 6.1.3, the relationship between practice and changes in muscle synergies is not clear yet and requires more research (Carson, 2006).

6.1.5 Limitations and future research directions

Study A1 has some limitations, which are discussed below in addition to those in section 2.5.7. Firstly, individual FF trials were performed at the beginning of the long-term test to address the warm-up decrement. In this phase, we found no group differences (CIE), i.e., overcoming the warm-up decrement with single FF trials may have masked the CIE. Secondly, the organization of practice variability was operationalized with a comparison of blocked and interleaved practice along the CIE. This type of variability concerns the scheduling aspect of practice (Raviv et al., 2022), i.e., participants learn from the same examples and the same number of examples but with different schedules. However, according to a recent feature review, there are several other types of variability, such as numerosity, heterogeneity, and situational (Raviv et al., 2022). Numerosity operationalizes variability with the difference in the number of practice items. Heterogeneity operationalizes variability with differences in practice items used by different groups, e.g., practicing less or more similar practice items. Situational refers to the difference in environmental conditions, e.g., in the same or different environments. From this broader perspective, study A1 improves our understanding of which kind of variability is effective; adapting using a more variable schedule shows superior performance in retention and spatial generalization. To improve practice schedules, future studies may investigate if any of the three other types of variability can further increase retention and spatial generalization. For example with numerosity, a recent study showed continued improvement in adaptation and retention even after multiple sessions and 7,000 force field trials (Franklin et al., 2025). Hence, it would be interesting to test, whether the CIE becomes more or less prominent with an increased number of trials. Lastly, the SSM could be further extended, for example, to include other aspects that may have played a role in the study: possible non-linear error sensitivity (Fine and Thoroughman, 2007, Wei and Körding, 2009), a context-dependent decay (Ingram et al., 2013), or additional ultraslow processes (Forano and Franklin, 2020). However, when including additional parameters such as the ones proposed, attention must be paid to overfitting problems (Kitago et al., 2013), which may reduce the external validity of the results (Badrulhisham et al., 2024).

Study A2 was the first to thoroughly investigate force field adaptation, retention, and spatial generalization with muscle synergies. Therefore, the experimental setup and the trial conditions were designed to align with former force field adaptation studies. However, especially for the unperturbed baseline trials, not much force and thus only minor muscle activity is required from the participant. Consequently, the modulations in the EMG data belonging to the movement are less distinguishable from other artifacts in the recorded EMG data, at least for a single-trial examination. Further studies may, therefore, consider testing force field adaptation with increased force field magnitudes and movement speeds and then being able to relate the computational level to the representational level more closely. In particular, this would open ways to relate mechanisms described using internal models (Kawato, 1999, Shadmehr and Mussa-Ivaldi, 1994) to the trial-by-trial alterations with a muscle synergy perspective. Another limitation is that even though the sampling of muscle activation patterns comprised a semi-circle, it cannot be excluded that a more extensive sampling, e.g., comprising a full circle or both reaching forward and backward, would have led to some different or additional muscle synergies. While the precise recording of surface EMG from the rotator cuff muscles is subject to debate (Waite et al., 2010), their contributions to muscle synergies could provide further information on coordination. These muscles are involved in horizontal reaching movements (Perotto, 2011) and may be activated earlier than the larger muscle groups, reflecting a predictive component (Day et al., 2012) and allow further associations with internal models.

The results of study A2, that structural changes and a novel four-phasic activation of muscle synergies are necessary for adaptation, raise further interesting questions: As Huang et al. (2012) showed that muscle activity continued to further decrease in force field adaptation even after a plateau in kinematic- and kinetic-dependent variables, it would be interesting to see, how muscle synergies evolve, when participants adapt to the force field over multiple sessions (Franklin et al., 2025). Often, it is assumed that the CNS aspires effort optimization (Huang et al., 2012). Accordingly, one could expect the CNS to optimize the muscle synergy structure so that the acceleration part of the reach movement is not made up of two successively activated muscle synergies, but only one, just like with unperturbed reaches.

Furthermore, it would be interesting to bring the findings of studies A1 and A2 together, to examine if the group differences in speed of adaptation, retention, and spatial generalization found in study A1 can be associated with changes at the muscular level. Possibly, the process and sub-process characteristics reflected by the SSM could be related to changes in the activations functions or muscle synergy structure.

Lastly, even if links to motor adaptation and skill learning in the sports context have been presented, it must be acknowledged that these links are hypotheses and must be carefully tested. As such, they should be seen as starting points for a step-by-step approach to studying the more complex movements in the sports context (Cisek and Green, 2024, Maselli et al., 2023).

6.2 Main findings in topic B – Effects of rollator support on the coordination of transitions between sitting and standing

In topic B, the complex skills of sit-to-stand and stand-to-sit with a robot rollator simulator were investigated. Sit-to-stand, and particularly stand-to-sit, had been vastly understudied, let alone with a rollator. This is surprising, as these movements are executed multiple times a day, important for independent living, and of special clinical interest (Yamada and Demura, 2009, Perry et al., 2006, Branch and Meyers, 1987, Frykberg and Häger, 2015). Furthermore, a rollator is a frequently used assistive device (Bateni and Maki, 2005, Bradley and Hernandez, 2011), but how rollators affect these movements has hardly found attention in the literature. Therefore, we comprehensively investigated the influence of rollator support on sit-to-stand and stand-to-sit movements.

6.2.1 Rollator support influences the movement strategy and muscle weightings, and the CNS controls balance-critical phases tightly

Sit-to-stand and stand-to-sit are complex multijoint movements and already multiple movement strategies have been identified in unassisted standing-up (Anan et al., 2012, Dolecka et al., 2015, Frykberg and Häger, 2015, Hughes et al., 1994, Komaris et al., 2018, van der Kruk et al., 2021b). Therefore, we expected multiple movement strategies in particular with the rollator (see section 1.5.2). In-line with this assumption, much variance in the high-dimensional biomechanical and EMG dataset was found and treated accordingly. The following parts extend the discussions from sections 4.5 and 5.5, firstly from a content-wise perspective and secondly from the methodological perspective.

Study B1 found that the young participants changed their movement strategy with rollator support, especially when their balance was challenged. The general trend was to stand up and sit down with less upper body forward lean when the handles were used. This switching of movement strategies indicates that rollator support affects the underlying coordination. This interference is of interest when trying to understand human-rollator interactions. The paradox that rollator use has been found to be a fall risk factor (Nickerson et al., 2023), even though they are built to support and stabilize human movements, could stem from the fact that they interfere with the movement strategies humans are used to. This is plausible as even simple reaching movements are influenced by the device used, and several possible factors are causing these differences: different biomechanical constraints, familiarity, or cognitive demands (Moher and Song, 2019). Accordingly, the findings that rollator support influences the movement strategy selection could help improve the human-rollator interaction, as elaborated in similar studies on sit-to-walk (Perera et al., 2023) or floor-to-stand movement strategies (Bohannon and Lusardi, 2004): A potential deduction for improvement could be to design rollators in a way that they assist the user in standing-up and sitting-down such that the user can utilize the strategies chosen by the young, healthy adults. Furthermore, users and therapists could be informed which specific strategy to train for, with the ones found in study B1 as references, as these are the naturally chosen strategies. Yet, further information regarding different strategies is required from additional studies. These ideas need to be tested with the target group, i.e., actual rollator users, for a more thorough evaluation to recommend strategies. For example, with the knowledge that different movement strategies are used and that participants switched them with rollator support, it is interesting how the CNS might control them and if they are controlled differently.

Therefore, in study B2, muscle synergy analysis was used based on full-body EMG measurements to unravel the underlying coordination at a muscular level with respect to the movement strategies. There were three major findings. First, the timings of the activation functions differed across the movement strategies. In particular, when comparing the activation functions of the muscle synergies between the movement strategies, there were specific time points during the trials at which a particular strategy showed muscle synergy activation, but the other strategies did not. These differences may reflect biomechanical requirements specific to this particular strategy. For example, a muscle synergy activation observed in the forward leaning strategy only relates to transferring the momentum generated by the upper body from the trunk to the thigh to stand up (Anan et al., 2012, Jeon et al., 2019, Riley et al., 1991). Hence, the differences in kinematics and kinetics found across the movement strategies in study B1, align with strategy-specific activations of muscle synergies. The second major finding was that muscle weightings increased in the arm and decreased in the lower body muscles with rollator support, especially during seat-off and seat-on. This is particularly relevant as lower limb muscle strength is one main predictors of successful sit-to-stand movements (Frykberg and Häger, 2015). This shows that rollator support can be a valuable way to cope with lower leg strength and potentially foster standing-up and sitting-down. The third major finding was that the width of the activation functions was narrower around the time of seat-off and seat-on than at the beginning and end of the movement. This is an intriguing finding providing insight into how the CNS controls movement: Recently, a study related the “intermittent control” theory to temporal muscle synergies (Brambilla et al., 2023a) stating that the CNS sends descending commands at designated times, which are then transformed into muscle activation profiles. We found multiple narrow, i.e., short in time, muscle synergy activations around the balance-critical seat-off and seat-on.

With the assumption that the CNS employs intermittent control and sends impulses with a high frequency, our results suggest that the CNS tightly controls the balance-critical seat-off and seat-on. With intermittent control, the CNS adjusts motor commands according to incoming, intermittent feedback in an open-loop way (Gawthrop et al., 2014). In particular, using sensory input, the CNS estimates a current state and plans muscle activations according to the body’s current state and the movement goal (Gawthrop et al., 2019, Karniel, 2011). According to Gawthrop et al. (2014), the sway motion in human balance tasks can be interpreted in the context of intermittent control (Gawthrop et al., 2014, Tanabe et al., 2017). In brief, bipedal standing could be achieved by monitoring stability and generating joint torques that stabilize the body when a certain balance threshold, a critical state with respect to the movement goal, is reached. For example, bipedal standing is considered stable when the CoM resides within the BoS provided by the feet (Shumway-Cook and Woollacott, 2007, Bateni and Maki, 2005). If the CoM moves outside the BoS, one way to avoid falling is to take a compensatory step. With respect to intermittent control, this means if the body’s CoM approaches the BoS edge critically, muscles are activated so that the CoM moves back inside the BoS so that the user’s balance is maintained (Loram et al., 2005). As during seat-off and seat-on, balance is critical (Pai et al., 1994, Frykberg and Häger, 2015, Schenkman et al., 1990), maybe the threshold that triggers corrective action is reached relatively fast, and multiple, successive pulses result in keeping the user in balance. A good example, already discussed in section 5.5.3, is the tight control around the seat-off in the exaggerated forward leaning strategy. This strategy is characterized by an extensive upper body forward lean and an early movement of the CoM over the BoS. Compared to the forward leaning strategy with less extensive upper body forward lean, three more temporal muscle synergies are found around seat-off. Accordingly, this higher number may reflect how the CNS copes to keep the CoM inside the BoS. This tight control may, for example, aim to prevent a sit-back. Indeed, Scarborough and colleagues 2007 argue that a sit-back can happen if no sufficient anterior and vertical momentums are generated. Taken together, the findings of the two studies hint that rollator support tends to let users stand up and sit down with less forward body lean, which may relate to less tight control required by the CNS. Referring back to potentially recommending specific movement strategies, a less tight control could be a beneficial aspect of the forward leaning strategy.

6.2.2 Practical implications for the analysis of human-robot interaction and complex whole-body movements

Analysis of high-dimensional data with an effective interpretation on the one hand and without losing essential information on the other hand is complex (Robertson et al., 2013). This holds especially in complex whole-body movements with many degrees of freedom due to the high variance (Reisman et al., 2002). Traditional statistics using discrete parameters that aggregate data (e.g., a knee angle time series is aggregated to the value of maximum knee flexion) bear the risk that further information inherent in the high-dimensional dataset is obscured (Stetter and Stein, 2024). High variation in the data can, for example, stem from users employing various movement strategies (James and Bates, 1997). Therefore, in study B1, movement strategies were identified, which facilitated further analyses. Therefore, a data-driven approach, a combination of PCA and clustering, was used. With PCA, the dimensionality of the data is reduced, such that most of the information of the original data is contained within the first few principal components (Robertson et al., 2013). This low-dimensional representation facilitates interpreting and further analyzing the data set. As employed in study B1, the first principal components can serve as input for subsequent clustering. With this approach, we could group the numerous trials into movement strategies. The following qualitative and quantitative analysis allowed us to discuss the movement strategy selection and the kinematic and kinetic differences between the strategies. As discussed in the next paragraph, identifying movement strategies paved the way for muscle synergy analysis. A follow-up analysis of the movement strategy analysis could have been done to narrow down the differences to presumably a few of the most distinguishable principal components using a support vector machine (SVM; Begg and Kamruzzaman 2005, Stetter et al. 2020). The thereby extracted condensed information could help instruct patients and therapists to use the appropriate movement strategy, allowing them to focus on only a few parameters instead of multiple ones.

The high variation in the data set described at the beginning of this section on kinematic and kinetic data applies also to EMG data, as elaborated in the section 1.4.2. This high variance was accounted for in two steps. Firstly, the previously identified movement strategies allowed a separate analysis for every movement strategy. This means muscle synergies were extracted separately per movement strategy. While muscle synergies are usually extracted separately per participant, the cross-validation results from this novel approach of pooling trials by movement strategy instead of by participant demonstrated the validity of the extracted muscle synergies, i.e., the validity of the approach. This way, the inter-strategy variability was omitted for the extractions, providing better data access and interpretability as the muscle synergies were less variable. Secondly, as it was not *a priori* clear which muscle synergy model best represented the data, we extracted spatial and temporal muscle synergies in the first step. We found that temporal muscle synergies provided a more compact representation than spatial muscle synergies (see section 5.4.1). For example, the forward leaning strategy in the sit-to-stand movement could be represented by eight muscle synergies less using temporal instead of spatial muscle synergies, easing the data interpretation. Taken together, these methodological steps provide insightful access to evaluating complex whole-body movements in human-robot interaction and provide a way to meaningfully reduce the dimension of the data to answer the research question.

6.2.3 Limitations and future research directions

The main limitation of topic B with respect to ecological validity is the participant sample. Although female and male participants were included, everyone was approximately 40 years younger than the usual population of rollator users (Charette et al., 2018). This is not untypical; a recent review showed that more than 20% of gait aid studies are conducted with younger adults (Zhang et al., 2025). Furthermore, the two studies had an exploratory character due to the limited existing research. This, in combination with an extensive methodological apparatus (e.g., full-body kinematics and EMG), would have been a burden for older and frail participants (Bowsher et al., 1993). However, the results and insights gained can now be further analyzed and verified with a rollator-prone sample while condensing the experimental protocol. While we have identified movement strategies that align with movement strategies described for older individuals in sit-to-stand without rollator support, it is possible that we would find further movement strategies when applying our methodology on rollator-prone users. Furthermore, rollator-prone users might have problems establishing the discussed tight control around seat-off and seat-on (Liaw et al., 2009). This is one probably important aspect of human-rollator interactions, which can now be addressed specifically in future studies.

Further valuable insights could be gained if the rollator handles provided precise force and torque data. From a methodological point of view, a quantitative assessment of the light touch condition would have been possible, such as controlling for a threshold of 1 N not to be exceeded (Kouzaki and Masani, 2008). From a content perspective, the human-rollator interaction could have been assessed in greater detail: Firstly, it would be interesting to see whether the previously discussed tight control is also reflected in the interaction forces, i.e., to what extent the CNS integrates the hand-handle interaction and possibly contributes to the balance (e.g., changing the CoM position by pulling on the handle). Secondly, the effects of rollator support on joint loading could have been addressed, e.g., to confirm proposed reductions in required lower limb strength. However, this would have needed to develop and validate a coupled human-rollator biomechanical model (Costamagna et al., 2017).

While the paradox that rollators should aid but have been associated with fall risk has motivated this research, a direct link between the movement strategies and fall risk needs further investigation in future studies. Disentangling the effects of different movement strategies and rollator support in relation to balance control, fall risk, and safety are promising directions to help develop protocols and instructions for safer rollator use. For example, it could be investigated if the proposed movement strategies with less tight control – e.g., the forward leaning instead of the exaggerated forward leaning strategy – can be carried out by rollator-prone users and if they show indeed better balance control (e.g., with center of pressure (CoP) sway as dependent variable; Shumway-Cook and Woollacott 2007).

In addition to the proposed directions, the presented findings motivate studies with human-rollator interaction in further movements in closely related movements such as sit-to-walk (Carey et al., 2021), for which research has shown that users struggle with, too. This includes walking downhill and uphill, backward, on uneven ground, while turning, or over the door threshold (Lindemann et al., 2016). Furthermore, various gait aids, such as orthoses or exoskeletons, can also be seen as human-robot interactions with potentially detrimental effects on balance, as shown by Dooley et al. (2023) and Panwalkar and Aruin (2013). According to our findings, the interaction could influence the movement strategy selection, the muscle weightings, and the CNS control. In fact, a recent study found that wearing an exoskeleton influences the users' strategies in balance tasks (Gonzalez et al., 2022). Future studies could also help improve rollator design and provide suggestions for smart assistance. There is growing interest in using rollators with sensors and actuators, such as to develop handles that assist in a good manner (Zhang et al., 2025). One example is the lift support for sit-to-stand movements provided by the handles of the SkyWalker (Mahdi et al., 2022).

6.3 Conclusion

This dissertation revealed novel insights into the coordination and adaptation of human movements. The findings in topic A facilitated a better understanding of the coordination and adaptation of human movements in human-robot interaction using the force field adaptation paradigm. Retention and spatial generalization benefit from a random compared to a blocked practice schedule in force field adaptation. These experimental results aligned well with the forgetting-and-reconstruction hypothesis of the CIE by means of a computational state-space model. Furthermore, it was found that force field adaptation, retention, and spatial generalization require structural changes of the muscle synergies underlying the movements. This novel characterization of force field adaptation adds to our understanding of how observable motor learning processes are represented at the muscular level, providing insights into how the CNS copes with the redundancy, versatility, and time-varying properties challenges at the muscular level during motor learning. Future studies can try to translate the findings regarding the organization of practice variability and the structural changes in muscle synergies underlying force field adaptation step-by-step to sports movements.

The findings in topic B showed that humans use different movement strategies to stand up and sit down when using a rollator. Furthermore, the findings showed that rollator support influences the movement strategy selection, such that humans stand up with less upper body forward lean and a more vertical trunk orientation when supported by a rollator. Furthermore, we found that the movement strategies differ regarding the timings of the temporal muscle synergies' activation profiles. Another finding was that rollator support affects the muscle weightings, such that arm muscle weighting increases and lower limb muscle weighting decreases. Lastly, our analysis suggests that the CNS controls the balance-critical seat-off and seat-on tightly. Hence, topic B provided insights into how the CNS copes with the redundancy and versatility challenges at the muscular level when using a rollator. These findings from experimental studies with young, healthy adults can now be verified with rollator-prone humans. In addition, certain movement strategies could be identified that required less tight CNS control and showed a shift in the muscle weighting to the arms. These movement strategies could potentially ease standing up and sitting down with a rollator and therefore be suitable for rollator users. Topic B further followed the methodological steps of using a data-driven way to group movement strategies and then to analyze these strategies further at a muscular level. As such, the steps provide a well-suited approach to analyze complex whole-body movements and further human-robot interactions. They demonstrate high potential to thoroughly unravel human-rollator interaction at different levels and pave the way for investigating complex whole-body movements with other interactive devices, such as prostheses, smart rollators, and exoskeletons.

To summarize, the scientific novelties and the developed and applied methodologies presented in this dissertation enhance our understanding of how the CNS meets the challenges of redundancy, versatility, and time-varying properties. Future research can benefit from and build upon these findings, in particular with respect to the organization of practice variability and coordination at a muscular level in motor adaptation, as well as the influence of rollator support on coordination. As such, the findings help us advance our understanding of the underlying CNS processes that facilitate our astonishing movements.

A Appendix

A.1 Supplementary material: topic A, study A1

A.1.1 Supplemental tables

Table A.1: Detailed description of the target ordering during short- and long-term transfer (in parentheses). Numbers are as follows. Practice targets: 1: 1.30, 2: 12, 3: 9, and 4: 7.30 h, 5: interpolation, 6: extrapolation, 7-10: targets with shifted origin in the same order as the practice targets.

Participant	EC				EC (FF)				EC		EC (FF)		EC				EC (FF)			
1	1	2	3	4	1	2	3	4	5	6	5	6	7	8	9	10	7	8	9	10
2	1	2	3	4	1	2	3	4	6	5	6	5	7	8	9	10	7	8	9	10
3	4	3	2	1	4	3	2	1	5	6	5	6	10	9	8	7	10	9	8	7
4	4	3	2	1	4	3	2	1	6	5	6	5	10	9	8	7	10	9	8	7
5	2	3	4	1	2	3	4	1	5	6	5	6	8	9	10	7	8	9	10	7
6	2	3	4	1	2	3	4	1	6	5	6	5	8	9	10	7	8	9	10	7
7	1	4	3	2	1	4	3	2	5	6	5	6	7	10	9	8	7	10	9	8
8	1	4	3	2	1	4	3	2	6	5	6	5	7	10	9	8	7	10	9	8
9	3	4	1	2	3	4	1	2	5	6	5	6	9	10	7	8	9	10	7	8
10	3	4	1	2	3	4	1	2	6	5	6	5	9	10	7	8	9	10	7	8
11	2	1	4	3	2	1	4	3	5	6	5	6	8	7	10	9	8	7	10	9
12	2	1	4	3	2	1	4	3	6	5	6	5	8	7	10	9	8	7	10	9
13	4	1	2	3	4	1	2	3	5	6	5	6	10	7	8	9	10	7	8	9
14	4	1	2	3	4	1	2	3	6	5	6	5	10	7	8	9	10	7	8	9
15	3	2	1	4	3	2	1	4	5	6	5	6	9	8	7	10	9	8	7	10
16	3	2	1	4	3	2	1	4	6	5	6	5	9	8	7	10	9	8	7	10

Table A.2: Results of the grid search with bootstrapping. Values in the RMSE and R^2 columns are mean and 97.5% confidence intervals

$\mathbf{A_s}$	$\mathbf{A_f}$	$\mathbf{b_f}$, $\mathbf{b_s}$	RMSE	$\mathbf{R^2}$
∈]0, 1[	∈]0, 1[	∈]0, 1[	4-1: 0.29 (0.11)	0.74 (0.14)
			1-4: 0.29 (0.10)	0.70 (0.29)
			4-4: 0.30 (0.13)	0.70 (0.18)
		∈]0, 0.5[	4-1: 0.28 (0.11)	0.74 (0.14)
			1-4: 0.29 (0.10)	0.72 (0.23)
			4-4: 0.30 (0. 3)	0.70 (0.19)
	∈]0.5, 1[	∈]0, 1[	4-1: 0.28 (0.11)	0.74 (0.14)
			1-4: 0.29 (0.09)	0.73 (0.15)
			4-4: 0.30 (0.13)	0.70 (0.19)
		∈]0, 0.5[	4-1: 0.28 (0.10)	0.75 (0.14)
			1-4: 0.29 (0.10)	0.74 (0.14)
			4-4: 0.30 (0.13)	0.70 (0.16)
	∈]0, 0.9]	∈]0, 1[	4-1: 0.29 (0.09)	0.73 (0.14)
			1-4: 0.30 (0.10)	0.72 (0.35)
			4-4: 0.30 (0.13)	0.70 (0.18)
		∈]0, 0.5[	4-1: 0.29 (0.11)	0.73 (0.18)
			1-4: 0.29 (0.10)	0.73 (0.23)
			4-4: 0.30 (0.11)	0.70 (0.23)
∈]0.9, 1[	∈]0, 0.9]	∈]0, 1[	4-1: 0.29 (0.09)	0.72 (0.17)
			1-4: 0.29 (0.09)	0.73 (0.17)
			4-4: 0.31 (0.11)	0.70 (0.18)
		∈]0, 0.5[	4-1: 0.30 (0.12)	0.72 (0.16)
			1-4: 0.29 (0.06)	0.73 (0.17)
			4-4: 0.30 (0.13)	0.70 (0.18)
	∈]0.5, 0.9]	∈]0, 1[	4-1: 0.29 (0.11)	0.73 (0.18)
			1-4: 0.29 (0.09)	0.73 (0.17)
			4-4: 0.30 (0.12)	0.70 (0.19)
		∈]0, 0.5[	4-1: 0.29 (0.11)	0.73 (0.18)
			1-4: 0.28 (0.08)	0.73 (0.15)
			4-4: 0.30 (0.12)	0.71 (0.19)

A.1.2 Supplemental data: detailed analysis of the model data

A.1.2.1 Practice

According to our experimental data analysis, we conducted an NOVA for the model data for the practice phase. It revealed significant time (F(1,30) = 315.515, p < 0.001, η_p^2 = 0.913), group (F(1,30) = 15.685, p < 0.001, η_p^2 = 0.343), and interaction effects (F(1,30) = 35.541, p < 0.001, η_p^2 = 0.541). Post-hoc t-tests revealed that both groups adapted to the force field (blocked: t(15) = -11.186, p < 0.001, |d| = 2.796; random: t(15) = -13.963, p < 0.001, |d| = 3.491). The groups differed at practice start (t(30) = -6.626, p < 0.001, |d| = 2.419), but not at practice end (t(21.482) = -1.371, p = 0.071, |d| = 0.819).

In summary, the model data reproduced the behavioral results, except for a significant group difference at practice start which was not present in the experimental data.

A.1.2.2 Retention

We conducted two ANOVAs, one regarding short-term retention ([Group: Blocked vs. Random, Time: Practice end, Short-term]) and the other regarding long-term retention ([Group: Blocked vs. Random, Time: Practice end, Long-term]). The ANOVA for the short-term retention revealed significant group (F(1,30) = 32.960, p < 0.001, η_p^2 = 0.988), time (F(1,30) = 46.655, p < 0.001, η_p^2 = 0.609), and interaction effects (F(1,30) = 12.191, p = 0.002, η_p^2 = 0.289). Post-hoc t-tests found a superior performance for the random group against the block group only in short term retention (t(30) = 6.416, p < 0.001, |d| = 2.343). Both groups showed a decrease with time (blocked: t(15) = 6.675, p < 0.002, |d| = 1.669; random: t(15) = 2.632, p = 0.019, |d| = 0.658).

The ANOVA for the long-term retention revealed a significant time effect (F(1,30) = 351.523, p < 0.001, η_p^2 = 0.921) but no significant interaction effect (F(1,30) = 2.617, p = 0.116, η_p^2 = 0.080), which resembles the experimental findings. Unlike the experimental findings, we found a significant group effect (F(1,30) = 24.628, p < 0.001, η_p^2 = 0.541). Post-hoc t-tests revealed a significant decrease in performance during the long-term retention for both groups (blocked: t(15) = 13.493, p < 0.001, |d| = 3.373; random: t(15) = 13.057, p < 0.001, |d| = 3.264), alike the behavioral results. In contrast to our behavioral findings, we found a significant difference in the long-term retention test between the groups (t(30) = 6.416, p < 0.001, |d| = 2.343).

In summary, the SSM reproduced the short-term retention performance of the experimental data, showing a better retention for the random group. Consistent with the behavioral results, the SSM was able to replicate the decline in performance in the long-term retention test for both groups. However, the model data revealed a significant group difference in the long-term retention test that was not present in the experimental data.

A.1.2.3 Spatial transfer

Analogously to our experimental statistics, we tested the model data for the interpolation, extrapolation, and shifted origin targets for both short- and long-term transfer. First, we tested for short-term transfer. The one- sample t-tests vs. 0 revealed transfer for all short-term transfer tasks for both the blocked (interpolation: t(15) = 12.910, p < 0.001, |d| = 3.228; extrapolation: t(15) = 2.437, p < 0.001, |d| = 0.609; shifted origin: t(15) = 12.068, p < 0.001, |d| = 3.017) and the random group (interpolation: t(15) = 22.432, p < 0.001, |d| = 5.608; extrapolation: t(15) = 4.518, p < 0.001, |d| = 1.129; shifted origin: t(15) = 16.218, p < 0.001, |d| = 4.054). Then, we tested for each target which group performed better. The t-tests showed a better performance for the interpolation and extrapolation target for the random group (interpolation: t(30) = 5.502, p < 0.001, |d| = 2.009; extrapolation: t(30) = 2.217, p = 0.035, |d| = 0.847). Further, the modelled performance was better for the random group for the shifted origin targets (t(30) = 4.605, p < 0.001, |d| = 1.681).
We tested long-term transfers analogously to the short-term transfers. The one-sample t-tests vs. 0 showed transfer for both the blocked and the random group for the interpolation target (blocked: t(15) = 4.606, p < 0.001, |d| = 1.151; random: t(15) = 5.488, p < 0.001, |d| = 1.372). However, the tests showed transfer to the extrapolation target only for the random group, but not for the blocked group (blocked: t(15) = 0.009, p = 0.993, |d| = 0.002; random: t(15) = -3.216, p = 0.006, |d| = 0.804). Both groups showed transfer to the shifted origin targets (blocked: t(15) = 20.986, p < 0.001, |d| = 5.246; random: t(15) = 31.579, p < 0.001, |d| = 7.895).
Then, we tested for each target if the groups' performances differ to each other. The t-tests showed no differences for the interpolation (t(30) = 0.248, p = 0.806, |d| = 0.090) and extrapolation target (t(30) = -1.940, p = 0.062, |d| = -0.708). The t-test to compare the shifted origin targets for the long-term transfer revealed a better transfer for the random compared to the blocked group (t(30) = 2.323, p = 0.027, |d| = 0.848). Except for the found transfer for the extrapolation target in the random group, these findings resemble those of the behavioral data.
To sum up, the SSM reproduced the behavioral results of all transfer tests, except for the extrapolation target. For the latter, the modelled data showed a low transfer for both groups during short-term tests and for the random group during long-term tests, though the behavioral data showed no transfer.

A.2 Supplementary material: topic B, study B1

A.2.1 Supplementary videos

The animated versions of the static figures below can be found online:

- Sit-to-stand, non-challenging condition: https://static-content.springer.com/esm/art%3A10.1038%2Fs41598-023-43401-6/MediaObjects/41598_2023_43401_MOESM2_ESM.gif
- Sit-to-stand, challenging condition: https://static-content.springer.com/esm/art%3A10.1038%2Fs41598-023-43401-6/MediaObjects/41598_2023_43401_MOESM1_ESM.gif
- Stand-to-sit, non-challenging condition: https://static-content.springer.com/esm/art%3A10.1038%2Fs41598-023-43401-6/MediaObjects/41598_2023_43401_MOESM4_ESM.gif
- Stand-to-sit, challenging condition: https://static-content.springer.com/esm/art%3A10.1038%2Fs41598-023-43401-6/MediaObjects/41598_2023_43401_MOESM3_ESM.gif

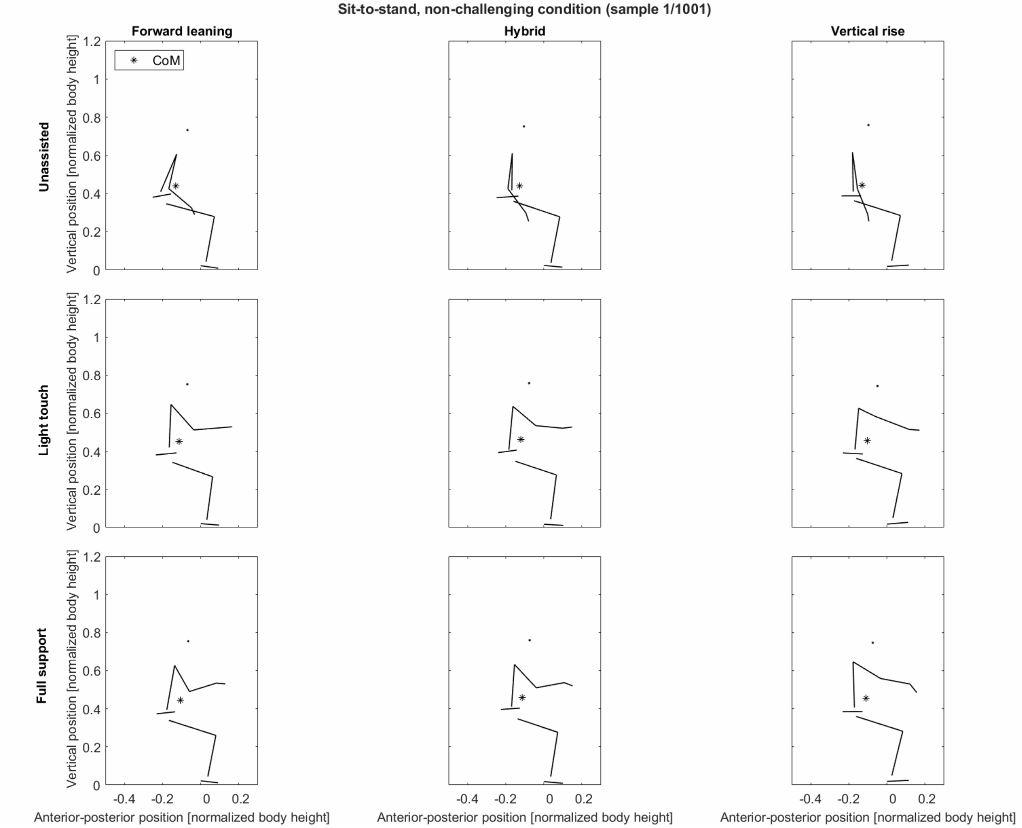

Figure A.1: Sit-to-stand, non-challenging condition. Animated version at https://static-content.springer.com/esm/art%3A10.1038%2Fs41598-023-43401-6/MediaObjects/41598_2023_43401_MOESM2_ESM.gif

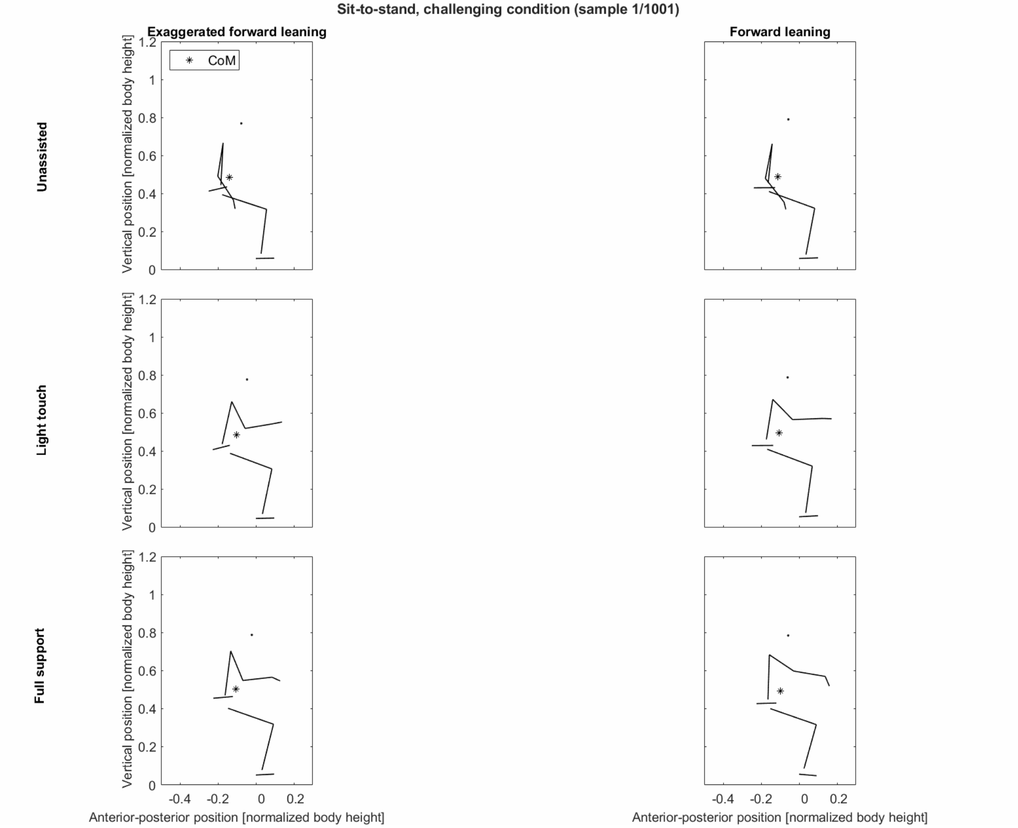

Figure A.2: Sit-to-stand, challenging condition. Animated version at https://static-content.springer.com/esm/art%3A10.1038%2Fs41598-023-43401-6/MediaObjects/41598_2023_43401_MOESM1_ESM.gif

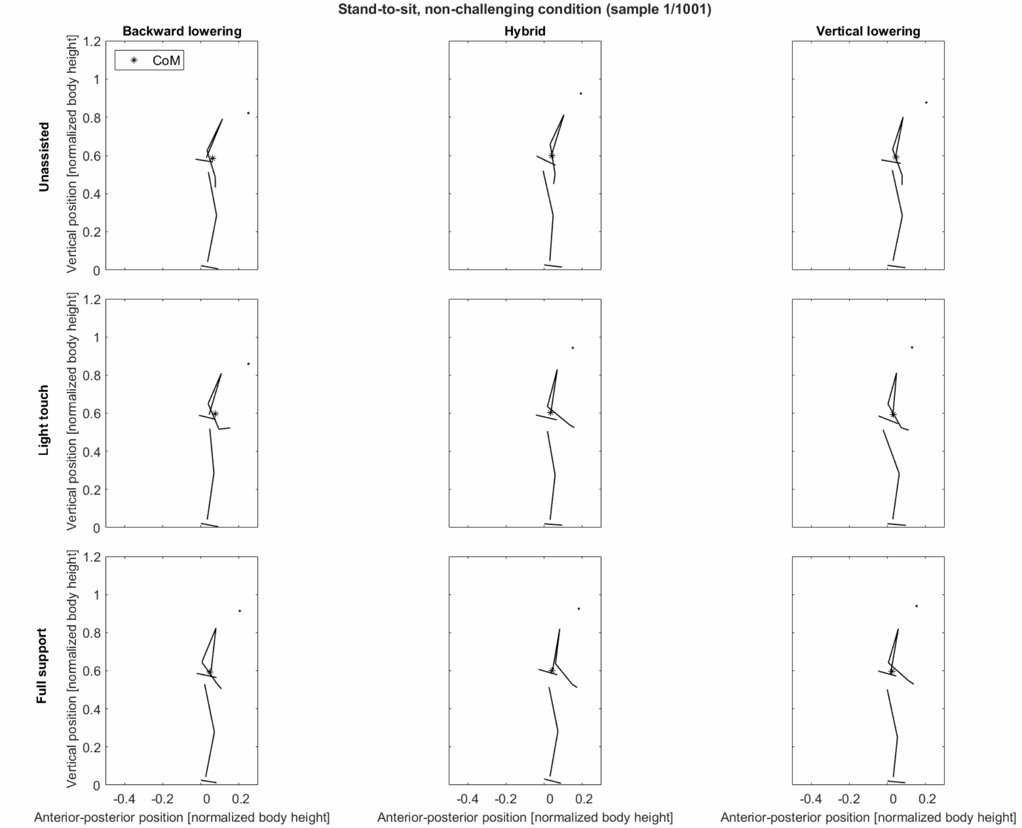

Figure A.3: Stand-to-sit, non-challenging condition. Animated version at https://static-content.springer.com/esm/art%3A10.1038%2Fs41598-023-43401-6/MediaObjects/41598_2023_43401_MOESM4_ESM.gif

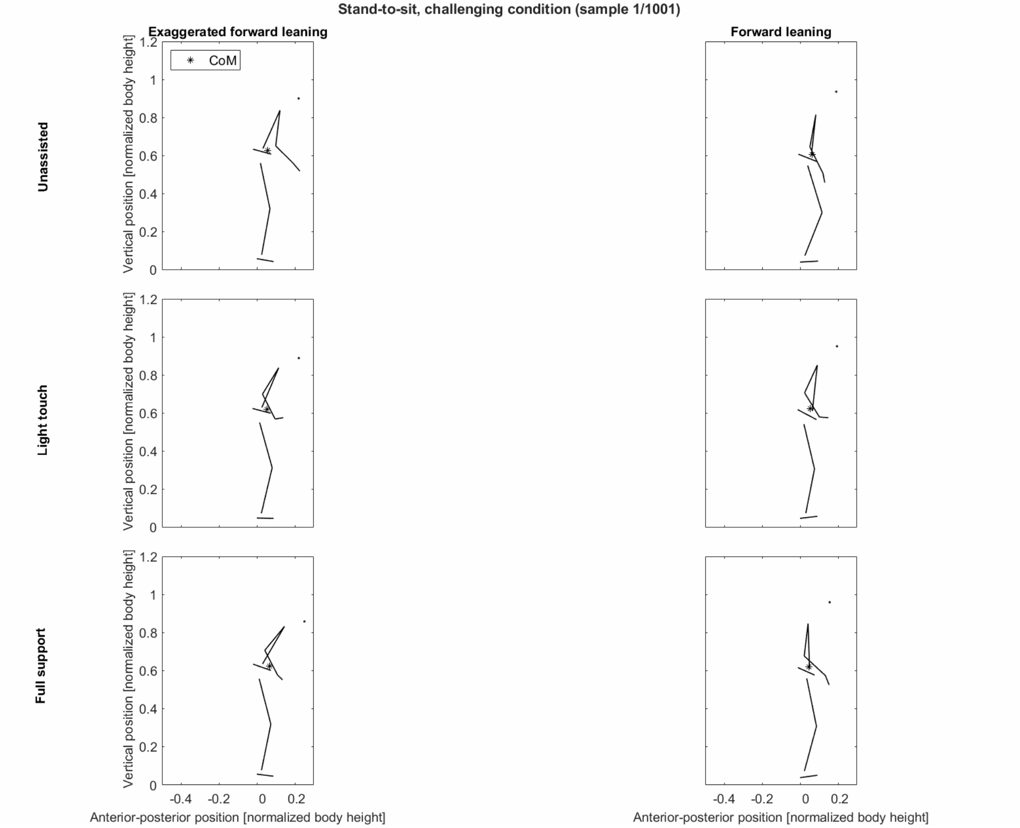

Figure A.4: Stand-to-sit, challenging condition. Animated version at https://static-content.springer.com/esm/art%3A10.1038%2Fs41598-023-43401-6/MediaObjects/41598_2023_43401_MOESM3_ESM.gif

A.2.2 Outlier trials in the sit-to-stand and stand-to-sit tasks

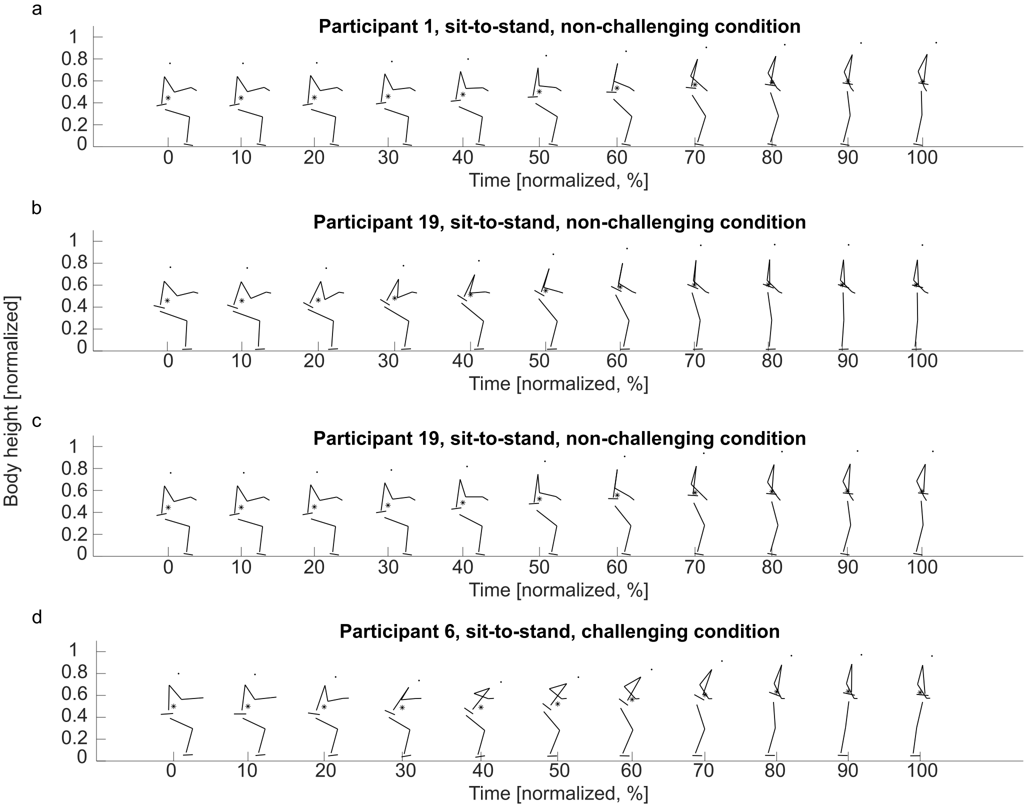

Figure continues on next page.

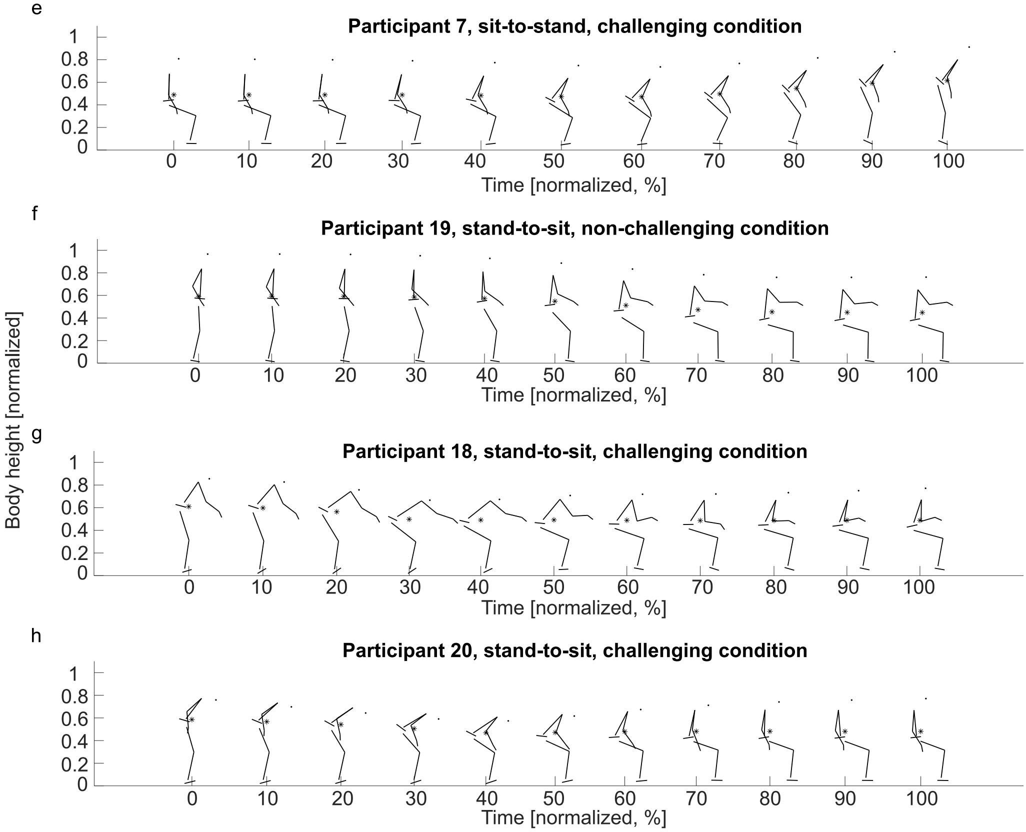

Figure A.5: Trials identified as outliers. These trials were first assigned to one of the strategies with k-means clustering but were later identified as outliers due to their large distance to the clusters' centroids. a-c: sit-to-stand, non- challenging, d-e: sit-to-stand, challenging, f: stand-to-sit, non-challenging, g-h: stand-to-sit, challenging condition. We call a-c "pulling strategy", as this movement execution is only possible with extensive pulling on the handles.

A.3 Supplementary material: topic B, study B2

A.3.1 Trials with corrupt EMG signals

Table A.3: Trials with corrupt EMG signals. Except for these trials, all EMG recordings were valid. l: left side, r: right side.

Participant	Movement and conditions	Trial	Strategy	Bic	Lat	Tra	GM	TF	RF	VM	BF	TA	PL	GA
2	Stand-to-sit, non-challenging, unassisted	1	Vertical lowering				l							
2	Stand-to-sit, non-challenging, unassisted	2	Vertical lowering				l							
2	Stand-to-sit, non-challenging, unassisted	3	Vertical lowering				l							
2	Sit-to-stand, non-challenging, light touch	1	Hybrid					l, r	l, r	l, r	l, r	l, r	l, r	l, r
2	Sit-to-stand, non-challenging, light touch	2	Hybrid					l, r	l, r	l, r	l, r	l, r	l, r	l, r
2	Sit-to-stand, non-challenging, light touch	3	Hybrid					l, r	l, r	l, r	l, r	l, r	l, r	l, r
2	Stand-to-sit, non-challenging, light touch	1	Vertical lowering					l, r	l, r	l, r	l, r	l, r	l, r	l, r
2	Stand-to-sit, non-challenging, light touch	2	Vertical lowering					l, r	l, r	l, r	l, r	l, r	l, r	l, r
2	Stand-to-sit, non-challenging, light touch	3	Vertical lowering					l, r	l, r	l, r	l, r	l, r	l, r	l, r
2	Sit-to-stand, non-challenging, full support	1	Vertical rise					l, r	l, r	l, r	l, r	l, r	l, r	l, r
2	Sit-to-stand, non-challenging, full support	2	Hybrid					l, r	l, r	l, r	l, r	l, r	l, r	l, r

2	Sit-to-stand, non-challenging, full support	2	Exaggerated forward leaning					l, r	l, r	l, r	l, r	l, r	l, r	l, r
2	Stand-to-sit, non-challenging, full support	1	Vertical lowering						l	l		l, r	l, r	l, r
2	Stand-to-sit, challenging, light touch	2	Backward lowering									l, r	l, r	l, r
4	Sit-to-stand, challenging, light touch	2	Forward leaning	l, r				r	l	l, r	l, r	l, r	l, r	r
4	Stand-to-sit, challenging, light touch	2	Exaggerated forward leaning	l, r				r	l	l, r	l, r	l, r	l, r	r
5	Sit-to-stand, non-challenging, light touch	1	Hybrid		l			l	l			l, r	l, r	l, r
5	Stand-to-sit, non-challenging, light touch	1	Backward lowering		l			l	l			l, r	l, r	l, r
9	Sit-to-stand, non-challenging, unassisted	3	Hybrid			r		l	l			l, r	r	l, r
9	Stand-to-sit, non-challenging, unassisted	3	Vertical lowering			r		l	l			l, r	r	l, r
9	Sit-to-stand, challenging, unassisted	3	Exaggerated forward leaning					l	l			l, r	r	l
9	Stand-to-sit, challenging, unassisted	3	Exaggerated forward leaning					l	l			l, r	r	l
12	Sit-to-stand, non-challenging, light touch	2	Forward leaning		l				l, r	l, r	l	l, r	r	l, r
12	Stand-to-sit, non-challenging, light touch	2	Vertical lowering		l				l, r	l, r	l	l, r	r	l, r

A.3.2 Distribution of trials among strategies

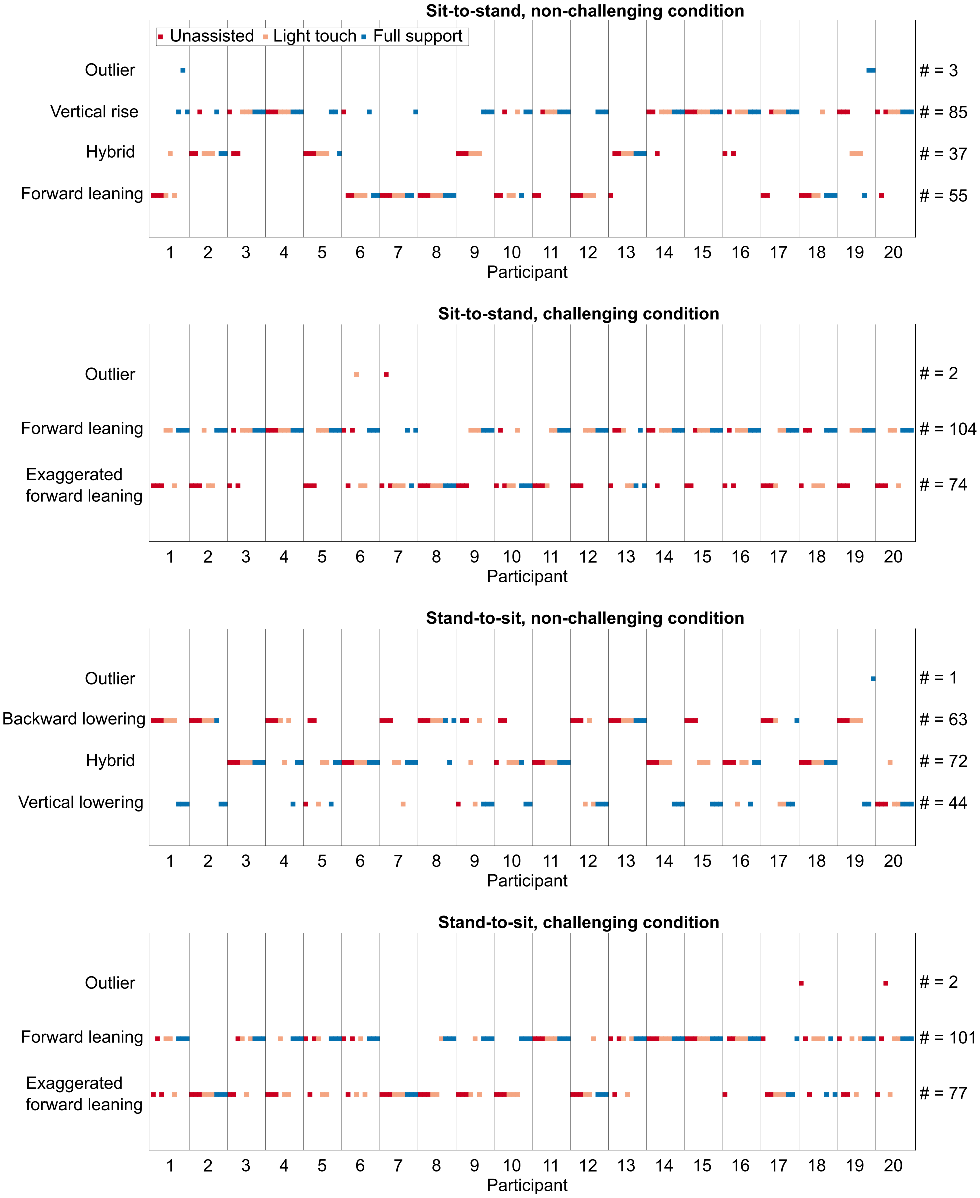

Figure A.6: Distribution of trials among strategies. One dot represents one trial. The row indicates the strategy to which it belongs. The column shows to which participant it belongs. The support conditions are color-coded as indicated by the legend. The labels on the right y-axis show how many trials were associated with the strategy written on the left y-axis. This figure is taken from Herzog et al. (2023).

A.3.3 Differences in the temporal composition remain with the R^2 > 0.9 (N^*_{strat}) criterion

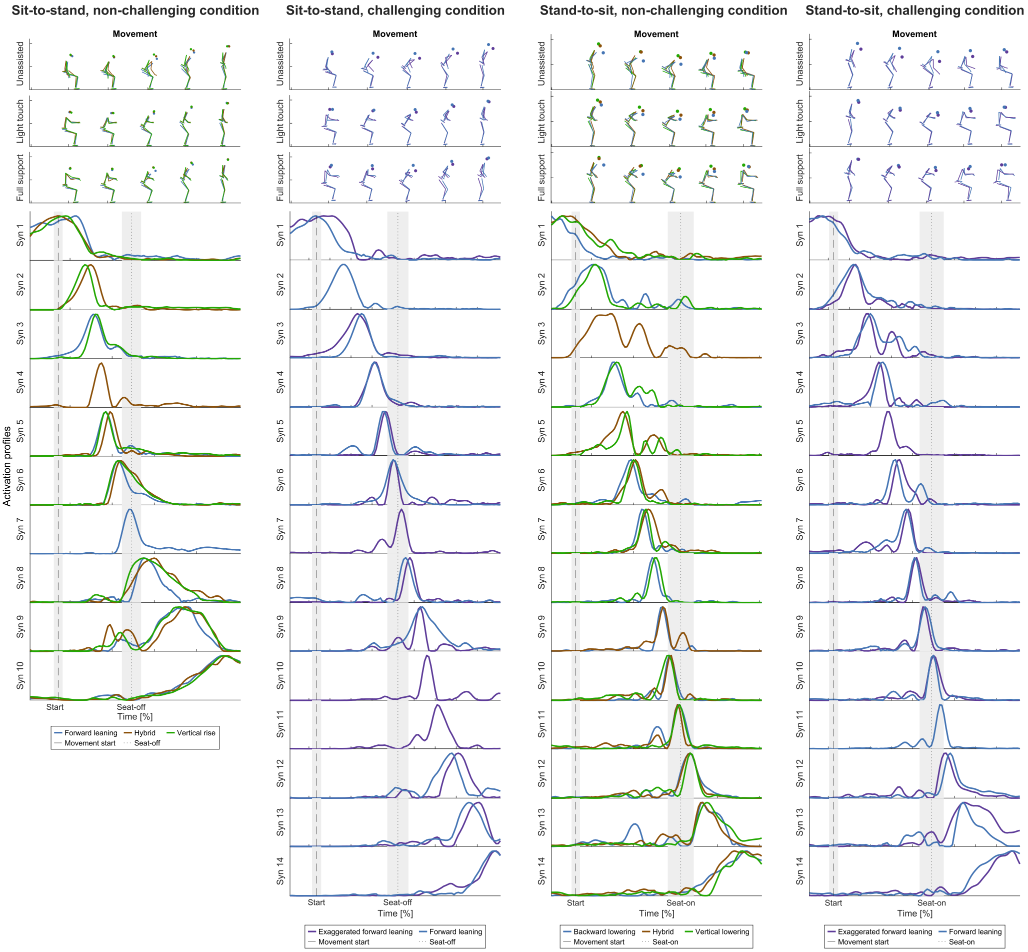

Figure A.7: Temporal synergies for every movement strategy with the $R^2 > 0.9$ (N^*_{strat}) criterion. Clustered and ordered chronologically.

A.3.4 Detailed linear mixed model statistics

Table A.4: Detailed statistics: sit-to-stand, non-challenging condition, forward leaning strategy, synergy 1

Reference group: UA

Model information	**Values**
Number of observations	864
Number of participants	12
ICC	0.502

Fixed effects	**Estimate**	**Lower 95% CI**	**Upper 95% CI**	**t**	**p**
(Intercept)	0.023	0.017	0.029	7.614	<.001
LT	0.008	0.003	0.014	7.614	0.047
FS	0.010	0.004	0.016	7.614	0.032
Random effects	**Estimate**	**Lower 95% CI**	**Upper 95% CI**		
(Intercept)	0.008	0.005	0.015		
Error	0.034	0.032	0.035		

Reference group: LT

Fixed effects	**Estimate**	**Lower 95% CI**	**Upper 95% CI**	**t**	**p**
(Intercept)	0.031	0.025	0.038	9.167	<.001
UA	0.031	-0.014	-0.003	-2.941	0.047
FS	0.031	-0.005	0.008	0.513	1.000
Random effects	**Estimate**	**Lower 95% CI**	**Upper 95% CI**		
(Intercept)	0.008	0.005	0.015		
Error	0.034	0.032	0.035		

Post-hoc UA vs. LT

Fixed effects	**Estimate**	**Lower 95% CI**	**Upper 95% CI**	**t**	**p**
RA:LT	-0.007	-0.023	0.008	-0.899	0.738
ES:LT	-0.007	-0.014	0.017	0.195	1.000
Pec:LT	-0.007	-0.018	0.013	-0.339	1.000
Lat:LT	-0.007	-0.007	0.024	1.055	0.584
Tra:LT	-0.007	0.036	0.067	6.553	<.001
Del:LT	-0.007	-0.010	0.021	0.661	1.000
Bic:LT	-0.007	-0.015	0.016	0.115	1.000
Tri:LT	-0.007	-0.014	0.017	0.251	1.000
GM:LT	-0.007	-0.025	0.006	-1.160	0.493
TF:LT	-0.007	-0.030	0.001	-1.886	0.119
RF:LT	-0.007	-0.024	0.007	-1.117	0.528
VM:LT	-0.007	-0.022	0.009	-0.869	0.770
BF:LT	-0.007	-0.022	0.009	-0.819	0.826
TA:LT	-0.007	-0.022	0.009	-0.805	0.843
PL:LT	-0.007	-0.020	0.011	-0.582	1.000
Random effects	**Estimate**	**Lower 95% CI**	**Upper 95% CI**		
(Intercept)	0.009	0.006	0.015		
Error	0.026	0.025	0.027		

Post-hoc UA vs. FS

Fixed effects	**Estimate**	**Lower 95% CI**	**Upper 95% CI**	**t**	**p**
RA:FS	-0.024	-0.041	-0.007	-2.725	0.013
ES:FS	-0.024	-0.025	0.009	-0.901	0.735
Pec:FS	-0.024	-0.010	0.024	0.795	0.854
Lat:FS	-0.024	-0.008	0.027	1.069	0.571
Tra:FS	-0.024	0.040	0.075	6.547	<.001
Del:FS	-0.024	-0.038	-0.003	-2.323	0.041
Bic:FS	-0.024	0.031	0.065	5.454	<.001
Tri:FS	-0.024	0.002	0.037	2.241	0.051
GM:FS	-0.024	-0.042	-0.008	-2.853	0.009
TF:FS	-0.024	-0.035	-0.001	-2.022	0.087
RF:FS	-0.024	-0.019	0.016	-0.178	1.000
VM:FS	-0.024	-0.020	0.015	-0.306	1.000
BF:FS	-0.024	-0.025	0.009	-0.924	0.711
TA:FS	-0.024	-0.032	0.003	-1.646	0.200
PL:FS	-0.024	-0.028	0.006	-1.263	0.414
Random effects	**Estimate**	**Lower 95% CI**	**Upper 95% CI**		
(Intercept)	0.009	0.006	0.015		
Error	0.026	0.025	0.027		

Table A.5: Detailed statistics: sit-to-stand, non-challenging condition, forward leaning strategy, synergy 3

Reference group: UA

Model information	**Values**
Number of observations	864
Number of participants	12
ICC	0.566

Fixed effects	**Estimate**	**Lower 95% CI**	**Upper 95% CI**	**t**	**p**
(Intercept)	0.020	0.014	0.027	6.490	<.001
LT	0.016	0.011	0.021	6.490	<.001
FS	0.011	0.005	0.017	6.490	0.008
Random effects	**Estimate**	**Lower 95% CI**	**Upper 95% CI**		
(Intercept)	0.009	0.005	0.015		
Error	0.032	0.031	0.034		

Reference group: LT

Fixed effects	**Estimate**	**Lower 95% CI**	**Upper 95% CI**	**t**	**p**
(Intercept)	0.036	0.029	0.043	10.350	<.001
UA	0.036	-0.021	-0.011	-5.924	<.001
FS	0.036	-0.011	0.001	-1.601	1.000
Random effects	**Estimate**	**Lower 95% CI**	**Upper 95% CI**		
(Intercept)	0.009	0.005	0.015		
Error	0.032	0.031	0.034		

Post-hoc UA vs. LT

Fixed effects	**Estimate**	**Lower 95% CI**	**Upper 95% CI**	**t**	**p**
RA:LT	-0.014	-0.032	0.003	-1.660	0.195
ES:LT	-0.014	-0.002	0.032	1.744	0.163
Pec:LT	-0.014	-0.031	0.004	-1.555	0.241
Lat:LT	-0.014	-0.009	0.026	0.980	0.655
Tra:LT	-0.014	-0.025	0.009	-0.937	0.698
Del:LT	-0.014	-0.000	0.034	1.937	0.106
Bic:LT	-0.014	-0.015	0.019	0.191	1.000
Tri:LT	-0.014	-0.019	0.015	-0.213	1.000
GM:LT	-0.014	-0.023	0.011	-0.698	0.971
TF:LT	-0.014	-0.018	0.016	-0.118	1.000
RF:LT	-0.014	-0.009	0.026	0.976	0.658
VM:LT	-0.014	0.006	0.040	2.622	0.018
BF:LT	-0.014	-0.025	0.009	-0.919	0.717
TA:LT	-0.014	-0.021	0.014	-0.412	1.000
PL:LT	-0.014	-0.023	0.011	-0.664	1.000
Random effects	**Estimate**	**Lower 95% CI**	**Upper 95% CI**		
(Intercept)	0.009	0.006	0.016		
Error	0.029	0.027	0.030		

Post-hoc UA vs. FS

Fixed effects	Estimate	Lower 95% CI	Upper 95% CI	t	p
RA:FS	-0.007	-0.026	0.012	-0.720	0.944
ES:FS	-0.007	-0.028	0.010	-0.929	0.706
Pec:FS	-0.007	-0.023	0.015	-0.438	1.000
Lat:FS	-0.007	-0.002	0.036	1.756	0.159
Tra:FS	-0.007	-0.032	0.006	-1.312	0.380
Del:FS	-0.007	-0.020	0.018	-0.119	1.000
Bic:FS	-0.007	0.010	0.049	3.036	0.005
Tri:FS	-0.007	-0.013	0.025	0.611	1.000
GM:FS	-0.007	-0.032	0.006	-1.343	0.359
TF:FS	-0.007	-0.015	0.023	0.383	1.000
RF:FS	-0.007	-0.016	0.023	0.359	1.000
VM:FS	-0.007	0.000	0.038	1.988	0.094
BF:FS	-0.007	-0.026	0.013	-0.672	1.000
TA:FS	-0.007	-0.027	0.012	-0.764	0.890
PL:FS	-0.007	-0.027	0.011	-0.834	0.809
Random effects	**Estimate**	**Lower 95% CI**	**Upper 95% CI**		
(Intercept)	0.009	0.006	0.016		
Error	0.029	0.027	0.030		

Table A.6: Detailed statistics: sit-to-stand, non-challenging condition, forward leaning strategy, synergy 4

Reference group: UA

Model information	**Values**
Number of observations	864
Number of participants	12
ICC	0.434

Fixed effects	**Estimate**	**Lower 95% CI**	**Upper 95% CI**	**t**	**p**
(Intercept)	0.030	0.024	0.036	10.441	<.001
LT	0.009	0.003	0.015	10.441	0.025
FS	0.005	-0.001	0.012	10.441	1.000
Random effects	**Estimate**	**Lower 95% CI**	**Upper 95% CI**		
(Intercept)	0.008	0.004	0.013		
Error	0.035	0.033	0.037		

Reference group: LT

Fixed effects	**Estimate**	**Lower 95% CI**	**Upper 95% CI**	**t**	**p**
(Intercept)	0.039	0.033	0.046	11.893	<.001
UA	0.039	-0.015	-0.003	-3.133	0.025
FS	0.039	-0.010	0.003	-1.083	1.000
Random effects	**Estimate**	**Lower 95% CI**	**Upper 95% CI**		
(Intercept)	0.008	0.004	0.013		
Error	0.035	0.033	0.037		

Post-hoc UA vs. LT

Fixed effects	**Estimate**	**Lower 95% CI**	**Upper 95% CI**	**t**	**p**
RA:LT	-0.011	-0.028	0.006	-1.281	0.201
ES:LT	-0.011	-0.036	-0.002	-2.187	0.029
Pec:LT	-0.011	-0.025	0.009	-0.907	0.365
Lat:LT	-0.011	-0.004	0.029	1.452	0.147
Tra:LT	-0.011	-0.020	0.014	-0.375	0.708
Del:LT	-0.011	0.015	0.049	3.674	<.001
Bic:LT	-0.011	-0.007	0.027	1.123	0.262
Tri:LT	-0.011	-0.025	0.009	-0.948	0.343
GM:LT	-0.011	-0.028	0.006	-1.295	0.196
TF:LT	-0.011	-0.009	0.025	0.955	0.340
RF:LT	-0.011	-0.014	0.019	0.289	0.772
VM:LT	-0.011	-0.012	0.022	0.553	0.580
BF:LT	-0.011	-0.010	0.024	0.815	0.415
TA:LT	-0.011	-0.020	0.014	-0.374	0.709
PL:LT	-0.011	-0.024	0.010	-0.796	0.426
Random effects	**Estimate**	**Lower 95% CI**	**Upper 95% CI**		
(Intercept)	0.008	0.005	0.013		
Error	0.028	0.027	0.030		

Table A.7: Detailed statistics: sit-to-stand, non-challenging condition, forward leaning strategy, synergy 5

Reference group: UA

Model information	**Values**
Number of observations	864
Number of participants	12
ICC	0.598

Fixed effects	**Estimate**	**Lower 95% CI**	**Upper 95% CI**	**t**	**p**
(Intercept)	0.039	0.032	0.047	10.559	<0.001
LT	-0.008	-0.014	-0.002	10.559	0.125
FS	-0.012	-0.018	-0.005	10.559	0.015
Random effects	**Estimate**	**Lower 95% CI**	**Upper 95% CI**		
(Intercept)	0.011	0.007	0.017		
Error	0.036	0.035	0.038		

Reference group: LT

Fixed effects	**Estimate**	**Lower 95% CI**	**Upper 95% CI**	**t**	**p**
(Intercept)	0.031	0.023	0.039	7.661	<0.001
UA	0.031	0.002	0.014	2.621	0.125
FS	0.031	-0.011	0.003	-1.019	1.000
Random effects	**Estimate**	**Lower 95% CI**	**Upper 95% CI**		
(Intercept)	0.011	0.007	0.017		
Error	0.036	0.035	0.038		

Post-hoc UA vs. FS

Fixed effects	**Estimate**	**Lower 95% CI**	**Upper 95% CI**	**t**	**p**
RA:FS	0.004	-0.013	0.022	0.509	0.611
ES:FS	0.004	-0.052	-0.018	-3.977	<0.001
Pec:FS	0.004	0.009	0.043	2.959	0.003
Lat:FS	0.004	0.002	0.036	2.144	0.032
Tra:FS	0.004	-0.002	0.032	1.739	0.082
Del:FS	0.004	0.023	0.057	4.545	<0.001
Bic:FS	0.004	0.007	0.041	2.752	0.006
Tri:FS	0.004	0.003	0.037	2.318	0.021
GM:FS	0.004	-0.013	0.021	0.440	0.660
TF:FS	0.004	-0.048	-0.013	-3.504	<0.001
RF:FS	0.004	-0.060	-0.026	-4.965	<0.001
VM:FS	0.004	-0.042	-0.008	-2.834	0.005
BF:FS	0.004	-0.026	0.008	-1.030	0.303
TA:FS	0.004	-0.030	0.004	-1.490	0.137
PL:FS	0.004	-0.019	0.015	-0.212	0.833
Random effects	**Estimate**	**Lower 95% CI**	**Upper 95% CI**		
(Intercept)	0.011	0.007	0.017		
Error	0.026	0.024	0.027		

Table A.8: Detailed statistics: sit-to-stand, non-challenging condition, forward leaning strategy, synergy 6

Reference group: UA

Model information	**Values**
Number of observations	864
Number of participants	12
ICC	0.576

Fixed effects	**Estimate**	**Lower 95% CI**	**Upper 95% CI**	**t**	**p**
(Intercept)	0.031	0.024	0.037	9.299	<0.001
LT	0.001	-0.005	0.006	9.299	1.000
FS	0.000	-0.006	0.006	9.299	1.000
Random effects	**Estimate**	**Lower 95% CI**	**Upper 95% CI**		
(Intercept)	0.010	0.006	0.017		
Error	0.033	0.032	0.035		

Reference group: LT

Fixed effects	**Estimate**	**Lower 95% CI**	**Upper 95% CI**	**t**	**p**
(Intercept)	0.031	0.024	0.039	8.560	<0.001
UA	0.031	-0.006	0.005	-0.202	1.000
FS	0.031	-0.007	0.006	-0.159	1.000
Random effects	**Estimate**	**Lower 95% CI**	**Upper 95% CI**		
(Intercept)	0.010	0.006	0.017		
Error	0.033	0.032	0.035		

Table A.9: Detailed statistics: sit-to-stand, non-challenging condition, forward leaning strategy, synergy 7

Reference group: UA

Model information	**Values**
Number of observations	864
Number of participants	12
ICC	0.339

Fixed effects	**Estimate**	**Lower 95% CI**	**Upper 95% CI**	**t**	**p**
(Intercept)	0.029	0.024	0.034	12.360	<0.001
LT	0.003	-0.002	0.008	12.360	1.000
FS	0.007	0.001	0.013	12.360	0.460
Random effects	**Estimate**	**Lower 95% CI**	**Upper 95% CI**		
(Intercept)	0.006	0.003	0.010		
Error	0.033	0.031	0.034		

Reference group: LT

Fixed effects	**Estimate**	**Lower 95% CI**	**Upper 95% CI**	**t**	**p**
(Intercept)	0.032	0.027	0.038	11.705	<0.001
UA	0.032	-0.008	0.002	-1.137	1.000
FS	0.032	-0.003	0.010	1.106	1.000
Random effects	**Estimate**	**Lower 95% CI**	**Upper 95% CI**		
(Intercept)	0.006	0.003	0.010		
Error	0.033	0.031	0.034		

Table A.10: Detailed statistics: sit-to-stand, non-challenging condition, forward leaning strategy, synergy 8

Reference group: UA

Model information	Values
Number of observations	864
Number of participants	12
ICC	0.346

Fixed effects	Estimate	Lower 95% CI	Upper 95% CI	t	p
(Intercept)	0.040	0.034	0.046	13.390	<0.001
LT	-0.005	-0.012	0.001	13.390	1.000
FS	-0.002	-0.010	0.005	13.390	1.000
Random effects	**Estimate**	**Lower 95% CI**	**Upper 95% CI**		
(Intercept)	0.007	0.004	0.013		
Error	0.041	0.039	0.043		

Reference group: LT

Fixed effects	Estimate	Lower 95% CI	Upper 95% CI	t	p
(Intercept)	0.035	0.028	0.041	9.985	<0.001
UA	0.035	-0.001	0.012	1.583	1.000
FS	0.035	-0.005	0.011	0.781	1.000
Random effects	**Estimate**	**Lower 95% CI**	**Upper 95% CI**		
(Intercept)	0.007	0.004	0.013		
Error	0.041	0.039	0.043		

Table A.11: Detailed statistics: sit-to-stand, non-challenging condition, hybrid strategy, synergy 1

Reference group: UA

Model information	Values
Number of observations	496
Number of participants	9
ICC	0.220

Fixed effects	Estimate	Lower 95% CI	Upper 95% CI	t	p
(Intercept)	0.029	0.024	0.035	9.978	<0.001
LT	0.000	-0.008	0.008	9.978	1.000
FS	0.011	0.001	0.021	9.978	0.346
Random effects	**Estimate**	**Lower 95% CI**	**Upper 95% CI**		
(Intercept)	0.004	0.001	0.023		
Error	0.037	0.035	0.040		

Reference group: LT

Fixed effects	Estimate	Lower 95% CI	Upper 95% CI	t	p
(Intercept)	0.030	0.023	0.036	9.124	<0.001
UA	0.030	-0.008	0.008	-0.065	1.000
FS	0.030	0.001	0.021	2.085	0.451
Random effects	**Estimate**	**Lower 95% CI**	**Upper 95% CI**		
(Intercept)	0.004	0.001	0.023		
Error	0.037	0.035	0.040		

Table A.12: Detailed statistics: sit-to-stand, non-challenging condition, hybrid strategy, synergy 3

Reference group: UA

Model information	**Values**
Number of observations	496
Number of participants	9
ICC	0.703

Fixed effects	**Estimate**	**Lower 95% CI**	**Upper 95% CI**	**t**	**p**
(Intercept)	0.025	0.014	0.035	4.797	<0.001
LT	0.022	0.014	0.031	4.797	<0.001
FS	0.034	0.024	0.044	4.797	<0.001
Random effects	**Estimate**	**Lower 95% CI**	**Upper 95% CI**		
(Intercept)	0.013	0.007	0.023		
Error	0.037	0.034	0.039		

Reference group: LT

Fixed effects	**Estimate**	**Lower 95% CI**	**Upper 95% CI**	**t**	**p**
(Intercept)	0.047	0.036	0.057	8.616	<0.001
UA	0.047	-0.031	-0.014	-5.026	<0.001
FS	0.047	0.001	0.023	2.118	0.416
Random effects	**Estimate**	**Lower 95% CI**	**Upper 95% CI**		
(Intercept)	0.013	0.007	0.023		
Error	0.037	0.034	0.039		

Post-hoc UA vs. LT

Fixed effects	**Estimate**	**Lower 95% CI**	**Upper 95% CI**	**t**	**p**
RA:LT	-0.005	-0.027	0.017	-0.429	1.000
ES:LT	-0.005	-0.014	0.029	0.672	1.000
Pec:LT	-0.005	-0.026	0.018	-0.337	1.000
Lat:LT	-0.005	0.002	0.045	2.108	0.071
Tra:LT	-0.005	-0.016	0.028	0.556	1.000
Del:LT	-0.005	-0.027	0.017	-0.447	1.000
Bic:LT	-0.005	-0.007	0.036	1.309	0.383
Tri:LT	-0.005	-0.031	0.012	-0.848	0.794
GM:LT	-0.005	-0.042	0.002	-1.823	0.138
TF:LT	-0.005	-0.026	0.018	-0.358	1.000
RF:LT	-0.005	-0.015	0.028	0.587	1.000
VM:LT	-0.005	-0.013	0.031	0.836	0.807
BF:LT	-0.005	-0.033	0.011	-1.019	0.618
TA:LT	-0.005	-0.013	0.031	0.825	0.820
PL:LT	-0.005	-0.022	0.022	0.012	1.000
Random effects	**Estimate**	**Lower 95% CI**	**Upper 95% CI**		
(Intercept)	0.014	0.008	0.023		
Error	0.029	0.027	0.031		

Post-hoc UA vs. FS

Fixed effects	**Estimate**	**Lower 95% CI**	**Upper 95% CI**	**t**	**p**
RA:FS	-0.003	-0.032	0.026	-0.211	1.000
ES:FS	-0.003	-0.017	0.041	0.845	0.797
Pec:FS	-0.003	-0.015	0.043	0.960	0.676
Lat:FS	-0.003	0.077	0.134	7.162	<0.001
Tra:FS	-0.003	-0.033	0.025	-0.254	1.000
Del:FS	-0.003	-0.067	-0.009	-2.576	0.021
Bic:FS	-0.003	0.064	0.122	6.324	<0.001
Tri:FS	-0.003	-0.002	0.056	1.861	0.127
GM:FS	-0.003	-0.075	-0.017	-3.125	0.004
TF:FS	-0.003	-0.060	-0.002	-2.122	0.069
RF:FS	-0.003	-0.043	0.014	-0.985	0.650
VM:FS	-0.003	-0.034	0.023	-0.375	1.000
BF:FS	-0.003	-0.060	-0.002	-2.117	0.070
TA:FS	-0.003	-0.040	0.017	-0.783	0.869
PL:FS	-0.003	-0.058	0.000	-1.964	0.100

Random effects	**Estimate**	**Lower 95% CI**	**Upper 95% CI**
(Intercept)	0.014	0.008	0.023
Error	0.029	0.027	0.031

Table A.13: Detailed statistics: sit-to-stand, non-challenging condition, hybrid strategy, synergy 4

Reference group: UA

Model information	**Values**
Number of observations	496
Number of participants	9
ICC	0.439

Fixed effects	**Estimate**	**Lower 95% CI**	**Upper 95% CI**	**t**	**p**
(Intercept)	0.046	0.038	0.054	11.567	<0.001
LT	-0.010	-0.019	-0.001	11.567	0.312
FS	-0.012	-0.023	-0.001	11.567	0.310

Random effects	**Estimate**	**Lower 95% CI**	**Upper 95% CI**
(Intercept)	0.009	0.004	0.018
Error	0.039	0.036	0.041

Reference group: LT

Fixed effects	**Estimate**	**Lower 95% CI**	**Upper 95% CI**	**t**	**p**
(Intercept)	0.036	0.028	0.045	8.327	<0.001
UA	0.036	0.001	0.019	2.233	0.312
FS	0.036	-0.014	0.009	-0.418	1.000

Random effects	**Estimate**	**Lower 95% CI**	**Upper 95% CI**
(Intercept)	0.009	0.004	0.018
Error	0.039	0.036	0.041

Table A.14: Detailed statistics: sit-to-stand, non-challenging condition, hybrid strategy, synergy 5

Reference group: UA					
Model information	**Values**				
Number of observations	496				
Number of participants	9				
ICC	0.527				
Fixed effects	**Estimate**	**Lower 95% CI**	**Upper 95% CI**	**t**	**p**
(Intercept)	0.045	0.035	0.055	9.198	<0.001
LT	0.003	-0.006	0.013	9.198	1.000
FS	0.000	-0.012	0.012	9.198	1.000
Random effects	**Estimate**	**Lower 95% CI**	**Upper 95% CI**		
(Intercept)	0.011	0.006	0.023		
Error	0.043	0.040	0.046		
Reference group: LT					
Fixed effects	**Estimate**	**Lower 95% CI**	**Upper 95% CI**	**t**	**p**
(Intercept)	0.049	0.038	0.059	9.145	<0.001
UA	0.049	-0.013	0.006	-0.679	1.000
FS	0.049	-0.015	0.010	-0.468	1.000
Random effects	**Estimate**	**Lower 95% CI**	**Upper 95% CI**		
(Intercept)	0.011	0.006	0.023		
Error	0.043	0.040	0.046		

Table A.15: Detailed statistics: sit-to-stand, non-challenging condition, hybrid strategy, synergy 7

Reference group: UA					
Model information	**Values**				
Number of observations	496				
Number of participants	9				
ICC	0.760				
Fixed effects	**Estimate**	**Lower 95% CI**	**Upper 95% CI**	**t**	**p**
(Intercept)	0.035	0.023	0.047	5.701	<0.001
LT	0.012	0.002	0.022	5.701	0.273
FS	0.005	-0.007	0.017	5.701	1.000
Random effects	**Estimate**	**Lower 95% CI**	**Upper 95% CI**		
(Intercept)	0.016	0.009	0.027		
Error	0.042	0.039	0.045		
Reference group: LT					
Fixed effects	**Estimate**	**Lower 95% CI**	**Upper 95% CI**	**t**	**p**
(Intercept)	0.047	0.034	0.060	7.175	<0.001
UA	0.047	-0.022	-0.002	-2.284	0.273
FS	0.047	-0.019	0.006	-1.072	1.000
Random effects	**Estimate**	**Lower 95% CI**	**Upper 95% CI**		
(Intercept)	0.016	0.009	0.027		
Error	0.042	0.039	0.045		

Table A.16: Detailed statistics: sit-to-stand, non-challenging condition, hybrid strategy, synergy 8

Reference group: UA

Model information	Values
Number of observations	496
Number of participants	9
ICC	0.304

Fixed effects	Estimate	Lower 95% CI	Upper 95% CI	t	p
(Intercept)	0.045	0.037	0.054	10.664	<0.001
LT	-0.005	-0.015	0.006	10.664	1.000
FS	-0.002	-0.015	0.012	10.664	1.000
Random effects	**Estimate**	**Lower 95% CI**	**Upper 95% CI**		
(Intercept)	0.007	0.003	0.018		
Error	0.049	0.046	0.052		

Reference group: LT

Fixed effects	Estimate	Lower 95% CI	Upper 95% CI	t	p
(Intercept)	0.040	0.031	0.050	8.655	<0.001
UA	0.040	-0.006	0.015	0.888	1.000
FS	0.040	-0.011	0.017	0.449	1.000
Random effects	**Estimate**	**Lower 95% CI**	**Upper 95% CI**		
(Intercept)	0.007	0.003	0.018		
Error	0.049	0.046	0.052		

Table A.17: Detailed statistics: sit-to-stand, non-challenging condition, vertical rise strategy, synergy 1

Reference group: UA

Model information	**Values**
Number of observations	1344
Number of participants	18
ICC	0.424

Fixed effects	**Estimate**	**Lower 95% CI**	**Upper 95% CI**	**t**	**p**
(Intercept)	0.026	0.020	0.032	8.712	<0.001
LT	0.005	-0.001	0.010	8.712	1.000
FS	0.010	0.005	0.016	8.712	0.004

Random effects	**Estimate**	**Lower 95% CI**	**Upper 95% CI**
(Intercept)	0.008	0.005	0.013
Error	0.038	0.036	0.039

Reference group: LT

Fixed effects	**Estimate**	**Lower 95% CI**	**Upper 95% CI**	**t**	**p**
(Intercept)	0.031	0.025	0.036	10.804	<0.001
UA	0.031	-0.010	0.001	-1.516	1.000
FS	0.031	0.001	0.011	2.259	0.288

Random effects	**Estimate**	**Lower 95% CI**	**Upper 95% CI**
(Intercept)	0.008	0.005	0.013
Error	0.038	0.036	0.039

Post-hoc UA vs. FS

Fixed effects	**Estimate**	**Lower 95% CI**	**Upper 95% CI**	**t**	**p**
RA:FS	-0.039	-0.054	-0.024	-4.976	<0.001
ES:FS	-0.039	-0.017	0.014	-0.188	0.851
Pec:FS	-0.039	0.009	0.039	3.080	0.002
Lat:FS	-0.039	-0.000	0.031	1.947	0.052
Tra:FS	-0.039	0.071	0.101	10.973	<0.001
Del:FS	-0.039	-0.029	0.002	-1.721	0.086
Bic:FS	-0.039	0.012	0.042	3.437	0.001
Tri:FS	-0.039	-0.005	0.026	1.299	0.194
GM:FS	-0.039	-0.038	-0.008	-2.951	0.003
TF:FS	-0.039	-0.037	-0.006	-2.789	0.005
RF:FS	-0.039	-0.022	0.008	-0.904	0.366
VM:FS	-0.039	-0.022	0.009	-0.840	0.401
BF:FS	-0.039	-0.022	0.009	-0.860	0.390
TA:FS	-0.039	-0.033	-0.002	-2.234	0.026
PL:FS	-0.039	-0.031	-0.001	-2.047	0.041

Random effects	**Estimate**	**Lower 95% CI**	**Upper 95% CI**
(Intercept)	0.009	0.006	0.013
Error	0.029	0.028	0.030

Table A.18: Detailed statistics: sit-to-stand, non-challenging condition, vertical rise strategy, synergy 2

Reference group: UA

Model information	**Values**
Number of observations	1344
Number of participants	18
ICC	0.827

Fixed effects	**Estimate**	**Lower 95% CI**	**Upper 95% CI**	**t**	**p**
(Intercept)	0.020	0.012	0.028	4.845	<0.001
LT	0.016	0.011	0.022	4.845	<0.001
FS	0.025	0.020	0.031	4.845	<0.001
Random effects	**Estimate**	**Lower 95% CI**	**Upper 95% CI**		
(Intercept)	0.015	0.010	0.021		
Error	0.036	0.034	0.037		

Reference group: LT

Fixed effects	**Estimate**	**Lower 95% CI**	**Upper 95% CI**	**t**	**p**
(Intercept)	0.036	0.028	0.044	8.988	<0.001
UA	0.036	-0.022	-0.011	-5.655	<0.001
FS	0.036	0.004	0.014	3.644	0.003
Random effects	**Estimate**	**Lower 95% CI**	**Upper 95% CI**		
(Intercept)	0.015	0.010	0.021		
Error	0.036	0.034	0.037		

Post-hoc UA vs. LT

Fixed effects	**Estimate**	**Lower 95% CI**	**Upper 95% CI**	**t**	**p**
RA:LT	-0.008	-0.026	0.009	-0.924	1.000
ES:LT	-0.008	-0.010	0.025	0.803	1.000
Pec:LT	-0.008	-0.038	-0.003	-2.347	0.057
Lat:LT	-0.008	-0.018	0.017	-0.068	1.000
Tra:LT	-0.008	0.006	0.041	2.583	0.030
Del:LT	-0.008	-0.013	0.022	0.491	1.000
Bic:LT	-0.008	0.002	0.037	2.224	0.079
Tri:LT	-0.008	-0.011	0.024	0.759	1.000
GM:LT	-0.008	-0.030	0.005	-1.386	0.498
TF:LT	-0.008	-0.019	0.016	-0.220	1.000
RF:LT	-0.008	-0.007	0.028	1.153	0.747
VM:LT	-0.008	-0.012	0.023	0.569	1.000
BF:LT	-0.008	-0.025	0.010	-0.820	1.000
TA:LT	-0.008	-0.016	0.019	0.193	1.000
PL:LT	-0.008	-0.030	0.005	-1.365	0.517
Random effects	**Estimate**	**Lower 95% CI**	**Upper 95% CI**		
(Intercept)	0.015	0.010	0.021		
Error	0.031	0.030	0.032		

Post-hoc UA vs. FS

Fixed effects	Estimate	Lower 95% CI	Upper 95% CI	t	p
RA:FS	-0.017	-0.033	-0.001	-2.038	0.125
ES:FS	-0.017	-0.020	0.012	-0.496	1.000
Pec:FS	-0.017	-0.029	0.004	-1.493	0.407
Lat:FS	-0.017	0.012	0.044	3.356	0.002
Tra:FS	-0.017	-0.015	0.017	0.100	1.000
Del:FS	-0.017	-0.040	-0.008	-2.881	0.012
Bic:FS	-0.017	0.011	0.043	3.289	0.003
Tri:FS	-0.017	-0.009	0.023	0.853	1.000
GM:FS	-0.017	-0.032	0.001	-1.886	0.179
TF:FS	-0.017	-0.009	0.024	0.915	1.000
RF:FS	-0.017	0.010	0.042	3.115	0.006
VM:FS	-0.017	0.017	0.049	3.984	<0.001
BF:FS	-0.017	-0.026	0.006	-1.217	0.672
TA:FS	-0.017	-0.018	0.015	-0.163	1.000
PL:FS	-0.017	-0.037	-0.005	-2.565	0.031
Random effects	**Estimate**	**Lower 95% CI**	**Upper 95% CI**		
(Intercept)	0.015	0.010	0.021		
Error	0.031	0.030	0.032		

Table A.19: Detailed statistics: sit-to-stand, non-challenging condition, vertical rise strategy, synergy 4

Reference group: UA

Model information	**Values**
Number of observations	1344
Number of participants	18
ICC	0.353

Fixed effects	**Estimate**	**Lower 95% CI**	**Upper 95% CI**	**t**	**p**
(Intercept)	0.037	0.031	0.043	11.650	<0.001
LT	0.013	0.006	0.020	11.650	0.001
FS	0.004	-0.003	0.010	11.650	1.000
Random effects	**Estimate**	**Lower 95% CI**	**Upper 95% CI**		
(Intercept)	0.008	0.005	0.012		
Error	0.043	0.041	0.044		

Reference group: LT

Fixed effects	**Estimate**	**Lower 95% CI**	**Upper 95% CI**	**t**	**p**
(Intercept)	0.050	0.044	0.056	16.823	<0.001
UA	0.050	-0.020	-0.006	-3.884	0.001
FS	0.050	-0.015	-0.004	-3.280	0.013
Random effects	**Estimate**	**Lower 95% CI**	**Upper 95% CI**		
(Intercept)	0.008	0.005	0.012		
Error	0.043	0.041	0.044		

Post-hoc UA vs. LT

Fixed effects	**Estimate**	**Lower 95% CI**	**Upper 95% CI**	**t**	**p**
RA:LT	-0.007	-0.025	0.011	-0.757	0.899
ES:LT	-0.007	-0.042	-0.006	-2.660	0.016
Pec:LT	-0.007	-0.024	0.012	-0.655	1.000
Lat:LT	-0.007	-0.019	0.017	-0.118	1.000
Tra:LT	-0.007	-0.024	0.012	-0.683	0.989
Del:LT	-0.007	-0.002	0.034	1.792	0.147
Bic:LT	-0.007	-0.015	0.021	0.319	1.000
Tri:LT	-0.007	-0.019	0.017	-0.150	1.000
GM:LT	-0.007	-0.018	0.018	0.019	1.000
TF:LT	-0.007	-0.005	0.031	1.458	0.290
RF:LT	-0.007	-0.001	0.035	1.886	0.119
VM:LT	-0.007	-0.008	0.028	1.053	0.586
BF:LT	-0.007	-0.014	0.022	0.401	1.000
TA:LT	-0.007	-0.014	0.022	0.472	1.000
PL:LT	-0.007	-0.028	0.008	-1.119	0.526
Random effects	**Estimate**	**Lower 95% CI**	**Upper 95% CI**		
(Intercept)	0.008	0.005	0.012		
Error	0.032	0.031	0.033		

Table A.20: Detailed statistics: sit-to-stand, non-challenging condition, vertical rise strategy, synergy 5

Reference group: UA

Model information	**Values**
Number of observations	1344
Number of participants	18
ICC	0.351

Fixed effects	**Estimate**	**Lower 95% CI**	**Upper 95% CI**	**t**	**p**
(Intercept)	0.058	0.051	0.065	15.893	<0.001
LT	-0.007	-0.014	0.001	15.893	1.000
FS	-0.013	-0.020	-0.005	15.893	0.007
Random effects	**Estimate**	**Lower 95% CI**	**Upper 95% CI**		
(Intercept)	0.009	0.005	0.014		
Error	0.049	0.047	0.051		

Reference group: LT

Fixed effects	**Estimate**	**Lower 95% CI**	**Upper 95% CI**	**t**	**p**
(Intercept)	0.051	0.045	0.058	15.032	<0.001
UA	0.051	-0.001	0.014	1.715	1.000
FS	0.051	-0.012	0.000	-1.820	0.827
Random effects	**Estimate**	**Lower 95% CI**	**Upper 95% CI**		
(Intercept)	0.009	0.005	0.014		
Error	0.049	0.047	0.051		

Post-hoc UA vs. FS

Fixed effects	**Estimate**	**Lower 95% CI**	**Upper 95% CI**	**t**	**p**
RA:FS	-0.003	-0.020	0.014	-0.370	0.711
ES:FS	-0.003	-0.043	-0.009	-3.065	0.002
Pec:FS	-0.003	0.020	0.053	4.259	<0.001
Lat:FS	-0.003	0.064	0.097	9.414	<0.001
Tra:FS	-0.003	-0.003	0.031	1.631	0.103
Del:FS	-0.003	0.033	0.067	5.824	<0.001
Bic:FS	-0.003	0.000	0.034	2.003	0.045
Tri:FS	-0.003	0.029	0.063	5.401	<0.001
GM:FS	-0.003	-0.027	0.006	-1.211	0.226
TF:FS	-0.003	-0.062	-0.028	-5.240	<0.001
RF:FS	-0.003	-0.080	-0.047	-7.427	<0.001
VM:FS	-0.003	-0.071	-0.037	-6.311	<0.001
BF:FS	-0.003	-0.013	0.020	0.392	0.695
TA:FS	-0.003	-0.051	-0.018	-4.014	<0.001
PL:FS	-0.003	-0.032	0.002	-1.757	0.079
Random effects	**Estimate**	**Lower 95% CI**	**Upper 95% CI**		
(Intercept)	0.010	0.007	0.015		
Error	0.032	0.031	0.033		

Table A.21: Detailed statistics: sit-to-stand, non-challenging condition, vertical rise strategy, synergy 7

Reference group: UA

Model information	**Values**
Number of observations	1344
Number of participants	18
ICC	0.197

Fixed effects	**Estimate**	**Lower 95% CI**	**Upper 95% CI**	**t**	**p**
(Intercept)	0.036	0.030	0.041	12.193	<0.001
LT	0.007	0.000	0.014	12.193	0.564
FS	0.013	0.007	0.020	12.193	0.001

Random effects	**Estimate**	**Lower 95% CI**	**Upper 95% CI**
(Intercept)	0.005	0.002	0.010
Error	0.046	0.044	0.048

Reference group: LT

Fixed effects	**Estimate**	**Lower 95% CI**	**Upper 95% CI**	**t**	**p**
(Intercept)	0.043	0.037	0.048	16.051	<0.001
UA	0.043	-0.014	-0.000	-1.988	0.564
FS	0.043	0.000	0.012	2.037	0.502

Random effects	**Estimate**	**Lower 95% CI**	**Upper 95% CI**
(Intercept)	0.005	0.002	0.010
Error	0.046	0.044	0.048

Post-hoc UA vs. FS

Fixed effects	**Estimate**	**Lower 95% CI**	**Upper 95% CI**	**t**	**p**
RA:FS	-0.015	-0.035	0.005	-1.477	0.140
ES:FS	-0.015	-0.058	-0.018	-3.716	<0.001
Pec:FS	-0.015	-0.012	0.028	0.818	0.414
Lat:FS	-0.015	0.001	0.041	2.081	0.038
Tra:FS	-0.015	-0.031	0.008	-1.131	0.258
Del:FS	-0.015	0.015	0.055	3.441	0.001
Bic:FS	-0.015	-0.025	0.015	-0.527	0.598
Tri:FS	-0.015	0.061	0.100	7.946	<0.001
GM:FS	-0.015	-0.013	0.027	0.721	0.471
TF:FS	-0.015	-0.023	0.017	-0.332	0.740
RF:FS	-0.015	-0.015	0.025	0.495	0.620
VM:FS	-0.015	-0.021	0.019	-0.090	0.928
BF:FS	-0.015	-0.039	0.001	-1.848	0.065
TA:FS	-0.015	-0.040	-0.001	-2.015	0.044
PL:FS	-0.015	-0.046	-0.006	-2.579	0.010

Random effects	**Estimate**	**Lower 95% CI**	**Upper 95% CI**
(Intercept)	0.005	0.003	0.010
Error	0.038	0.036	0.039

Table A.22: Detailed statistics: sit-to-stand, non-challenging condition, vertical rise strategy, synergy 8

Reference group: UA					
Model information	**Values**				
Number of observations	1344				
Number of participants	18				
ICC	0.338				
Fixed effects	**Estimate**	**Lower 95% CI**	**Upper 95% CI**	**t**	**p**
(Intercept)	0.049	0.042	0.056	13.873	<0.001
LT	-0.003	-0.010	0.004	13.873	1.000
FS	-0.005	-0.013	0.002	13.873	1.000
Random effects	**Estimate**	**Lower 95% CI**	**Upper 95% CI**		
(Intercept)	0.008	0.005	0.014		
Error	0.048	0.047	0.050		
Reference group: LT					
Fixed effects	**Estimate**	**Lower 95% CI**	**Upper 95% CI**	**t**	**p**
(Intercept)	0.046	0.040	0.053	13.941	<0.001
UA	0.046	-0.004	0.010	0.787	1.000
FS	0.046	-0.009	0.004	-0.766	1.000
Random effects	**Estimate**	**Lower 95% CI**	**Upper 95% CI**		
(Intercept)	0.008	0.005	0.014		
Error	0.048	0.047	0.050		

Table A.23: Detailed statistics: sit-to-stand, challenging condition, exaggerated forward leaning strategy, synergy 2

Reference group: UA

Model information	**Values**
Number of observations	1152
Number of participants	19
ICC	0.458

Fixed effects	**Estimate**	**Lower 95% CI**	**Upper 95% CI**	**t**	**p**
(Intercept)	0.029	0.024	0.034	11.991	<0.001
LT	0.011	0.005	0.016	11.991	0.002
FS	0.015	0.007	0.023	11.991	0.003

Random effects	**Estimate**	**Lower 95% CI**	**Upper 95% CI**
(Intercept)	0.008	0.006	0.013
Error	0.037	0.035	0.038

Reference group: LT

Fixed effects	**Estimate**	**Lower 95% CI**	**Upper 95% CI**	**t**	**p**
(Intercept)	0.040	0.034	0.046	13.020	<0.001
UA	0.040	-0.016	-0.005	-3.853	0.002
FS	0.040	-0.003	0.012	1.091	1.000

Random effects	**Estimate**	**Lower 95% CI**	**Upper 95% CI**
(Intercept)	0.008	0.006	0.013
Error	0.037	0.035	0.038

Post-hoc UA vs. LT

Fixed effects	**Estimate**	**Lower 95% CI**	**Upper 95% CI**	**t**	**p**
RA:LT	-0.009	-0.023	0.004	-1.387	0.331
ES:LT	-0.009	-0.003	0.023	1.467	0.285
Pec:LT	-0.009	-0.036	-0.009	-3.251	0.002
Lat:LT	-0.009	-0.018	0.009	-0.608	1.000
Tra:LT	-0.009	0.033	0.060	6.854	<0.001
Del:LT	-0.009	-0.012	0.015	0.165	1.000
Bic:LT	-0.009	-0.001	0.026	1.798	0.145
Tri:LT	-0.009	-0.005	0.022	1.254	0.420
GM:LT	-0.009	-0.028	-0.002	-2.186	0.058
TF:LT	-0.009	-0.025	0.001	-1.753	0.160
RF:LT	-0.009	-0.018	0.009	-0.697	0.972
VM:LT	-0.009	-0.023	0.003	-1.467	0.285
BF:LT	-0.009	-0.022	0.005	-1.209	0.454
TA:LT	-0.009	-0.001	0.026	1.814	0.140
PL:LT	-0.009	-0.013	0.014	0.103	1.000

Random effects	**Estimate**	**Lower 95% CI**	**Upper 95% CI**
(Intercept)	0.009	0.006	0.013
Error	0.026	0.025	0.027

Post-hoc UA vs. FS

Fixed effects	Estimate	Lower 95% CI	Upper 95% CI	t	p
RA:FS	-0.005	-0.023	0.013	-0.541	1.000
ES:FS	-0.005	-0.032	0.004	-1.506	0.265
Pec:FS	-0.005	-0.006	0.031	1.362	0.347
Lat:FS	-0.005	-0.007	0.029	1.171	0.484
Tra:FS	-0.005	0.058	0.094	8.219	<0.001
Del:FS	-0.005	-0.064	-0.027	-4.937	<0.001
Bic:FS	-0.005	0.048	0.085	7.207	<0.001
Tri:FS	-0.005	-0.008	0.028	1.052	0.586
GM:FS	-0.005	-0.039	-0.003	-2.242	0.050
TF:FS	-0.005	-0.034	0.002	-1.768	0.155
RF:FS	-0.005	-0.024	0.012	-0.687	0.985
VM:FS	-0.005	-0.027	0.010	-0.918	0.717
BF:FS	-0.005	-0.026	0.010	-0.880	0.758
TA:FS	-0.005	-0.044	-0.008	-2.783	0.011
PL:FS	-0.005	-0.034	0.002	-1.717	0.172

Random effects	Estimate	Lower 95% CI	Upper 95% CI
(Intercept)	0.009	0.006	0.013
Error	0.026	0.025	0.027

Table A.24: Detailed statistics: sit-to-stand, challenging condition, exaggerated forward leaning strategy, synergy 3

Reference group: UA

Model information	Values
Number of observations	1152
Number of participants	19
ICC	0.437

Fixed effects	Estimate	Lower 95% CI	Upper 95% CI	t	p
(Intercept)	0.032	0.027	0.036	14.212	<0.001
LT	0.007	0.002	0.012	14.212	0.204
FS	-0.002	-0.009	0.005	14.212	1.000

Random effects	Estimate	Lower 95% CI	Upper 95% CI
(Intercept)	0.008	0.005	0.012
Error	0.035	0.033	0.036

Reference group: LT

Fixed effects	Estimate	Lower 95% CI	Upper 95% CI	t	p
(Intercept)	0.038	0.033	0.044	13.535	<0.001
UA	0.038	-0.012	-0.002	-2.573	0.204
FS	0.038	-0.016	-0.001	-2.331	0.398

Random effects	Estimate	Lower 95% CI	Upper 95% CI
(Intercept)	0.008	0.005	0.012
Error	0.035	0.033	0.036

Table A.25: Detailed statistics: sit-to-stand, challenging condition, exaggerated forward leaning strategy, synergy 4

Reference group: UA

Model information	Values
Number of observations	1152
Number of participants	19
ICC	0.482

Fixed effects	Estimate	Lower 95% CI	Upper 95% CI	t	p
(Intercept)	0.034	0.029	0.038	15.385	<0.001
LT	0.002	-0.003	0.007	15.385	1.000
FS	-0.003	-0.010	0.004	15.385	1.000
Random effects	**Estimate**	**Lower 95% CI**	**Upper 95% CI**		
(Intercept)	0.008	0.005	0.012		
Error	0.032	0.031	0.034		

Reference group: LT

Fixed effects	Estimate	Lower 95% CI	Upper 95% CI	t	p
(Intercept)	0.036	0.031	0.041	13.089	<0.001
UA	0.036	-0.007	0.003	-0.901	1.000
FS	0.036	-0.012	0.002	-1.396	1.000
Random effects	**Estimate**	**Lower 95% CI**	**Upper 95% CI**		
(Intercept)	0.008	0.005	0.012		
Error	0.032	0.031	0.034		

Table A.26: Detailed statistics: sit-to-stand, challenging condition, exaggerated forward leaning strategy, synergy 5

Reference group: UA

Model information	**Values**
Number of observations	1152
Number of participants	19
ICC	0.607

Fixed effects	**Estimate**	**Lower 95% CI**	**Upper 95% CI**	**t**	**p**
(Intercept)	0.038	0.033	0.042	15.178	<0.001
LT	-0.009	-0.014	-0.005	15.178	0.002
FS	-0.012	-0.019	-0.006	15.178	0.006
Random effects	**Estimate**	**Lower 95% CI**	**Upper 95% CI**		
(Intercept)	0.009	0.006	0.014		
Error	0.031	0.030	0.032		

Reference group: LT

Fixed effects	**Estimate**	**Lower 95% CI**	**Upper 95% CI**	**t**	**p**
(Intercept)	0.028	0.022	0.034	9.526	<0.001
UA	0.028	0.005	0.014	3.879	0.002
FS	0.028	-0.010	0.004	-0.867	1.000
Random effects	**Estimate**	**Lower 95% CI**	**Upper 95% CI**		
(Intercept)	0.009	0.006	0.014		
Error	0.031	0.030	0.032		

Post-hoc UA vs. LT

Fixed effects	**Estimate**	**Lower 95% CI**	**Upper 95% CI**	**t**	**p**
RA:LT	-0.003	-0.015	0.010	-0.408	1.000
ES:LT	-0.003	-0.030	-0.005	-2.657	0.016
Pec:LT	-0.003	-0.009	0.017	0.617	1.000
Lat:LT	-0.003	-0.007	0.019	0.877	0.761
Tra:LT	-0.003	-0.014	0.012	-0.203	1.000
Del:LT	-0.003	0.021	0.047	5.198	<0.001
Bic:LT	-0.003	0.006	0.032	2.890	0.008
Tri:LT	-0.003	0.015	0.041	4.242	<0.001
GM:LT	-0.003	-0.023	0.003	-1.572	0.232
TF:LT	-0.003	-0.039	-0.013	-3.988	<0.001
RF:LT	-0.003	-0.027	-0.002	-2.205	0.055
VM:LT	-0.003	-0.019	0.006	-0.994	0.641
BF:LT	-0.003	-0.021	0.005	-1.217	0.448
TA:LT	-0.003	-0.015	0.011	-0.329	1.000
PL:LT	-0.003	-0.017	0.009	-0.605	1.000
Random effects	**Estimate**	**Lower 95% CI**	**Upper 95% CI**		
(Intercept)	0.010	0.007	0.015		
Error	0.025	0.024	0.026		

Post-hoc UA vs. FS

Fixed effects	Estimate	Lower 95% CI	Upper 95% CI	t	p
RA:FS	0.009	-0.008	0.026	1.017	0.619
ES:FS	0.009	-0.039	-0.004	-2.446	0.029
Pec:FS	0.009	-0.000	0.035	1.945	0.104
Lat:FS	0.009	0.002	0.036	2.136	0.066
Tra:FS	0.009	-0.014	0.021	0.385	1.000
Del:FS	0.009	-0.001	0.034	1.884	0.120
Bic:FS	0.009	-0.000	0.035	1.935	0.107
Tri:FS	0.009	0.015	0.050	3.687	<0.001
GM:FS	0.009	-0.022	0.012	-0.561	1.000
TF:FS	0.009	-0.052	-0.017	-3.870	<0.001
RF:FS	0.009	-0.035	0.000	-1.945	0.104
VM:FS	0.009	-0.028	0.007	-1.191	0.467
BF:FS	0.009	-0.021	0.014	-0.356	1.000
TA:FS	0.009	-0.035	-0.001	-2.031	0.085
PL:FS	0.009	-0.027	0.007	-1.143	0.507
Random effects	**Estimate**	**Lower 95% CI**	**Upper 95% CI**		
(Intercept)	0.010	0.007	0.015		
Error	0.025	0.024	0.026		

Table A.27: Detailed statistics: sit-to-stand, challenging condition, exaggerated forward leaning strategy, synergy 6

Reference group: UA

Model information	**Values**
Number of observations	1152
Number of participants	19
ICC	0.449

Fixed effects	**Estimate**	**Lower 95% CI**	**Upper 95% CI**	**t**	**p**
(Intercept)	0.031	0.028	0.035	17.801	<0.001
LT	-0.009	-0.013	-0.005	17.801	<0.001
FS	-0.005	-0.010	0.001	17.801	1.000
Random effects	**Estimate**	**Lower 95% CI**	**Upper 95% CI**		
(Intercept)	0.006	0.004	0.010		
Error	0.027	0.026	0.028		

Reference group: LT

Fixed effects	**Estimate**	**Lower 95% CI**	**Upper 95% CI**	**t**	**p**
(Intercept)	0.022	0.017	0.026	9.841	<0.001
UA	0.022	0.005	0.013	4.493	<0.001
FS	0.022	-0.001	0.010	1.624	1.000
Random effects	**Estimate**	**Lower 95% CI**	**Upper 95% CI**		
(Intercept)	0.006	0.004	0.010		
Error	0.027	0.026	0.028		

Post-hoc UA vs. LT

Fixed effects	**Estimate**	**Lower 95% CI**	**Upper 95% CI**	**t**	**p**
RA:LT	0.001	-0.011	0.014	0.208	0.835
ES:LT	0.001	-0.018	0.007	-0.833	0.405
Pec:LT	0.001	-0.014	0.011	-0.184	0.854
Lat:LT	0.001	-0.001	0.024	1.773	0.077
Tra:LT	0.001	-0.007	0.018	0.805	0.421
Del:LT	0.001	0.006	0.030	2.837	0.005
Bic:LT	0.001	-0.004	0.021	1.380	0.168
Tri:LT	0.001	0.013	0.038	4.045	<0.001
GM:LT	0.001	-0.025	0.000	-1.938	0.053
TF:LT	0.001	-0.023	0.002	-1.633	0.103
RF:LT	0.001	-0.017	0.007	-0.790	0.430
VM:LT	0.001	-0.005	0.020	1.159	0.247
BF:LT	0.001	-0.012	0.013	0.044	0.965
TA:LT	0.001	-0.035	-0.010	-3.509	<0.001
PL:LT	0.001	-0.030	-0.005	-2.807	0.005
Random effects	**Estimate**	**Lower 95% CI**	**Upper 95% CI**		
(Intercept)	0.006	0.004	0.010		
Error	0.024	0.023	0.025		

Table A.28: Detailed statistics: sit-to-stand, challenging condition, exaggerated forward leaning strategy, synergy 7

Reference group: UA

Model information	**Values**
Number of observations	1152
Number of participants	19
ICC	0.473

Fixed effects	**Estimate**	**Lower 95% CI**	**Upper 95% CI**	**t**	**p**
(Intercept)	0.035	0.031	0.039	16.607	<0.001
LT	-0.016	-0.021	-0.012	16.607	<0.001
FS	-0.016	-0.023	-0.010	16.607	<0.001

Random effects	**Estimate**	**Lower 95% CI**	**Upper 95% CI**
(Intercept)	0.007	0.005	0.012
Error	0.031	0.030	0.033

Reference group: LT

Fixed effects	**Estimate**	**Lower 95% CI**	**Upper 95% CI**	**t**	**p**
(Intercept)	0.019	0.014	0.024	7.047	<0.001
UA	0.019	0.012	0.021	6.769	<0.001
FS	0.019	-0.007	0.007	-0.021	1.000

Random effects	**Estimate**	**Lower 95% CI**	**Upper 95% CI**
(Intercept)	0.007	0.005	0.012
Error	0.031	0.030	0.033

Post-hoc UA vs. LT

Fixed effects	**Estimate**	**Lower 95% CI**	**Upper 95% CI**	**t**	**p**
RA:LT	0.003	-0.011	0.017	0.457	1.000
ES:LT	0.003	-0.027	0.001	-1.768	0.155
Pec:LT	0.003	-0.007	0.022	1.029	0.607
Lat:LT	0.003	-0.002	0.026	1.657	0.196
Tra:LT	0.003	-0.003	0.025	1.545	0.245
Del:LT	0.003	0.009	0.037	3.234	0.003
Bic:LT	0.003	0.002	0.031	2.283	0.045
Tri:LT	0.003	0.029	0.057	5.992	<0.001
GM:LT	0.003	-0.013	0.015	0.130	1.000
TF:LT	0.003	-0.030	-0.002	-2.236	0.051
RF:LT	0.003	-0.024	0.005	-1.335	0.365
VM:LT	0.003	-0.016	0.012	-0.238	1.000
BF:LT	0.003	-0.019	0.009	-0.686	0.986
TA:LT	0.003	-0.038	-0.010	-3.365	0.002
PL:LT	0.003	-0.042	-0.014	-3.849	<0.001

Random effects	**Estimate**	**Lower 95% CI**	**Upper 95% CI**
(Intercept)	0.008	0.005	0.012
Error	0.027	0.026	0.029

Post-hoc UA vs. FS

Fixed effects	**Estimate**	**Lower 95% CI**	**Upper 95% CI**	**t**	**p**
RA:FS	0.002	-0.017	0.022	0.252	1.000
ES:FS	0.002	-0.045	-0.007	-2.647	0.016
Pec:FS	0.002	0.002	0.040	2.163	0.061
Lat:FS	0.002	-0.001	0.037	1.864	0.125
Tra:FS	0.002	-0.010	0.028	0.895	0.742
Del:FS	0.002	0.009	0.047	2.839	0.009
Bic:FS	0.002	-0.002	0.036	1.748	0.162
Tri:FS	0.002	0.041	0.080	6.210	<0.001
GM:FS	0.002	-0.026	0.012	-0.720	0.943
TF:FS	0.002	-0.038	-0.000	-1.981	0.096
RF:FS	0.002	-0.032	0.006	-1.371	0.342
VM:FS	0.002	-0.023	0.015	-0.378	1.000
BF:FS	0.002	-0.024	0.014	-0.490	1.000
TA:FS	0.002	-0.042	-0.004	-2.393	0.034
PL:FS	0.002	-0.051	-0.013	-3.248	0.002
Random effects	**Estimate**	**Lower 95% CI**	**Upper 95% CI**		
(Intercept)	0.008	0.005	0.012		
Error	0.027	0.026	0.029		

Table A.29: Detailed statistics: sit-to-stand, challenging condition, exaggerated forward leaning strategy, synergy 8

Reference group: UA

Model information	Values
Number of observations	1152
Number of participants	19
ICC	0.355

Fixed effects	Estimate	Lower 95% CI	Upper 95% CI	t	p
(Intercept)	0.032	0.029	0.035	20.775	<0.001
LT	-0.015	-0.019	-0.011	20.775	<0.001
FS	-0.016	-0.021	-0.010	20.775	<0.001
Random effects	**Estimate**	**Lower 95% CI**	**Upper 95% CI**		
(Intercept)	0.005	0.003	0.008		
Error	0.027	0.026	0.028		

Reference group: LT

Fixed effects	Estimate	Lower 95% CI	Upper 95% CI	t	p
(Intercept)	0.017	0.013	0.021	8.527	<0.001
UA	0.017	0.011	0.019	7.143	<0.001
FS	0.017	-0.007	0.005	-0.345	1.000
Random effects	**Estimate**	**Lower 95% CI**	**Upper 95% CI**		
(Intercept)	0.005	0.003	0.008		
Error	0.027	0.026	0.028		

Post-hoc UA vs. LT

Fixed effects	Estimate	Lower 95% CI	Upper 95% CI	t	p
RA:LT	0.003	-0.009	0.016	0.502	1.000
ES:LT	0.003	-0.023	0.002	-1.672	0.189
Pec:LT	0.003	-0.009	0.016	0.535	1.000
Lat:LT	0.003	-0.007	0.017	0.780	0.871
Tra:LT	0.003	-0.001	0.024	1.771	0.154
Del:LT	0.003	0.009	0.034	3.364	0.002
Bic:LT	0.003	0.001	0.025	2.076	0.076
Tri:LT	0.003	0.027	0.051	6.180	<0.001
GM:LT	0.003	-0.011	0.013	0.163	1.000
TF:LT	0.003	-0.020	0.004	-1.250	0.423
RF:LT	0.003	-0.025	0.000	-1.934	0.107
VM:LT	0.003	-0.012	0.013	0.131	1.000
BF:LT	0.003	-0.020	0.005	-1.158	0.495
TA:LT	0.003	-0.023	0.002	-1.633	0.206
PL:LT	0.003	-0.043	-0.018	-4.819	<0.001
Random effects	**Estimate**	**Lower 95% CI**	**Upper 95% CI**		
(Intercept)	0.005	0.003	0.008		
Error	0.024	0.023	0.025		

Post-hoc UA vs. FS

Fixed effects	**Estimate**	**Lower 95% CI**	**Upper 95% CI**	**t**	**p**
RA:FS	0.011	-0.006	0.028	1.316	0.377
ES:FS	0.011	-0.026	0.007	-1.089	0.553
Pec:FS	0.011	-0.007	0.027	1.169	0.486
Lat:FS	0.011	-0.009	0.024	0.906	0.730
Tra:FS	0.011	-0.001	0.032	1.787	0.148
Del:FS	0.011	-0.004	0.029	1.487	0.275
Bic:FS	0.011	0.003	0.037	2.325	0.041
Tri:FS	0.011	0.022	0.056	4.588	<0.001
GM:FS	0.011	-0.020	0.013	-0.409	1.000
TF:FS	0.011	-0.034	-0.000	-1.974	0.097
RF:FS	0.011	-0.019	0.014	-0.313	1.000
VM:FS	0.011	-0.019	0.014	-0.281	1.000
BF:FS	0.011	-0.019	0.014	-0.263	1.000
TA:FS	0.011	-0.030	0.004	-1.536	0.250
PL:FS	0.011	-0.056	-0.023	-4.663	<0.001
Random effects	**Estimate**	**Lower 95% CI**	**Upper 95% CI**		
(Intercept)	0.005	0.003	0.008		
Error	0.024	0.023	0.025		

Table A.30: Detailed statistics: sit-to-stand, challenging condition, exaggerated forward leaning strategy, synergy 9

Reference group: UA

Model information	**Values**
Number of observations	1152
Number of participants	19
ICC	0.253

Fixed effects	**Estimate**	**Lower 95% CI**	**Upper 95% CI**	**t**	**p**
(Intercept)	0.039	0.036	0.042	23.596	<0.001
LT	-0.018	-0.023	-0.014	23.596	<0.001
FS	-0.014	-0.021	-0.007	23.596	0.001

Random effects	**Estimate**	**Lower 95% CI**	**Upper 95% CI**
(Intercept)	0.004	0.002	0.009
Error	0.034	0.033	0.036

Reference group: LT

Fixed effects	**Estimate**	**Lower 95% CI**	**Upper 95% CI**	**t**	**p**
(Intercept)	0.021	0.016	0.025	8.973	<0.001
UA	0.021	0.014	0.023	7.429	<0.001
FS	0.021	-0.003	0.012	1.232	1.000

Random effects	**Estimate**	**Lower 95% CI**	**Upper 95% CI**
(Intercept)	0.004	0.002	0.009
Error	0.034	0.033	0.036

Post-hoc UA vs. LT

Fixed effects	**Estimate**	**Lower 95% CI**	**Upper 95% CI**	**t**	**p**
RA:LT	0.009	-0.006	0.024	1.161	0.492
ES:LT	0.009	-0.018	0.012	-0.440	1.000
Pec:LT	0.009	-0.006	0.024	1.189	0.469
Lat:LT	0.009	-0.006	0.024	1.211	0.453
Tra:LT	0.009	0.001	0.031	2.121	0.068
Del:LT	0.009	-0.002	0.028	1.746	0.162
Bic:LT	0.009	-0.003	0.027	1.628	0.208
Tri:LT	0.009	0.032	0.062	6.201	<0.001
GM:LT	0.009	-0.019	0.010	-0.600	1.000
TF:LT	0.009	-0.021	0.008	-0.853	0.788
RF:LT	0.009	-0.016	0.013	-0.205	1.000
VM:LT	0.009	-0.005	0.025	1.337	0.363
BF:LT	0.009	-0.031	-0.001	-2.060	0.079
TA:LT	0.009	-0.032	-0.003	-2.299	0.043
PL:LT	0.009	-0.059	-0.029	-5.784	<0.001

Random effects	**Estimate**	**Lower 95% CI**	**Upper 95% CI**
(Intercept)	0.005	0.003	0.009
Error	0.029	0.028	0.030

Post-hoc UA vs. FS

Fixed effects	**Estimate**	**Lower 95% CI**	**Upper 95% CI**	**t**	**p**
RA:FS	0.014	-0.007	0.034	1.327	0.370
ES:FS	0.014	-0.032	0.009	-1.101	0.542
Pec:FS	0.014	0.022	0.062	4.050	<0.001
Lat:FS	0.014	-0.006	0.034	1.363	0.346
Tra:FS	0.014	-0.002	0.039	1.811	0.141
Del:FS	0.014	-0.005	0.035	1.448	0.296
Bic:FS	0.014	0.006	0.047	2.589	0.020
Tri:FS	0.014	0.030	0.070	4.861	<0.001
GM:FS	0.014	-0.026	0.014	-0.574	1.000
TF:FS	0.014	-0.031	0.010	-1.018	0.617
RF:FS	0.014	-0.028	0.012	-0.756	0.899
VM:FS	0.014	-0.020	0.020	0.021	1.000
BF:FS	0.014	-0.058	-0.018	-3.711	<0.001
TA:FS	0.014	-0.042	-0.002	-2.135	0.066
PL:FS	0.014	-0.068	-0.027	-4.625	<0.001
Random effects	**Estimate**	**Lower 95% CI**	**Upper 95% CI**		
(Intercept)	0.005	0.003	0.009		
Error	0.029	0.028	0.030		

Table A.31: Detailed statistics: sit-to-stand, challenging condition, exaggerated forward leaning strategy, synergy 10

Reference group: UA

Model information	**Values**
Number of observations	1152
Number of participants	19
ICC	0.210

Fixed effects	**Estimate**	**Lower 95% CI**	**Upper 95% CI**	**t**	**p**
(Intercept)	0.032	0.030	0.035	24.172	<0.001
LT	-0.014	-0.018	-0.009	24.172	<0.001
FS	-0.011	-0.017	-0.006	24.172	0.002

Random effects	**Estimate**	**Lower 95% CI**	**Upper 95% CI**
(Intercept)	0.003	0.001	0.008
Error	0.029	0.028	0.031

Reference group: LT

Fixed effects	**Estimate**	**Lower 95% CI**	**Upper 95% CI**	**t**	**p**
(Intercept)	0.019	0.015	0.022	9.915	<0.001
UA	0.019	0.009	0.018	6.465	<0.001
FS	0.019	-0.004	0.008	0.685	1.000

Random effects	**Estimate**	**Lower 95% CI**	**Upper 95% CI**
(Intercept)	0.003	0.001	0.008
Error	0.029	0.028	0.031

Post-hoc UA vs. LT

Fixed effects	**Estimate**	**Lower 95% CI**	**Upper 95% CI**	**t**	**p**
RA:LT	0.006	-0.007	0.019	0.929	0.706
ES:LT	0.006	-0.009	0.016	0.553	1.000
Pec:LT	0.006	-0.005	0.020	1.130	0.517
Lat:LT	0.006	-0.010	0.015	0.411	1.000
Tra:LT	0.006	0.001	0.026	2.165	0.061
Del:LT	0.006	0.001	0.026	2.084	0.075
Bic:LT	0.006	-0.003	0.022	1.515	0.260
Tri:LT	0.006	0.017	0.042	4.537	<0.001
GM:LT	0.006	-0.019	0.007	-0.936	0.699
TF:LT	0.006	-0.014	0.011	-0.184	1.000
RF:LT	0.006	-0.012	0.013	0.067	1.000
VM:LT	0.006	-0.002	0.023	1.689	0.183
BF:LT	0.006	-0.031	-0.005	-2.806	0.010
TA:LT	0.006	-0.031	-0.006	-2.919	0.007
PL:LT	0.006	-0.037	-0.012	-3.817	<0.001

Random effects	**Estimate**	**Lower 95% CI**	**Upper 95% CI**
(Intercept)	0.004	0.002	0.007
Error	0.024	0.024	0.026

Post-hoc UA vs. FS

Fixed effects	Estimate	Lower 95% CI	Upper 95% CI	t	p
RA:FS	0.015	-0.002	0.032	1.723	0.170
ES:FS	0.015	-0.000	0.034	1.916	0.111
Pec:FS	0.015	0.017	0.051	3.959	<0.001
Lat:FS	0.015	-0.005	0.029	1.359	0.349
Tra:FS	0.015	-0.002	0.032	1.738	0.165
Del:FS	0.015	0.001	0.035	2.032	0.085
Bic:FS	0.015	0.013	0.048	3.514	0.001
Tri:FS	0.015	0.015	0.049	3.708	<0.001
GM:FS	0.015	-0.024	0.010	-0.783	0.867
TF:FS	0.015	-0.028	0.007	-1.203	0.458
RF:FS	0.015	-0.028	0.006	-1.304	0.385
VM:FS	0.015	-0.027	0.007	-1.161	0.492
BF:FS	0.015	-0.052	-0.018	-4.024	<0.001
TA:FS	0.015	-0.038	-0.003	-2.364	0.037
PL:FS	0.015	-0.052	-0.018	-4.063	<0.001
Random effects	**Estimate**	**Lower 95% CI**	**Upper 95% CI**		
(Intercept)	0.004	0.002	0.007		
Error	0.024	0.024	0.026		

Table A.32: Detailed statistics: sit-to-stand, challenging condition, exaggerated forward leaning strategy, synergy 11

Reference group: UA

Model information	Values
Number of observations	1152
Number of participants	19
ICC	0.211

Fixed effects	Estimate	Lower 95% CI	Upper 95% CI	t	p
(Intercept)	0.038	0.035	0.041	24.836	<0.001
LT	-0.015	-0.019	-0.010	24.836	<0.001
FS	-0.015	-0.022	-0.009	24.836	<0.001

Random effects	Estimate	Lower 95% CI	Upper 95% CI
(Intercept)	0.003	0.001	0.008
Error	0.033	0.032	0.035

Reference group: LT

Fixed effects	Estimate	Lower 95% CI	Upper 95% CI	t	p
(Intercept)	0.023	0.019	0.027	10.644	<0.001
UA	0.023	0.010	0.019	6.246	<0.001
FS	0.023	-0.007	0.006	-0.137	1.000

Random effects	Estimate	Lower 95% CI	Upper 95% CI
(Intercept)	0.003	0.001	0.008
Error	0.033	0.032	0.035

Post-hoc UA vs. LT

Fixed effects	Estimate	Lower 95% CI	Upper 95% CI	t	p
RA:LT	0.015	0.001	0.028	2.153	0.063
ES:LT	0.015	-0.018	0.009	-0.652	1.000
Pec:LT	0.015	-0.003	0.024	1.533	0.251
Lat:LT	0.015	-0.005	0.022	1.288	0.396
Tra:LT	0.015	-0.001	0.027	1.885	0.119
Del:LT	0.015	-0.005	0.022	1.274	0.406
Bic:LT	0.015	-0.004	0.023	1.346	0.357
Tri:LT	0.015	0.014	0.041	3.940	<0.001
GM:LT	0.015	-0.022	0.005	-1.296	0.390
TF:LT	0.015	-0.012	0.015	0.208	1.000
RF:LT	0.015	-0.016	0.011	-0.376	1.000
VM:LT	0.015	-0.003	0.024	1.518	0.259
BF:LT	0.015	-0.037	-0.010	-3.365	0.002
TA:LT	0.015	-0.037	-0.010	-3.405	0.001
PL:LT	0.015	-0.032	-0.005	-2.677	0.015

Random effects	Estimate	Lower 95% CI	Upper 95% CI
(Intercept)	0.005	0.003	0.008
Error	0.026	0.025	0.027

Post-hoc UA vs. FS

Fixed effects	Estimate	Lower 95% CI	Upper 95% CI	t	p
RA:FS	0.014	-0.005	0.032	1.469	0.284
ES:FS	0.014	-0.011	0.025	0.747	0.910
Pec:FS	0.014	0.009	0.046	2.921	0.007
Lat:FS	0.014	0.004	0.041	2.410	0.032
Tra:FS	0.014	0.000	0.037	1.996	0.092
Del:FS	0.014	-0.014	0.023	0.473	1.000
Bic:FS	0.014	0.010	0.046	2.988	0.006
Tri:FS	0.014	0.007	0.043	2.685	0.015
GM:FS	0.014	-0.018	0.018	0.002	1.000
TF:FS	0.014	-0.021	0.015	-0.337	1.000
RF:FS	0.014	-0.029	0.008	-1.100	0.544
VM:FS	0.014	-0.022	0.015	-0.378	1.000
BF:FS	0.014	-0.052	-0.016	-3.647	0.001
TA:FS	0.014	-0.043	-0.006	-2.633	0.017
PL:FS	0.014	-0.045	-0.009	-2.901	0.008
Random effects	**Estimate**	**Lower 95% CI**	**Upper 95% CI**		
(Intercept)	0.005	0.003	0.008		
Error	0.026	0.025	0.027		

Table A.33: Detailed statistics: sit-to-stand, challenging condition, forward leaning strategy, synergy 1

Reference group: UA					
Model information	**Values**				
Number of observations	1648				
Number of participants	19				
ICC	0.436				
Fixed effects	**Estimate**	**Lower 95% CI**	**Upper 95% CI**	**t**	**p**
(Intercept)	0.021	0.015	0.027	6.954	<0.001
LT	0.002	-0.004	0.008	6.954	1.000
FS	0.012	0.006	0.017	6.954	<0.001
Random effects	**Estimate**	**Lower 95% CI**	**Upper 95% CI**		
(Intercept)	0.008	0.005	0.011		
Error	0.035	0.034	0.036		
Reference group: LT					
Fixed effects	**Estimate**	**Lower 95% CI**	**Upper 95% CI**	**t**	**p**
(Intercept)	0.023	0.018	0.028	9.926	<0.001
UA	0.023	-0.008	0.004	-0.661	1.000
FS	0.023	0.006	0.014	5.137	<0.001
Random effects	**Estimate**	**Lower 95% CI**	**Upper 95% CI**		
(Intercept)	0.008	0.005	0.011		
Error	0.035	0.034	0.036		
Post-hoc UA vs. FS					
Fixed effects	**Estimate**	**Lower 95% CI**	**Upper 95% CI**	**t**	**p**
RA:FS	-0.018	-0.033	-0.003	-2.406	0.033
ES:FS	-0.018	-0.022	0.007	-0.986	0.649
Pec:FS	-0.018	0.003	0.033	2.389	0.034
Lat:FS	-0.018	-0.020	0.010	-0.669	1.000
Tra:FS	-0.018	0.053	0.082	8.864	<0.001
Del:FS	-0.018	-0.038	-0.008	-3.044	0.005
Bic:FS	-0.018	0.029	0.059	5.779	<0.001
Tri:FS	-0.018	0.004	0.034	2.456	0.028
GM:FS	-0.018	-0.049	-0.019	-4.455	<0.001
TF:FS	-0.018	-0.026	0.003	-1.519	0.258
RF:FS	-0.018	-0.022	0.008	-0.913	0.723
VM:FS	-0.018	-0.021	0.009	-0.843	0.799
BF:FS	-0.018	-0.034	-0.004	-2.516	0.024
TA:FS	-0.018	-0.010	0.020	0.651	1.000
PL:FS	-0.018	-0.020	0.010	-0.649	1.000
Random effects	**Estimate**	**Lower 95% CI**	**Upper 95% CI**		
(Intercept)	0.008	0.006	0.012		
Error	0.027	0.026	0.028		

Table A.34: Detailed statistics: sit-to-stand, challenging condition, forward leaning strategy, synergy 2

Reference group: UA

Model information	**Values**
Number of observations	1648
Number of participants	19
ICC	0.439

Fixed effects	**Estimate**	**Lower 95% CI**	**Upper 95% CI**	**t**	**p**
(Intercept)	0.023	0.016	0.029	6.983	<0.001
LT	0.008	0.002	0.014	6.983	0.233
FS	0.015	0.009	0.021	6.983	<0.001
Random effects	**Estimate**	**Lower 95% CI**	**Upper 95% CI**		
(Intercept)	0.008	0.006	0.012		
Error	0.038	0.036	0.039		

Reference group: LT

Fixed effects	**Estimate**	**Lower 95% CI**	**Upper 95% CI**	**t**	**p**
(Intercept)	0.031	0.026	0.036	12.207	<0.001
UA	0.031	-0.014	-0.002	-2.445	0.233
FS	0.031	0.003	0.012	3.634	0.005
Random effects	**Estimate**	**Lower 95% CI**	**Upper 95% CI**		
(Intercept)	0.008	0.006	0.012		
Error	0.038	0.036	0.039		

Post-hoc UA vs. FS

Fixed effects	**Estimate**	**Lower 95% CI**	**Upper 95% CI**	**t**	**p**
RA:FS	-0.018	-0.034	-0.001	-2.123	0.068
ES:FS	-0.018	-0.014	0.019	0.259	1.000
Pec:FS	-0.018	-0.027	0.006	-1.247	0.425
Lat:FS	-0.018	-0.001	0.031	1.791	0.147
Tra:FS	-0.018	-0.002	0.031	1.767	0.155
Del:FS	-0.018	-0.045	-0.013	-3.472	0.001
Bic:FS	-0.018	0.063	0.096	9.470	<0.001
Tri:FS	-0.018	0.012	0.045	3.371	0.002
GM:FS	-0.018	-0.035	-0.002	-2.253	0.049
TF:FS	-0.018	-0.019	0.014	-0.316	1.000
RF:FS	-0.018	-0.009	0.024	0.875	0.763
VM:FS	-0.018	-0.018	0.015	-0.208	1.000
BF:FS	-0.018	-0.028	0.005	-1.354	0.352
TA:FS	-0.018	-0.035	-0.002	-2.258	0.048
PL:FS	-0.018	-0.033	0.000	-1.929	0.108
Random effects	**Estimate**	**Lower 95% CI**	**Upper 95% CI**		
(Intercept)	0.009	0.006	0.012		
Error	0.029	0.028	0.030		

Table A.35: Detailed statistics: sit-to-stand, challenging condition, forward leaning strategy, synergy 3

Reference group: UA					
Model information	**Values**				
Number of observations	1648				
Number of participants	19				
ICC	0.500				
Fixed effects	**Estimate**	**Lower 95% CI**	**Upper 95% CI**	**t**	**p**
(Intercept)	0.038	0.031	0.044	10.893	<0.001
LT	0.005	-0.001	0.012	10.893	1.000
FS	0.003	-0.003	0.009	10.893	1.000
Random effects	**Estimate**	**Lower 95% CI**	**Upper 95% CI**		
(Intercept)	0.009	0.006	0.014		
Error	0.038	0.036	0.039		
Reference group: LT					
Fixed effects	**Estimate**	**Lower 95% CI**	**Upper 95% CI**	**t**	**p**
(Intercept)	0.043	0.038	0.048	15.793	<0.001
UA	0.043	-0.012	0.001	-1.695	1.000
FS	0.043	-0.006	0.002	-1.108	1.000
Random effects	**Estimate**	**Lower 95% CI**	**Upper 95% CI**		
(Intercept)	0.009	0.006	0.014		
Error	0.038	0.036	0.039		

Table A.36: Detailed statistics: sit-to-stand, challenging condition, forward leaning strategy, synergy 4

Reference group: UA

Model information	**Values**
Number of observations	1648
Number of participants	19
ICC	0.284

Fixed effects	**Estimate**	**Lower 95% CI**	**Upper 95% CI**	**t**	**p**
(Intercept)	0.044	0.039	0.048	18.266	<0.001
LT	-0.008	-0.013	-0.003	18.266	0.020
FS	-0.014	-0.019	-0.010	18.266	<0.001
Random effects	**Estimate**	**Lower 95% CI**	**Upper 95% CI**		
(Intercept)	0.004	0.003	0.007		
Error	0.031	0.030	0.032		

Reference group: LT

Fixed effects	**Estimate**	**Lower 95% CI**	**Upper 95% CI**	**t**	**p**
(Intercept)	0.035	0.032	0.039	21.006	<0.001
UA	0.035	0.003	0.013	3.230	0.020
FS	0.035	-0.009	-0.003	-3.531	0.007
Random effects	**Estimate**	**Lower 95% CI**	**Upper 95% CI**		
(Intercept)	0.004	0.003	0.007		
Error	0.031	0.030	0.032		

Post-hoc UA vs. LT

Fixed effects	**Estimate**	**Lower 95% CI**	**Upper 95% CI**	**t**	**p**
RA:LT	-0.001	-0.017	0.015	-0.067	1.000
ES:LT	-0.001	-0.000	0.032	1.920	0.165
Pec:LT	-0.001	-0.013	0.019	0.336	1.000
Lat:LT	-0.001	-0.008	0.024	0.983	0.977
Tra:LT	-0.001	-0.021	0.011	-0.588	1.000
Del:LT	-0.001	0.011	0.043	3.275	0.003
Bic:LT	-0.001	-0.001	0.031	1.818	0.208
Tri:LT	-0.001	0.011	0.042	3.258	0.003
GM:LT	-0.001	-0.029	0.003	-1.567	0.352
TF:LT	-0.001	-0.027	0.005	-1.385	0.499
RF:LT	-0.001	-0.008	0.024	1.008	0.940
VM:LT	-0.001	-0.016	0.015	-0.062	1.000
BF:LT	-0.001	-0.022	0.010	-0.749	1.000
TA:LT	-0.001	-0.032	0.000	-1.955	0.152
PL:LT	-0.001	-0.050	-0.018	-4.186	<0.001
Random effects	**Estimate**	**Lower 95% CI**	**Upper 95% CI**		
(Intercept)	0.005	0.003	0.007		
Error	0.027	0.027	0.028		

Table A.37: Detailed statistics: sit-to-stand, challenging condition, forward leaning strategy, synergy 5

Reference group: UA					
Model information	**Values**				
Number of observations	1648				
Number of participants	19				
ICC	0.425				
Fixed effects	**Estimate**	**Lower 95% CI**	**Upper 95% CI**	**t**	**p**
(Intercept)	0.041	0.035	0.046	14.535	<0.001
LT	0.002	-0.003	0.007	14.535	1.000
FS	-0.011	-0.016	-0.006	14.535	<0.001
Random effects	**Estimate**	**Lower 95% CI**	**Upper 95% CI**		
(Intercept)	0.007	0.005	0.010		
Error	0.033	0.032	0.034		
Reference group: LT					
Fixed effects	**Estimate**	**Lower 95% CI**	**Upper 95% CI**	**t**	**p**
(Intercept)	0.043	0.039	0.047	20.042	<0.001
UA	0.043	-0.007	0.003	-0.733	1.000
FS	0.043	-0.017	-0.010	-7.349	<0.001
Random effects	**Estimate**	**Lower 95% CI**	**Upper 95% CI**		
(Intercept)	0.007	0.005	0.010		
Error	0.033	0.032	0.034		

Table A.38: Detailed statistics: sit-to-stand, challenging condition, forward leaning strategy, synergy 6

Reference group: UA					
Model information	**Values**				
Number of observations	1648				
Number of participants	19				
ICC	0.491				
Fixed effects	**Estimate**	**Lower 95% CI**	**Upper 95% CI**	**t**	**p**
(Intercept)	0.047	0.041	0.053	15.373	<0.001
LT	-0.006	-0.012	-0.001	15.373	0.369
FS	-0.021	-0.026	-0.016	15.373	<0.001
Random effects	**Estimate**	**Lower 95% CI**	**Upper 95% CI**		
(Intercept)	0.008	0.006	0.012		
Error	0.034	0.033	0.035		
Reference group: LT					
Fixed effects	**Estimate**	**Lower 95% CI**	**Upper 95% CI**	**t**	**p**
(Intercept)	0.040	0.036	0.045	16.853	<0.001
UA	0.040	0.001	0.012	2.275	0.369
FS	0.040	-0.018	-0.011	-7.813	<0.001
Random effects	**Estimate**	**Lower 95% CI**	**Upper 95% CI**		
(Intercept)	0.008	0.006	0.012		
Error	0.034	0.033	0.035		

Table A.39: Detailed statistics: sit-to-stand, challenging condition, forward leaning strategy, synergy 9

Reference group: UA					
Model information	**Values**				
Number of observations	1648				
Number of participants	19				
ICC	0.392				
Fixed effects	**Estimate**	**Lower 95% CI**	**Upper 95% CI**	**t**	**p**
(Intercept)	0.063	0.057	0.069	20.377	<0.001
LT	-0.025	-0.031	-0.019	20.377	<0.001
FS	-0.031	-0.036	-0.025	20.377	<0.001
Random effects	**Estimate**	**Lower 95% CI**	**Upper 95% CI**		
(Intercept)	0.007	0.005	0.011		
Error	0.037	0.036	0.038		
Reference group: LT					
Fixed effects	**Estimate**	**Lower 95% CI**	**Upper 95% CI**	**t**	**p**
(Intercept)	0.038	0.033	0.043	16.412	<0.001
UA	0.038	0.019	0.031	8.061	<0.001
FS	0.038	-0.010	-0.002	-2.722	0.105
Random effects	**Estimate**	**Lower 95% CI**	**Upper 95% CI**		
(Intercept)	0.007	0.005	0.011		
Error	0.037	0.036	0.038		

Table A.40: Detailed statistics: sit-to-stand, challenging condition, forward leaning strategy, synergy 11

Reference group: UA					
Model information	**Values**				
Number of observations	1648				
Number of participants	19				
ICC	0.308				
Fixed effects	**Estimate**	**Lower 95% CI**	**Upper 95% CI**	**t**	**p**
(Intercept)	0.069	0.062	0.076	18.872	<0.001
LT	-0.026	-0.034	-0.019	18.872	<0.001
FS	-0.028	-0.035	-0.021	18.872	<0.001
Random effects	**Estimate**	**Lower 95% CI**	**Upper 95% CI**		
(Intercept)	0.007	0.004	0.012		
Error	0.047	0.045	0.048		
Reference group: LT					
Fixed effects	**Estimate**	**Lower 95% CI**	**Upper 95% CI**	**t**	**p**
(Intercept)	0.042	0.037	0.048	16.357	<0.001
UA	0.042	0.019	0.034	6.779	<0.001
FS	0.042	-0.007	0.003	-0.653	1.000
Random effects	**Estimate**	**Lower 95% CI**	**Upper 95% CI**		
(Intercept)	0.007	0.004	0.012		
Error	0.047	0.045	0.048		

Table A.41: Detailed statistics: stand-to-sit, non-challenging condition, backward lowering strategy, synergy 1

Reference group: UA

Model information	Values
Number of observations	672
Number of participants	14
ICC	0.542

Fixed effects	Estimate	Lower 95% CI	Upper 95% CI	t	p
(Intercept)	0.024	0.018	0.030	8.040	<0.001
LT	-0.004	-0.011	0.002	8.040	1.000
FS	-0.005	-0.011	0.000	8.040	0.919
Random effects	**Estimate**	**Lower 95% CI**	**Upper 95% CI**		
(Intercept)	0.005	0.003	0.009		
Error	0.020	0.019	0.021		

Reference group: LT

Fixed effects	Estimate	Lower 95% CI	Upper 95% CI	t	p
(Intercept)	0.020	0.015	0.024	8.254	<0.001
UA	0.020	-0.002	0.011	1.421	1.000
FS	0.020	-0.005	0.003	-0.405	1.000
Random effects	**Estimate**	**Lower 95% CI**	**Upper 95% CI**		
(Intercept)	0.005	0.003	0.009		
Error	0.020	0.019	0.021		

Table A.42: Detailed statistics: stand-to-sit, non-challenging condition, backward lowering strategy, synergy 2

Reference group: UA

Model information	Values
Number of observations	672
Number of participants	14
ICC	0.632

Fixed effects	Estimate	Lower 95% CI	Upper 95% CI	t	p
(Intercept)	0.027	0.020	0.034	7.185	<0.001
LT	0.005	-0.002	0.013	7.185	1.000
FS	0.002	-0.004	0.009	7.185	1.000
Random effects	**Estimate**	**Lower 95% CI**	**Upper 95% CI**		
(Intercept)	0.008	0.005	0.012		
Error	0.024	0.023	0.025		

Reference group: LT

Fixed effects	Estimate	Lower 95% CI	Upper 95% CI	t	p
(Intercept)	0.032	0.026	0.038	10.525	<0.001
UA	0.032	-0.013	0.002	-1.382	1.000
FS	0.032	-0.008	0.002	-1.100	1.000
Random effects	**Estimate**	**Lower 95% CI**	**Upper 95% CI**		
(Intercept)	0.008	0.005	0.012		
Error	0.024	0.023	0.025		

Table A.43: Detailed statistics: stand-to-sit, non-challenging condition, backward lowering strategy, synergy 3

Reference group: UA					
Model information	**Values**				
Number of observations	672				
Number of participants	14				
ICC	0.708				
Fixed effects	**Estimate**	**Lower 95% CI**	**Upper 95% CI**	**t**	**p**
(Intercept)	0.024	0.016	0.032	6.075	<0.001
LT	0.007	-0.000	0.015	6.075	0.920
FS	0.002	-0.004	0.009	6.075	1.000
Random effects	**Estimate**	**Lower 95% CI**	**Upper 95% CI**		
(Intercept)	0.009	0.005	0.014		
Error	0.024	0.023	0.025		
Reference group: LT					
Fixed effects	**Estimate**	**Lower 95% CI**	**Upper 95% CI**	**t**	**p**
(Intercept)	0.031	0.025	0.038	9.557	<0.001
UA	0.031	-0.015	0.000	-1.903	0.920
FS	0.031	-0.010	0.000	-1.835	1.000
Random effects	**Estimate**	**Lower 95% CI**	**Upper 95% CI**		
(Intercept)	0.009	0.005	0.014		
Error	0.024	0.023	0.025		

Table A.44: Detailed statistics: stand-to-sit, non-challenging condition, backward lowering strategy, synergy 5

Reference group: UA					
Model information	**Values**				
Number of observations	672				
Number of participants	14				
ICC	0.593				
Fixed effects	**Estimate**	**Lower 95% CI**	**Upper 95% CI**	**t**	**p**
(Intercept)	0.025	0.019	0.032	7.354	<0.001
LT	-0.002	-0.009	0.005	7.354	1.000
FS	-0.005	-0.011	0.001	7.354	1.000
Random effects	**Estimate**	**Lower 95% CI**	**Upper 95% CI**		
(Intercept)	0.007	0.004	0.011		
Error	0.022	0.021	0.024		
Reference group: LT					
Fixed effects	**Estimate**	**Lower 95% CI**	**Upper 95% CI**	**t**	**p**
(Intercept)	0.023	0.018	0.029	8.349	<0.001
UA	0.023	-0.005	0.009	0.619	1.000
FS	0.023	-0.007	0.002	-1.040	1.000
Random effects	**Estimate**	**Lower 95% CI**	**Upper 95% CI**		
(Intercept)	0.007	0.004	0.011		
Error	0.022	0.021	0.024		

Table A.45: Detailed statistics: stand-to-sit, non-challenging condition, backward lowering strategy, synergy 6

Reference group: UA

Model information	Values
Number of observations	672
Number of participants	14
ICC	0.484

Fixed effects	Estimate	Lower 95% CI	Upper 95% CI	t	p
(Intercept)	0.025	0.017	0.033	6.271	<0.001
LT	-0.003	-0.011	0.005	6.271	1.000
FS	0.000	-0.007	0.008	6.271	1.000

Random effects	Estimate	Lower 95% CI	Upper 95% CI
(Intercept)	0.007	0.004	0.011
Error	0.027	0.026	0.029

Reference group: LT

Fixed effects	Estimate	Lower 95% CI	Upper 95% CI	t	p
(Intercept)	0.022	0.016	0.028	6.965	<0.001
UA	0.022	-0.005	0.011	0.759	1.000
FS	0.022	-0.002	0.009	1.161	1.000

Random effects	Estimate	Lower 95% CI	Upper 95% CI
(Intercept)	0.007	0.004	0.011
Error	0.027	0.026	0.029

Table A.46: Detailed statistics: stand-to-sit, non-challenging condition, backward lowering strategy, synergy 8

Reference group: UA

Model information	Values
Number of observations	672
Number of participants	14
ICC	0.817

Fixed effects	Estimate	Lower 95% CI	Upper 95% CI	t	p
(Intercept)	0.027	0.019	0.036	6.465	<0.001
LT	-0.005	-0.012	0.003	6.465	1.000
FS	-0.006	-0.013	0.001	6.465	1.000

Random effects	Estimate	Lower 95% CI	Upper 95% CI
(Intercept)	0.010	0.006	0.016
Error	0.024	0.023	0.026

Reference group: LT

Fixed effects	Estimate	Lower 95% CI	Upper 95% CI	t	p
(Intercept)	0.023	0.016	0.030	6.376	<0.001
UA	0.023	-0.003	0.012	1.176	1.000
FS	0.023	-0.007	0.004	-0.476	1.000

Random effects	Estimate	Lower 95% CI	Upper 95% CI
(Intercept)	0.010	0.006	0.016
Error	0.024	0.023	0.026

Table A.47: Detailed statistics: stand-to-sit, non-challenging condition, backward lowering strategy, synergy 9

Reference group: UA

Model information	Values
Number of observations	672
Number of participants	14
ICC	0.711

Fixed effects	Estimate	Lower 95% CI	Upper 95% CI	t	p
(Intercept)	0.015	0.008	0.022	4.170	0.001
LT	0.007	0.000	0.014	4.170	0.675
FS	0.006	-0.000	0.012	4.170	0.814

Random effects	Estimate	Lower 95% CI	Upper 95% CI
(Intercept)	0.008	0.005	0.012
Error	0.022	0.021	0.023

Reference group: LT

Fixed effects	Estimate	Lower 95% CI	Upper 95% CI	t	p
(Intercept)	0.022	0.016	0.028	7.400	<0.001
UA	0.022	-0.014	-0.000	-2.036	0.675
FS	0.022	-0.006	0.004	-0.409	1.000

Random effects	Estimate	Lower 95% CI	Upper 95% CI
(Intercept)	0.008	0.005	0.012
Error	0.022	0.021	0.023

Table A.48: Detailed statistics: stand-to-sit, non-challenging condition, backward lowering strategy, synergy 10

Reference group: UA

Model information	Values
Number of observations	672
Number of participants	14
ICC	0.373

Fixed effects	Estimate	Lower 95% CI	Upper 95% CI	t	p
(Intercept)	0.018	0.010	0.025	4.679	<0.001
LT	0.002	-0.006	0.010	4.679	1.000
FS	0.003	-0.004	0.010	4.679	1.000

Random effects	Estimate	Lower 95% CI	Upper 95% CI
(Intercept)	0.005	0.003	0.009
Error	0.027	0.026	0.029

Reference group: LT

Fixed effects	Estimate	Lower 95% CI	Upper 95% CI	t	p
(Intercept)	0.019	0.014	0.025	6.745	<0.001
UA	0.019	-0.010	0.006	-0.430	1.000
FS	0.019	-0.004	0.007	0.476	1.000

Random effects	Estimate	Lower 95% CI	Upper 95% CI
(Intercept)	0.005	0.003	0.009
Error	0.027	0.026	0.029

Table A.49: Detailed statistics: stand-to-sit, non-challenging condition, hybrid strategy, synergy 1

Reference group: UA					
Model information	**Values**				
Number of observations	1152				
Number of participants	14				
ICC	0.723				
Fixed effects	**Estimate**	**Lower 95% CI**	**Upper 95% CI**	**t**	**p**
(Intercept)	0.021	0.016	0.026	8.813	<0.001
LT	0.002	-0.002	0.005	8.813	1.000
FS	0.003	-0.000	0.006	8.813	1.000
Random effects	**Estimate**	**Lower 95% CI**	**Upper 95% CI**		
(Intercept)	0.007	0.005	0.011		
Error	0.020	0.019	0.021		
Reference group: LT					
Fixed effects	**Estimate**	**Lower 95% CI**	**Upper 95% CI**	**t**	**p**
(Intercept)	0.023	0.018	0.027	10.327	<0.001
UA	0.023	-0.005	0.002	-0.995	1.000
FS	0.023	-0.002	0.004	0.948	1.000
Random effects	**Estimate**	**Lower 95% CI**	**Upper 95% CI**		
(Intercept)	0.007	0.005	0.011		
Error	0.020	0.019	0.021		

Table A.50: Detailed statistics: stand-to-sit, non-challenging condition, hybrid strategy, synergy 2

Reference group: UA					
Model information	**Values**				
Number of observations	1152				
Number of participants	14				
ICC	0.367				
Fixed effects	**Estimate**	**Lower 95% CI**	**Upper 95% CI**	**t**	**p**
(Intercept)	0.031	0.027	0.035	15.256	<0.001
LT	-0.002	-0.006	0.001	15.256	1.000
FS	-0.004	-0.008	0.000	15.256	0.950
Random effects	**Estimate**	**Lower 95% CI**	**Upper 95% CI**		
(Intercept)	0.005	0.003	0.008		
Error	0.025	0.024	0.026		
Reference group: LT					
Fixed effects	**Estimate**	**Lower 95% CI**	**Upper 95% CI**	**t**	**p**
(Intercept)	0.029	0.025	0.032	16.716	<0.001
UA	0.029	-0.001	0.006	1.259	1.000
FS	0.029	-0.005	0.002	-0.798	1.000
Random effects	**Estimate**	**Lower 95% CI**	**Upper 95% CI**		
(Intercept)	0.005	0.003	0.008		
Error	0.025	0.024	0.026		

Table A.51: Detailed statistics: stand-to-sit, non-challenging condition, hybrid strategy, synergy 3

Reference group: UA

Model information	**Values**
Number of observations	1152
Number of participants	14
ICC	0.090

Fixed effects	**Estimate**	**Lower 95% CI**	**Upper 95% CI**	**t**	**p**
(Intercept)	0.030	0.027	0.033	18.009	<.001
LT	-0.002	-0.006	0.002	18.009	1.000
FS	-0.003	-0.007	0.001	18.009	1.000

Random effects	**Estimate**	**Lower 95% CI**	**Upper 95% CI**
(Intercept)	0.001	0.000	0.029
Error	0.028	0.026	0.029

Reference group: LT

Fixed effects	**Estimate**	**Lower 95% CI**	**Upper 95% CI**	**t**	**p**
(Intercept)	0.027	0.025	0.030	20.889	<0.001
UA	0.027	-0.002	0.006	1.153	1.000
FS	0.027	-0.005	0.003	-0.399	1.000

Random effects	**Estimate**	**Lower 95% CI**	**Upper 95% CI**
(Intercept)	0.001	0.000	0.029
Error	0.028	0.026	0.029

Table A.52: Detailed statistics: stand-to-sit, non-challenging condition, hybrid strategy, synergy 5

Reference group: UA

Model information	**Values**
Number of observations	1152
Number of participants	14
ICC	0.220

Fixed effects	**Estimate**	**Lower 95% CI**	**Upper 95% CI**	**t**	**p**
(Intercept)	0.027	0.023	0.030	15.080	<0.001
LT	-0.004	-0.007	0.000	15.080	1.000
FS	0.002	-0.002	0.006	15.080	1.000

Random effects	**Estimate**	**Lower 95% CI**	**Upper 95% CI**
(Intercept)	0.003	0.001	0.006
Error	0.026	0.025	0.027

Reference group: LT

Fixed effects	**Estimate**	**Lower 95% CI**	**Upper 95% CI**	**t**	**p**
(Intercept)	0.023	0.021	0.026	16.262	<0.001
UA	0.023	-0.000	0.007	1.799	1.000
FS	0.023	0.002	0.009	2.877	0.065

Random effects	**Estimate**	**Lower 95% CI**	**Upper 95% CI**
(Intercept)	0.003	0.001	0.006
Error	0.026	0.025	0.027

Table A.53: Detailed statistics: stand-to-sit, non-challenging condition, hybrid strategy, synergy 6

Reference group: UA

Model information	Values
Number of observations	1152
Number of participants	14
ICC	0.233

Fixed effects	Estimate	Lower 95% CI	Upper 95% CI	t	p
(Intercept)	0.032	0.028	0.036	15.827	<0.001
LT	-0.005	-0.010	-0.001	15.827	0.254
FS	-0.006	-0.011	-0.002	15.827	0.134

Random effects	Estimate	Lower 95% CI	Upper 95% CI
(Intercept)	0.003	0.002	0.008
Error	0.029	0.028	0.031

Reference group: LT

Fixed effects	Estimate	Lower 95% CI	Upper 95% CI	t	p
(Intercept)	0.027	0.024	0.030	16.341	<0.001
UA	0.027	0.001	0.010	2.415	0.254
FS	0.027	-0.005	0.003	-0.418	1.000

Random effects	Estimate	Lower 95% CI	Upper 95% CI
(Intercept)	0.003	0.002	0.008
Error	0.029	0.028	0.031

Table A.54: Detailed statistics: stand-to-sit, non-challenging condition, hybrid strategy, synergy 7

Reference group: UA

Model information	Values
Number of observations	1152
Number of participants	14
ICC	0.451

Fixed effects	Estimate	Lower 95% CI	Upper 95% CI	t	p
(Intercept)	0.022	0.017	0.026	9.963	<0.001
LT	0.004	0.001	0.008	9.963	0.346
FS	0.003	-0.001	0.007	9.963	1.000

Random effects	Estimate	Lower 95% CI	Upper 95% CI
(Intercept)	0.005	0.003	0.009
Error	0.024	0.023	0.025

Reference group: LT

Fixed effects	Estimate	Lower 95% CI	Upper 95% CI	t	p
(Intercept)	0.026	0.022	0.030	13.827	<0.001
UA	0.026	-0.008	-0.001	-2.300	0.346
FS	0.026	-0.005	0.002	-0.873	1.000

Random effects	Estimate	Lower 95% CI	Upper 95% CI
(Intercept)	0.005	0.003	0.009
Error	0.024	0.023	0.025

Table A.55: Detailed statistics: stand-to-sit, non-challenging condition, hybrid strategy, synergy 8

Reference group: UA

Model information	**Values**
Number of observations	1152
Number of participants	14
ICC	0.700

Fixed effects	**Estimate**	**Lower 95% CI**	**Upper 95% CI**	**t**	**p**
(Intercept)	0.022	0.016	0.029	6.893	<0.001
LT	0.007	0.003	0.012	6.893	0.012
FS	0.002	-0.002	0.007	6.893	1.000

Random effects	**Estimate**	**Lower 95% CI**	**Upper 95% CI**
(Intercept)	0.010	0.006	0.015
Error	0.028	0.027	0.029

Reference group: LT

Fixed effects	**Estimate**	**Lower 95% CI**	**Upper 95% CI**	**t**	**p**
(Intercept)	0.030	0.024	0.036	10.032	<0.001
UA	0.030	-0.012	-0.003	-3.381	0.012
FS	0.030	-0.009	-0.001	-2.545	0.177

Random effects	**Estimate**	**Lower 95% CI**	**Upper 95% CI**
(Intercept)	0.010	0.006	0.015
Error	0.028	0.027	0.029

Table A.56: Detailed statistics: stand-to-sit, non-challenging condition, hybrid strategy, synergy 10

Reference group: UA

Model information	**Values**
Number of observations	1152
Number of participants	14
ICC	0.536

Fixed effects	**Estimate**	**Lower 95% CI**	**Upper 95% CI**	**t**	**p**
(Intercept)	0.022	0.016	0.027	8.094	<0.001
LT	0.008	0.004	0.012	8.094	0.002
FS	0.004	-0.001	0.008	8.094	1.000

Random effects	**Estimate**	**Lower 95% CI**	**Upper 95% CI**
(Intercept)	0.007	0.005	0.011
Error	0.027	0.026	0.028

Reference group: LT

Fixed effects	**Estimate**	**Lower 95% CI**	**Upper 95% CI**	**t**	**p**
(Intercept)	0.030	0.025	0.035	12.642	<0.001
UA	0.030	-0.012	-0.004	-3.899	0.002
FS	0.030	-0.009	-0.001	-2.318	0.330

Random effects	**Estimate**	**Lower 95% CI**	**Upper 95% CI**
(Intercept)	0.007	0.005	0.011
Error	0.027	0.026	0.028

Table A.57: Detailed statistics: stand-to-sit, non-challenging condition, vertical lowering strategy, synergy 1

Reference group: UA

Model information	**Values**
Number of observations	864
Number of participants	12
ICC	0.674

Fixed effects	**Estimate**	**Lower 95% CI**	**Upper 95% CI**	**t**	**p**
(Intercept)	0.022	0.018	0.027	9.218	<0.001
LT	0.001	-0.003	0.005	9.218	1.000
FS	0.003	-0.003	0.008	9.218	1.000

Random effects	**Estimate**	**Lower 95% CI**	**Upper 95% CI**
(Intercept)	0.008	0.005	0.012
Error	0.023	0.022	0.024

Reference group: LT

Fixed effects	**Estimate**	**Lower 95% CI**	**Upper 95% CI**	**t**	**p**
(Intercept)	0.023	0.018	0.029	8.453	<0.001
UA	0.023	-0.005	0.003	-0.444	1.000
FS	0.023	-0.004	0.008	0.665	1.000

Random effects	**Estimate**	**Lower 95% CI**	**Upper 95% CI**
(Intercept)	0.008	0.005	0.012
Error	0.023	0.022	0.024

Table A.58: Detailed statistics: stand-to-sit, non-challenging condition, vertical lowering strategy, synergy 2

Reference group: UA

Model information	**Values**
Number of observations	864
Number of participants	12
ICC	0.383

Fixed effects	**Estimate**	**Lower 95% CI**	**Upper 95% CI**	**t**	**p**
(Intercept)	0.025	0.021	0.028	13.619	<0.001
LT	0.005	0.000	0.009	13.619	0.450
FS	-0.004	-0.010	0.003	13.619	1.000

Random effects	**Estimate**	**Lower 95% CI**	**Upper 95% CI**
(Intercept)	0.005	0.003	0.008
Error	0.025	0.024	0.026

Reference group: LT

Fixed effects	**Estimate**	**Lower 95% CI**	**Upper 95% CI**	**t**	**p**
(Intercept)	0.029	0.025	0.034	12.879	<0.001
UA	0.029	-0.009	-0.000	-2.199	0.450
FS	0.029	-0.014	-0.002	-2.540	0.180

Random effects	**Estimate**	**Lower 95% CI**	**Upper 95% CI**
(Intercept)	0.005	0.003	0.008
Error	0.025	0.024	0.026

Table A.59: Detailed statistics: stand-to-sit, non-challenging condition, vertical lowering strategy, synergy 3

Reference group: UA

Model information	**Values**
Number of observations	864
Number of participants	12
ICC	0.321

Fixed effects	**Estimate**	**Lower 95% CI**	**Upper 95% CI**	**t**	**p**
(Intercept)	0.023	0.020	0.026	14.452	<0.001
LT	-0.001	-0.005	0.003	14.452	1.000
FS	0.002	-0.004	0.008	14.452	1.000
Random effects	**Estimate**	**Lower 95% CI**	**Upper 95% CI**		
(Intercept)	0.004	0.002	0.008		
Error	0.025	0.024	0.026		

Reference group: LT

Fixed effects	**Estimate**	**Lower 95% CI**	**Upper 95% CI**	**t**	**p**
(Intercept)	0.022	0.018	0.026	10.817	<0.001
UA	0.022	-0.003	0.005	0.369	1.000
FS	0.022	-0.003	0.009	0.960	1.000
Random effects	**Estimate**	**Lower 95% CI**	**Upper 95% CI**		
(Intercept)	0.004	0.002	0.008		
Error	0.025	0.024	0.026		

Table A.60: Detailed statistics: stand-to-sit, non-challenging condition, vertical lowering strategy, synergy 4

Reference group: UA

Model information	**Values**
Number of observations	864
Number of participants	12
ICC	0.222

Fixed effects	**Estimate**	**Lower 95% CI**	**Upper 95% CI**	**t**	**p**
(Intercept)	0.023	0.021	0.025	18.385	<0.001
LT	-0.004	-0.008	-0.001	18.385	0.353
FS	-0.006	-0.011	-0.000	18.385	0.639
Random effects	**Estimate**	**Lower 95% CI**	**Upper 95% CI**		
(Intercept)	0.003	0.001	0.006		
Error	0.023	0.022	0.024		

Reference group: LT

Fixed effects	**Estimate**	**Lower 95% CI**	**Upper 95% CI**	**t**	**p**
(Intercept)	0.019	0.016	0.022	11.107	<0.001
UA	0.019	0.001	0.008	2.293	0.353
FS	0.019	-0.007	0.004	-0.489	1.000
Random effects	**Estimate**	**Lower 95% CI**	**Upper 95% CI**		
(Intercept)	0.003	0.001	0.006		
Error	0.023	0.022	0.024		

Table A.61: Detailed statistics: stand-to-sit, non-challenging condition, vertical lowering strategy, synergy 5

Reference group: UA

Model information	**Values**
Number of observations	864
Number of participants	12
ICC	0.261

Fixed effects	**Estimate**	**Lower 95% CI**	**Upper 95% CI**	**t**	**p**
(Intercept)	0.025	0.022	0.028	16.516	<0.001
LT	-0.000	-0.004	0.004	16.516	1.000
FS	-0.002	-0.008	0.004	16.516	1.000

Random effects	**Estimate**	**Lower 95% CI**	**Upper 95% CI**
(Intercept)	0.003	0.001	0.007
Error	0.026	0.024	0.027

Reference group: LT

Fixed effects	**Estimate**	**Lower 95% CI**	**Upper 95% CI**	**t**	**p**
(Intercept)	0.024	0.020	0.028	12.222	<0.001
UA	0.024	-0.004	0.004	0.180	1.000
FS	0.024	-0.008	0.005	-0.464	1.000

Random effects	**Estimate**	**Lower 95% CI**	**Upper 95% CI**
(Intercept)	0.003	0.001	0.007
Error	0.026	0.024	0.027

Table A.62: Detailed statistics: stand-to-sit, non-challenging condition, vertical lowering strategy, synergy 6

Reference group: UA

Model information	**Values**
Number of observations	864
Number of participants	12
ICC	0.513

Fixed effects	**Estimate**	**Lower 95% CI**	**Upper 95% CI**	**t**	**p**
(Intercept)	0.022	0.018	0.026	10.413	<0.001
LT	0.007	0.003	0.011	10.413	0.013
FS	0.002	-0.004	0.008	10.413	1.000

Random effects	**Estimate**	**Lower 95% CI**	**Upper 95% CI**
(Intercept)	0.006	0.004	0.010
Error	0.024	0.023	0.025

Reference group: LT

Fixed effects	**Estimate**	**Lower 95% CI**	**Upper 95% CI**	**t**	**p**
(Intercept)	0.028	0.024	0.033	11.478	<0.001
UA	0.028	-0.011	-0.003	-3.353	0.013
FS	0.028	-0.011	0.001	-1.570	1.000

Random effects	**Estimate**	**Lower 95% CI**	**Upper 95% CI**
(Intercept)	0.006	0.004	0.010
Error	0.024	0.023	0.025

Table A.63: Detailed statistics: stand-to-sit, non-challenging condition, vertical lowering strategy, synergy 8

Reference group: UA

Model information	Values
Number of observations	864
Number of participants	12
ICC	0.672

Fixed effects	Estimate	Lower 95% CI	Upper 95% CI	t	p
(Intercept)	0.017	0.013	0.022	7.464	<0.001
LT	0.011	0.007	0.015	7.464	<0.001
FS	0.018	0.012	0.023	7.464	<0.001
Random effects	**Estimate**	**Lower 95% CI**	**Upper 95% CI**		
(Intercept)	0.007	0.005	0.012		
Error	0.022	0.021	0.023		

Reference group: LT

Fixed effects	Estimate	Lower 95% CI	Upper 95% CI	t	p
(Intercept)	0.028	0.023	0.033	10.791	<0.001
UA	0.028	-0.015	-0.007	-6.036	<0.001
FS	0.028	0.001	0.012	2.343	0.309
Random effects	**Estimate**	**Lower 95% CI**	**Upper 95% CI**		
(Intercept)	0.007	0.005	0.012		
Error	0.022	0.021	0.023		

Table A.64: Detailed statistics: stand-to-sit, non-challenging condition, vertical lowering strategy, synergy 10

Reference group: UA

Model information	Values
Number of observations	864
Number of participants	12
ICC	0.377

Fixed effects	Estimate	Lower 95% CI	Upper 95% CI	t	p
(Intercept)	0.018	0.014	0.022	8.754	<0.001
LT	0.009	0.004	0.013	8.754	0.005
FS	0.011	0.004	0.018	8.754	0.037
Random effects	**Estimate**	**Lower 95% CI**	**Upper 95% CI**		
(Intercept)	0.005	0.003	0.009		
Error	0.029	0.028	0.030		

Reference group: LT

Fixed effects	Estimate	Lower 95% CI	Upper 95% CI	t	p
(Intercept)	0.027	0.022	0.032	10.309	<0.001
UA	0.027	-0.013	-0.004	-3.617	0.005
FS	0.027	-0.005	0.009	0.598	1.000
Random effects	**Estimate**	**Lower 95% CI**	**Upper 95% CI**		
(Intercept)	0.005	0.003	0.009		
Error	0.029	0.028	0.030		

Table A.65: Detailed statistics: stand-to-sit, challenging condition, exaggerated forward leaning strategy, synergy 1

Reference group: UA

Model information	**Values**
Number of observations	1200
Number of participants	17
ICC	0.591

Fixed effects	**Estimate**	**Lower 95% CI**	**Upper 95% CI**	**t**	**p**
(Intercept)	0.034	0.029	0.038	14.297	<0.001
LT	-0.007	-0.011	-0.004	14.297	0.001
FS	-0.007	-0.012	-0.002	14.297	0.129

Random effects	**Estimate**	**Lower 95% CI**	**Upper 95% CI**
(Intercept)	0.008	0.005	0.012
Error	0.028	0.027	0.029

Reference group: LT

Fixed effects	**Estimate**	**Lower 95% CI**	**Upper 95% CI**	**t**	**p**
(Intercept)	0.026	0.022	0.031	10.759	<0.001
UA	0.026	0.004	0.011	4.019	0.001
FS	0.026	-0.004	0.006	0.265	1.000

Random effects	**Estimate**	**Lower 95% CI**	**Upper 95% CI**
(Intercept)	0.008	0.005	0.012
Error	0.028	0.027	0.029

Table A.66: Detailed statistics: stand-to-sit, challenging condition, exaggerated forward leaning strategy, synergy 2

Reference group: UA

Model information	**Values**
Number of observations	1200
Number of participants	17
ICC	0.426

Fixed effects	**Estimate**	**Lower 95% CI**	**Upper 95% CI**	**t**	**p**
(Intercept)	0.034	0.029	0.038	15.929	<0.001
LT	-0.005	-0.009	-0.001	15.929	0.315
FS	-0.003	-0.008	0.002	15.929	1.000

Random effects	**Estimate**	**Lower 95% CI**	**Upper 95% CI**
(Intercept)	0.007	0.004	0.010
Error	0.031	0.030	0.032

Reference group: LT

Fixed effects	**Estimate**	**Lower 95% CI**	**Upper 95% CI**	**t**	**p**
(Intercept)	0.029	0.025	0.033	13.014	<0.001
UA	0.029	0.001	0.009	2.285	0.315
FS	0.029	-0.004	0.007	0.560	1.000

Random effects	**Estimate**	**Lower 95% CI**	**Upper 95% CI**
(Intercept)	0.007	0.004	0.010
Error	0.031	0.030	0.032

Table A.67: Detailed statistics: stand-to-sit, challenging condition, exaggerated forward leaning strategy, synergy 3

Reference group: UA					
Model information	**Values**				
Number of observations	1200				
Number of participants	17				
ICC	0.554				
Fixed effects	**Estimate**	**Lower 95% CI**	**Upper 95% CI**	**t**	**p**
(Intercept)	0.035	0.030	0.040	15.109	<0.001
LT	-0.003	-0.007	0.001	15.109	1.000
FS	0.002	-0.003	0.007	15.109	1.000
Random effects	**Estimate**	**Lower 95% CI**	**Upper 95% CI**		
(Intercept)	0.008	0.005	0.012		
Error	0.029	0.028	0.030		
Reference group: LT					
Fixed effects	**Estimate**	**Lower 95% CI**	**Upper 95% CI**	**t**	**p**
(Intercept)	0.032	0.027	0.037	13.210	<0.001
UA	0.032	-0.001	0.007	1.651	1.000
FS	0.032	-0.000	0.010	1.933	0.749
Random effects	**Estimate**	**Lower 95% CI**	**Upper 95% CI**		
(Intercept)	0.008	0.005	0.012		
Error	0.029	0.028	0.030		

Table A.68: Detailed statistics: stand-to-sit, challenging condition, exaggerated forward leaning strategy, synergy 4

Reference group: UA					
Model information	**Values**				
Number of observations	1200				
Number of participants	17				
ICC	0.694				
Fixed effects	**Estimate**	**Lower 95% CI**	**Upper 95% CI**	**t**	**p**
(Intercept)	0.025	0.021	0.030	11.068	<0.001
LT	0.000	-0.003	0.003	11.068	1.000
FS	0.002	-0.002	0.007	11.068	1.000
Random effects	**Estimate**	**Lower 95% CI**	**Upper 95% CI**		
(Intercept)	0.008	0.006	0.012		
Error	0.024	0.023	0.025		
Reference group: LT					
Fixed effects	**Estimate**	**Lower 95% CI**	**Upper 95% CI**	**t**	**p**
(Intercept)	0.026	0.021	0.030	10.869	<0.001
UA	0.026	-0.003	0.003	-0.212	1.000
FS	0.026	-0.002	0.006	0.916	1.000
Random effects	**Estimate**	**Lower 95% CI**	**Upper 95% CI**		
(Intercept)	0.008	0.006	0.012		
Error	0.024	0.023	0.025		

Table A.69: Detailed statistics: stand-to-sit, challenging condition, exaggerated forward leaning strategy, synergy 5

Reference group: UA					
Model information	**Values**				
Number of observations	1200				
Number of participants	17				
ICC	0.672				
Fixed effects	**Estimate**	**Lower 95% CI**	**Upper 95% CI**	**t**	**p**
(Intercept)	0.026	0.021	0.031	10.766	<0.001
LT	0.003	-0.000	0.007	10.766	0.723
FS	0.002	-0.002	0.007	10.766	1.000
Random effects	**Estimate**	**Lower 95% CI**	**Upper 95% CI**		
(Intercept)	0.009	0.006	0.013		
Error	0.026	0.025	0.027		
Reference group: LT					
Fixed effects	**Estimate**	**Lower 95% CI**	**Upper 95% CI**	**t**	**p**
(Intercept)	0.029	0.024	0.034	11.749	<0.001
UA	0.029	-0.007	0.000	-1.948	0.723
FS	0.029	-0.006	0.004	-0.378	1.000
Random effects	**Estimate**	**Lower 95% CI**	**Upper 95% CI**		
(Intercept)	0.009	0.006	0.013		
Error	0.026	0.025	0.027		

Table A.70: Detailed statistics: stand-to-sit, challenging condition, exaggerated forward leaning strategy, synergy 6

Reference group: UA					
Model information	**Values**				
Number of observations	1200				
Number of participants	17				
ICC	0.680				
Fixed effects	**Estimate**	**Lower 95% CI**	**Upper 95% CI**	**t**	**p**
(Intercept)	0.023	0.018	0.028	9.766	<0.001
LT	0.005	0.002	0.009	9.766	0.013
FS	0.008	0.004	0.013	9.766	0.005
Random effects	**Estimate**	**Lower 95% CI**	**Upper 95% CI**		
(Intercept)	0.009	0.006	0.013		
Error	0.025	0.024	0.026		
Reference group: LT					
Fixed effects	**Estimate**	**Lower 95% CI**	**Upper 95% CI**	**t**	**p**
(Intercept)	0.028	0.024	0.033	11.705	<0.001
UA	0.028	-0.009	-0.002	-3.322	0.013
FS	0.028	-0.002	0.007	1.166	1.000
Random effects	**Estimate**	**Lower 95% CI**	**Upper 95% CI**		
(Intercept)	0.009	0.006	0.013		
Error	0.025	0.024	0.026		

Table A.71: Detailed statistics: stand-to-sit, challenging condition, exaggerated forward leaning strategy, synergy 8

Reference group: UA

Model information	Values
Number of observations	1200
Number of participants	17
ICC	0.383

Fixed effects	Estimate	Lower 95% CI	Upper 95% CI	t	p
(Intercept)	0.021	0.017	0.025	10.160	<0.001
LT	0.009	0.005	0.013	10.160	<0.001
FS	0.004	-0.001	0.010	10.160	1.000
Random effects	**Estimate**	**Lower 95% CI**	**Upper 95% CI**		
(Intercept)	0.006	0.004	0.010		
Error	0.032	0.030	0.033		

Reference group: LT

Fixed effects	Estimate	Lower 95% CI	Upper 95% CI	t	p
(Intercept)	0.029	0.025	0.034	13.597	<0.001
UA	0.029	-0.013	-0.005	-4.217	<0.001
FS	0.029	-0.010	0.001	-1.510	1.000
Random effects	**Estimate**	**Lower 95% CI**	**Upper 95% CI**		
(Intercept)	0.006	0.004	0.010		
Error	0.032	0.030	0.033		

Table A.72: Detailed statistics: stand-to-sit, challenging condition, forward leaning strategy, synergy 1

Reference group: UA

Model information	Values
Number of observations	1616
Number of participants	18
ICC	0.510

Fixed effects	Estimate	Lower 95% CI	Upper 95% CI	t	p
(Intercept)	0.042	0.037	0.048	15.997	<0.001
LT	-0.010	-0.014	-0.005	15.997	<0.001
FS	-0.014	-0.018	-0.010	15.997	<0.001
Random effects	**Estimate**	**Lower 95% CI**	**Upper 95% CI**		
(Intercept)	0.008	0.005	0.012		
Error	0.032	0.031	0.033		

Reference group: LT

Fixed effects	Estimate	Lower 95% CI	Upper 95% CI	t	p
(Intercept)	0.033	0.028	0.038	13.316	<0.001
UA	0.033	0.005	0.014	4.201	<0.001
FS	0.033	-0.008	-0.000	-2.153	0.440
Random effects	**Estimate**	**Lower 95% CI**	**Upper 95% CI**		
(Intercept)	0.008	0.005	0.012		
Error	0.032	0.031	0.033		

Table A.73: Detailed statistics: stand-to-sit, challenging condition, forward leaning strategy, synergy 2

Reference group: UA

Model information	Values
Number of observations	1616
Number of participants	18
ICC	0.488

Fixed effects	Estimate	Lower 95% CI	Upper 95% CI	t	p
(Intercept)	0.034	0.029	0.039	13.269	<0.001
LT	-0.001	-0.006	0.003	13.269	1.000
FS	-0.003	-0.007	0.001	13.269	1.000

Random effects	Estimate	Lower 95% CI	Upper 95% CI
(Intercept)	0.008	0.005	0.012
Error	0.032	0.030	0.033

Reference group: LT

Fixed effects	Estimate	Lower 95% CI	Upper 95% CI	t	p
(Intercept)	0.032	0.028	0.037	13.755	<0.001
UA	0.032	-0.003	0.006	0.581	1.000
FS	0.032	-0.005	0.002	-0.771	1.000

Random effects	Estimate	Lower 95% CI	Upper 95% CI
(Intercept)	0.008	0.005	0.012
Error	0.032	0.030	0.033

Table A.74: Detailed statistics: stand-to-sit, challenging condition, forward leaning strategy, synergy 3

Reference group: UA

Model information	Values
Number of observations	1616
Number of participants	18
ICC	0.557

Fixed effects	Estimate	Lower 95% CI	Upper 95% CI	t	p
(Intercept)	0.032	0.027	0.038	11.290	<0.001
LT	0.006	0.001	0.011	11.290	0.147
FS	0.005	0.000	0.009	11.290	0.567

Random effects	Estimate	Lower 95% CI	Upper 95% CI
(Intercept)	0.009	0.006	0.014
Error	0.033	0.032	0.034

Reference group: LT

Fixed effects	Estimate	Lower 95% CI	Upper 95% CI	t	p
(Intercept)	0.038	0.033	0.044	14.282	<0.001
UA	0.038	-0.011	-0.001	-2.561	0.147
FS	0.038	-0.005	0.002	-0.735	1.000

Random effects	Estimate	Lower 95% CI	Upper 95% CI
(Intercept)	0.009	0.006	0.014
Error	0.033	0.032	0.034

Table A.75: Detailed statistics: stand-to-sit, challenging condition, forward leaning strategy, synergy 4

Reference group: UA

Model information	**Values**
Number of observations	1616
Number of participants	18
ICC	0.500

Fixed effects	**Estimate**	**Lower 95% CI**	**Upper 95% CI**	**t**	**p**
(Intercept)	0.035	0.031	0.040	14.533	<0.001
LT	0.001	-0.003	0.005	14.533	1.000
FS	-0.000	-0.004	0.003	14.533	1.000
Random effects	**Estimate**	**Lower 95% CI**	**Upper 95% CI**		
(Intercept)	0.007	0.005	0.011		
Error	0.030	0.029	0.031		

Reference group: LT

Fixed effects	**Estimate**	**Lower 95% CI**	**Upper 95% CI**	**t**	**p**
(Intercept)	0.036	0.032	0.041	15.988	<0.001
UA	0.036	-0.005	0.003	-0.375	1.000
FS	0.036	-0.005	0.002	-0.704	1.000
Random effects	**Estimate**	**Lower 95% CI**	**Upper 95% CI**		
(Intercept)	0.007	0.005	0.011		
Error	0.030	0.029	0.031		

Table A.76: Detailed statistics: stand-to-sit, challenging condition, forward leaning strategy, synergy 6

Reference group: UA

Model information	**Values**
Number of observations	1616
Number of participants	18
ICC	0.460

Fixed effects	**Estimate**	**Lower 95% CI**	**Upper 95% CI**	**t**	**p**
(Intercept)	0.034	0.030	0.038	15.283	<0.001
LT	-0.005	-0.009	-0.001	15.283	0.267
FS	-0.004	-0.008	-0.000	15.283	0.409
Random effects	**Estimate**	**Lower 95% CI**	**Upper 95% CI**		
(Intercept)	0.007	0.004	0.010		
Error	0.029	0.028	0.030		

Reference group: LT

Fixed effects	**Estimate**	**Lower 95% CI**	**Upper 95% CI**	**t**	**p**
(Intercept)	0.029	0.025	0.033	14.253	<0.001
UA	0.029	0.001	0.009	2.347	0.267
FS	0.029	-0.003	0.004	0.341	1.000
Random effects	**Estimate**	**Lower 95% CI**	**Upper 95% CI**		
(Intercept)	0.007	0.004	0.010		
Error	0.029	0.028	0.030		

Table A.77: Detailed statistics: stand-to-sit, challenging condition, forward leaning strategy, synergy 7

Reference group: UA					
Model information	**Values**				
Number of observations	1616				
Number of participants	18				
ICC	0.674				
Fixed effects	**Estimate**	**Lower 95% CI**	**Upper 95% CI**	**t**	**p**
(Intercept)	0.030	0.025	0.035	11.029	<0.001
LT	-0.004	-0.008	0.000	11.029	0.737
FS	-0.005	-0.009	-0.001	11.029	0.106
Random effects	**Estimate**	**Lower 95% CI**	**Upper 95% CI**		
(Intercept)	0.009	0.006	0.014		
Error	0.028	0.027	0.029		
Reference group: LT					
Fixed effects	**Estimate**	**Lower 95% CI**	**Upper 95% CI**	**t**	**p**
(Intercept)	0.026	0.021	0.031	10.130	<0.001
UA	0.026	-0.000	0.008	1.940	0.737
FS	0.026	-0.004	0.002	-0.686	1.000
Random effects	**Estimate**	**Lower 95% CI**	**Upper 95% CI**		
(Intercept)	0.009	0.006	0.014		
Error	0.028	0.027	0.029		

Table A.78: Detailed statistics: stand-to-sit, challenging condition, forward leaning strategy, synergy 8

Reference group: UA					
Model information	**Values**				
Number of observations	1616				
Number of participants	18				
ICC	0.628				
Fixed effects	**Estimate**	**Lower 95% CI**	**Upper 95% CI**	**t**	**p**
(Intercept)	0.027	0.020	0.033	8.006	<0.001
LT	0.005	-0.000	0.010	8.006	0.764
FS	0.002	-0.003	0.007	8.006	1.000
Random effects	**Estimate**	**Lower 95% CI**	**Upper 95% CI**		
(Intercept)	0.011	0.008	0.016		
Error	0.036	0.035	0.037		
Reference group: LT					
Fixed effects	**Estimate**	**Lower 95% CI**	**Upper 95% CI**	**t**	**p**
(Intercept)	0.032	0.026	0.038	10.016	<0.001
UA	0.032	-0.010	0.000	-1.924	0.764
FS	0.032	-0.007	0.002	-1.261	1.000
Random effects	**Estimate**	**Lower 95% CI**	**Upper 95% CI**		
(Intercept)	0.011	0.008	0.016		
UA	-0.005	-0.010	0.000		

Bibliography

Aarts, E., Verhage, M., Veenvliet, J. V., Dolan, C. V. and Van Der Sluis, S. (2014). A solution to dependency: using multilevel analysis to accommodate nested data. *Nature Neuroscience* 17: 491–496, doi:10.1038/nn.3648.

Afsar, M. R., Ashiquzzaman, A., Martelli, D. and Shen, X. (2023). Sw-sista2: A new-generation semi-wearable device for sit-to-stand assistance. *Journal of Medical Devices* 17: 031001, doi:10.1115/1.4062337.

Ahmad, I., Ansari, F. and Dey, U. K. (2013). Power line noise reduction in ecg by butterworth notch filters: A comparative study. *International Journal of Electronics, Communication & Instrumentation Engineering Research and Development* 3: 65–74.

Albert, S. T. and Shadmehr, R. (2016). The neural feedback response to error as a teaching signal for the motor learning system. *Journal of Neuroscience* 36: 4832–4845, doi:10.1523/JNEUROSCI.0159-16.2016.

Albert, S. T. and Shadmehr, R. (2018). Estimating properties of the fast and slow adaptive processes during sensorimotor adaptation. *Journal of Neurophysiology* 119: 1367–1393, doi:10.1152/jn.00197.2017.

Aleshinsky, S. Y. (1986). An energy ‘sources’ and ‘fractions’ approach to the mechanical energy expenditure problem—v. the mechanical energy expenditure reduction during motion of the multi-link system. *Journal of Biomechanics* 19: 311–315, doi:10.1016/0021-9290(86)90007-2.

Alessandro, C., Delis, I., Nori, F., Panzeri, S. and Berret, B. (2013). Muscle synergies in neuroscience and robotics: from input-space to task-space perspectives. *Frontiers in Computational Neuroscience* 7, doi:10.3389/fncom.2013.00043.

Alexander, N. B., Schultz, A. B., Ashton-Miller, J. A., Gross, M. and Giordani, B. (1997). Muscle strength and rising from a chair in older adults. *Muscle & Nerve* 20: 56–59, doi:10.1002/(SICI)1097-4598(1997)5+<56::AID-MUS14>3.0.CO;2-X.

Alkjær, T., Larsen, P. K., Pedersen, G., Nielsen, L. H. and Simonsen, E. B. (2006). Biomechanical analysis of rollator walking. *BioMedical Engineering OnLine* 5: 2, doi:10.1186/1475-925X-5-2.

Alkner, B. A., Tesch, P. A. and Berg, H. E. (2000). Quadriceps emg/force relationship in knee extension and leg press:. *Medicine & Science in Sports & Exercise* 32: 459, doi:10.1097/00005768-200002000-00030.

Allen, J. L., Kesar, T. M. and Ting, L. H. (2019). Motor module generalization across balance and walking is impaired after stroke. *Journal of Neurophysiology* 122: 277–289, doi:10.1152/jn.00561.2018.

Allen, T., Choppin, S. and Knudson, D. (2016). A review of tennis racket performance parameters. *Sports Engineering* 19: 1–11, doi:10.1007/s12283-014-0167-x.

Ambrose, A. F., Paul, G. and Hausdorff, J. M. (2013). Risk factors for falls among older adults: A review of the literature. *Maturitas* 75: 51–61, doi:10.1016/j.maturitas.2013.02.009.

Amiridis, I. G., Hatzitaki, V. and Arabatzi, F. (2003). Age-induced modifications of static postural control in humans. *Neuroscience Letters* 350: 137–140, doi:10.1016/S0304-3940(03)00878-4.

Ammar, A., Trabelsi, K., Boujelbane, M. A., Boukhris, O., Glenn, J. M., Chtourou, H. and Schöllhorn, W. I. (2023). The myth of contextual interference learning benefit in sports practice: A systematic review and meta-analysis. *Educational Research Review* 39: 1–27, doi:10.1016/j.edurev.2023.100537.

An, Q., Ikemoto, Y. and Asama, H. (2013). Muscle synergy analysis between young and elderly people in standing-up motion. *Journal of Robotics and Mechatronics* 25: 1038–1049, doi:10.20965/jrm.2013.p1038.

Anan, M., Ibara, T., Kito, N. and Shinkoda, K. (2012). The clarification of the strategy during sit-to-stand motion from the standpoint of mechanical energy transfer. *Journal of Physical Therapy Science* 24: 231–236, doi:10.1589/jpts.24.231.

Anderson, K. and Behm, D. G. (2005). The impact of instability resistance training on balance and stability. *Sports Medicine* 35: 43–53, doi:10.2165/00007256-200535010-00004.

Anwar, M. N., Tomi, N. and Ito, K. (2011). Motor imagery facilitates force field learning. *Brain Research* 13: 21–29, doi:10.1016/j.brainres.2011.04.030.

Arborelius, U. P., Wretenberg, P. and Lindberg, F. (1992). The effects of armrests and high seat heights on lower-limb joint load and muscular activity during sitting and rising. *Ergonomics* 35: 1377–1391, doi:10.1080/00140139208967399.

Ashford, S. and De Souza, L. (2000). A comparison of the timing of muscle activity during sitting down compared to standing up. *Physiotherapy Research International* 5: 111–128, doi:10.1002/pri.190.

Atkeson, C. G. (1989). Learning arm kinematics and dynamics. *Annual Review of Neuroscience* 12: 157–183, doi:10.1146/annurev.ne.12.030189.001105.

Bach, M. M., Daffertshofer, A. and Dominici, N. (2021). Muscle synergies in children walking and running on a treadmill. *Frontiers in Human Neuroscience* 15: 1–14, doi:10.3389/fnhum.2021.637157.

Badrulhisham, F., Pogatzki-Zahn, E., Segelcke, D., Spisak, T. and Vollert, J. (2024). Machine learning and artificial intelligence in neuroscience: A primer for researchers. *Brain, Behavior, and Immunity* 115: 470–479, doi:10.1016/j.bbi.2023.11.005.

Bahrami, F., Riener, R., Jabedar-Maralani, P. and Schmidt, G. (2000). Biomechanical analysis of sit-to-stand transfer in healthy and paraplegic subjects. *Clinical Biomechanics* 15: 123–133, doi:10.1016/S0268-0033(99)00044-3.

Banks, C. L., Pai, M. M., McGuirk, T. E., Fregly, B. J. and Patten, C. (2017). Methodological choices in muscle synergy analysis impact differentiation of physiological characteristics following stroke. *Frontiers in Computational Neuroscience* 11: 1–12, doi:10.3389/fncom.2017.00078.

Bateni, H. and Maki, B. E. (2005). Assistive devices for balance and mobility: Benefits, demands, and adverse consequences. *Archives of Physical Medicine and Rehabilitation* 86: 134–145, doi:10.1016/j.apmr.2004.04.023.

Battig, W. F. (1972). Intratask interference as a source of facilitation in transfer and retention. In Thompson, R. F. and Voss, J. F. (eds), *Topics in learning and performance*. New York: Academic Press, 1–17.

Beckerle, P., Salvietti, G., Unal, R., Prattichizzo, D., Rossi, S., Castellini, C., Hirche, S., Endo, S., Amor, H. B., Ciocarlie, M., Mastrogiovanni, F., Argall, B. D. and Bianchi, M. (2017). A human-robot interaction perspective on assistive and rehabilitation robotics. *Frontiers in Neurorobotics* 11: 1–6, doi:10.3389/fnbot.2017.00024.

Begg, R. and Kamruzzaman, J. (2005). A machine learning approach for automated recognition of movement patterns using basic, kinetic and kinematic gait data. *Journal of Biomechanics* 38: 401–408, doi:10.1016/j.jbiomech.2004.05.002.

Bellman, R. (1966). Dynamic programming. *Science* 153: 34–37, doi:10.1126/science.153.3731.34.

Berger, D. J., Borzelli, D. and d'Avella, A. (2022). Task space exploration improves adaptation after incompatible virtual surgeries. *Journal of Neurophysiology* 127: 1127–1146, doi:10.1152/jn.00356.2021.

Berger, D. J., Gentner, R., Edmunds, T., Pai, D. K. and d'Avella, A. (2013). Differences in adaptation rates after virtual surgeries provide direct evidence for modularity. *Journal of Neuroscience* 33: 12384–12394, doi:10.1523/JNEUROSCI.0122-13.2013.

Berger, D. J., Masciullo, M., Molinari, M., Lacquaniti, F. and d'Avella, A. (2020). Does the cerebellum shape the spatiotemporal organization of muscle patterns? insights from subjects with cerebellar ataxias. *Journal of Neurophysiology* 123: 1691–1710, doi:10.1152/jn.00657.2018.

Berniker, M., Franklin, D. W., Flanagan, J. R., Wolpert, D. M. and Kording, K. (2014). Motor learning of novel dynamics is not represented in a single global coordinate system: evaluation of mixed coordinate representations and local learning. *Journal of Neurophysiology* 111: 1165–1182, doi:10.1152/jn.00493.2013.

Berniker, M., Jarc, A., Bizzi, E. and Tresch, M. C. (2009). Simplified and effective motor control based on muscle synergies to exploit musculoskeletal dynamics. *Proceedings of the National Academy of Sciences* 106: 7601–7606, doi:10.1073/pnas.0901512106.

Bernstein, N. A. (1967). *The co-ordination and regulation of movements*. Oxford: Pergamon Press.

Berret, B., Delis, I., Gaveau, J. and Jean, F. (2019). Optimality and modularity in human movement: From optimal control to muscle synergies. In Venture, G., Laumond, J.-P. and Watier, B. (eds), *Biomechanics of Anthropomorphic Systems*. Champaign: Springer, Springer Tracts in Advanced Robotics *124*, 105–133, doi:10.1007/978-3-319-93870-7_6.

Bishop, N. (1997). *The Secrets of Animal Flight*. New York: Houghton Mifflin Harcourt.

Bizzi, E. and Ajemian, R. (2015). A hard scientific quest: Understanding voluntary movements. *Daedalus* 144: 83–95, doi:10.1162/DAED_a_00324.

Bizzi, E., Cheung, V., d'Avella, A., Saltiel, P. and Tresch, M. (2008). Combining modules for movement. *Brain Research Reviews* 57: 125–133, doi:10.1016/j.brainresrev.2007.08.004.

Bizzi, E. and Cheung, V. C. (2013). The neural origin of muscle synergies. *Frontiers in Computational Neuroscience* 7: 1–6, doi:10.3389/fncom.2013.00051.

Bizzi, E., D'Avella, A., Saltiel, P. and Tresch, M. (2002). Book review: Modular organization of spinal motor systems. *The Neuroscientist* 8: 437–442, doi:10.1177/107385802236969.

Bizzi, E., Mussa-Ivaldi, F. A. and Giszter, S. (1991). Computations underlying the execution of movement: a biological perspective. *Science* 253: 287–291, doi:10.1126/science.1857964.

Bizzi, E., Tresch, M. C., Saltiel, P. and d'Avella, A. (2000). New perspectives on spinal motor systems. *Nature Reviews Neuroscience* 1: 101–108, doi:10.1038/35039000.

Boelen, M. P. (2009). *Health professionals' guide to physical management of parkinson's disease*. Champaign: Human Kinetics.

Bohannon, R. W. (2012). Measurement of sit-to-stand among older adults. *Topics in Geriatric Rehabilitation* 28: 11–16, doi:10.1097/TGR.0b013e31823415fa.

Bohannon, R. W. and Corrigan, D. L. (2003). Strategies community dwelling elderly women employ to ease the task of standing up from household surfaces. *Topics in Geriatric Rehabilitation* 19: 137–144, doi:10.1097/00013614-200304000-00007.

Bohannon, R. W. and Lusardi, M. M. (2004). Getting up from the floor. determinants and techniques among healthy older adults. *Physiotherapy Theory and Practice* 20: 233–241, doi:10.1080/09593980490887993.

Borzelli, D., De Marchis, C., Quercia, A., De Pasquale, P., Casile, A., Quartarone, A., Calabrò, R. S. and d'Avella, A. (2024). Muscle synergy analysis as a tool for assessing the effectiveness of gait rehabilitation therapies: A methodological review and perspective. *Bioengineering* 11: 793, doi:10.3390/bioengineering11080793.

Borzelli, D., Gurgone, S., Mezzetti, M., De Pasquale, P., Berger, D. J., Milardi, D., Acri, G. and D'Avella, A. (2022). Adaptation to virtual surgeries across multiple practice sessions. In Torricelli, D., Akay, M. and Pons, J. L. (eds), *Converging Clinical and Engineering Research on Neurorehabilitation IV*. Champaign: Springer International Publishing, Biosystems & Biorobotics *28*, 563–568.

Borzelli, G., Cappizzo, A. and Papa, E. (1999). Inter- and intra-individual variability of ground reaction forces during sit-to-stand with principal component analysis. *Medical Engineering & Physics* 21: 235–240, doi:10.1016/S1350-4533(99)00050-8.

Bowsher, J., Bramlett, M., Burnside, I. M. and Gueldner, S. H. (1993). Methodological considerations in the study of frail elderly people. *Journal of Advanced Nursing* 18: 873–879, doi:10.1046/j.1365-2648.1993.18060873.x.

Boyer, M., Bouyer, L., Roy, J.-S. and Campeau-Lecours, A. (2023). Reducing noise, artifacts and interference in single-channel emg signals: A review. *Sensors* 23: 2927, doi:10.3390/s23062927.

Bradley, S. M. and Hernandez, C. R. (2011). Geriatric assistive devices. *American family physician* 84: 405–411.

Brambilla, C., Atzori, M., Müller, H., d'Avella, A. and Scano, A. (2023a). Spatial and temporal muscle synergies provide a dual characterization of low-dimensional and intermittent control of upper-limb movements. *Neuroscience* 514: 100–122, doi:10.1016/j.neuroscience.2023.01.017.

Brambilla, C., Russo, M., d'Avella, A. and Scano, A. (2023b). Phasic and tonic muscle synergies are different in number, structure and sparseness. *Human Movement Science* 92: 103148, doi:10.1016/j.humov.2023.103148.

Branch, L. G. and Meyers, A. R. (1987). Assessing physical function in the elderly. *Clinics in Geriatric Medicine* 3: 29–51, doi:10.1016/S0749-0690(18)30825-5.

Brashers-Krug, T., Shadmehr, R. and Bizzi, E. (1996). Consolidation in human motor memory. *Nature* 382: 252–255, doi:10.1038/382252a0.

Bruton, M. and O'Dwyer, N. (2018). Synergies in coordination: a comprehensive overview of neural, computational, and behavioral approaches. *Journal of Neurophysiology* 120: 2761–2774, doi:10.1152/jn.00052.2018.

Burdet, E., Franklin, D. W. and Milner, T. E. (2013). *Human robotics: neuromechanics and motor control*. Neuroscience/Robotics. Cambridge: MIT Press, doi:10.7551/mitpress/9007.001.0001, collection-title: Neuroscience/Robotics.

Candow, D. G. and Chilibeck, P. D. (2005). Differences in size, strength, and power of upper and lower body muscle groups in young and older men. *The Journals of Gerontology Series A: Biological Sciences and Medical Sciences* 60: 148–156, doi:10.1093/gerona/60.2.148.

Cappellini, G., Ivanenko, Y. P., Poppele, R. E. and Lacquaniti, F. (2006). Motor patterns in human walking and running. *Journal of Neurophysiology* 95: 3426–3437, doi:10.1152/jn.00081.2006.

Cappozzo, A., Catani, F., Della Croce, U. and Leardini, A. (1995). Position and orientation in space of bones during movement: anatomical frame definition and determination. *Clinical Biomechanics* 10: 171–178, doi:10.1016/0268-0033(95)91394-T.

Carey, H. D., Liss, D. J. and Allen, J. L. (2021). Young adults recruit similar motor modules across walking, turning, and chair transfers. *Physiological Reports* 9: e15050, doi:10.14814/phy2.15050.

Carr, J. H. (1992). Balancing the centre of body mass during standing up. *Physiotherapy Theory and Practice* 8: 159–164, doi:10.3109/09593989209108095.

Carr, J. H. and Gentile, A. M. (1994). The effect of arm movement on the biomechanics of standing up. *Human Movement Science* 13: 175–193, doi:10.1016/0167-9457(94)90035-3.

Carson, R. G. (2006). Changes in muscle coordination with training. *Journal of Applied Physiology* 101: 1506–1513, doi:10.1152/japplphysiol.00544.2006.

Castro, L. N. G., Wu, H. G. and Smith, M. A. (2011). Adaptation to dynamic environments displays local generalization for voluntary reaching movements. In *EMBC 2011: 33rd Annual International Conference of the IEEE Engineering in Medicine and Biology Society*. Boston, 4050–4052, doi:10.1109/IEMBS.2011.6091006.

Chadwick, E. K., Blana, D., Kirsch, R. F. and Bogert, A. J. van den (2014). Real-time simulation of three-dimensional shoulder girdle and arm dynamics. *IEEE Transactions on Biomedical Engineering* 61: 1947–1956, doi:10.1109/TBME.2014.2309727.

Chalavi, S., Pauwels, L., Heise, K.-F., Zivari Adab, H., Maes, C., Puts, N. A., Edden, R. A. and Swinnen, S. P. (2018). The neurochemical basis of the contextual interference effect. *Neurobiology of Aging* 66: 85–96, doi:10.1016/j.neurobiolaging.2018.02.014.

Chang, S. R., Kobetic, R. and Triolo, R. J. (2014). Understanding stand-to-sit maneuver: Implications for motor system neuroprostheses after paralysis. *Journal of Rehabilitation Research and Development* 51: 1339–1352, doi:10.1682/JRRD.2013.12.0264.

Charette, C., Best, K. L., Smith, E. M., Miller, W. C. and Routhier, F. (2018). Walking aid use in canada: Prevalence and demographic characteristics among community-dwelling users. *Physical Therapy* 98: 571–577, doi:10.1093/ptj/pzy038.

Cheesborough, J. E., Smith, L. H., Kuiken, T. A. and Dumanian, G. A. (2015). Targeted muscle reinnervation and advanced prosthetic arms. *Seminars in Plastic Surgery* 29: 062–072, doi: 10.1055/s-0035-1544166.

Cheng, Y.-Y., Wei, S.-H., Chen, P.-Y., Tsai, M.-W., Cheng, I.-C., Liu, D.-H. and Kao, C.-L. (2014). Can sit-to-stand lower limb muscle power predict fall status? *Gait & Posture* 40: 403–407, doi:10.1016/j.gaitpost.2014.05.064.

Cheung, V. C. K., Cheung, B. M. F., Zhang, J. H., Chan, Z. Y. S., Ha, S. C. W., Chen, C.-Y. and Cheung, R. T. H. (2020). Plasticity of muscle synergies through fractionation and merging during development and training of human runners. *Nature Communications* 11: 4356, doi:10.1038/s41467-020-18210-4.

Cheung, V. C. K., d'Avella, A. and Bizzi, E. (2009). Adjustments of motor pattern for load compensation via modulated activations of muscle synergies during natural behaviors. *Journal of Neurophysiology* 101: 1235–1257, doi:10.1152/jn.01387.2007.

Cheung, V. C. K., d'Avella, A., Tresch, M. C. and Bizzi, E. (2005). Central and sensory contributions to the activation and organization of muscle synergies during natural motor behaviors. *Journal of Neuroscience* 25: 6419–6434, doi:10.1523/JNEUROSCI.4904-04.2005.

Cheung, V. C. K. and Seki, K. (2021). Approaches to revealing the neural basis of muscle synergies: a review and a critique. *Journal of Neurophysiology* 125: 1580–1597, doi:10.1152/jn.00625.2019.

Cheung, V. C. K., Turolla, A., Agostini, M., Silvoni, S., Bennis, C., Kasi, P., Paganoni, S., Bonato, P. and Bizzi, E. (2012). Muscle synergy patterns as physiological markers of motor cortical damage. *Proceedings of the National Academy of Sciences* 109: 14652–14656, doi:10.1073/pnas.1212056109.

Chihara, T. and Seo, A. (2014). Evaluation of multiple muscle loads through multi-objective optimization with prediction of subjective satisfaction level: Illustration by an application to handrail position for standing. *Applied Ergonomics* 45: 261–269, doi:10.1016/j.apergo.2013.04.006.

Chiovetto, E., Berret, B., Delis, I., Panzeri, S. and Pozzo, T. (2013). Investigating reduction of dimensionality during single-joint elbow movements: a case study on muscle synergies. *Frontiers in Computational Neuroscience* 7: 1–12, doi:10.3389/fncom.2013.00011.

Choudry, M. U., Beach, T. A. C., Callaghan, J. P. and Kulić, D. (2013). A stochastic framework for movement strategy identification and analysis. *IEEE Transactions on Human-Machine Systems* 43: 314–327, doi:10.1109/TSMC.2013.2251629.

Cichocki, A., Zdunek, R., Phan, A. H. and Amari, S.-i. (2009). *Nonnegative Matrix and Tensor Factorizations: Applications to Exploratory Multi-way Data Analysis and Blind Source Separation*. Chichester: John Wiley & Sons.

Cifuentes, C. A. and Frizera, A. (2016). Assistive devices for human mobility and gait rehabilitation. In Cifuentes, C. A. and Frizera, A. (eds), *Human-Robot Interaction Strategies for Walker-Assisted Locomotion*, Springer Tracts in Advanced Robotics. Champaign: Springer International Publishing, 1–15, doi:10.1007/978-3-319-34063-0_1.

Cisek, P. and Green, A. M. (2024). Toward a neuroscience of natural behavior. *Current Opinion in Neurobiology* 86, doi:10.1016/j.conb.2024.102859.

Coghlin, S. S. and McFadyen, B. J. (1994). Transfer strategies used to rise from a chair in normal and low back pain subjects. *Clinical Biomechanics* 9: 85–92, doi:10.1016/0268-0033(94)90029-9.

Cohen, J. (1988). *Statistical power for the behavioural sciences*. Hilsdale: Lawrence Erlbaum Associates, 2nd ed.

Coltman, S. K., Cashaback, J. G. A. and Gribble, P. L. (2019). Both fast and slow learning processes contribute to savings following sensorimotor adaptation. *Journal of Neurophysiology* 121: 1575–1583, doi:10.1152/jn.00794.2018.

Coscia, M., Cheung, V. C., Tropea, P., Koenig, A., Monaco, V., Bennis, C., Micera, S. and Bonato, P. (2014). The effect of arm weight support on upper limb muscle synergies during reaching movements. *Journal of NeuroEngineering and Rehabilitation* 11: 22, doi:10.1186/1743-0003-11-22.

Coser, O., Tamantini, C., Soda, P. and Zollo, L. (2024). Ai-based methodologies for exoskeleton-assisted rehabilitation of the lower limb: a review. *Frontiers in Robotics and AI* 11: 1–19, doi:10.3389/frobt.2024.1341580.

Costamagna, E., Thies, S., Kenney, L., Howard, D., Liu, A. and Ogden, D. (2017). A generalisable methodology for stability assessment of walking aid users. *Medical Engineering & Physics* 47: 167–175, doi:10.1016/j.medengphy.2017.06.013.

Cowin, J., Nimphius, S., Fell, J., Culhane, P. and Schmidt, M. (2022). A proposed framework to describe movement variability within sporting tasks: A scoping review. *Sports Medicine - Open* 8: 85, doi:10.1186/s40798-022-00473-4.

Crevecoeur, F. and Scott, S. H. (2014). Beyond muscles stiffness: Importance of state-estimation to account for very fast motor corrections. *PLOS Computational Biology* 10: e1003869, doi: 10.1371/journal.pcbi.1003869.

Crevecoeur, F., Scott, S. H. and Cluff, T. (2019). Robust control in human reaching movements: A model-free strategy to compensate for unpredictable disturbances. *Journal of Neuroscience* 39: 8135–8148, doi:10.1523/JNEUROSCI.0770-19.2019.

Criscimagna-Hemminger, S. E., Donchin, O., Gazzaniga, M. S. and Shadmehr, R. (2003). Learned dynamics of reaching movements generalize from dominant to nondominant arm. *Journal of Neurophysiology* 89: 168–176, doi:10.1152/jn.00622.2002.

Criscimagna-Hemminger, S. E. and Shadmehr, R. (2008). Consolidation patterns of human motor memory. *Journal of Neuroscience* 28: 9610–9618, doi:10.1523/JNEUROSCI.3071-08.2008.

Cunha, C. P. D., Rao, P. T. and Karthikbabu, S. (2021). Clinical features contributing to the sit-to-stand transfer in people with parkinson's disease: a systematic review. *The Egyptian Journal of Neurology, Psychiatry and Neurosurgery* 57: 1–15, doi:10.1186/s41983-021-00396-z.

Czyż, S. H., Wójcik, A. M. and Solarská, P. (2024a). The effect of contextual interference on transfer in motor learning - a systematic review and meta-analysis. *Frontiers in Psychology* 15, doi:10.3389/fpsyg.2024.1377122.

Czyż, S. H., Wójcik, A. M., Solarská, P. and Kiper, P. (2024b). High contextual interference improves retention in motor learning: systematic review and meta-analysis. *Scientific Reports* 14: 15974, doi:10.1038/s41598-024-65753-3.

Daffertshofer, A., Lamoth, C. J. C., Meijer, O. G. and Beek, P. J. (2004). PCA in studying coordination and variability: a tutorial. *Clinical Biomechanics* 19: 415–428, doi:10.1016/j.clinbiomech.2004.01.005.

Dall, P. M. and Kerr, A. (2010). Frequency of the sit to stand task: An observational study of free-living adults. *Applied Ergonomics* 41: 58–61, doi:10.1016/j.apergo.2009.04.005.

Daly, C. (2021). Factors associated with increased terminal swing knee flexion in cerebral palsy. *Gait & Posture* 89: 126–131, doi:10.1016/j.gaitpost.2021.07.007.

Darainy, M. and Ostry, D. J. (2008). Muscle cocontraction following dynamics learning. *Experimental Brain Research* 190: 153–163, doi:10.1007/s00221-008-1457-y.

d'Avella, A. (2016). Modularity for motor control and motor learning. In *Progress in Motor Control: Theories and Translations*, Advances in Experimental Medicine and Biology. Champaign: Springer International Publishing, 3–19, doi:10.1007/978-3-319-47313-0_1.

d'Avella, A. and Bizzi, E. (2005). Shared and specific muscle synergies in natural motor behaviors. *Proceedings of the National Academy of Sciences* 102: 3076–3081, doi: 10.1073/pnas.0500199102.

d'Avella, A., Fernandez, L., Portone, A. and Lacquaniti, F. (2008). Modulation of phasic and tonic muscle synergies with reaching direction and speed. *Journal of Neurophysiology* 100: 1433–1454, doi:10.1152/jn.01377.2007.

d'Avella, A., Portone, A., Fernandes, L. and Lacquaniti, F. (2006). Control of fast-reaching movements by muscle synergy combinations. *Journal of Neuroscience* 26: 7791–7810, doi: 10.1523/JNEUROSCI.0830-06.2006.

d'Avella, A., Portone, A. and Lacquaniti, F. (2011). Superposition and modulation of muscle synergies for reaching in response to a change in target location. *Journal of Neurophysiology* 106: 2796–2812, doi:10.1152/jn.00675.2010.

d'Avella, A., Saltiel, P. and Bizzi, E. (2003). Combinations of muscle synergies in the construction of a natural motor behavior. *Nature neuroscience* 6: 300–308, doi:10.1038/nn1010.

d'Avella, A. and Tresch, M. C. (2002). Modularity in the motor system: decomposition of muscle patterns as combinations of time-varying synergies. In *Advances in neural information processing systems*, 141–148.

Davidson, P. R. and Wolpert, D. M. (2004). Scaling down motor memories: de-adaptation after motor learning. *Neuroscience Letters* 370: 102–107, doi:10.1016/j.neulet.2004.08.003.

Day, A., Taylor, N. F. and Green, R. A. (2012). The stabilizing role of the rotator cuff at the shoulder—responses to external perturbations. *Clinical Biomechanics* 27: 551–556, doi:10.1016/j.clinbiomech.2012.02.003.

De Marchis, C., Di Somma, J., Zych, M., Conforto, S. and Severini, G. (2018). Consistent visuomotor adaptations and generalizations can be achieved through different rotations of robust motor modules. *Scientific Reports* 8: 12657, doi:10.1038/s41598-018-31174-2.

Dehail, P., Bestaven, E., Muller, F., Mallet, A., Robert, B., Bourdel-Marchasson, I. and Petit, J. (2007). Kinematic and electromyographic analysis of rising from a chair during a "sit-to-walk" task in elderly subjects: Role of strength. *Clinical Biomechanics* 22: 1096–1103, doi:10.1016/j.clinbiomech.2007.07.015.

Dekker, D., Buzink, S. N., Molenbroek, J. F. and De Bruin, R. (2007). Hand supports to assist toilet use among the elderly. *Applied Ergonomics* 38: 109–118, doi:10.1016/j.apergo.2005.07.010.

Delis, I., Hilt, P. M., Pozzo, T., Panzeri, S. and Berret, B. (2018). Deciphering the functional role of spatial and temporal muscle synergies in whole-body movements. *Scientific Reports* 8: 8391, doi:10.1038/s41598-018-26780-z.

Delis, I., Panzeri, S., Pozzo, T. and Berret, B. (2014). A unifying model of concurrent spatial and temporal modularity in muscle activity. *Journal of Neurophysiology* 111: 675–693, doi:10.1152/jn.00245.2013.

Delp, S. L., Anderson, F. C., Arnold, A. S., Loan, P., Habib, A., John, C. T., Guendelman, E. and Thelen, D. G. (2007). Opensim: Open-source software to create and analyze dynamic simulations of movement. *IEEE Transactions on Biomedical Engineering* 54: 1940–1950, doi:10.1109/TBME.2007.901024.

Deluzio, K. J. and Astephen, J. L. (2007). Biomechanical features of gait waveform data associated with knee osteoarthritis: An application of principal component analysis. *Gait & Posture* 25: 86–93, doi:10.1016/j.gaitpost.2006.01.007.

Devarajan, K. and Cheung, V. C. K. (2014). On nonnegative matrix factorization algorithms for signal-dependent noise with application to electromyography data. *Neural Computation* 26: 1128–1168, doi:10.1162/NECO_a_00576.

Diedrichsen, J. and Kornysheva, K. (2015). Motor skill learning between selection and execution. *Trends in Cognitive Sciences* 19: 227–233, doi:10.1016/j.tics.2015.02.003.

Diedrichsen, J., White, O., Newman, D. and Lally, N. (2010). Use-dependent and error-based learning of motor behaviors. *The Journal of Neuroscience* 30: 5159–5166, doi:10.1523/JNEUROSCI.5406-09.2010.

Dietz, V., Zijlstra, W. and Duysens, J. (1994). Human neuronal interlimb coordination during split-belt locomotion. *Experimental Brain Research* 101: 513–520, doi:10.1007/BF00227344.

Djaldetti, R., Lorberboym, M. and Melamed, E. (2006). Primary postural instability: a cause of recurrent sudden falls in the elderly. *Neurological Sciences* 27: 412–416, doi:10.1007/s10072-006-0720-x.

Dolecka, U. E., Ownsworth, T. and Kuys, S. S. (2015). Comparison of sit-to-stand strategies used by older adults and people living with dementia. *Archives of Gerontology and Geriatrics* 60: 528–534, doi:10.1016/j.archger.2014.12.007.

Dollar, A. M. and Herr, H. (2008). Lower extremity exoskeletons and active orthoses: Challenges and state-of-the-art. *IEEE Transactions on robotics* 24: 144–158, doi:10.1109/TRO.2008.915453.

Dominici, N., Ivanenko, Y. P., Cappellini, G., d'Avella, A., Mondì, V., Cicchese, M., Fabiano, A., Silei, T., Di Paolo, A., Giannini, C., Poppele, R. E. and Lacquaniti, F. (2011). Locomotor primitives in newborn babies and their development. *Science* 334: 997–999, doi:10.1126/science.1210617.

Donath, L., Kurz, E., Roth, R., Zahner, L. and Faude, O. (2015). Different ankle muscle coordination patterns and co-activation during quiet stance between young adults and seniors do not change after a bout of high intensity training. *BMC Geriatrics* 15: 19, doi:10.1186/s12877-015-0017-0.

Donchin, O., Francis, J. T. and Shadmehr, R. (2003). Quantifying generalization from trial-by-trial behavior of adaptive systems that learn with basis functions: Theory and experiments in human motor control. *The Journal of Neuroscience* 23: 9032–9045, doi:10.1523/JNEUROSCI.23-27-09032.2003.

Dooley, S., Kim, S., Nussbaum, M. A. and Madigan, M. L. (2023). A passive leg-support exoskeleton adversely affects reactive balance after simulated slips and trips on a treadmill. *Journal of Biomechanics* 151: 111533, doi:10.1016/j.jbiomech.2023.111533.

Doorenbosch, C. A. M., Harlaar, J., Roebroeck, M. E. and Lankhorst, G. J. (1994). Two strategies of transferring from sit-to-stand; the activation of monoarticular and biarticular muscles. *Journal of Biomechanics* 27: 1299–1307, doi:10.1016/0021-9290(94)90039-6.

Drongelen, S. van, Stetter, B. J., Böhm, H., Stief, F., Stein, T. and Meurer, A. (2021). Identification of patients with similar gait compensating strategies due to unilateral hip osteoarthritis and the effect of total hip replacement: a secondary analysis. *Journal of Clinical Medicine* 10: 2167, doi:10.3390/jcm10102167.

Dubost, V., Beauchet, O., Manckoundia, P., Herrmann, F. and Mourey, F. (2005). Decreased trunk angular displacement during sitting down: an early feature of aging. *Physical Therapy* 85: 404–412, doi:10.1093/ptj/85.5.404.

Duffield, D. (2018). Marr's vision ii. In Duffield, D. (ed.), *Reflections on Psycholinguistic Theories: Raiding the Inarticulate*. Cambridge: Cambridge University Press, 34–46, doi: 10.1017/9781108264969.004.

Ethier, V., Zee, D. S. and Shadmehr, R. (2008). Spontaneous recovery of motor memory during saccade adaptation. *Journal of Neurophysiology* 99: 2577–2583, doi:10.1152/jn.00015.2008.

Etnyre, B. and Thomas, D. Q. (2007). Event standardization of sit-to-stand movements. *Physical Therapy* 87: 1651–1666, doi:10.2522/ptj.20060378.

Farrens, A. J. and Sergi, F. (2019). Identifying the neural representation of fast and slow states in force field adaptation via fMRI. In *2019 IEEE 16th International Conference on Rehabilitation Robotics (ICORR)*, 1007–1012, doi:10.1109/ICORR.2019.8779512.

FIG (2024). FÉdÉration internationale de gymnastique. code of points 2025-2028. women's artistic gymnastics.

Fine, M. S. and Thoroughman, K. A. (2007). Trial-by-trial transformation of error into sensorimotor adaptation changes with environmental dynamics. *Journal of Neurophysiology* 98: 1392–1404, doi:10.1152/jn.00196.2007.

Flanders, M. (1991). Temporal patterns of muscle activation for arm movements in three- dimensional space. *The Journal of Neuroscience* 11: 2680–2693, doi:10.1523/JNEUROSCI.11-09-02680.1991.

Flanders, M., Pellegrini, J. J. and Soechting, J. F. (1994). Spatial/temporal characteristics of a motor pattern for reaching. *Journal of Neurophysiology* 71: 811–813, doi:10.1152/jn.1994.71.2.811.

Flash, T. and Bizzi, E. (2016). Cortical circuits and modules in movement generation: experiments and theories. *Current Opinion in Neurobiology* 41: 174–178, doi:10.1016/j.conb.2016.09.013.

Flash, T. and Hochner, B. (2005). Motor primitives in vertebrates and invertebrates. *Current Opinion in Neurobiology* 15: 660–666, doi:10.1016/j.conb.2005.10.011.

Fleisig, G., Nicholls, R., Elliott, B. and Escamilla, R. (2003). Tennis: Kinematics used by world class tennis players to produce high-velocity serves. *Sports Biomechanics* 2: 51–64, doi:10.1080/14763140308522807.

Floreano, D., Ijspeert, A. J. and Schaal, S. (2014). Robotics and neuroscience. *Current Biology* 24: R910–R920, doi:10.1016/j.cub.2014.07.058.

Forano, M. and Franklin, D. W. (2020). Timescales of motor memory formation in dual-adaptation. *PLOS Computational Biology* 16: e1008373, doi:10.1371/journal.pcbi.1008373.

Franklin, D. W., Batchelor, A. V. and Wolpert, D. M. (2016). The sensorimotor system can sculpt behaviorally relevant representations for motor learning. *eneuro* 3: ENEURO.0070–16.2016, doi:10.1523/ENEURO.0070-16.2016.

Franklin, D. W., Nietschmann, P., Papadopoulou, T. and Franklin, S. (2025). Long-term development of a motor memory. *bioRxiv* doi:10.1101/2025.02.22.639647.

Franklin, D. W., Osu, R., Burdet, E., Kawato, M. and Milner, T. E. (2003). Adaptation to stable and unstable dynamics achieved by combined impedance control and inverse dynamics model. *Journal of Neurophysiology* 90: 3270–3282, doi:10.1152/jn.01112.2002.

Franklin, D. W. and Wolpert, D. M. (2011). Computational mechanisms of sensorimotor control. *Neuron* 72: 425–442, doi:10.1016/j.neuron.2011.10.006.

Franklin, S. and Franklin, D. W. (2021). Feedback gains modulate with motor memory uncertainty. *Neurons, Behavior, Data analysis, and Theory* 5: 1–28, doi:10.51628/001c.22336.

Franklin, S., Wolpert, D. M. and Franklin, D. W. (2012). Visuomotor feedback gains upregulate during the learning of novel dynamics. *Journal of Neurophysiology* 108: 467–478, doi:10.1152/jn.01123.2011.

Franklin, S., Wolpert, D. M. and Franklin, D. W. (2017). Rapid visuomotor feedback gains are tuned to the task dynamics. *Journal of Neurophysiology* 118: 2711–2726, doi:10.1152/jn.00748.2016.

Friston, K., Holmes, A., Worsley, K., Poline, J.-B., Frith, C. and Frackowiak, R. (1994). Statistical parametric maps in functional imaging: a general linear approach. *Human Brain Mapping* 2: 189–210, doi:10.1002/hbm.460020402.

Frykberg, G. E. and Häger, C. K. (2015). Movement analysis of sit-to-stand - research informing clinical practice. *Physical Therapy Reviews* 20: 156–167, doi:10.1179/1743288X15Y.0000000005.

Gandolfo, F., Mussa-Ivaldi, F. A. and Bizzi, E. (1996). Motor learning by field approximation. *Proceedings of the National Academy of Sciences of the United States of America* 93: 3843–3846, doi:10.1073/pnas.93.9.3843.

Gawthrop, P., Gollee, H., Lakie, M. and Loram, I. D. (2019). Intermittent control of movement and balance. In Jaeger, D. and Jung, R. (eds), *Encyclopedia of Computational Neuroscience*. New York, NY: Springer, 1–6, doi:10.1007/978-1-4614-7320-6_100701-1.

Gawthrop, P., Loram, I., Gollee, H. and Lakie, M. (2014). Intermittent control models of human standing: similarities and differences. *Biological Cybernetics* 108: 159–168, doi: 10.1007/s00422-014-0587-5.

Gaxatte, C., Nguyen, T., Chourabi, F., Salleron, J., Pardessus, V., Delabrière, I., Thévenon, A. and Puisieux, F. (2011). Fear of falling as seen in the multidisciplinary falls consultation. *Annals of Physical and Rehabilitation Medicine* 54: 248–258, doi:10.1016/j.rehab.2011.04.002.

Gelbard, R., Inaba, K., Okoye, O. T., Morrell, M., Saadi, Z., Lam, L., Talving, P. and Demetriades, D. (2014). Falls in the elderly: a modern look at an old problem. *The American Journal of Surgery* 208: 249–253, doi:10.1016/j.amjsurg.2013.12.034.

Gentner, R., Edmunds, T., Pai, D. K. and d'Avella, A. (2013). Robustness of muscle synergies during visuomotor adaptation. *Frontiers in Computational Neuroscience* 7, doi:10.3389/fncom.2013.00120.

Ghez, C., Krakauer, J. W., Sainburg, R. L. and Ghilardi, M. F. (1999). Spatial representations and internal models of limb dynamics in motor learning. In Gazzaniga, M. (ed.), *The New Cognitive Neurosciences*. Cambridge: The MIT Press, 2nd ed., 501–514.

Gilleard, W., Crosbie, J. and Smith, R. (2008). Rising to stand from a chair: Symmetry, and frontal and transverse plane kinematics and kinetics. *Gait & Posture* 27: 8–15, doi:10.1016/j.gaitpost.2006.11.002.

Giszter, S. F. (2015). Motor primitives—new data and future questions. *Current Opinion in Neurobiology* 33: 156–165, doi:10.1016/j.conb.2015.04.004.

Giszter, S. F. and Hart, C. B. (2013). Motor primitives and synergies in the spinal cord and after injury-the current state of play: Spinal motor primitives, modularity, and disease. *Annals of the New York Academy of Sciences* 1279: 114–126, doi:10.1111/nyas.12065.

Giszter, S. F., Hart, C. B. and Silfies, S. P. (2010). Spinal cord modularity: evolution, development, and optimization and the possible relevance to low back pain in man. *Experimental Brain Research* 200: 283–306, doi:10.1007/s00221-009-2016-x.

Giszter, S. F., Mussa-Ivaldi, F. A. and Bizzi, E. (1993). Convergent force fields organized in the frog's spinal cord. *Journal of Neuroscience* 13: 467–491, doi:10.1523/JNEUROSCI.13-02-00467.1993.

Gollhofer, A., Taube, W. and Nielsen, J. B. (eds) (2012). *Routledge Handbook of Motor Control and Motor Learning*. Routledge International Handbooks. London, New York: Routledge, doi:10.4324/9780203132746.

Golub, G. H. and Van Loan, C. F. (1989). *Matrix Computations*. Johns Hopkins series in the mathematical sciences. Baltimore: Johns Hopkins University Press, 2nd ed.

Gonzalez, S., Stegall, P., Cain, S. M., Siu, H. C. and Stirling, L. (2022). Assessment of a powered ankle exoskeleton on human stability and balance. *Applied Ergonomics* 103, doi: 10.1016/j.apergo.2022.103768.

Gonzalez Castro, L. N., Hadjiosif, A. M., Hemphill, M. A. and Smith, M. A. (2014). Environmental consistency determines the rate of motor adaptation. *Current Biology* 24: 1050–1061, doi: 10.1016/j.cub.2014.03.049.

Goodbody, S. J. and Wolpert, D. M. (1998). Temporal and amplitude generalization in motor learning. *Journal of Neurophysiology* 79: 1825–1838, doi:10.1152/jn.1998.79.4.1825.

Goode, S. and Magill, R. A. (1986). Contextual interference effects in learning three badminton serves. *Research quarterly for exercise and sport* 57: 308–314, doi:10.1080/02701367.1986.10608091.

Goodpaster, B. H., Park, S. W., Harris, T. B., Kritchevsky, S. B., Nevitt, M., Schwartz, A. V., Simonsick, E. M., Tylavsky, F. A., Visser, M., Newman, A. B. and Health ABC Study for the (2006). The loss of skeletal muscle strength, mass, and quality in older adults: The health, aging and body composition study. *The Journals of Gerontology Series A: Biological Sciences and Medical Sciences* 61: 1059–1064, doi:10.1093/gerona/61.10.1059.

Gottschalk, F., Kourosh, S. and Leveau, B. (1989). The functional anatomy of tensor fasciae latae and gluteus medius and minimus. *Journal of anatomy* : 179–189.

Goulart, F. R.-d.-P. and Valls-Solé, J. (1999). Patterned electromyographic activity in the sit-to-stand movement. *Clinical neurophysiology* 110: 1634–1640, doi:10.1016/S1388-2457(99)00109-1.

Grillner, S. (1981). Control of locomotion in bipeds, tetrapods, and fish. In Brooks, V. B. (ed.), *Handbook of physiology: section I. The nervous system*. Bethesda: American Physiological Society, 1179–1236.

Gross, J., Timmermann, L., Kujala, J., Dirks, M., Schmitz, F., Salmelin, R. and Schnitzler, A. (2002). The neural basis of intermittent motor control in humans. *Proceedings of the National Academy of Sciences* 99: 2299–2302, doi:10.1073/pnas.032682099.

Guadagnoli, M. A. and Lee, T. D. (2004). Challenge point: A framework for conceptualizing the effects of various practice conditions in motor learning. *Journal of Motor Behavior* 36: 212–224, doi:10.3200/JMBR.36.2.212-224.

Haith, A. M. and Krakauer, J. W. (2012). Theoretical models of motor control and motor learning. In Gollhofer, A., Taube, W. and Nielsen, J. B. (eds), *Routledge Handbook of Motor Control and Motor Learning*, Routledge International Handbooks. London, New York: Routledge, 7–28, doi:10.4324/9780203132746.

Haith, A. M. and Krakauer, J. W. (2014). Motor learning: The great rate debate. *Current Biology* 24: R386–R388, doi:10.1016/j.cub.2014.03.077.

Halilaj, E., Rajagopal, A., Fiterau, M., Hicks, J. L., Hastie, T. J. and Delp, S. L. (2018). Machine learning in human movement biomechanics: Best practices, common pitfalls, and new opportunities. *Journal of Biomechanics* 81: 1–11, doi:10.1016/j.jbiomech.2018.09.009.

Hamill, J. and Knutzen, K. M. (2009). *Biomechanical basis of human movement*. Philadelphia: Wolters Kluwer Health/Lippincott Williams and Wilkins, 3rd ed.

Hanawa, H., Kubota, K., Kokubun, T., Marumo, T., Hoshi, F., Kobayashi, A. and Kanemura, N. (2017). Muscle synergies underlying sit-to-stand tasks in elderly people and their relationship with kinetic characteristics. *Journal of Electromyography and Kinesiology* 37: 15–20, doi:10.1016/j.jelekin.2017.08.004.

Happee, R. (1992). Goal-directed arm movements: I. analysis of emg records in shoulder and elbow muscles. *Journal of Electromyography and Kinesiology* 2: 165–178, doi:10.1016/1050-6411(92)90014-A.

Harman, E. A., Rosenstein, M. T., Frykman, P. N. and Rosenstein, R. M. (1990). The effects of arms and countermovement on vertical jumping. *Medicine and Science in Sports and Exercise* 22: 825–833, doi:10.1249/00005768-199012000-00015.

Hart, C. B. (2004). Modular premotor drives and unit bursts as primitives for frog motor behaviors. *Journal of Neuroscience* 24: 5269–5282, doi:10.1523/JNEUROSCI.5626-03.2004.

Hart, C. B. and Giszter, S. F. (2010). A neural basis for motor primitives in the spinal cord. *Journal of Neuroscience* 30: 1322–1336, doi:10.1523/JNEUROSCI.5894-08.2010.

Hayes, H. B., Chvatal, S. A., French, M. A., Ting, L. H. and Trumbower, R. D. (2014). Neuromuscular constraints on muscle coordination during overground walking in persons with chronic incomplete spinal cord injury. *Clinical Neurophysiology* 125: 2024–2035, doi: 10.1016/j.clinph.2014.02.001.

Heald, J. B., Franklin, D. W. and Wolpert, D. M. (2018). Increasing muscle co-contraction speeds up internal model acquisition during dynamic motor learning. *Scientific Reports* 8: 1–11, doi:10.1038/s41598-018-34737-5.

Henry, M. and Baudry, S. (2019). Age-related changes in leg proprioception: implications for postural control. *Journal of Neurophysiology* 122: 525–538, doi:10.1152/jn.00067.2019.

Hermens, H. J., Freriks, B., Disselhorst-Klug, C. and Rau, G. (2000). Development of recommendations for semg sensors and sensor placement procedures. *Journal of Electromyography and Kinesiology* 10: 361–374, doi:10.1016/S1050-6411(00)00027-4.

Herzfeld, D. J., Vaswani, P. A., Marko, M. K. and Shadmehr, R. (2014). A memory of errors in sensorimotor learning. *Science* 345: 1349–1353, doi:10.1126/science.1253138.

Herzog, M., Focke, A., Maurus, P., Thürer, B. and Stein, T. (2022). Random practice enhances retention and spatial transfer in force field adaptation. *Frontiers in Human Neuroscience* 16: 1–19, doi:10.3389/fnhum.2022.816197.

Herzog, M., Krafft, F. C., Stetter, B. J., d'Avella, A., Sloot, L. H. and Stein, T. (2023). Rollator usage lets young individuals switch movement strategies in sit-to-stand and stand-to-sit tasks. *Scientific Reports* 13: 16901, doi:10.1038/s41598-023-43401-6.

Hesse, S., Schauer, M., Malezic, M., Jahnke, M. and Mauritz, K. H. (1994). Quantitative analysis of rising from a chair in healthy and hemiparetic subjects. *Scandinavian Journal of Rehabilitation Medicine* 26: 161–166, doi:10.2340/165019771994263160166.

Hinnekens, E., Berret, B., Morard, E., Do, M.-C., Barbu-Roth, M. and Teulier, C. (2024). Optimization of modularity during development to simplify walking control across multiple steps. *Frontiers in Neural Circuits* 17: 1–14, doi:10.3389/fncir.2023.1340298.

Holm, S. (1979). A simple sequentially rejective multiple test procedure. *Scandinavian journal of statistics* 2: 65–70.

Honert, E. C. and Pataky, T. C. (2021). Timing of gait events affects whole trajectory analyses: A statistical parametric mapping sensitivity analysis of lower limb biomechanics. *Journal of Biomechanics* 119: 1–7, doi:10.1016/j.jbiomech.2021.110329.

Hotelling, H. (1933). Analysis of a complex of statistical variables into principal components. *Journal of educational psychology* 24: 417.

Howard, I. S. and Franklin, D. W. (2015). Neural tuning functions underlie both generalization and interference. *PLOS ONE* 10: e0131268, doi:10.1371/journal.pone.0131268.

Hox, J., Moerbeek, M. and Schoot, R. van de (2017). *Multilevel Analysis : Techniques and Applications*. Quantitative Methodology Series. London: Routledge, 3rd ed., doi:10.4324/9781315650982.

Huang, H. J., Kram, R. and Ahmed, A. A. (2012). Reduction of metabolic cost during motor learning of arm reaching dynamics. *The Journal of Neuroscience* 32: 2182–2190, doi:10.1523/JNEUROSCI.4003-11.2012.

Huang, V. S., Haith, A., Mazzoni, P. and Krakauer, J. W. (2011). Rethinking motor learning and savings in adaptation paradigms: model-free memory for successful actions combines with internal models. *Neuron* 70: 787–801, doi:10.1016/j.neuron.2011.04.012.

Huang, V. S. and Shadmehr, R. (2007). Evolution of motor memory during the seconds after observation of motor error. *Journal of Neurophysiology* 97: 3976–3985, doi:10.1152/jn.01281.2006.

Huberdeau, D. M., Haith, A. M. and Krakauer, J. W. (2015a). Formation of a long-term memory for visuomotor adaptation following only a few trials of practice. *Journal of Neurophysiology* 114: 969–977, doi:10.1152/jn.00369.2015.

Huberdeau, D. M., Krakauer, J. W. and Haith, A. M. (2015b). Dual-process decomposition in human sensorimotor adaptation. *Current Opinion in Neurobiology* 33: 71–77, doi:10.1016/j.conb.2015.03.003.

Hug, F., Turpin, N. A., Guével, A. and Dorel, S. (2010). Is interindividual variability of emg patterns in trained cyclists related to different muscle synergies? *Journal of applied physiology* 108: 1727–1736, doi:10.1152/japplphysiol.01305.2009.

Hughes, M. A., Myers, B. S. and Schenkman, M. L. (1996). The role of strength in rising from a chair in the functionally impaired elderly. *Journal of Biomechanics* 29: 1509–1513, doi:10.1016/S0021-9290(96)80001-7.

Hughes, M. A., Weiner, D. K., Schenkman, M. L., Long, R. M. and Studenski, S. A. (1994). Chair rise strategies in the elderly. *Clinical Biomechanics* 9: 187–192, doi:10.1016/0268-0033(94)90020-5.

Iglewicz, B. and Hoaglin, D. C. (1993). *How to detect and handle outliers*, *16*. Milwaukee, WI: ASQC Quality Press.

IJmker, T., Lamoth, C. J., Houdijk, H., Tolsma, M., Woude, L. H. V. van der, Daffertshofer, A. and Beek, P. J. (2015). Effects of handrail hold and light touch on energetics, step parameters, and neuromuscular activity during walking after stroke. *Journal of NeuroEngineering and Rehabilitation* 12, doi:10.1186/s12984-015-0051-3.

Ingram, J. N., Flanagan, J. R. and Wolpert, D. M. (2013). Context-dependent decay of motor memories during skill acquisition. *Current Biology* 23: 1107–1112, doi:10.1016/j.cub.2013.04.079.

Ingram, J. N., Howard, I. S., Flanagan, J. R. and Wolpert, D. M. (2011). A single-rate context-dependent learning process underlies rapid adaptation to familiar object dynamics. *PLOS Computational Biology* 7: e1002196, doi:10.1371/journal.pcbi.1002196.

Ippersiel, P., Preuss, R., Fillion, A., Jean-Louis, J., Woodrow, R., Zhang, Q. and Robbins, S. M. (2021). Inter-joint coordination and the flexion-relaxation phenomenon among adults with low back pain during bending. *Gait & Posture* 85: 164–170, doi:10.1016/j.gaitpost.2021.02.001.

Irwin, G., Hanton, S. and Kerwin, D. G. (2005). The conceptual process of skill progression development in artistic gymnastics. *Journal of Sports Sciences* 23: 1089–1099, doi:10.1080/02640410500130763.

Ivanenko, Y. P., Cappellini, G., Dominici, N., Poppele, R. E. and Lacquaniti, F. (2005). Coordination of locomotion with voluntary movements in humans. *Journal of Neuroscience* 25: 7238–7253, doi:10.1523/JNEUROSCI.1327-05.2005.

Ivanenko, Y. P., Cappellini, G., Poppele, R. E. and Lacquaniti, F. (2008). Spatiotemporal organization of α-motoneuron activity in the human spinal cord during different gaits and gait transitions. *European Journal of Neuroscience* 27: 3351–3368, doi:10.1111/j.1460-9568.2008.06289.x.

Ivanenko, Y. P., Poppele, R. E. and Lacquaniti, F. (2004). Five basic muscle activation patterns account for muscle activity during human locomotion. *The Journal of Physiology* 556: 267–282, doi:10.1113/jphysiol.2003.057174.

Ivanenko, Y. P., Poppele, R. E. and Lacquaniti, F. (2006). Motor control programs and walking. *The Neuroscientist* 12: 339–348, doi:10.1177/1073858406287987.

James, C. R. and Bates, B. T. (1997). Experimental and statistical design issues in human movement research. *Measurement in Physical Education and Exercise Science* 1: 55–69, doi:10.1207/s15327841mpee0101_4.

Jeka, J. J. (1997). Light touch contact as a balance aid. *Physical Therapy* 77: 476–487, doi:10.1093/ptj/77.5.476.

Jeka, J. J. and Lackner, J. R. (1994). Fingertip contact influences human postural control. *Experimental Brain Research* 100: 8, doi:10.1007/BF02738408.

Jeon, W., Jensen, J. L. and Griffin, L. (2019). Muscle activity and balance control during sit-to-stand across symmetric and asymmetric initial foot positions in healthy adults. *Gait & Posture* 71: 138–144, doi:10.1016/j.gaitpost.2019.04.030.

Jeon, W., Whitall, J., Griffin, L. and Westlake, K. P. (2021). Trunk kinematics and muscle activation patterns during stand-to-sit movement and the relationship with postural stability in aging. *Gait & Posture* 86: 292–298, doi:10.1016/j.gaitpost.2021.03.025.

Jeyasurya, J., Loos, H. F. M. Van der, Hodgson, A. and Croft, E. A. (2013). Comparison of seat, waist, and arm sit-to-stand assistance modalities in elderly population. *Journal of Rehabilitation Research and Development* 50: 835–844, doi:10.1682/JRRD.2011.12.0233.

Joiner, W. M., Ajayi, O., Sing, G. C. and Smith, M. A. (2010). Linear hypergeneralization of learned dynamics across movement speeds reveals anisotropic, gain-encoding primitives for motor adaptation. *Journal of Neurophysiology* 105: 45–59, doi:10.1152/jn.00884.2009.

Joiner, W. M., Brayanov, J. B. and Smith, M. A. (2013). The training schedule affects the stability, not the magnitude, of the interlimb transfer of learned dynamics. *Journal of Neurophysiology* 110: 984–998, doi:10.1152/jn.01072.2012.

Joiner, W. M., Sing, G. C. and Smith, M. A. (2017). Temporal specificity of the initial adaptive response in motor adaptation. *PLOS Computational Biology* 13: e1005438, doi:10.1371/journal.pcbi.1005438.

Joiner, W. M. and Smith, M. A. (2008). Long-term retention explained by a model of short-term learning in the adaptive control of reaching. *Journal of Neurophysiology* 100: 2948–2955, doi:10.1152/jn.90706.2008.

Jolliffe, I. T. (1986). *Principal Component Analysis*. Springer Series in Statistics. New York: Springer.

Jolliffe, I. T. (2002). *Principal Component Analysis*. Springer Series in Statistics. New York: Springer, 2nd ed., doi:10.1007/b98835.

Jonas, E. and Kording, K. P. (2017). Could a neuroscientist understand a microprocessor? *PLOS Computational Biology* 13: e1005268, doi:10.1371/journal.pcbi.1005268.

Joyce, B. M. and Kirby, R. L. (1991). Canes, crutches and walkers. *American family physician* 43: 535–542.

Jutten, C. and Herault, J. (1991). Blind separation of sources, part i: An adaptive algorithm based on neuromimetic architecture. *Signal Processing* 24: 1–10, doi:10.1016/0165-1684(91)90079-X.

Kallin, K., Jensen, J., Olsson, L. L., Nyberg, L. and Gustafson, Y. (2004). Why the elderly fall in residential care facilities, and suggested remedies. *The Journal of family practice* 53: 41–52.

Kantak, S. S., Sullivan, K. J., Fisher, B. E., Knowlton, B. J. and Winstein, C. J. (2010). Neural substrates of motor memory consolidation depend on practice structure. *Nature Neuroscience* 13: 923–925, doi:10.1038/nn.2596.

Kantak, S. S. and Winstein, C. J. (2012). Learning-performance distinction and memory processes for motor skills: A focused review and perspective. *Behavioural Brain Research* 228: 219–231, doi:10.1016/j.bbr.2011.11.028.

Karniel, A. (2011). Open questions in computational motor control. *Journal of Integrative Neuroscience* 10: 385–411, doi:10.1142/S0219635211002749.

Karst, G. M. and Hasan, Z. (1991). Initiation rules for planar, two-joint arm movements: agonist selection for movements throughout the work space. *Journal of Neurophysiology* 66: 1579–1593, doi:10.1152/jn.1991.66.5.1579.

Kato, T., Sekiguchi, Y., Honda, K., Izumi, S.-I. and Kanetaka, H. (2020). Comparison of handrail reaction forces between two different handrails during sit-to-stand movement in the elderly. *Clinical Biomechanics* 80: 1–5, doi:10.1016/j.clinbiomech.2020.105130.

Kawato, M. (1999). Internal models for motor control and trajectory planning. *Current Opinion in Neurobiology* 9: 718–727, doi:10.1016/S0959-4388(99)00028-8.

Kenny, R. A., Romero-Ortuno, R. and Kumar, P. (2017). Falls in older adults. *Medicine* 45: 28–33, doi:10.1016/j.mpmed.2016.10.007.

Kholinne, E., Zulkarnain, R. F., Sun, Y. C., Lim, S., Chun, J.-M. and Jeon, I.-H. (2018). The different role of each head of the triceps brachii muscle in elbow extension. *Acta Orthopaedica et Traumatologica Turcica* 52: 201–205, doi:10.1016/j.aott.2018.02.005.

Khuna, L., Thaweewannakij, T., Wattanapan, P., Amatachaya, P. and Amatachaya, S. (2020). Five times sit-to-stand test for ambulatory individuals with spinal cord injury: a psychometric study on the effects of arm placements. *Spinal Cord* 58: 356–364, doi:10.1038/s41393-019-0372-3.

Kieliba, P., Tropea, P., Pirondini, E., Coscia, M., Micera, S. and Artoni, F. (2018). How are muscle synergies affected by electromyography pre-processing? *IEEE Transactions on Neural Systems and Rehabilitation Engineering* 26: 882–893, doi:10.1109/TNSRE.2018.2810859.

Kim, H. E., Avraham, G. and Ivry, R. B. (2021). The psychology of reaching: action selection, movement implementation, and sensorimotor learning. *Annual Review of Psychology* 72: 61–95, doi:10.1146/annurev-psych-010419-051053.

Kim, M., Kim, Y., Kim, H. and Yoon, B. (2018). Specific muscle synergies in national elite female ice hockey players in response to unexpected external perturbation. *Journal of sports sciences* 36: 319–325, doi:10.1080/02640414.2017.1306090.

Kim, M. H., Yi, C. H., Yoo, W. G. and Choi, B. R. (2011). Emg and kinematics analysis of the trunk and lower extremity during the sit-to-stand task while wearing shoes with different heel heights in healthy young women. *Human Movement Science* 30: 596–605, doi:10.1016/j.humov.2010.09.003.

Kim, S., Ogawa, K., Lv, J., Schweighofer, N. and Imamizu, H. (2015a). Neural substrates related to motor memory with multiple timescales in sensorimotor adaptation. *PLOS Biology* 13: e1002312, doi:10.1371/journal.pbio.1002312.

Kim, S., Oh, Y. and Schweighofer, N. (2015b). Between-trial forgetting due to interference and time in motor adaptation. *PLOS ONE* 10: e0142963, doi:10.1371/journal.pone.0142963.

King, M. A. and Yeadon, M. R. (2004). Maximising somersault rotation in tumbling. *Journal of Biomechanics* 37: 471–477, doi:10.1016/j.jbiomech.2003.09.008.

Kitago, T. and Krakauer, J. W. (2013). Chapter 8 - motor learning principles for neurorehabilitation. In Barnes, M. P. and Good, D. C. (eds), *Neurological Rehabilitation*. Elsevier, Handbook of Clinical Neurology *110*, 93–103, doi:https://doi.org/10.1016/B978-0-444-52901-5.00008-3.

Kitago, T., Ryan, S. L., Mazzoni, P., Krakauer, J. W. and Haith, A. M. (2013). Unlearning versus savings in visuomotor adaptation: comparing effects of washout, passage of time, and removal of errors on motor memory. *Frontiers in Human Neuroscience* 7: 1–7, doi: 10.3389/fnhum.2013.00307.

Ko, C.-Y., Kim, S.-B., Chang, Y., Choi, H.-J., Kang, S., Heo, Y., Ryu, J., Mun, M. and Kim, G. (2014). Assessment of forearm and plantar foot load in the elderly using a four-wheeled walker with armrest and the effect of armrest height. *Clinical Interventions in Aging* 9: 1759–1765, doi:10.2147/CIA.S70722.

Kogami, H., An, Q., Yang, N., Wang, R., Yoshida, K., Hamada, H., Yamakawa, H., Tamura, Y., Shimoda, S., Yamasaki, H., Yokoyama, M., Alnajjar, F., Hattori, N., Takahashi, K., Fujii, T., Otomune, H., Miyai, I., Yamashita, A. and Asama, H. (2021). Analysis of muscle synergy and kinematics in sit-to-stand motion of hemiplegic patients in subacute period. *Advanced Robotics* 35: 867–877, doi:10.1080/01691864.2021.1928547.

Komaris, D.-S., Govind, C., Murphy, A., Ewen, A. and Riches, P. (2018). Identification of movement strategies during the sit-to-walk movement in patients with knee osteoarthritis. *Journal of Applied Biomechanics* 34: 96–103, doi:10.1123/jab.2016-0279.

Komisar, V., Schooten, K. S. van, Aguiar, O. M. G., Shishov, N. and Robinovitch, S. N. (2023). Circumstances of falls during sit-to-stand transfers in older people: A cohort study of video-captured falls in long-term care. *Archives of Physical Medicine and Rehabilitation* 104: 533–540, doi:10.1016/j.apmr.2022.10.012.

Kotake, T., Dohi, N., Kajiwara, T., Sumi, N., Koyama, Y. and Miura, T. (1993). An analysis of sit-to-stand movements. *Archives of Physical Medicine and Rehabilitation* 74: 1095–1099, doi:10.1016/0003-9993(93)90068-L.

Kouzaki, M. and Masani, K. (2008). Reduced postural sway during quiet standing by light touch is due to finger tactile feedback but not mechanical support. *Experimental Brain Research* 188: 153–158, doi:10.1007/s00221-008-1426-5.

Krafft, F. C., Herzog, M., Stein, T. and Sloot, L. H. (2022). Young individuals are more stable and stand more upright when using rollator assistance during standing up and sitting down. *Frontiers in Bioengineering and Biotechnology* 10: 1–12, doi:10.3389/fbioe.2022.876349.

Krakauer, J. W. (2005). Adaptation to visuomotor transformations: Consolidation, interference, and forgetting. *Journal of Neuroscience* 25: 473–478, doi:10.1523/JNEUROSCI.4218-04.2005.

Krakauer, J. W. (2009). Motor learning and consolidation: The case of visuomotor rotation. In Sternad, D. (ed.), *Progress in Motor Control: A Multidisciplinary Perspective*. Boston: Springer, 405–421, doi:10.1007/978-0-387-77064-2_21.

Krakauer, J. W., Ghazanfar, A. A., Gomez-Marin, A., MacIver, M. A. and Poeppel, D. (2017). Neuroscience needs behavior: Correcting a reductionist bias. *Neuron* 93: 480–490, doi:10.1016/j.neuron.2016.12.041.

Krakauer, J. W., Ghilardi, M.-F. and Ghez, C. (1999). Independent learning of internal models for kinematic and dynamic control of reaching. *Nature Neuroscience* 2: 1026–1031, doi:10.1038/14826.

Krakauer, J. W., Hadjiosif, A. M., Xu, J., Wong, A. L. and Haith, A. M. (2019). Motor learning. *Comprehensive Physiology* 9: 613–663, doi:10.1002/cphy.

Krakauer, J. W. and Mazzoni, P. (2011). Human sensorimotor learning: adaptation, skill, and beyond. *Current Opinion in Neurobiology* 21: 636–644, doi:10.1016/j.conb.2011.06.012.

Krakauer, J. W., Mazzoni, P., Ghazizadeh, A., Ravindran, R. and Shadmehr, R. (2006). Generalization of motor learning depends on the history of prior action. *PLOS Biology* 4: e316, doi:10.1371/journal.pbio.0040316.

Krakauer, J. W., Pine, Z. M., Ghilardi, M.-F. and Ghez, C. (2000). Learning of visuomotor transformations for vectorial planning of reaching trajectories. *Journal of Neuroscience* 20: 8916–8924, doi:10.1523/JNEUROSCI.20-23-08916.2000.

Krakauer, J. W. and Shadmehr, R. (2006). Consolidation of motor memory. *Trends in Neurosciences* 29: 58–64, doi:10.1016/j.tins.2005.10.003.

Kriegeskorte, N. and Douglas, P. K. (2018). Cognitive computational neuroscience. *Nature Neuroscience* 21: 1148–1160, doi:10.1038/s41593-018-0210-5.

Kristiansen, M., Madeleine, P., Hansen, E. A. and Samani, A. (2015). Inter-subject variability of muscle synergies during bench press in power lifters and untrained individuals. *Scandinavian journal of medicine & science in sports* 25: 89–97, doi:10.1111/sms.12167.

Kruk, E. van der, Silverman, A. K., Koizia, L., Reilly, P., Fertleman, M. and Bull, A. M. J. (2021a). Age-related compensation: Neuromusculoskeletal capacity, reserve & movement objectives. *Journal of Biomechanics* 122, doi:10.1016/j.jbiomech.2021.110385.

Kruk, E. van der, Silverman, A. K., Reilly, P. and Bull, A. M. J. (2021b). Compensation due to age-related decline in sit-to-stand and sit-to-walk. *Journal of Biomechanics* 122, doi:10.1016/j.jbiomech.2021.110411.

Kruk, E. van der, Strutton, P., Koizia, L. J., Fertleman, M., Reilly, P. and Bull, A. M. J. (2022). Why do older adults stand-up differently to young adults?: investigation of compensatory movement strategies in sit-to-walk. *npj Aging* 8: 1–19, doi:10.1038/s41514-022-00094-x.

Künzell, S. and Lukas, S. (2011). Facilitation effects of a preparatory skateboard training on the learning of snowboarding. *Kinesiology* 43: 56–63.

Lacquaniti, F., Ivanenko, Y. P. and Zago, M. (2012). Patterned control of human locomotion: Control of human locomotion. *The Journal of Physiology* 590: 2189–2199, doi:10.1113/jphysiol.2011.215137.

Landin, D. K., Hebert, E. P. and Fairweather, M. (1993). The effects of variable practice on the performance of a basketball skill. *Research Quarterly for Exercise and Sport* 64: 232–237, doi:10.1080/02701367.1993.10608803.

Lanza, M. B., Arbuco, B., Ryan, A. S., Shipper, A. G., Gray, V. L. and Addison, O. (2022). Systematic review of the importance of hip muscle strength, activation, and structure in balance and mobility tasks. *Archives of Physical Medicine and Rehabilitation* 103: 1651–1662, doi: 10.1016/j.apmr.2021.12.008.

Lavallière, M., D'Ambrosio, L., Gennis, A., Burstein, A., Godfrey, K. M., Waerstad, H., Puleo, R. M., Lauenroth, A. and Coughlin, J. F. (2017). Walking a mile in another's shoes: The impact of wearing an age suit. *Gerontology & Geriatrics Education* 38: 171–187, doi:10.1080/02701960.2015.1079706.

Leardini, A., Biagi, F., Merlo, A., Belvedere, C. and Benedetti, M. G. (2011). Multi-segment trunk kinematics during locomotion and elementary exercises. *Clinical Biomechanics* 26: 562–571, doi:10.1016/j.clinbiomech.2011.01.015.

Lee, D. and Seung, H. S. (2001). Algorithms for non-negative matrix factorization. In Leen, T., Dietterich, T. and Tresp, V. (eds), *Advances in Neural Information Processing Systems 13 - Proceedings of the 2000 Conference, NIPS 2000*. Neural information processing systems foundation, Advances in Neural Information Processing Systems *13*, 556–563.

Lee, D.-C. A., Dissanayaka, T., Burton, E., Meyer, C., Hunter, S. W., Suttanon, P., Ekegren, C. L., Stout, J. C., Dawes, H. and Hill, K. D. (2022). Effectiveness of gait aid prescription for improving spatiotemporal gait parameters and associated outcomes in community-dwelling older people: a systematic review. *Disability and Rehabilitation* 44: 6139–6154, doi:10.1080/09638288.2021.1958930.

Lee, D. D. and Seung, H. S. (1999). Learning the parts of objects by non-negative matrix factorization. *Nature* 401: 788–791, doi:10.1038/44565.

Lee, J.-Y. and Schweighofer, N. (2009). Dual adaptation supports a parallel architecture of motor memory. *Journal of Neuroscience* 29: 10396–10404, doi:10.1523/JNEUROSCI.1294-09.2009.

Lee, T. D. and Magill, R. A. (1983). The locus of contextual interference in motor-skill acquisition. *Journal of Experimental Psychology: Learning, Memory, and Cognition* 9: 730, doi:10.1037/0278-7393.9.4.730.

Lee, T. D., Magill, R. A. and Weeks, D. J. (1985). Influence of practice schedule on testing schema theory predictions in adults. *Journal of motor behavior* 17: 283–299, doi:10.1080/00222895.1985.10735350.

Lee, W. A. (1984). Neuromotor synergies as a basis for coordinated intentional action. *Journal of Motor Behavior* 16: 135–170, doi:10.1080/00222895.1984.10735316.

Lees, A., Vanrenterghem, J. and Clercq, D. D. (2004). Understanding how an arm swing enhances performance in the vertical jump. *Journal of Biomechanics* 37: 1929–1940, doi:10.1016/j.jbiomech.2004.02.021.

Lehtola, S., Koistinen, P. and Luukinen, H. (2006). Falls and injurious falls late in home-dwelling life. *Archives of Gerontology and Geriatrics* 42: 217–224, doi:10.1016/j.archger.2005.07.002.

Leib, R., Howard, I. S., Millard, M. and Franklin, D. W. (2024). Behavioral motor performance. *Comprehensive Physiology* 14: 5179–5224, doi:10.1002/cphy.c220032.

Leib, R., Russo, M., d'Avella, A. and Nisky, I. (2020). A bang-bang control model predicts the triphasic muscles activity during hand reaching. *Journal of Neurophysiology* 124: 295–304, doi:10.1152/jn.00132.2020.

Lelis-Torres, N., Ugrinowitsch, H., Apolinário-Souza, T. and Lage, G. M. (2018). The contextual interference effect in the learning of a manual aiming task. *Journal of Physical Education* 29: e2904, doi:10.4025/jphyseduc.v29i1.2904.

Lemay, M. A., Calagan, J., Hogan, N. and Bizzi, E. (2001). Modulation and vectorial summation of the spinalized frog's hindlimb end-point force produced by intraspinal electrical stimulation of the cord. *IEEE transactions on neural systems and rehabilitation engineering* 9: 12–23.

Leporace, G., Batista, L. A., Muniz, A. M., Zeitoune, G., Luciano, T., Metsavaht, L. and Nadal, J. (2012). Classification of gait kinematics of anterior cruciate ligament reconstructed subjects using principal component analysis and regressions modelling. In *2012 Annual International Conference of the IEEE Engineering in Medicine and Biology Society*, 6514–6517, doi: 10.1109/EMBC.2012.6347486.

Leung, C.-Y. and Yeh, P.-C. (2011). Vertical force and wrist deviation angle when using a walker to stand up and sit down. *Perceptual and Motor Skills* 113: 229–241, doi:10.2466/10.15.26.PMS.113.4.229-241.

Levine, A. J., Hinckley, C. A., Hilde, K. L., Driscoll, S. P., Poon, T. H., Montgomery, J. M. and Pfaff, S. L. (2014). Identification of a cellular node for motor control pathways. *Nature Neuroscience* 17: 586–593, doi:10.1038/nn.3675.

Liaw, M.-Y., Chen, C.-L., Pei, Y.-C., Leong, C.-P. and Lau, Y.-C. (2009). Comparison of the static and dynamic balance performance in young, middle-aged, and elderly healthy people. *Chang Gung Medical Journal* 32: 297–304.

Lindemann, U., Schwenk, M., Klenk, J., Kessler, M., Weyrich, M., Kurz, F. and Becker, C. (2016). Problems of older persons using a wheeled walker. *Aging Clinical and Experimental Research* 28: 215–220, doi:10.1007/s40520-015-0410-8.

Lockette, K. (2011). *A caregiver's complete guide for safe mobility and independence in the home*. Minneapolis, MN: Two Harbors Press.

Loram, I. D., Maganaris, C. N. and Lakie, M. (2005). Human postural sway results from frequent, ballistic bias impulses by soleus and gastrocnemius. *The Journal of Physiology* 564: 295–311, doi:10.1113/jphysiol.2004.076307.

Louwerens, J. W. K., Linge, B. V., De Klerk, L. W. L., Mulder, P. G. H. and Snijders, C. J. (1995). Peroneus longus and tibialis anterior muscle activity in the stance phase: A quantified electromyographic study of 10 controls and 25 patients with chronic ankle instability. *Acta Orthopaedica Scandinavica* 66: 517–523, doi:10.3109/17453679509002306.

Lynch, N. A., Metter, E. J., Lindle, R. S., Fozard, J. L., Tobin, J. D., Roy, T. A., Fleg, J. L. and Hurley, B. F. (1999). Muscle quality. I. Age-associated differences between arm and leg muscle groups. *Journal of applied physiology* 86: 188–194, doi:10.1152/jappl.1999.86.1.188.

Magill, R. and Anderson, D. I. (2010). *Motor learning and control*. New York: McGraw-Hill Publishing.

Magill, R. A. and Hall, K. G. (1990). A review of the contextual interference effect in motor skill acquisition. *Human movement science* 9: 241–289, doi:10.1016/0167-9457(90)90005-X.

Mahdi, A., Lin, J. F.-S. and Mombaur, K. (2022). Maintaining mobility in older age - design and initial evaluation of the robot SkyWalker for walking & sit-to-stand assistance. In *2022 9th IEEE RAS/EMBS International Conference for Biomedical Robotics and Biomechatronics (BioRob)*, 01–08, doi:10.1109/BioRob52689.2022.9925362.

Malfait, N., Shiller, D. M. and Ostry, D. J. (2002). Transfer of motor learning across arm configurations. *The Journal of Neuroscience* 22: 9656–9660, doi:10.1523/JNEUROSCI.22-22-09656.2002.

Mann, W. C., Hurren, D., Tomita, M. and Charvat, B. (1995). An analysis of problems with walkers encountered by elderly persons. *Physical & Occupational Therapy in Geriatrics* 13: 1–23, doi:10.1080/J148v13n01_01.

Mardia, K. V., Kent, J. T. and Bibby, J. M. (1979). *Multivariate analysis*. Probability and mathematical statistics. London, New York: Academic Press.

Marr, D. (1982). *Vision: A Computational Investigation into the Human Representation and Processing of Visual Information.* USA: Henry Holt and Co., Inc.

Martin, T. A., Keating, J. G., Goodkin, H. P., Bastian, A. J. and Thach, W. T. (1996). Throwing while looking through prisms: I. focal olivocerebellar lesions impair adaptation. *Brain* 119: 1183–1198, doi:10.1093/brain/119.4.1183.

Maselli, A., Gordon, J., Eluchans, M., Lancia, G. L., Thiery, T., Moretti, R., Cisek, P. and Pezzulo, G. (2023). Beyond simple laboratory studies: Developing sophisticated models to study rich behavior. *Physics of Life Reviews* 46: 220–244, doi:10.1016/j.plrev.2023.07.006.

Maslovat, D., Chua, R., Lee, T. D. and Franks, I. M. (2004). Contextual interference: Single task versus multi-task learning. *Motor Control* 8: 213–233, doi:10.1123/mcj.8.2.213.

Mathew, J., Lefèvre, P. and Crevecoeur, F. (2021). Savings in human force field learning supported by feedback adaptation. *eneuro* 8: ENEURO.0088–21.2021, doi:10.1523/ENEURO.0088-21.2021.

Mattar, A. A. G. and Ostry, D. J. (2007). Modifiability of generalization in dynamics learning. *Journal of Neurophysiology* 98: 3321–3329, doi:10.1152/jn.00576.2007.

Mattar, A. A. G. and Ostry, D. J. (2010). Generalization of dynamics learning across changes in movement amplitude. *Journal of Neurophysiology* 104: 426–438, doi:10.1152/jn.00886.2009.

Mazzà, C., Benvenuti, F., Bimbi, C. and Stanhope, S. (2004). Association between subject functional status, seat height, and movement strategy in sit-to-stand performance. *Journal of the American Geriatrics Society* 52: 1750–1754, doi:10.1111/j.1532-5415.2004.52472.x.

McDougle, S. D., Bond, K. M. and Taylor, J. A. (2015). Explicit and implicit processes constitute the fast and slow processes of sensorimotor learning. *Journal of Neuroscience* 35: 9568–9579, doi:10.1523/JNEUROSCI.5061-14.2015.

McLaughlin, S. C. (1967). Parametric adjustment in saccadic eye movements. *Perception & Psychophysics* 2: 359–362, doi:10.3758/BF03210071.

McLeod, P., Kettelkamp, D., Srinivasan, V. and Henderson, O. (1975). Measurements of repetitive activities of the knee. *Journal of Biomechanics* 8: 369–373, doi:10.1016/0021-9290(75)90072-X.

McNamee, D. and Wolpert, D. M. (2019). Internal models in biological control. *Annual Review of Control, Robotics, and Autonomous Systems* 2: 339–364, doi:10.1146/annurev-control-060117-105206.

Mileti, I., Zampogna, A., Santuz, A., Asci, F., Del Prete, Z., Arampatzis, A., Palermo, E. and Suppa, A. (2020). Muscle synergies in parkinson's disease. *Sensors* 20: 3209, doi:10.3390/s20113209.

Millington, P. J., Myklebust, B. M. and Shambes, G. M. (1992). Biomechanical analysis of the sit-to-stand motion in elderly persons. *Archives of Physical Medicine and Rehabilitation* 73: 609–617., doi:10.5555/uri:pii:000399939290124F.

Milner, T. and Franklin, D. W. (2005). Impedance control and internal model use during the initial stage of adaptation to novel dynamics in humans. *The Journal of physiology* 567: 651–64, doi:10.1113/jphysiol.2005.090449.

Mohamad, I. B. and Usman, D. (2013). Standardization and its effects on k-means clustering algorithm. *Research Journal of Applied Sciences, Engineering and Technology* 6: 3299–3303, doi:10.19026/rjaset.6.3638.

Mohebbi, A. (2020). Human-robot interaction in rehabilitation and assistance: a review. *Current Robotics Reports* 1: 131–144, doi:10.1007/s43154-020-00015-4.

Moher, J. and Song, J.-H. (2019). A comparison of simple movement behaviors across three different devices. *Attention, Perception, & Psychophysics* 81: 2558–2569, doi:10.3758/s13414-019-01856-8.

Molier, B. I., Prange, G. B., Buurke, J. H. and Asseldonk, E. H. F. van (2011). Influence of reaching direction on visuomotor adaptation: An explorative study. In *2011 IEEE International Conference on Rehabilitation Robotics*, 1–5, doi:10.1109/ICORR.2011.5975374.

Morasso, P. (1981). Spatial control of arm movements. *Experimental Brain Research* 42: 223–227, doi:10.1007/BF00236911.

Moreland, J. D., Richardson, J. A., Goldsmith, C. H. and Clase, C. M. (2004). Muscle weakness and falls in older adults: A systematic review and meta-analysis. *Journal of the American Geriatrics Society* 52: 1121–1129, doi:10.1111/j.1532-5415.2004.52310.x.

Mouritz, A. P. (2012). *Introduction to Aerospace Materials*. Cambridge: Woodhead Publishing.

Muceli, S., Boye, A. T., d'Avella, A. and Farina, D. (2010). Identifying representative synergy matrices for describing muscular activation patterns during multidirectional reaching in the horizontal plane. *Journal of Neurophysiology* 103: 1532–1542, doi:10.1152/jn.00559.2009.

Mundt, M., Batista, J. P., Markert, B., Bollheimer, C. and Laurentius, T. (2019). Walking with rollator: a systematic review of gait parameters in older persons. *European Review of Aging and Physical Activity* 16: 15, doi:10.1186/s11556-019-0222-5.

Munro, B. J. and Steele, J. R. (1998). Facilitating the sit-to-stand transfer: a review. *Physical Therapy Reviews* 3: 213–224, doi:10.1179/ptr.1998.3.4.213.

Mussa-Ivaldi, F. (1997). Nonlinear force fields: a distributed system of control primitives for representing and learning movements. In *Proceedings 1997 IEEE International Symposium on Computational Intelligence in Robotics and Automation CIRA'97. "Towards New Computational Principles for Robotics and Automation"*, 84–90, doi:10.1109/CIRA.1997.613842.

Mussa-Ivaldi, F. A. (1999). Modular features of motor control and learning. *Current Opinion in Neurobiology* 9: 713–717, doi:10.1016/S0959-4388(99)00029-X.

Mussa-Ivaldi, F. A. and Bizzi, E. (2000). Motor learning through the combination of primitives. *Philosophical Transactions of the Royal Society of London. Series B: Biological Sciences* 355: 1755–1769, doi:10.1098/rstb.2000.0733.

Mussa-Ivaldi, F. A. and Giszter, S. F. (1992). Vector field approximation: a computational paradigm for motor control and learning. *Biological Cybernetics* 67: 491–500, doi:10.1007/BF00198756.

Mussa-Ivaldi, F. A., Giszter, S. F. and Bizzi, E. (1994). Linear combinations of primitives in vertebrate motor control. *Proceedings of the National Academy of Sciences* 91: 7534–7538, doi:10.1073/pnas.91.16.7534.

Neptune, R. R., Clark, D. J. and Kautz, S. A. (2009). Modular control of human walking: A simulation study. *Journal of Biomechanics* 42: 1282–1287, doi:10.1016/j.jbiomech.2009.03.009.

Nickerson, K. A., Diaz, K. and Muir, B. C. (2023). Circumstances of falls among older adult walker users in long-term care and the associated walker design deficits. *Assistive Technology* 0: 1–6, doi:10.1080/10400435.2023.2267623.

Nickerson, K. A., Diaz, K. and Muir, B. C. (2024). Circumstances of falls among older adult walker users in long-term care and the associated walker design deficits. *Assistive Technology* 36: 248–53, doi:10.1080/10400435.2023.2267623.

Nikfekr, E., Kerr, K., Attfield, S. and Playford, E. (2002). Trunk movement in parkinson's disease during rising from seated position. *Movement Disorders* 17: 274–282, doi:10.1002/mds.10073.

Norman-Gerum, V. and McPhee, J. (2020). Comprehensive description of sit-to-stand motions using force and angle data. *Journal of Biomechanics* 112, doi:10.1016/j.jbiomech.2020.110046.

Nüesch, C., Valderrabano, V., Huber, C., Tscharner, V. von and Pagenstert, G. (2012). Gait patterns of asymmetric ankle osteoarthritis patients. *Clinical Biomechanics* 27: 613–618, doi:10.1016/j.clinbiomech.2011.12.016.

Oates, A., Unger, J., Arnold, C., Fung, J. and Lanovaz, J. (2017). The effect of light touch on balance control during overground walking in healthy young adults. *Heliyon* 3: e00484, doi:10.1016/j.heliyon.2017.e00484.

Oldfield, R. C. (1971). The assessment and analysis of handedness: The edinburgh inventory. *Neuropsychologia* 9: 97–113, doi:10.1016/0028-3932(71)90067-4.

O'Loughlin, J. L., Robitaille, Y., Boivin, J.-F. and Suissa, S. (1993). Incidence of and risk factors for falls and injurious falls among the community-dwelling elderly. *American journal of epidemiology* 137: 342–354, doi:10.1093/oxfordjournals.aje.a116681.

Orozco, S. P., Albert, S. T. and Shadmehr, R. (2021). Adaptive control of movement deceleration during saccades. *PLOS Computational Biology* 17: e1009176, doi:10.1371/journal.pcbi.1009176.

Oscari, F., Finetto, C., Kautz, S. A. and Rosati, G. (2016). Changes in muscle coordination patterns induced by exposure to a viscous force field. *Journal of NeuroEngineering and Rehabilitation* 13: 58, doi:10.1186/s12984-016-0164-3.

Overduin, S. A., d'Avella, A., Roh, J. and Bizzi, E. (2008). Modulation of muscle synergy recruitment in primate grasping. *Journal of Neuroscience* 28: 880–892, doi:10.1523/JNEUROSCI.2869-07.2008.

Pai, Y.-C., Naughton, B., Chang, R. and Rogers, M. (1994). Control of body centre of mass momentum during sit-to-stand among young and elderly adults. *Gait & Posture* 2: 109–116, doi:10.1016/0966-6362(94)90100-7.

Panwalkar, N. and Aruin, A. S. (2013). Role of ankle foot orthoses in the outcome of clinical tests of balance. *Disability and Rehabilitation: Assistive Technology* 8: 314–320, doi:10.3109/17483107.2012.721158.

Papa, E. and Cappozzo, A. (2000). Sit-to-stand motor strategies investigated in able-bodied young and elderly subjects. *Journal of Biomechanics* 33: 1113–1122, doi:10.1016/S0021-9290(00)00046-4.

Park, S. and Caldwell, G. E. (2022). Muscle synergies are modified with improved task performance in skill learning. *Human Movement Science* 83, doi:10.1016/j.humov.2022.102946.

Pataky, T. C., Robinson, M. A. and Vanrenterghem, J. (2016). Region-of-interest analyses of one-dimensional biomechanical trajectories: bridging 0d and 1d theory, augmenting statistical power. *PeerJ* 4, doi:10.7717/peerj.2652.

Pataky, T. C., Vanrenterghem, J., Robinson, M. A. and Liebl, D. (2019). On the validity of statistical parametric mapping for nonuniformly and heterogeneously smooth one-dimensional biomechanical data. *Journal of Biomechanics* 91: 114–123, doi:10.1016/j.jbiomech.2019.05.018.

Pauwels, L., Swinnen, S. P. and Beets, I. A. M. (2014). Contextual interference in complex bimanual skill learning leads to better skill persistence. *PLOS ONE* 9: e100906, doi:10.1371/journal.pone.0100906.

Pearson, K. (1901). Liii. on lines and planes of closest fit to systems of points in space. *The London, Edinburgh, and Dublin Philosophical Magazine and Journal of Science* 2: 559–572.

Perera, C. K., Gopalai, A. A., Gouwanda, D., Ahmad, S. A. and Salim, M. S. B. (2023). Sit-to-walk strategy classification in healthy adults using hip and knee joint angles at gait initiation. *Scientific Reports* 13: 16640, doi:10.1038/s41598-023-43148-0.

Peri, E., Xu, L., Ciccarelli, C., Vandenbussche, N. L., Xu, H., Long, X., Overeem, S., Dijk, J. P. van and Mischi, M. (2021). Singular value decomposition for removal of cardiac interference from trunk electromyogram. *Sensors* 21: 573, doi:10.3390/s21020573.

Perotto, A. O. (2011). *ANATOMICAL GUIDE FOR THE ELECTROMYOGRAPHER: The Limbs and Trunk*. Springfield, IL: Charles C Thomas Publisher, 5th ed.

Perry, S. B., Marchetti, G. F., Wagner, S. and Wilton, W. (2006). Predicting caregiver assistance required for sit-to-stand following rehabilitation for acute stroke. *Journal of Neurologic Physical Therapy* 30: 2–11, doi:10.1097/01.NPT.0000282144.72703.cb.

Pickle, N. T., Silverman, A. K., Wilken, J. M. and Fey, N. P. (2019). Statistical analysis of timeseries data reveals changes in 3d segmental coordination of balance in response to prosthetic ankle power on ramps. *Scientific Reports* 9: 1272, doi:10.1038/s41598-018-37581-9.

Poggensee, K. L. and Collins, S. H. (2021). How adaptation, training, and customization contribute to benefits from exoskeleton assistance. *Science Robotics* 6: eabf1078, doi:10.1126/scirobotics.abf1078.

Porter, C., Greenwood, D., Panchuk, D. and Pepping, G.-J. (2020). Learner-adapted practice promotes skill transfer in unskilled adults learning the basketball set shot. *European Journal of Sport Science* 20: 61–71, doi:10.1080/17461391.2019.1611931.

Prudente, C., Paula, F. Rodrigues-de and Faria, C. D. C. M. (2013). Lower limb muscle activation during the sit-to-stand task in subjects who have had a stroke. *American Journal of Physical Medicine & Rehabilitation* 92: 666, doi:10.1097/PHM.0b013e318282c87a.

Ranaldi, S., Gizzi, L., Severini, G. and Marchis, C. D. (2023). Optimal identification of muscle synergies from typical sit-to-stand clinical tests. *IEEE Open Journal of Engineering in Medicine and Biology* : 1–8doi:10.1109/OJEMB.2023.3263123.

Rand, M. K. and Rentsch, S. (2017). Eye-hand coordination during visuomotor adaptation: effects of hemispace and joint coordination. *Experimental Brain Research* 235: 3645–3661, doi:10.1007/s00221-017-5088-z.

Ranganathan, R., Lee, M.-H. and Newell, K. M. (2020). Repetition without repetition: Challenges in understanding behavioral flexibility in motor skill. *Frontiers in Psychology* 11, doi:10.3389/fpsyg.2020.02018.

Rapp, K., Becker, C., Cameron, I. D., König, H.-H. and Büchele, G. (2012). Epidemiology of falls in residential aged care: analysis of more than 70,000 falls from residents of bavarian nursing homes. *Journal of the American Medical Directors Association* 13: p187.e1–187.e6, doi:10.1016/j.jamda.2011.06.011.

Raviv, L., Lupyan, G. and Green, S. C. (2022). How variability shapes learning and generalization. *Trends in Cognitive Sciences* 26: 462–483, doi:10.1016/j.tics.2022.03.007.

Rein, R., Button, C., Davids, K. and Summers, J. (2010). Cluster analysis of movement patterns in multiarticular actions: a tutorial. *Motor Control* 14: 211–239, doi:10.1123/mcj.14.2.211.

Reisman, D. S., Scholz, J. P. and Schöner, G. (2002). Coordination underlying the control of whole body momentum during sit-to-stand. *Gait & Posture* 15: 45–55, doi:10.1016/S0966-6362(01)00158-8.

Rezazadeh, A. and Berniker, M. (2019). Force field generalization and the internal representation of motor learning. *PLOS ONE* 14: e0225002, doi:10.1371/journal.pone.0225002.

Richmond, S. B., Fling, B. W., Lee, H. and Peterson, D. S. (2021). The assessment of center of mass and center of pressure during quiet stance: Current applications and future directions. *Journal of Biomechanics* 123: 110485, doi:10.1016/j.jbiomech.2021.110485.

Riley, P. O., Schenkman, M. L., Mann, R. W. and Hodge, W. A. (1991). Mechanics of a constrained chair-rise. *Journal of Biomechanics* 24: 77–85, doi:10.1016/0021-9290(91)90328-K.

Rinaldi, L., Yeung, L.-F., Lam, P. C.-H., Pang, M. Y. C., Tong, R. K.-Y. and Cheung, V. C. K. (2020). Adapting to the mechanical properties and active force of an exoskeleton by altering muscle synergies in chronic stroke survivors. *IEEE Transactions on Neural Systems and Rehabilitation Engineering* 28: 2203–2213, doi:10.1109/TNSRE.2020.3017128.

Robertson, G., Caldwell, G., Hamill, J., Kamen, G. and Whittlesey, S. (2013). *Research methods in biomechanics*. Champaign: Human Kinetics, 2nd ed.

Robinovitch, S. N., Feldman, F., Yang, Y., Schonnop, R., Leung, P. M., Sarraf, T., Sims-Gould, J. and Loughin, M. (2013). Video capture of the circumstances of falls in elderly people residing in long-term care: an observational study. *The Lancet* 381: 47–54, doi:10.1016/S0140-6736(12)61263-X.

Roebroeck, M., Doorenbosch, C., Harlaar, J., Jacobs, R. and Lankhorst, G. (1994). Biomechanics and muscular activity during sit-to-stand transfer. *Clinical Biomechanics* 9: 235–244, doi:10.1016/0268-0033(94)90004-3.

Rosenbaum, D. A. (2009). *Human Motor Control*. London, Oxford, Boston, New York, San Diego: Academic Press, 2nd ed., doi:10.1016/B978-0-12-374226-1.X0001-0.

Rosner, B. (1983). Percentage points for a generalized ESD many-outlier procedure. *Technometrics* 25: 165–172, doi:10.2307/1268549.

Rubenstein, L. Z. (2006). Falls in older people: epidemiology, risk factors and strategies for prevention. *Age and ageing* 35: ii37–ii41, doi:10.1093/ageing/afl084.

Rucci, M., Bullock, D. and Santini, F. (2007). Integrating robotics and neuroscience: brains for robots, bodies for brains. *Advanced Robotics* 21: 1115–1129, doi:10.1163/156855307781389428.

Rugy, A. de, Loeb, G. E. and Carroll, T. J. (2012). Muscle coordination is habitual rather than optimal. *Journal of Neuroscience* 32: 7384–7391, doi:10.1523/JNEUROSCI.5792-11.2012.

Russell, D. M. and Haworth, J. L. (2014). Walking at the preferred stride frequency maximizes local dynamic stability of knee motion. *Journal of Biomechanics* 47: 102–108, doi:10.1016/j.jbiomech.2013.10.012.

Russo, M., D'Andola, M., Portone, A., Lacquaniti, F. and d'Avella, A. (2014). Dimensionality of joint torques and muscle patterns for reaching. *Frontiers in Computational Neuroscience* 8, doi:10.3389/fncom.2014.00024.

Russo, M., Scano, A., Brambilla, C. and d'Avella, A. (2024). Synergyanalyzer: A matlab toolbox implementing mixed-matrix factorization to identify kinematic-muscular synergies. *Computer Methods and Programs in Biomedicine* 251, doi:10.1016/j.cmpb.2024.108217.

Sadeghi, M., Ingram, J. N. and Wolpert, D. M. (2018). Adaptive coupling influences generalization of sensorimotor learning. *PLOS ONE* 13: e0207482, doi:10.1371/journal.pone.0207482.

Sadeh, S., Gobert, D., Shen, K.-H., Foroughi, F. and Hsiao, H.-Y. (2023). Biomechanical and neuromuscular control characteristics of sit-to-stand transfer in young and older adults: A systematic review with implications for balance regulation mechanisms. *Clinical Biomechanics* 109, doi:10.1016/j.clinbiomech.2023.106068.

Safavynia, S. A. and Ting, L. H. (2012). Task-level feedback can explain temporal recruitment of spatially fixed muscle synergies throughout postural perturbations. *Journal of Neurophysiology* 107: 159–177, doi:10.1152/jn.00653.2011.

Safavynia, S. A., Torres-Oviedo, G. and Ting, L. H. (2011). Muscle synergies: Implications for clinical evaluation and rehabilitation of movement. *Topics in Spinal Cord Injury Rehabilitation* 17: 16–24, doi:10.1310/sci1701-16.

Salari, N., Darvishi, N., Ahmadipanah, M., Shohaimi, S. and Mohammadi, M. (2022). Global prevalence of falls in the older adults: a comprehensive systematic review and meta-analysis. *Journal of Orthopaedic Surgery and Research* 17: 334, doi:10.1186/s13018-022-03222-1.

Saltiel, P., d'Avella, A., Wyler-Duda, K. and Bizzi, E. (2016). Synergy temporal sequences and topography in the spinal cord: evidence for a traveling wave in frog locomotion. *Brain Structure and Function* 221: 3869–3890, doi:10.1007/s00429-015-1133-5.

Saltiel, P., Wyler-Duda, K., D'Avella, A., Tresch, M. C. and Bizzi, E. (2001). Muscle synergies encoded within the spinal cord: Evidence from focal intraspinal nmda iontophoresis in the frog. *Journal of Neurophysiology* 85: 605–619, doi:10.1152/jn.2001.85.2.605.

Salzman, A., Torburn, L. and Perry, J. (1993). Contribution of rectus femoris and vasti to knee extension. an electromyographic study. *Clinical Orthopaedics and Related Research* : 236–243.

Sands, W. A. (2018). Transfer of learning tasks to a final skill. In Jemni, M. (ed.), *The science of gymnastics: advanced concepts*. London: Routledge, 2nd ed., 233–235, doi:10.4324/9781315203805.

Santello, M., Flanders, M. and Soechting, J. F. (1998). Postural hand synergies for tool use. *Journal of Neuroscience* 18: 10105–10115, doi:10.1523/JNEUROSCI.18-23-10105.1998.

Sarwary, A. M. E., Wischnewski, M., Schutter, D. J. L. G., Selen, L. P. J. and Medendorp, W. P. (2018). Corticospinal correlates of fast and slow adaptive processes in motor learning. *Journal of Neurophysiology* 120: 2011–2019, doi:10.1152/jn.00488.2018.

Savelsbergh, G., Wimmers, R., Van Der Kamp, J. and Davids, K. (1999). The development of movement control and coordination. In Kalverboer, A. F., Genta, M. L. and Hopkins, J. B. (eds), *Current Issues in Developmental Psychology: Biopsychological Perspectives*. Dordrecht: Springer Netherlands, 107–136, doi:10.1007/978-94-011-4507-7_5.

Sawers, A., Allen, J. L. and Ting, L. H. (2015). Long-term training modifies the modular structure and organization of walking balance control. *Journal of Neurophysiology* 114: 3359–3373, doi:10.1152/jn.00758.2015.

Scano, A., Mira, R. M. and d'Avella, A. (2022). Mixed matrix factorization: a novel algorithm for the extraction of kinematic-muscular synergies. *Journal of Neurophysiology* 127: 529–547, doi:10.1152/jn.00379.2021.

Scarborough, D. M., McGibbon, C. A. and Krebs, D. E. (2007). Chair rise strategies in older adults with functional limitations. *The Journal of Rehabilitation Research and Development* 44: 33, doi:10.1682/JRRD.2005.08.0134.

Schaal, S. (2007). The new robotics—towards human-centered machines. *HFSP Journal* 1: 115–126, doi:10.2976/1.2748612.

Scheidt, R. A., Reinkensmeyer, D. J., Conditt, M. A., Rymer, W. Z. and Mussa-Ivaldi, F. A. (2000). Persistence of motor adaptation during constrained, multi-joint, arm movements. *Journal of Neurophysiology* 84: 853–862, doi:10.1152/jn.2000.84.2.853.

Schenkman, M., Berger, R. A., Riley, P. O., Mann, R. W. and Hodge, W. A. (1990). Whole-body movements during rising to standing from sitting. *Physical Therapy* 70: 638–648, doi: 10.1093/ptj/70.10.638.

Schmidt, R. A. and Lee, T. D. (2011). *Motor control and learning: a behavioral emphasis*. Champaign: Human Kinetics, 5th ed.

Schmidt, R. A., Lee, T. D., Winstein, C. J., Wulf, G. and Zelaznik, H. N. (2019). *Motor control and learning: a behavioral emphasis*. Champaign: Human Kinetics, 6th ed.

Schooten, K. S. van, Yang, Y., Feldman, F., Leung, M., McKay, H., Sims-Gould, J. and Robinovitch, S. N. (2018). The association between fall frequency, injury risk, and characteristics of falls in older residents of long-term care: Do recurrent fallers fall more safely? *The Journals of Gerontology: Series A* 73: 786–791, doi:10.1093/gerona/glx196.

Schultz, A. B., Alexander, N. B. and Ashton-Miller, J. A. (1992). Biomechanical analyses of rising from a chair. *Journal of Biomechanics* 25: 1383–1391, doi:10.1016/0021-9290(92)90052-3.

Schweighofer, N., Lee, J.-Y., Goh, H.-T., Choi, Y., Kim, S. S., Stewart, J. C., Lewthwaite, R. and Winstein, C. J. (2011). Mechanisms of the contextual interference effect in individuals poststroke. *Journal of Neurophysiology* 106: 2632–2641, doi:10.1152/jn.00399.2011.

Scott, S. H. (2004). Optimal feedback control and the neural basis of volitional motor control. *Nature Reviews Neuroscience* 5: 532–545, doi:10.1038/nrn1427.

Seidler, R. D., Bernard, J. A., Burutolu, T. B., Fling, B. W., Gordon, M. T., Gwin, J. T., Kwak, Y. and Lipps, D. B. (2010). Motor control and aging: Links to age-related brain structural, functional, and biochemical effects. *Neuroscience and biobehavioral reviews* 34: 721–733, doi:10.1016/j.neubiorev.2009.10.005.

Sensinger, J. W. and Dosen, S. (2020). A review of sensory feedback in upper-limb prostheses from the perspective of human motor control. *Frontiers in Neuroscience* 14, doi:10.3389/fnins.2020.00345.

Severini, G. and Zych, M. (2020). Characterization of the adaptation to visuomotor rotations in the muscle synergies space. *Frontiers in Bioengineering and Biotechnology* 8, doi:10.3389/fbioe.2020.00605.

Shadmehr, R. (2004). Generalization as a behavioral window to the neural mechanisms of learning internal models. *Human Movement Science* 23: 543–568, doi:10.1016/j.humov.2004.04.003.

Shadmehr, R. (2017). Learning to predict and control the physics of our movements. *The Journal of Neuroscience* 37: 1663–1671, doi:10.1523/JNEUROSCI.1675-16.2016.

Shadmehr, R. and Brashers-Krug, T. (1997). Functional stages in the formation of human long-term motor memory. *Journal of Neuroscience* 17: 409–419, doi:10.1523/JNEUROSCI.17-01-00409.1997.

Shadmehr, R. and Krakauer, J. W. (2008). A computational neuroanatomy for motor control. *Experimental Brain Research* 185: 359–381, doi:10.1007/s00221-008-1280-5.

Shadmehr, R. and Moussavi, Z. M. K. (2000). Spatial generalization from learning dynamics of reaching movements. *The Journal of Neuroscience* 20: 7807–7815, doi:10.1523/JNEUROSCI.20-20-07807.2000.

Shadmehr, R. and Mussa-Ivaldi, F. A. (1994). Adaptive representation of dynamics during learning of a motor task. *The Journal of Neuroscience* 14: 3208–3224, doi:10.1523/JNEUROSCI.14-05-03208.1994.

Shadmehr, R., Smith, M. A. and Krakauer, J. W. (2010). Error correction, sensory prediction, and adaptation in motor control. *Annual Review of Neuroscience* 33: 89–108, doi:10.1146/annurev-neuro-060909-153135.

Shadmehr, R. and Wise, S. P. (2005). *The Computational Neurobiology of Reaching and Pointing: A Foundation for Motor Learning*. Cambridge: MIT Press.

Shea, J. B. and Morgan, R. L. (1979). Contextual interference effects on the acquisition, retention, and transfer of a motor skill. *Journal of Experimental Psychology: Human Learning and Memory* 5: 179–187, doi:10.1037/0278-7393.5.2.179.

Shea, J. B. and Titzer, R. C. (1993). The influence of reminder trials on contextual interference effects. *Journal of Motor Behavior* 25: 264–274.

Sheridan, T. B. (2016). Human–robot interaction: Status and challenges. *Human Factors* 58: 525–532, doi:10.1177/0018720816644364.

Sherrington, C. S. (1910). Flexion-reflex of the limb, crossed extension-reflex, and reflex stepping and standing. *The Journal of physiology* 40: 28.

Shum, G. L. K., Crosbie, J. and Lee, R. Y. W. (2005). Effect of low back pain on the kinematics and joint coordination of the lumbar spine and hip during sit-to-stand and stand-to-sit. *Spine* 30: 1998–2004, doi:10.1097/01.brs.0000176195.16128.27.

Shumway-Cook, A. and Woollacott, M. H. (2007). *Motor Control: Translating Research Into Clinical Practice*. Philadelphia: Lippincott Williams & Wilkins, 3rd ed.

Sing, G. C., Joiner, W. M., Nanayakkara, T., Brayanov, J. B. and Smith, M. A. (2009). Primitives for motor adaptation reflect correlated neural tuning to position and velocity. *Neuron* 64: 575–589, doi:10.1016/j.neuron.2009.10.001.

Singh, R. E., Iqbal, K., White, G. and Hutchinson, T. E. (2018). A systematic review on muscle synergies: From building blocks of motor behavior to a neurorehabilitation tool. *Applied Bionics and Biomechanics* 2018: 1–15, doi:10.1155/2018/3615368.

Sloot, L. H., Millard, M., Werner, C. and Mombaur, K. (2020). Slow but steady: similar sit-to-stand balance at seat-off in older vs. younger adults. *Frontiers in sports and active living* 2, doi:10.3389/fspor.2020.548174.

Smith, M. A., Ghazizadeh, A. and Shadmehr, R. (2006). Interacting adaptive processes with different timescales underlie short-term motor learning. *PLOS Biology* 4: e179, doi:10.1371/journal.pbio.0040179.

Snijders, T. A. B. and Bosker, R. J. (2012). *Multilevel analysis: an introduction to basic and advanced multilevel modeling*. Los Angeles, Calif: SAGE, 2nd ed.

Spampinato, D. and Celnik, P. (2021). Multiple motor learning processes in humans: Defining their neurophysiological bases. *The Neuroscientist: A Review Journal Bringing Neurobiology, Neurology and Psychiatry* 27: 246–267, doi:10.1177/1073858420939552.

Steele, K. M., Tresch, M. C. and Perreault, E. J. (2013). The number and choice of muscles impact the results of muscle synergy analyses. *Frontiers in Computational Neuroscience* 7, doi:10.3389/fncom.2013.00105.

Steele, K. M., Tresch, M. C. and Perreault, E. J. (2015). Consequences of biomechanically constrained tasks in the design and interpretation of synergy analyses. *Journal of Neurophysiology* 113: 2102–2113, doi:10.1152/jn.00769.2013.

Stetter, B., Möhler, F., Krafft, F., Sell, S. and Stein, T. (2020). Identification of fatigue-related kinematic changes in elite runners using a support vector machine approach. *ISBS Proceedings Archive* 38: 264.

Stetter, B. J. and Stein, T. (2024). Machine learning in biomechanics: Enhancing human movement analysis. In Dindorf, C., Bartaguiz, E., Gassmann, F. and Fröhlich, M. (eds), *Artificial Intelligence in Sports, Movement, and Health*. Champaign: Springer Nature Switzerland, 139–160, doi:10.1007/978-3-031-67256-9_9.

Stevens, J. A. (2005). Falls among older adults—risk factors and prevention strategies. *Journal of Safety Research* 36: 409–411, doi:10.1016/j.jsr.2005.08.001.

Stief, F., Holder, J., Feja, Z., Lotfolahpour, A., Meurer, A. and Wilke, J. (2021). Impact of subject-specific step width modification on the knee and hip adduction moments during gait. *Gait & Posture* 89: 161–168, doi:10.1016/j.gaitpost.2021.07.008.

Stockinger, C., Pöschl, M., Focke, A. and Stein, T. (2012). Manipanalysis - a software application for the analysis of force field experiments. *International Journal of Computer Science in Sport* 11: 52–27.

Stockinger, C., Thürer, B., Focke, A. and Stein, T. (2015). Intermanual transfer characteristics of dynamic learning: direction, coordinate frame, and consolidation of interlimb generalization. *Journal of Neurophysiology* 114: 3166–3176, doi:10.1152/jn.00727.2015.

Stone, M. (1974). Cross-validatory choice and assessment of statistical predictions. *Journal of the Royal Statistical Society Series B: Statistical Methodology* 36: 111–133, doi:10.1111/j.2517-6161.1974.tb00994.x.

Suica, Z., Romkes, J., Tal, A. and Maguire, C. (2016). Walking with a four wheeled walker (rollator) significantly reduces emg lower-limb muscle activity in healthy subjects. *Journal of Bodywork and Movement Therapies* 20: 65–73, doi:10.1016/j.jbmt.2015.06.002.

Swearingen, J. J. (1962). Determination of centers of gravity of man. Tech. Rep. 14, Civil Aeromedical Research Institute, Oklahoma City.

Sylos-Labini, F., La Scaleia, V., Cappellini, G., Fabiano, A., Picone, S., Keshishian, E. S., Zhvansky, D. S., Paolillo, P., Solopova, I. A., d'Avella, A., Ivanenko, Y. and Lacquaniti, F. (2020). Distinct locomotor precursors in newborn babies. *Proceedings of the National Academy of Sciences* 117: 9604–9612, doi:10.1073/pnas.1920984117.

Taborri, J., Agostini, V., Artemiadis, P. K., Ghislieri, M., Jacobs, D. A., Roh, J. and Rossi, S. (2018). Feasibility of muscle synergy outcomes in clinics, robotics, and sports: A systematic review. *Applied Bionics and Biomechanics* 2018: 1–19, doi:10.1155/2018/3934698.

Tanabe, H., Fujii, K. and Kouzaki, M. (2017). Intermittent muscle activity in the feedback loop of postural control system during natural quiet standing. *Scientific Reports* 7: 10631, doi:10.1038/s41598-017-10015-8.

Tanaka, H., Krakauer, J. W. and Sejnowski, T. J. (2012). Generalization and multirate models of motor adaptation. *Neural Computation* 24: 939–966, doi:10.1162/NECO_a_00262.

Taubert, M., Stein, T., Kreutzberg, T., Stockinger, C., Hecker, L., Focke, A., Ragert, P., Villringer, A. and Pleger, B. (2016). Remote effects of non-invasive cerebellar stimulation on error processing in motor re-learning. *Brain Stimulation* 9: 692–699, doi:10.1016/j.brs.2016.04.007.

Thoroughman, K. A. and Shadmehr, R. (1999). Electromyographic correlates of learning an internal model of reaching movements. *The Journal of Neuroscience* 19: 8573–8588, doi: 10.1523/JNEUROSCI.19-19-08573.1999.

Thoroughman, K. A. and Shadmehr, R. (2000). Learning of action through adaptive combination of motor primitives. *Nature* 407: 742–747, doi:10.1038/35037588.

Thürer, B., Gedemer, S., Focke, A. and Stein, T. (2019). Contextual interference effect is independent of retroactive inhibition but variable practice is not always beneficial. *Frontiers in Human Neuroscience* 13, doi:10.3389/fnhum.2019.00165.

Thürer, B., Stockinger, C., Putze, F., Schultz, T. and Stein, T. (2017). Mechanisms within the parietal cortex correlate with the benefits of random practice in motor adaptation. *Frontiers in Human Neuroscience* 11, doi:10.3389/fnhum.2017.00403.

Thürer, B., Weber, F. D., Born, J. and Stein, T. (2018). Variable training but not sleep improves consolidation of motor adaptation. *Scientific Reports* 8: 15977, doi:10.1038/s41598-018-34225-w.

Tinetti, M. E., Speechley, M. and Ginter, S. F. (1988). Risk factors for falls among elderly persons living in the community. *New England journal of medicine* 319: 1701–1707, doi: 10.1056/NEJM198812293192604.

Ting, L. H. and Chiel, H. J. (2017). Muscle, biomechanics, and implications for neural control. In Hooper, S. L. and Büschges, A. (eds), *Neurobiology of Motor Control*. Hoboken: John Wiley & Sons, Inc., 365–416, doi:10.1002/9781118873397.ch12.

Ting, L. H., Chiel, H. J., Trumbower, R. D., Allen, J. L., McKay, J. L., Hackney, M. E. and Kesar, T. M. (2015). Neuromechanical principles underlying movement modularity and their implications for rehabilitation. *Neuron* 86: 38–54, doi:10.1016/j.neuron.2015.02.042.

Ting, L. H. and Chvatal, S. A. (2010). Decomposing muscle activity in motor tasks. In Danion, F. and Latash, M. (eds), *Motor Control: Theories, Experiments, and Applications*. New York: Oxford University Press, 102–138, doi:10.1093/acprof:oso/9780195395273.003.0005.

Ting, L. H. and Macpherson, J. M. (2005). A limited set of muscle synergies for force control during a postural task. *Journal of neurophysiology* 93: 609–613, doi:10.1152/jn.00681.2004.

Ting, L. H. and McKay, J. L. (2007). Neuromechanics of muscle synergies for posture and movement. *Current Opinion in Neurobiology* 17: 622–628, doi:10.1016/j.conb.2008.01.002.

Tirrell, T. F., Rademaker, A. W. and Lieber, R. L. (2018). Analysis of hierarchical biomechanical data structures using mixed-effects models. *Journal of Biomechanics* 69: 34–39, doi:10.1016/j.jbiomech.2018.01.013.

Todorov, E. (2004). Optimality principles in sensorimotor control. *Nature Neuroscience* 7: 907–915, doi:10.1038/nn1309.

Todorov, E. and Jordan, M. I. (2002). Optimal feedback control as a theory of motor coordination. *Nature neuroscience* 5: 1226, doi:10.1038/nn963.

Torres-Oviedo, G., Macpherson, J. M. and Ting, L. H. (2006). Muscle synergy organization is robust across a variety of postural perturbations. *Journal of Neurophysiology* 96: 1530–1546, doi:10.1152/jn.00810.2005.

Torres-Oviedo, G. and Ting, L. H. (2007). Muscle synergies characterizing human postural responses. *Journal of Neurophysiology* 98: 2144–2156, doi:10.1152/jn.01360.2006.

Torricelli, D., Barroso, F., Coscia, M., Alessandro, C., Lunardini, F. and Esteban, E. B. (2016). Muscle synergies in clinical practice: Theoretical and practical implications. In Pons, J. L., Raya, R. and González, J. (eds), *Emerging Therapies in Neurorehabilitation II. Biosystems & Biorobotics*. Champaign: Springer, *10*, 22, doi:10.1007/978-3-319-24901-8_10.

Torricelli, D., De Marchis, C., d'Avella, A., Tobaruela, D. N., Barroso, F. O. and Pons, J. L. (2020). Reorganization of muscle coordination underlying motor learning in cycling tasks. *Frontiers in Bioengineering and Biotechnology* 8, doi:10.3389/fbioe.2020.00800.

Tresch, M. C. and Bizzi, E. (1999). Responses to spinal microstimulation in the chronically spinalized rat and their relationship to spinal systems activated by low threshold cutaneous stimulation. *Experimental Brain Research* 129: 0401–0416, doi:10.1007/s002210050908.

Tresch, M. C., Cheung, V. C. K. and d'Avella, A. (2006). Matrix factorization algorithms for the identification of muscle synergies: evaluation on simulated and experimental data sets. *Journal of Neurophysiology* 95: 2199–2212, doi:10.1152/jn.00222.2005.

Tresch, M. C. and Jarc, A. (2009). The case for and against muscle synergies. *Current Opinion in Neurobiology* 19: 601–607, doi:10.1016/j.conb.2009.09.002.

Tresch, M. C., Saltiel, P. and Bizzi, E. (1999). The construction of movement by the spinal cord. *Nature Neuroscience* 2: 162–167, doi:10.1038/5721.

Trewartha, K. M., Garcia, A., Wolpert, D. M. and Flanagan, J. R. (2014). Fast but fleeting: Adaptive motor learning processes associated with aging and cognitive decline. *Journal of Neuroscience* 34: 13411–13421, doi:10.1523/JNEUROSCI.1489-14.2014.

Truong, C., Ruffino, C., Crognier, A., Paizis, C., Crognier, L. and Papaxanthis, C. (2023). Error-based and reinforcement learning in basketball free throw shooting. *Scientific Reports* 13: 499, doi:10.1038/s41598-022-26568-2.

Turpin, N. A., Guével, A., Durand, S. and Hug, F. (2011). Effect of power output on muscle coordination during rowing. *European journal of applied physiology* 111: 3017–3029, doi: 10.1007/s00421-011-1928-x.

Turpin, N. A., Uriac, S. and Dalleau, G. (2021). How to improve the muscle synergy analysis methodology? *European Journal of Applied Physiology* 121, doi:10.1007/s00421-021-04604-9.

Twisk, J. W. R. (2019). Multivariate mixed model analysis. In *Applied Mixed Model Analysis: A Practical Guide*, Practical Guides to Biostatistics and Epidemiology. Cambridge University Press, 151–165.

Van Ingen Schenau, G. J. (1989). From rotation to translation: Constraints on multi-joint movements and the unique action of bi-articular muscles. *Human Movement Science* 8: 301–337, doi:10.1016/0167-9457(89)90037-7.

Vander Linden, D. W., Brunt, D. and McCulloch, M. U. (1994). Variant and invariant characteristics of the sit-to-stand task in healthy elderly adults. *Archives of Physical Medicine and Rehabilitation* 75: 653–660, doi:10.1016/0003-9993(94)90188-0.

Vaz, J. R., Olstad, B. H., Cabri, J., Kjendlie, P.-L., Pezarat-Correia, P. and Hug, F. (2016). Muscle coordination during breaststroke swimming: comparison between elite swimmers and beginners. *Journal of sports sciences* 34: 1941–1948, doi:10.1080/02640414.2016.1143109.

Vera, M. J., Dubravka, B., Nikola, J., Vojin, I. and Bojana, P.-B. (2013). Detecting and removing outlier(s) in electromyographic gait-related patterns. *Journal of Applied Statistics* 40: 1319–1332, doi:10.1080/02664763.2013.785495.

Wadman, W. J., Gon, J. Denier Van der, Geuze, R. H. and Mol, C. R. (1979). Control of fast goal-directed arm movements. *Journal of Human Movement Studies* 5: 3–17.

Wagner, M. J. and Smith, M. A. (2008). Shared internal models for feedforward and feedback control. *Journal of Neuroscience* 28: 10663–10673, doi:10.1523/JNEUROSCI.5479-07.2008.

Waite, D. L., Brookham, R. L. and Dickerson, C. R. (2010). On the suitability of using surface electrode placements to estimate muscle activity of the rotator cuff as recorded by intramuscular electrodes. *Journal of Electromyography and Kinesiology* 20: 903–911, doi:10.1016/j.jelekin.2009.10.003.

Wang, T., Okada, S., Guo, A., Makikawa, M. and Shiozawa, N. (2021). Effect of Assist Robot on Muscle Synergy during Sit-to-Stand Movement. In *2021 IEEE International Conference on Intelligence and Safety for Robotics (ISR)*, 367–368, doi:10.1109/ISR50024.2021.9419525.

Wei, K. and Körding, K. (2009). Relevance of error: What drives motor adaptation? *Journal of Neurophysiology* 101: 655–664, doi:10.1152/jn.90545.2008.

Wiesmeier, I. K., Dalin, D. and Maurer, C. (2015). Elderly use proprioception rather than visual and vestibular cues for postural motor control. *Frontiers in Aging Neuroscience* 7, doi:10.3389/fnagi.2015.00097.

Wilkins, L. W. . (2008). *Perfecting clinical procedures*. Nursing: The series for clinical excellence. Philadelphia, PA: Wolters Kluwer Health, Lippincott Williams & Wilkins.

Windrich, M., Grimmer, M., Christ, O., Rinderknecht, S. and Beckerle, P. (2016). Active lower limb prosthetics: a systematic review of design issues and solutions. *Biomedical engineering online* 15: 5–19, doi:10.1186/s12938-016-0284-9.

Wolpert, D. M. and Bastian, A. J. (2021). Principles of sensorimotor control. In Kandel, E., Schwartz, J., Jessell, T., Siegelbaum, S. and Hudspeth, A. (eds), *Principles of Neural Science*. New York: McGraw Hill, 6th ed., 713–973.

Wolpert, D. M., Diedrichsen, J. and Flanagan, J. R. (2011). Principles of sensorimotor learning. *Nature Reviews Neuroscience* 12: 739–751, doi:10.1038/nrn3112.

Wolpert, D. M. and Flanagan, J. (2010a). Motor learning. *Current biology* 20: R467–R472, doi:10.1016/j.cub.2010.04.035.

Wolpert, D. M. and Flanagan, J. R. (2010b). Q&a: Robotics as a tool to understand the brain. *BMC Biology* 8: 92, doi:10.1186/1741-7007-8-92.

Wolpert, D. M. and Ghahramani, Z. (2000). Computational principles of movement neuroscience. *Nature Neuroscience* 3: 1212–1217, doi:10.1038/81497.

Wolpert, D. M. and Kawato, M. (1998). Multiple paired forward and inverse models for motor control. *Neural Networks* 11: 1317–1329, doi:10.1016/S0893-6080(98)00066-5.

Wolpert, D. M., Pearson, K. and Ghez, C. (2012). The organization and planning of movement. In Kandel, E., Schwartz, J., Jessell, T., Siegelbaum, S. and Hudspeth, A. (eds), *Principles of Neural Science*. New York, London: McGraw-Hill Publishing, 5th ed., 743–767.

Wretenberg, P., Lindberg, F. and Arborelius, U. P. (1993). Effect of armrests and different ways of using them on hip and knee load during rising. *Clinical Biomechanics* 8: 95–101, doi:10.1016/S0268-0033(93)90039-K.

Wright, D. L. and Kim, T. (2019). Contextual interference. In Hodges, N. J. and Williams, A. M. (eds), *Skill Acquisition in Sport*. New York: Routledge, 3rd ed., 99–118, doi:10.4324/9781351189750-6.

Wulf, G. and Shea, C. H. (2002). Principles derived from the study of simple skills do not generalize to complex skill learning. *Psychonomic Bulletin & Review* 9: 185–211, doi:10.3758/BF03196276.

Yamada, T. and Demura, S.-i. (2009). Relationships between ground reaction force parameters during a sit-to-stand movement and physical activity and falling risk of the elderly and a comparison of the movement characteristics between the young and the elderly. *Archives of gerontology and geriatrics* 48: 73–77, doi:10.1016/j.archger.2007.10.006.

Yamasaki, H. R. and Shimoda, S. (2016). Spatiotemporal modular organization of muscle torques for sit-to-stand movements. *Journal of Biomechanics* 49: 3268–3274, doi:10.1016/j.jbiomech.2016.08.010.

Yan, T., Cempini, M., Oddo, C. M. and Vitiello, N. (2015). Review of assistive strategies in powered lower-limb orthoses and exoskeletons. *Robotics and Autonomous Systems* 64: 120–136, doi:10.1016/j.robot.2014.09.032.

Yang, N., An, Q., Yamakawa, H., Tamura, Y., Yamashita, A. and Asama, H. (2017). Muscle synergy structure using different strategies in human standing-up motion. *Advanced Robotics* 31: 40–54, doi:10.1080/01691864.2016.1238781.

Yoshida, K., An, Q., Yozu, A., Chiba, R., Takakusaki, K., Yamakawa, H., Tamura, Y., Yamashita, A. and Asama, H. (2019). Visual and vestibular inputs affect muscle synergies responsible for body extension and stabilization in sit-to-stand motion. *Frontiers in Neuroscience* 12, doi:10.3389/fnins.2018.01042.

Youdas, J. W., Kotajarvi, B. J., Padgett, D. J. and Kaufman, K. R. (2005). Partial weight-bearing gait using conventional assistive devices. *Archives of Physical Medicine and Rehabilitation* 86: 394–398, doi:10.1016/j.apmr.2004.03.026.

Zajac, F. E. (1989). Muscle and tendon: properties, models, scaling, and application to biomechanics and motor control. *Critical reviews in biomedical engineering* 17: 359–411.

Zarahn, E., Weston, G. D., Liang, J., Mazzoni, P. and Krakauer, J. W. (2008). Explaining savings for visuomotor adaptation: linear time-invariant state-space models are not sufficient. *Journal of neurophysiology* 100: 2537–2548, doi:10.1152/jn.90529.2008.

Zhang, Y., Tao, C., Wang, H. and Fan, Y. (2025). Biomechanical effects of human-mobility aid interaction: A narrative review. *Gait & Posture* 118, doi:10.1016/j.gaitpost.2025.01.009.

Zhao, K., Zhang, Z., Wen, H., Liu, B., Li, J., d'Avella, A. and Scano, A. (2023). Muscle synergies for evaluating upper limb in clinical applications: A systematic review. *Heliyon* 9: e16202, doi:10.1016/j.heliyon.2023.e16202.

Michael Herzog studied at the Karlsruhe Institute of Technology, the North Carolina State University, and the École Nationale Supérieure de Techniques Avancées ParisTech, and double-majored in computer science and sports science. He works as a research assistant in Thorsten Stein's group at the BioMotion Center at the Institute of Sports and Sports Science at the Karlsruhe Institute of Technology and received a scholarship for a research stay during his doctoral studies at the Istituto di Ricovero e Cura a Carattere Scientifico in Rome with Andrea d'Avella.

In his research, he investigates human movement coordination with robotic devices. This includes tasks such as reaching in perturbing viscous force fields and standing-up and sitting-down with robotic rollator assistance. His primary approach is to analyze the synergistic muscle activations underlying these movements. As a sports enthusiast and computer scientist, he bridges the gap between real-world settings and advanced data-driven methodologies.

KARLSRUHE SPORTS SCIENCE RESEARCH | BAND 91

ISSN 2943-0380